School of Industrial and

ICT Engineering

Impact of generator speed filtering process on wind turbine structural loads

Bachelor's Degree

In Industrial Engineering

Final Degree Project

Miren Bontigui Vallejos

Director: Asier Díaz de Corcuera Martínez

Co-director: Jorge Elso Torralba

Pamplona, June 10th 2019

upna Universidad Pública de Navarra Nafarroako Unibertsitate Publikoa

upna
Universidad
Pública de Navarra
Nafarroako
Unibertsitate Publikoa

ACKNOWLEDGEMENTS

After the months that I have dedicated to this project, I am more than happy of what I have learned out of it. There are many people whose support and guidance have been crucial for the development of this project and I couldn't go without thanking them.

First of all, I would like to thank my parents and sister. Thank you for putting up with me, not only through this project but throughout my whole career, I can only imagine how hard that must be.

I would like to say a special thank you to my dad. None of this would have been possible without you. You are the best.

I want to thank my friends, for all the good times and for making the worst ones better. Thank you for always being there.

I also want to thank you, Javi, for always cheering me up. You are awesome.

I would like to thank everyone in the Siemens Gamesa R.E. Control Department for making everything a little easier and particularly to Mikel and Aitor for always helping me out.

I would also like to thank Marta and Jesús for giving me this golden oportunity. And to Jorge, for your advice throughout this project.

Finally, I am extremely thankful to Asier, you are the mentor any student would be happy to have. The love you have for what you do makes everything better and I can't thank you enough for your guidance during this project.

ABSTRACT

This Final Degree Project has been carried out in the company Siemens Gamesa Renewable Energy, in Sarriguren (Navarra, Spain). Particularly, it has been developed in the Control Department of the Technology area of the company.

The aim of this project is to study the influence that filtering the generator speed has on wind turbine structural loads. First, a classical control strategy has been designed and then, a load and fatigue analysis has been carried out. This allows the comparison of the structural loads that appear when changes are introduced in the filtering process.

When designing a wind turbine control strategy, two main objectives are pursued. On one hand, there is power regulation. It is a **regulation control** strategy and its aim is to maximize the turbine's AEP (Annual Energy Production). On the other hand, there is load reduction, which is an **active control** strategy and it is designed with the aim of reducing structural loads therefore extending the turbine's time life. Both of them are developed in the control scheme of this project.

The wind turbine control scheme that has been designed in this project is a classical control strategy and it is based on traditional wind turbine control, particularly it is based on a variable speed turbine control design article by Bossanyi [1].

The **regulation control** strategy is composed by two control loops: the pitch control loop and the torque control loop. Both are designed to control generator speed, but the first one controls it by acting on the blade pitch angle and the second one does it by acting on the generator torque. This regulation control is set to **follow the torque vs. generator speed curve** of the wind turbine. Then, the **active control** strategy is designed to give **damping** to the drive train and the 1st tower fore-aft excited modes.

Besides, the generator speed is thoroughly filtered in the regulation control loops with the objective of eliminating any unnecessary control action in the frequencies that must be avoided due to their effect in the wind turbine's structural loads.

For that purpose a Simulink library containing filters and PIDs has been built. This library contains several filters such as a notch filter, low pass 1st and 2nd order filters, a band pass filter and a high pass filter as well as a PID block that is used in both regulation control loops.

This control scheme is implemented in Simulink and it is simulated with a wind turbine model developed by the **aeroelastic FAST code** (Fatigue, Aerodynamics, Structures and Turbulence). Specifically, the model that has been used for this project is the Upwind 5MW onshore baseline turbine model from NREL (National Renewable Energy Laboratory). This free, publicly available wind turbine model is a pitch-regulated, variable-speed wind turbine model that has the rotor facing the wind (upwind position).

The aeroelastic FAST code has not only been chosen because it is public but also because it allows the incorporation of its equations of motion to a **Simulink** model, which can be done because Simulink can incorporate the FAST routines in a block called S-Function. This makes feasible designing the control strategy in the Simulink environment and simulating it with the complete aeroelastic nonlinear model of the wind turbine.

FAST is also capable of extracting **linearized representations** of the wind turbine model. From these linear models, the plants of the system are obtained in the Laplace continuous-time form. These plants are necessary for designing and validating the control strategy and its performance in the frequency domain, which is done by adjusting the control until the system's desired closed loop behaviors are obtained.

Once the control strategy has been validated, the next step is to proceed with the **load and statistical analysis**. The objective is to check the fatigue load reduction capacity of the active control elements, this is, the ones that have been designed to give damping to the wind turbine's most excited structural modes.

This project's classical control scheme is also validated by comparing it to another Simulink implemented control strategy, the control strategy published by the DELFT University [2]. Again, a load and statistical analysis is carried out and both control strategies have been compared.

Finally, the actual study of the **pitch control's filtering process** is carried out. **AEP**, **pitch duty**, tower base and low speed shaft **loads** are analyzed by performing a study of the influence of the filters' parameters.

As a result of this study, an optimized filtering process for this specific wind turbine and this control scheme's pitch loop is obtained. Finally, a pitch control filtering process guide is proposed. Depending on the control's objectives such as lower loads, higher AEP or lower pitch duty, different filtering configurations are proposed.

LIST OF KEY WORDS

· Wind turbine

· Generator speed

· Control strategy

· Bode diagram

· Structural load

· Blade pitch angle

· Generator demanded torque

· Disturbance rejection sensibility

· Tracking sensibility

· Rated power

· Drive train mode

· 1st tower fore-aft mode

· Regulatory control

· Active control

· Closed loop control

· Damping of structural mode

upna Universidad Pública de Navarra Nafarroako Unibertsitate Publikoa

Index of contents

Chapter 1: Introduction 1
1.1. Background 1
1.2. Objectives of the study 2
Chapter 2: Wind turbine fundamentals 3
2.1. History 3
2.2. Modern wind turbines 5
2.2.1. Rotor 6
2.2.2. Nacelle 8
2.2.3. Tower 8
2.3. Wind energy 9
2.3.1. Available power and power coefficient 9
Chapter 3: Modelling of the reference wind turbine 13
3.1. Introduction 13
3.2. Upwind 5MW wind turbine modelled in FASTv7 (Simulink Environment) 13
3.3. Upwind 5MW wind turbine model 15
3.3.1. Upwind 5MW wind turbine model characteristics 15
3.3.2. Upwind 5MW wind turbine model coordinate systems 17
3.4. Linearization process in FASTv7 19
Chapter 4: Wind Turbine Simulink Controller Block 23
4.1. Introduction 23
4.2. Control library 24
4.2.1. Introduction 24
4.2.2. Discretization 24
4.2.3. 1st order Low Pass filter 26
4.2.4. 2nd order Low Pass filter 28
4.2.5. High Pass 30
4.2.6. Band Pass 32
4.2.7. Notch filter 34
4.2.8. PID block 36
4.3. Wind Turbine Control blocks 39
4.3.1. Main structure 39
4.3.2. Supervisory Control 40
4.3.3. Torque Control 44
4.3.4. Pitch Control 44
4.3.5. DTD 45
4.3.6. ATD 47

4.3.7. Main Supervisory Control 50
4.4. Simulink model and parameter file 50
4.4.1. Supervisory control 50
4.4.2. Pitch control loop 55
4.4.3. Torque control loop 60
4.4.4. DTD 66
4.4.5. ATD 69
Chapter 5: Baseline Control Tuning for 5MW Upwind model in FASTv7 72
5.1. Introduction 72
5.2. Supervisory Control 73
5.2.1. Parameters 73
5.3. DTD 73
5.3.1. Control performance 73
5.3.2. Parameters 79
5.4. Torque Control 79
5.4.1. Control performance 79
5.4.2. Parameters 85
5.5. Pitch Control 87
5.5.1. Control performance 87
5.5.2. Parameters 92
5.6. ATD 94
5.6.1. Control performance 94
5.6.2. Parameters 97
Chapter 6: Validation of baseline Control Tuning for 5MW Upwind model in FASTv7 99
6.1. Introduction 99
6.2. Time-series simulation analysis 99
6.3. Statistical analysis 104
6.4. Frequency analysis in power production wind of 25m/s 107
6.5. Fatigue Load analysis (minirainflows) 114
6.5.1. Fatigue load analysis process 114
6.5.2. Fatigue load analysis results 118
6.6. Conclusions 119
Chapter 7: Analysis of generator speed filtering process in Pitch Control Loop vs baseline 120
7.1. Introduction 120
7.2. Control scenario 1, 1st order Low Pass filter 124
7.2.1. Control performance (open loop, sensitivities) vs baseline 124
7.2.2. Statistical analysis 127

7.2.3. Fatigue load analysis 129
7.3. Control scenario 2, Notch DT filter 130
7.3.1. Control performance (open loop, sensitivities) vs baseline 130
7.3.2. Statistical analysis 133
7.3.3. Fatigue load analysis 136
7.4. Control scenario 3, Notch Symmetric filter 136
7.4.1. Control performance (open loop, sensitivities) vs baseline 136
7.4.2. Statistical analysis 139
7.4.3. Fatigue load analysis 141
7.5. Control scenario 4, Notch Side-to-side filter 141
7.5.1. Control performance (open loop, sensitivities) vs baseline 141
7.5.2. Statistical analysis 144
7.5.3. Fatigue load analysis 146
7.6. Control scenario 5, Notch 1P filter 146
7.6.1. Control performance (open loop, sensitivities) vs baseline 146
7.6.2. Statistical analysis 149
7.6.3. Fatigue load analysis 151
7.7. Control scenario 6, Notch 3P filter 152
7.7.1. Control performance (open loop, sensitivities) vs baseline 152
7.7.2. Statistical analysis 155
7.7.3. Fatigue load analysis 157
7.8. Conclusions 157
7.8.1. Scenario 1, Low Pass filter 158
7.8.2. Scenario 2, Notch DT 158
7.8.3. Scenario 3, Notch Sym 158
7.8.4. Scenario 4, Notch 2Tss 159
7.8.5. Scenario 5 159
7.8.6. Scenario 6 160
Chapter 8: Conclusions 161
8.1. Conclusions 161
8.2. Industrial implementation 163
8.3. Future work 164
Chapter 9: References 165

Index of figures

Figure 1: Wind power global capacity and annual additions, 2007-2017 1
Figure 2: James Blyth's windmill, 1887 3
Figure 3: Charles F. Brush 12kW wind turbine, 1887 3
Figure 4: Wind power capacity and additions, 2017 4
Figure 5: Eolic systems' contribution to the electric demand [4] 4
Figure 6: Wind Power Capacity and Additions, Top 10 Countries, 2017 5
Figure 7: Main elements of a modern wind turbine 5
Figure 8: Wind turbine hub 6
Figure 9: Wind turbine blade profile. Aerodynamic forces 6
Figure 10: Torsion angle along blade profile 7
Figure 11: Generator power for passive stall and pitch control wind turbines (kW) 7
Figure 12: Wind turbine blade 8
Figure 13: Wind turbine drive train 8
Figure 14: Lattice tower wind turbine 9
Figure 15: Tubular steel tower wind turbine 9
Figure 16: Upwind and downwind wind turbine configurations 9
Figure 17: Wind turbine rotor control volume 10
Figure 18: Cp vs tip speed ratio λ 11
Figure 19: FAST S-Function in Simulink 14
Figure 20: FAST diagram 14
Figure 21: Campbell diagram of the 5MW Upwind baseline model 17
Figure 22: Tower-Base Coordinate System 18
Figure 23: Tower-Top Coordinate System 18
Figure 24: Nacelle or Yaw Coordinate System 18
Figure 25: Hub Coordinate System 18
Figure 26: Coned Coordinate System 19
Figure 27: Blade Coordinate System 19
Figure 28: Generator speed vs. wind speed linearization points 20
Figure 29: Pitch angle vs. wind speed linearization points 21
Figure 30: Generator torque vs. wind speed linearization points 21
Figure 31: Generator torque vs. generator speed linearization points 22
Figure 32: Scheme of the control loops and active control strategies 23
Figure 33: Generator torque to generator speed curve 24
Figure 34: Discretization diagram 25
Figure 35: 1st order low pass filter Bode diagram 26
Figure 36: 1st order low pass continuous filter vs. discrete filter 27
Figure 37: 1st and 2nd order filter Bode diagram 28
Figure 38: 2nd order low pass continuous filter vs. discrete filter 29
Figure 39: 1st and 2nd order low pass filter attenuation comparison 29
Figure 40: 2nd order high pass filter Bode diagram 31
Figure 41: 2nd order high pass continuous filter vs. discrete filter 31
Figure 42: 2nd order band pass filter Bode diagram 33
Figure 43: 2nd order band pass continuous filter vs. discrete filter 33
Figure 44: Notch filter Bode diagram 35
Figure 45: Notch continuous filter vs. discrete filter 35
Figure 46: Bode diagram of a PID block 37
Figure 47: Bode diagram of a PID and a PID with a filter 38
Figure 48: Diagram of the control's main structure 40
Figure 49: Supervisory control zones in generator torque vs. speed graph 41

Figure 50: First vertical control scheme. Block diagram of Torque Control Loop and DTD 41
Figure 51: Quadratic curve control scheme. Block diagram of DTD 42
Figure 52: Second vertical control scheme. Block diagram of Torque Control Loop and DTD ... 43
Figure 53: Above rated control scheme. Block diagram of the Pitch Control Loop, ATD and DTD 43
Figure 54: Torque control loop scheme 44
Figure 55: Pitch control loop scheme 45
Figure 56: Kp, pitch control PID's gain scheduling 45
Figure 57: Ki, pitch control PID's gain scheduling 45
Figure 58: Open loop Bode diagram of the DTD at 11m/s 46
Figure 59: Bode diagram of the plant drom torque to generator speed with and without DTD at 11m/s 47
Figure 60: ATD gain scheduling 48
Figure 61: Open loop Bode diagram of the ATD at 13m/s 49
Figure 62: Bode diagram of the plant from pitch to nacelle fore-aft with and without ATD at 13m/s 50
Figure 63: Simulink model of the Supervisory Control 51
Figure 64: Internal Simulink model of the Supervisory Control 51
Figure 65: Simulink model of the Pitch Control Loop 55
Figure 66: Internal Simulink model of the Pitch Control Loop, filters 56
Figure 67: Internal Simulink model of the Pitch Control Loop, PID and gain schedulings 56
Figure 68:Simulink model of the Torque Control Loop 60
Figure 69: Internal Simulink model of the Torque Control Loop, filters and PID 61
Figure 70: Internal Simulink model of the Torque Control Loop, torque limits 62
Figure 71: Simulink model of the DTD 66
Figure 72: Internal Simulink model of the DTD, filters 66
Figure 73: Internal Simulink model of the DTD, DTD gains and limits 67
Figure 74: Simulink model of the ATD 69
Figure 75: Internal Simulink model of the ATD, filters 69
Figure 76: Internal Simulink model of the ATD, ATD gain scheduling and limits 70
Figure 77: Bode diagram of the plant from torque to generator speed with and without DTD at 5m/s 74
Figure 78: Bode diagram of the DTD's disturbance sensibility S(s) at 5m/s 75
Figure 79: Bode diagram of the plant from torque to generator speed with and without DTD at 9m/s 75
Figure 80: Bode diagram of the DTD's disturbance sensibility S(s) at 9m/s 76
Figure 81: Bode diagram of the plant from torque to generator speed with and without DTD at 11m/s 76
Figure 82: Bode diagram of the DTD's disturbance sensibility S(s) at 11m/s 77
Figure 83: Bode diagram of the plant from torque to generator speed with and without DTD at 19m/s 78
Figure 84: Bode diagram of the DTD's disturbance sensibility S(s) at 19m/s 78
The behavior of the torque control loop is going to be explained in every operating zone. These zones correspond to the ones explained in Figure 85 in Chapter 4: Wind Turbine Simulink Controller Block. 80
Figure 86: Bode diagram of the torque control, DTD, plant with DTD and open loop at 5m/s .. 80
Figure 87: Gain and phase margins of the torque control at 5m/s 81
Figure 88: Bode diagram of torque control's disturbance sensibility S(s) at 5m/s 82
Figure 89: Band width and magnitude peak of the torque control's S(s) at 5m/s 82
Figure 90: Bode diagram of the torque control, DTD, plant with DTD and open loop at 11m/s 83
Figure 91: Gain and phase margins of the torque control at 11m/s 84
Figure 92: Bode diagram of torque control's disturbance sensibility S(s) at 11m/s 84

Figure 93: Band width and magnitude peak of the torque control's S(s) at 11m/s 85
Figure 94: Pitch Control disturbance sensibility requirements 87
Figure 95: Bode diagram of the pitch control, ATD, plant with ATD and open loop at 19m/s ... 88
Figure 96: Gain and phase margins of the pitch control at 19m/s 88
Figure 97: Bode diagram of pitch control's disturbance sensibility S(s) at 13m/s 89
Figure 98: Band width and magnitude peak of the pitch control's S(s) at 13m/s 90
Figure 99: Bode diagram of pitch control's disturbance sensibility S(s) at 19m/s 90
Figure 100: Band width and magnitude peak of the pitch control's S(s) at 19m/s 91
Figure 101: Bode diagram of pitch control's disturbance sensibility S(s) at 25m/s 91
Figure 102: Band width and magnitude peak of the pitch control's S(s) at 25m/s 92
Figure 103: Bode diagram of the plant from pitch to nacelle fore-aft with and without ATD at 13m/s 94
Figure 104: Bode diagram of the plant from pitch to nacelle fore-aft with and without ATD at 19m/s 95
Figure 105: Bode diagram of the plant from pitch to nacelle fore-aft with and without ATD at 25m/s 95
Figure 106: Bode diagram of the ATD's disturbance sensibility S(s) at 13m/s 96
Figure 107: Bode diagram of the ATD's disturbance sensibility S(s) at m/s 97
Figure 108: Generator torque vs. generator speed with a ramp input 100
Figure 109: Generator power vs. generator speed with a ramp input 101
Figure 110: Wind, generator speed, torque and pitch angle vs. time with a ramp input 101
Figure 111: Generator torque vs. generator speed with unitary step inputs 102
Figure 112: Generator power vs. generator speed with unitary step inputs 103
Figure 113: Wind, generator speed, torque and pitch angle vs. time with unitary step inputs 103
Figure 114: Generator speed vs. time with unitary step inputs 104
Figure 115: Generated power statistics for 600s simulations 105
Figure 116: Pitch standard deviation for 600s simulations 105
Figure 117: Tower base "y" momentum statistics for 600s simulations 106
Figure 118: Low speed shaft "x" momentum statistics for 600s simulations 107
Figure 119: Generator speed vs. time in 60s simulations 108
Figure 120: Generator speed FFT in 600s simulations 109
Figure 121: Blade pitch angle vs. time for 600s simulations 109
Figure 122: Blade pitch angle FFT in 600s simulations 110
Figure 123: Generator power vs. time in 600s simulations 111
Figure 124: Generator power FFT in 600s simulations 111
Figure 125: Nacelle fore-aft acceleration vs. time in 600s simulations 112
Figure 126: Nacelle fore-aft acceleration FFT in 600s simulations 112
Figure 127: ATD Demanded pitch angle vs. time in 600s simulations 113
Figure 128: ATD Demanded pitch vs. time in 600s simulations 113
Figure 129: Typical S-N or Wöhler curve 114
Figure 130: Weibull distribution used for load and statistical analysis 115
Figure 131: Blade coordinate system for blade root loads 116
Figure 132: Tower coordinate system for tower base loads 116
Figure 133: Yaw coordinate system for yaw bearing loads 117
Figure 134: Shaft coordinate system for low speed shaft loads 117
Figure 135: Fatigue load analysis spider chart for 600s simulations 118
Figure 136: Notch filter parameter interpretation 120
Figure 137: Bode diagram of the pitch control open loop for Scenario 1 at 19m/s 124
Figure 138: Bode diagram of the closed loop pitch control's S(s) for Scenario 1 at 19m/s 125
Figure 139: Bode diagram of the closed loop pitch control's T(s) for Scenario 1 at 19m/s 125
Figure 140: Bode diagram of the closed loop pitch control's U(s) for Scenario 1 at 19m/s 126
Figure 141: Generated power statistics for Scenario 1 127

Figure 142: Pitch standard deviation for Scenario 1 128
Figure 143: Tower base "y" momentum statistics for Scenario 1 129
Figure 144: Low speed shaft "x" momentum statistics for Scenario 1 129
Figure 145: Fatigue load analysis spider chart for Scenario 1 130
Figure 146: Bode diagram of the pitch control open loop for Scenario 2 at 19m/s 131
Figure 147: Bode diagram of the closed loop pitch control's S(s) for Scenario 2 at 19m/s 131
Figure 148: Bode diagram of the closed loop pitch control's T(s) for Scenario 2 at 19m/s 132
Figure 149: Bode diagram of the closed loop pitch control's U(s) for Scenario 2 at 19m/s 133
Figure 150: Generated power statistics for Scenario 2 133
Figure 151: Pitch standard deviation for Scenario 2 134
Figure 152: Tower base "y" momentum statistics for Scenario 2 135
Figure 153: Low speed shaft "x" momentum statistics for Scenario 2 135
Figure 154: Fatigue load analysis spider chart for Scenario 2 136
Figure 155: Bode diagram of the pitch control open loop for Scenario 3 at 19m/s 137
Figure 156: Bode diagram of the closed loop pitch control's S(s) for Scenario 3 at 19m/s 137
Figure 157: Bode diagram of the closed loop pitch control's T(s) for Scenario 3 at 19m/s 138
Figure 158: Bode diagram of the closed loop pitch control's U(s) for Scenario 3 at 19m/s 138
Figure 159: Generated power statistics for Scenario 3 139
Figure 160: Pitch standard deviation for Scenario 3 139
Figure 161: Tower base "y" momentum statistics for Scenario 3 140
Figure 162: Low speed shaft "x" momentum statistics for Scenario 3 140
Figure 163: Fatigue load analysis spider chart for Scenario 3 141
Figure 164: Bode diagram of the pitch control open loop for Scenario 4 at 19m/s 142
Figure 165: Bode diagram of the closed loop pitch control's S(s) for Scenario 4 at 19m/s 142
Figure 166: Bode diagram of the closed loop pitch control's T(s) for Scenario 4 at 19m/s 143
Figure 167: Bode diagram of the closed loop pitch control's U(s) for Scenario 4 at 19m/s 143
Figure 168: Generated power statistics for Scenario 4 144
Figure 169: Pitch standard deviation for Scenario 4 144
Figure 170: Tower base "y" momentum statistics for Scenario 4 145
Figure 171: Low speed shaft "x" momentum statistics for Scenario 4 145
Figure 172: Fatigue load analysis spider chart for Scenario 4 146
Figure 173: Bode diagram of the pitch control open loop for Scenario 5 at 19m/s 147
Figure 174: Bode diagram of the closed loop pitch control's S(s) for Scenario 5 at 19m/s 147
Figure 175: Bode diagram of the closed loop pitch control's T(s) for Scenario 5 at 19m/s 148
Figure 176: Bode diagram of the closed loop pitch control's U(s) for Scenario 5 at 19m/s 148
Figure 177: Generated power statistics for Scenario 5 149
Figure 178: Pitch standard deviation for Scenario 5 150
Figure 179: Tower base "y" momentum statistics for Scenario 5 150
Figure 180: Low speed shaft "x" momentum statistics for Scenario 5 151
Figure 181: Fatigue load analysis spider chart for Scenario 5 152
Figure 182: Bode diagram of the pitch control open loop for Scenario 6 at 19m/s 153
Figure 183: Bode diagram of the closed loop pitch control's S(s) for Scenario 6 at 19m/s 153
Figure 184: Bode diagram of the closed loop pitch control's T(s) for Scenario 6 at 19m/s 154
Figure 185: Bode diagram of the closed loop pitch control's U(s) for Scenario 6 at 19m/s 154
Figure 186: Generated power statistics for Scenario 6 155
Figure 187: Pitch standard deviation for Scenario 6 155
Figure 188: Tower base "y" momentum statistics for Scenario 6 156
Figure 189: Low speed shaft "x" momentum statistics for Scenario 6 156
Figure 190: Fatigue load analysis spider chart for Scenario 6 157
Figure 191: Wind turbine PLC scheme 163

Index of tables

Table 1: Upwind 5MW model general properties 15
Table 2: Upwind 5MW model blade properties 15
Table 3: Upwind 5MW model hub and nacelle properties 16
Table 4: Upwind 5MW tower properties 16
Table 5: Upwind 5MW model drive train properties 16
Table 6: Upwind 5MW model natural mode frequencies 16
Table 7: Generator torque vs. speed curve parameters 24
Table 8: Supervisory control parameter explanation 54
Table 9: Pitch control parameter explanation 59
Table 10: Torque control parameter explanation 65
Table 11: DTD parameter explanation 68
Table 12: ATD parameter explanation 71
Table 13: Supervisory control parameter values 73
Table 14: DTD parameter values 79
Table 15: Torque Control disturbance sensibility requirements 79
Table 16: Torque control parameter values 86
Table 17: Pitch control parameter values 94
Table 18: ATD parameter values 98
Table 19: Pitch control filtering process study Scenarios 121
Table 20: Pitch control filtering process study Scenarios' parameters 123
Table 21: Filtering process configuration ranking for Scenario 1 158
Table 22: Filtering process configuration ranking for Scenario 2 158
Table 23: Filtering process configuration ranking for Scenario 3 159
Table 24: Filtering process configuration ranking for Scenario 4 159
Table 25: Filtering process configuration ranking for Scenario 5 160
Table 26: Filtering process configuration ranking for Scenario 6 160

Chapter 1: Introduction

1.1. Background

At the end of 2017, over 150 countries in the world had set a target share for renewable energy contribution to the power sector. This, together with the increasing renewable energy regulatory policies in 128 countries, will not only help reduce global warming emissions such as CO_2 and other greenhouse gasses but it will also promote a more sustainable energy system as it will lower the dependence on fossil fuels and other finite resources.

Spain has set a target of 20% of final energy consumption by renewable energy sources by the year 2020. Denmark is the only country in the world whose goal is to have a 100% of the share of renewable energy in final energy by 2050. Developing wind power technology is key to achieve this goal as wind energy is a cost-efficient, nonpolluting source of electricity with a renewable supply. On top of that, it is becoming one of the cheapest energy sources available nowadays.

According to [3], by the end of 2017, the worldwide installed wind power capacity was 539GW. This is 5.73 times the amount installed in 2007. China is, by far, the country with the largest wind power industry (around 1/3 of the world's total capacity).

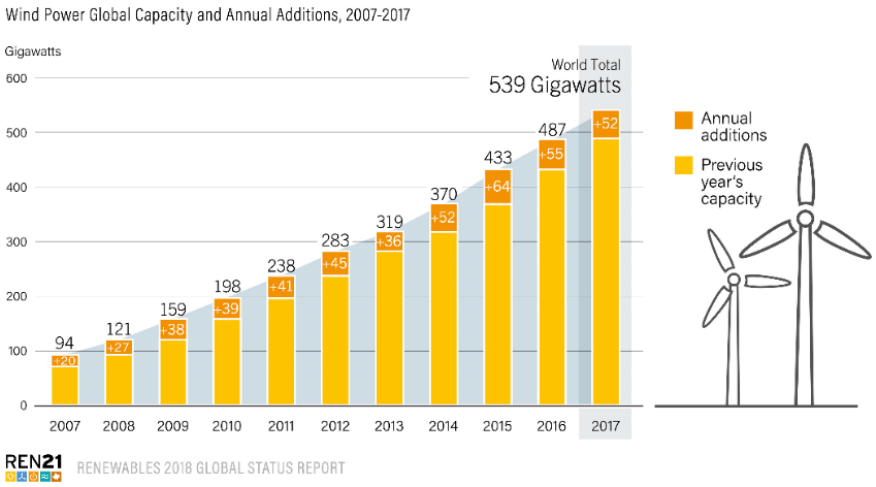

Figure 1: Wind power global capacity and annual additions, 2007-2017

As the wind power industry grows the market is becoming more and more competitive, which forces companies to focus on lowering production costs. This leads to building larger wind turbines aiming for a higher energy capture. This growth translates into larger blades, higher towers, larger drive train torque multipliers… In essence, higher costs.

To keep these costs at competitive levels, optimized designs must be developed. To minimize maintenance costs and ensure efficient energy production, wind turbine control strategies must be implemented.

By acting on the blade pitch angle and the generator torque, these control strategies optimize the energy capture while reducing the wind turbine's structural loads. This is done by increasing the damping of the wind turbine's structural modes such as the drive train mode as well as reducing the tower's fore-aft and side-to-side accelerations, etc.

Another aspect the wind power industry is focused on is improving wind predictions leading to a more reliable and efficient power source. Due to this issue and the stochastic nature of wind,

controllers are designed with the aim of keeping the wind turbines under the desired performance despite the wind conditions.

1.2. Objectives of the study

The aim of this project named "Impact of generator speed filtering process on wind turbine structural loads" is to analyze the effect that changing the parameters of the pitch control filters has on the different loads of the wind turbine.

Once this analysis has been done, an adequate filtering process has been defined depending on the desired objectives and specific needs of each wind turbine and each control strategy.

When pursuing the main objective of this project, several other ones have been fulfilled:

· Learning of an aeroelastic computer-aided engineering code for simulating the dynamic response of wind turbines

· **Discretization** of continuous-time functions and their implementation on Simulink. Creation of a **Simulink library** containing discrete-time filters and a PID

· Learning **linearization** of nonlinear dynamic systems

· Design of classical wind turbine **control strategy** and implementation on **Simulink**

· Control tuning with **sisotool**, a single-input, single-output MATLAB design application for controllers of feedback systems

· Study of the fatigue loads in the wind turbine components and load mitigation analysis when simulating with the control strategy

· Definition of a **guide on generator speed filtering design** depending on the specific load restrictions of each wind turbine and its structural limitations

Chapter 2: Wind turbine fundamentals

2.1. History

The capacity of wind energy has been used by mankind since ancient times. The earliest known use of wind power was in sailboats in Ancient Egypt back in 3.000 a.C. It was not until the seventh century that the first windmills appeared in Persia (Afghanistan) and they did not reach Europe until the twelfth century in France and England. Those windmills were used for mechanical purposes such as grinding corn and flour or pumping water.

The first known wind turbine that was used to produce electricity was built by James Blyth, a Scottish electrical engineer, in 1887. It was a 10m high wind turbine and it was used to charge accumulators to power the lighting of his holiday cottage. That same year, in the United States, professor Charles F. Brush built a 12kW wind turbine with a 17m diameter and 144 blades.

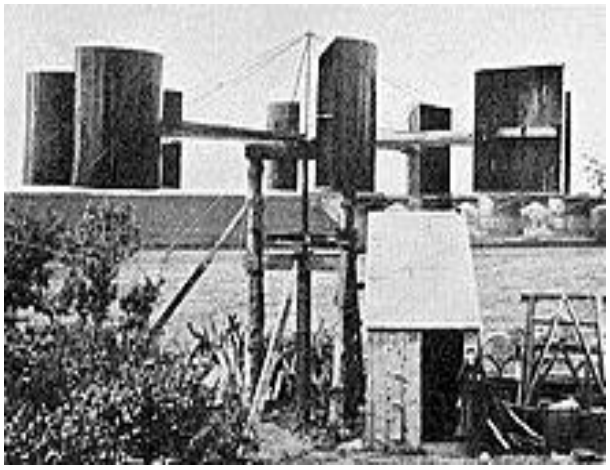

Figure 2: James Blyth's windmill, 1887

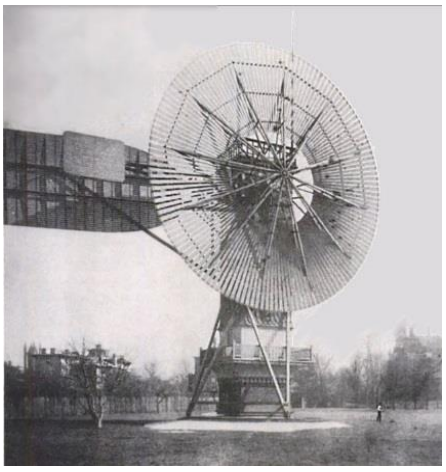

Figure 3: Charles F. Brush 12kW wind turbine, 1887

During the end of the XIX century and beginning of the XX, wind energy did not succeed as a source of electric energy, with the exception of some rural areas. In the 1930's, when power lines where built to transport electricity, it started to decline in those areas too. It was not until the 70's that the oil crisis lead to a greater interest in renewable energies such as wind energy, especially after the arising of movements against nuclear energy during the 80's.

That was when the United States federal and state policies started to encourage the installation, research and development of wind turbines. As well as the United States, other countries economically encouraged wind energy due to its high cost at the time.

The power capacity of these wind turbines went from 100 kW (1931) up to 2MW in the year 2000. By that year, the worldwide wind power installed capacity was 17GW. Nowadays, the total installed capacity in the world is 30 times that, 539 GW total. China, the U.S. and Germany are the top three countries with the largest wind energy market, with over half of the total wind energy capacity installed in the world [3].

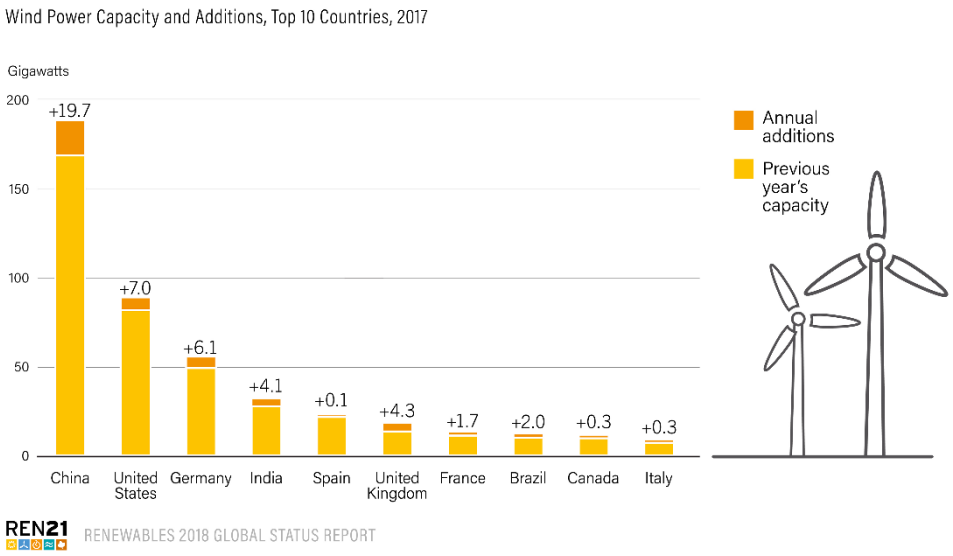

Figure 4: Wind power capacity and additions, 2017

Spain is the fifth county in the world, with a total of 23GW of wind energy installed in 2017, even though the previous 5 years barely 300MW were installed due to country policies. This resulted in the county being the fourth county in the world exporting wind turbines, practically 100% of the ones produced in the country from 2014 to 2017.

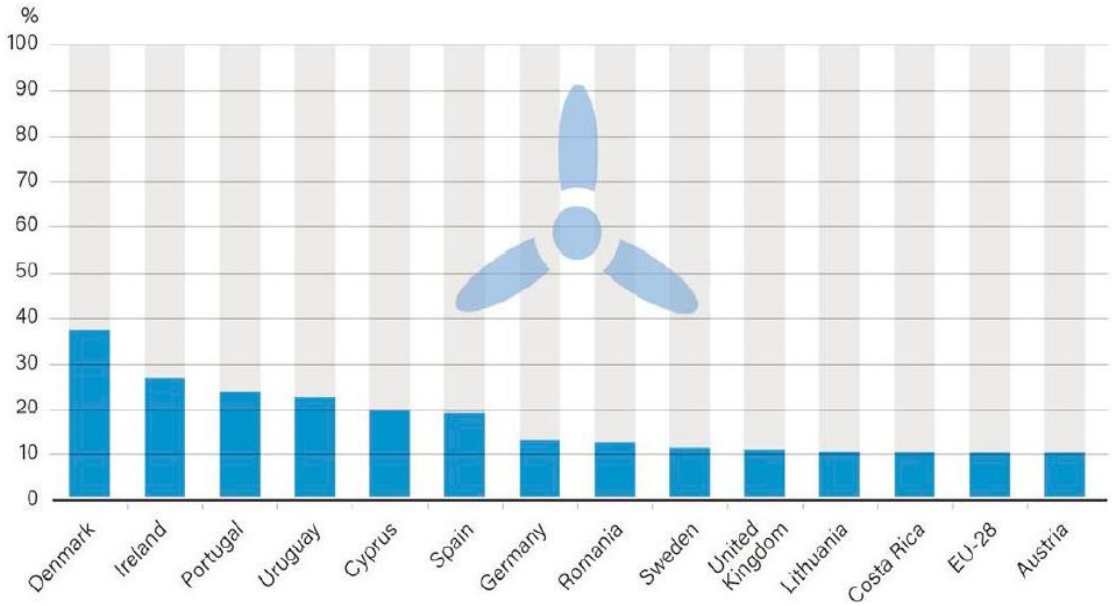

Figure 5: Eolic systems' contribution to the electric demand [4]

Despite of this, the objectives imposed by the UE for countries to have a 20% of their generated power come from renewable sources have forced the installation of wind energy capacity in Spain. Renewable energy auctions that took place in 2016 and 2017 prove that Spain is leading from its 17% of energy generated by renewable source towards the European objectives.

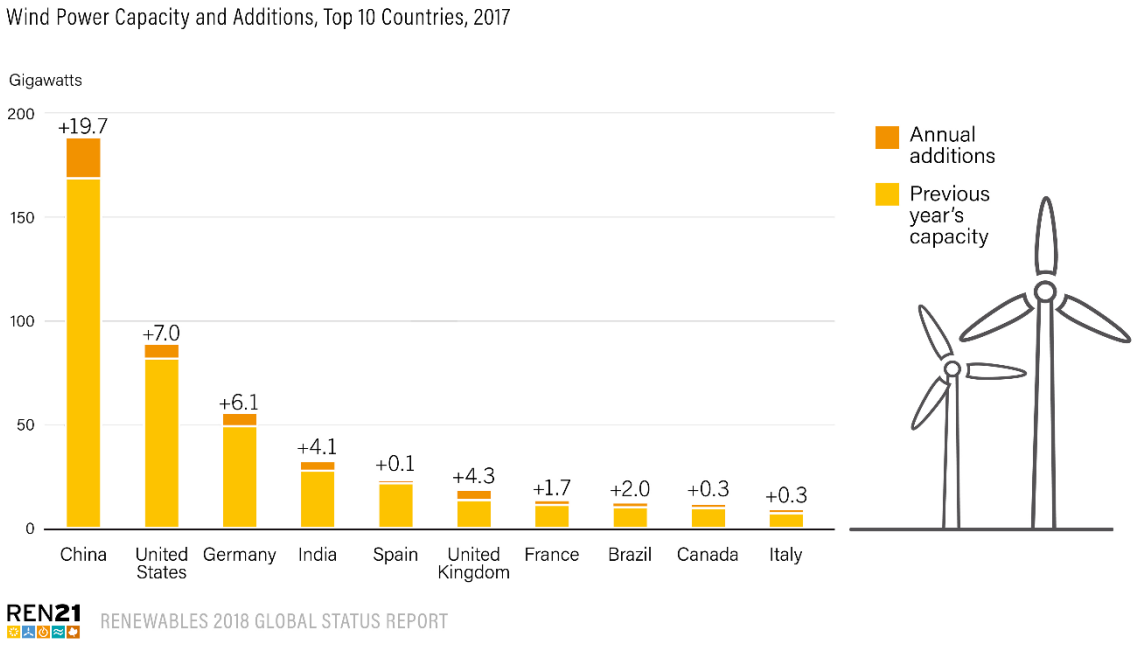

Figure 6: Wind Power Capacity and Additions, Top 10 Countries, 2017

Nowadays, wind energy is a cost-effective source of energy and it is competitive with traditional fossil-fuel energy sources. In Spain, it contributes to lower the final price of energy due to the energy pool.

2.2. Modern wind turbines

In this section the main elements that compose a modern wind turbine are described.

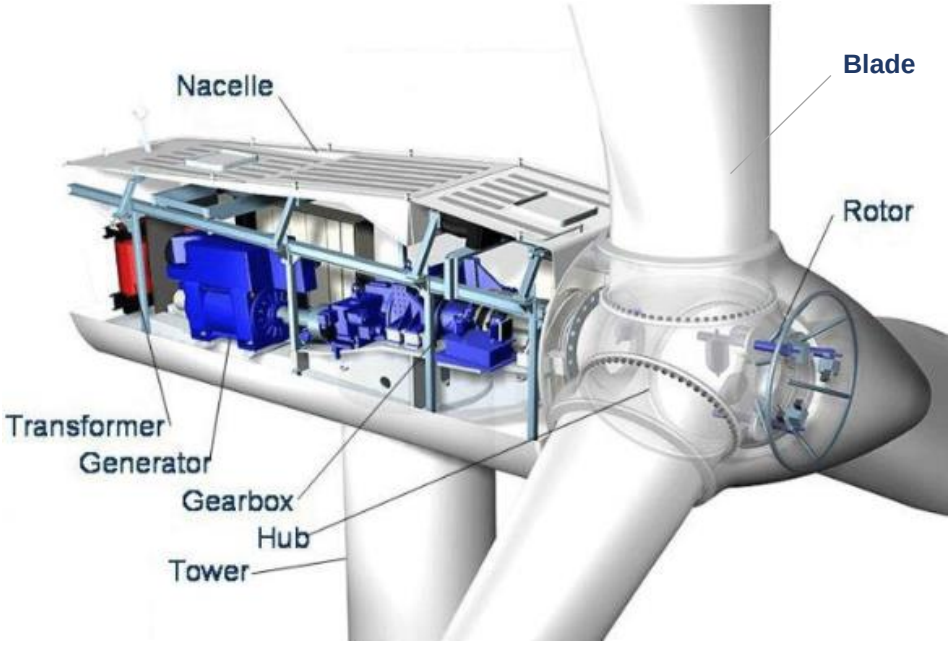

Figure 7: Main elements of a modern wind turbine

2.2.1.Rotor

The wind turbine rotor is composed of the **blades** and the **hub**.

The **hub** is the element that attaches the blades to the nacelle and it is generally made of steel, either welded or cast. There are two types of hub configurations. Depending on if the blades are variable-pitch blades or if there is a passive stall control, the blades will be directly attached to the hub or they will be bolted to the pitch bearing, respectively. In this second configuration there will be a hydraulic pitch actuator.

Figure 8: Wind turbine hub

The **blades** are the element of the wind turbine in charge of capturing the winds energy. When wind flows through them, there are two main forces that appear, **lift** (perpendicular to the wind flow direction) and **drag** (force parallel to wind flow), and they both depend on the angle of attack (angle between the resulting wind direction and the blade profile chord). When designing the blades, a high lift-to-drag ratio must be obtained by using sophisticated aerodynamic principles.

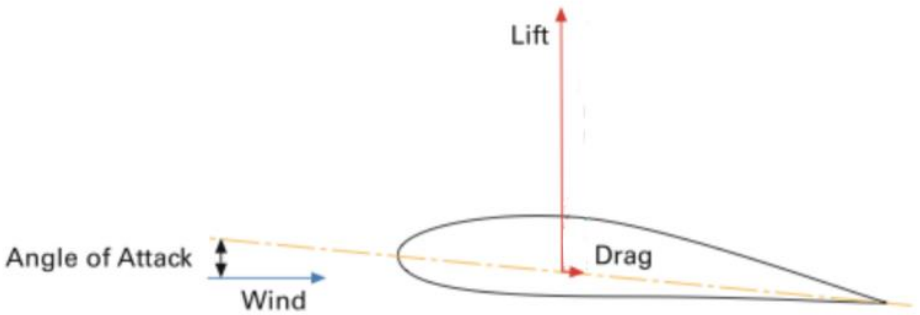

Figure 9: Wind turbine blade profile. Aerodynamic forces

The resultant wind inflow is the sum between the profile's speed and the wind speed. Since the profile's velocity increases as the profile gets further from the hub, the blades are designed with a torsion angle along their longitudinal axis in order to get all the profiles to have an optimum attack angle.

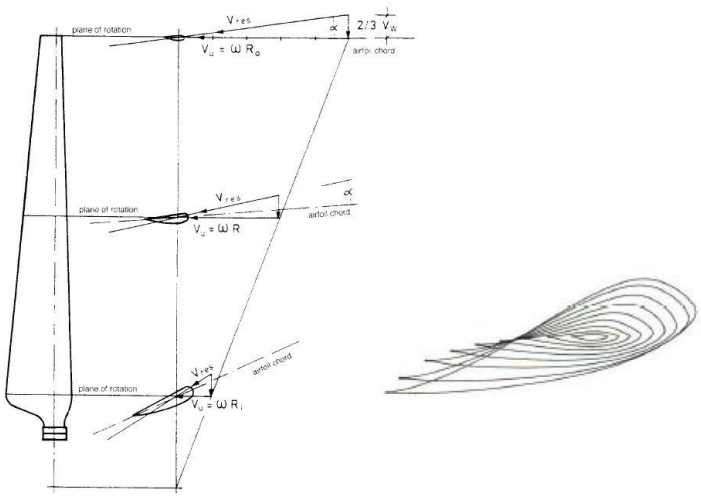

Figure 10: Torsion angle along blade profile

Passive stall control wind turbines (those that do not have variable-pitch control and whose blades are fixed to the hub) have blades whose aerodynamic profile has been designed to gradually decrease the lift force whenever wind speed exceeds a certain limit. This is because when the angle of attack exceeds a certain angle (due to wind speed increasing), turbulence appears and the blades begin to stall.

Variable pitch control, on the other hand, allows changing the blade pitch angle, which will change the angle of attack along the whole blade. This means that the optimal angle of attack can be obtained for each wind speed by changing the blade pitch. As a result, a much higher aerodynamic efficiency is obtained at high wind speeds (wind speeds above rated).

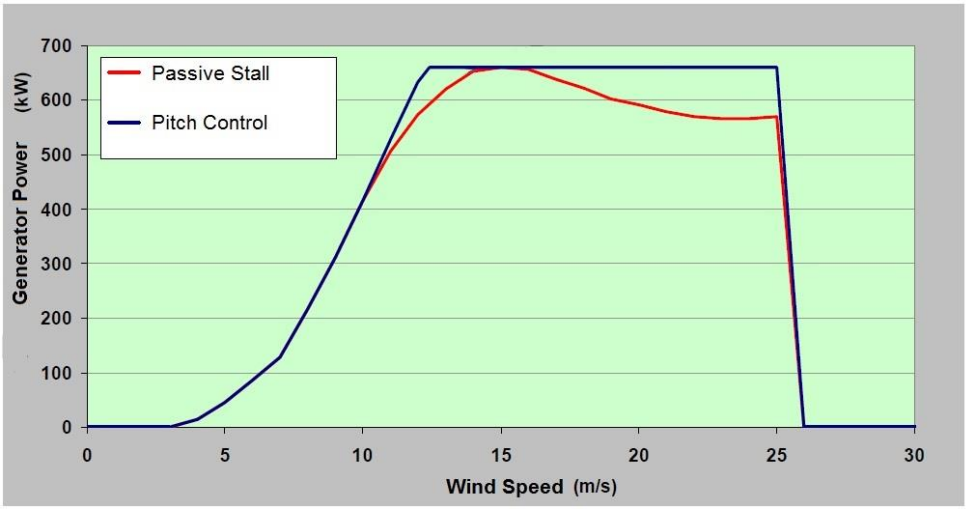

Figure 11: Generator power for passive stall and pitch control wind turbines (kW)

Most commercial wind turbines are three-bladed wind turbines, due to aerodynamic efficiency, that increases with the number of blades. Increasing the number of blades from 1 to 2 gives a 6% increase in aerodynamic efficiency, but increasing the number from 2 to 3 blades would increase a 3%. A higher number of blades would sacrifice the blades' stiffness as they become thinner without a worthy aerodynamic efficiency increase.

Blades are made either with glass or carbon fiber reinforced epoxy or polyester, because the composites between carbon or glass fibers and a resin matrix make a strong, light weighted, corrosion-resistant **composite**.

Figure 12: Wind turbine blade

2.2.2.Nacelle

The **nacelle** sits at the top of the tower and contains the **drive train** of the wind turbine, which transforms mechanical energy into electric energy. The low speed shaft is turned by the rotor and it connects, through the gearbox, to the high speed shaft, which drives the generator.

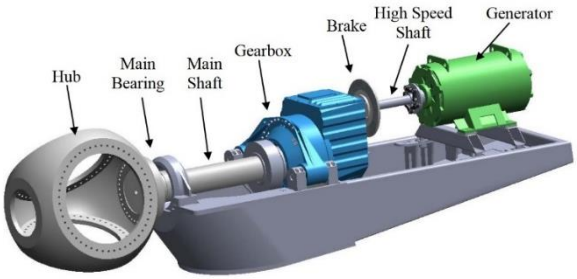

Figure 13: Wind turbine drive train

2.2.3.Tower

The **tower** carries the nacelle and the rotor. At first, for hub heights lower than 50m, lattice steel towers were used. Later, as towers got taller aiming a higher energy capture, the technology developed into **tubular steel**, concrete and hybrid (steel and concrete) towers, the first ones being the most popular.

Figure 14: Lattice tower wind turbine

Figure 15: Tubular steel tower wind turbine

Between the nacelle and the tower there is a **yaw system**, which is responsible for aligning upwind wind turbines towards the wind. Downwind wind turbines, on the other hand, are passively placed facing the wind utilizing the wind's own force. The vast majority of commercial wind turbines have an upwind design.

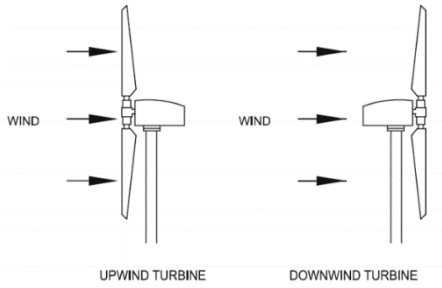

Figure 16: Upwind and downwind wind turbine configurations

2.3. Wind energy

2.3.1. Available power and power coefficient

In order to analyze the available power in wind, a control volume is considered and conservation of mass is applied to it. The mass that flows through the rotor is given by [5]:

$$\dot{m} = \rho \cdot A_1 \cdot U_1 = \rho \cdot A \cdot U = \rho \cdot A_2 \cdot U_2 = const.$$

Where ρ is the wind density (1.225kg/m^3 in standard conditions: 15ºC and sea level), A is the area swept by rotor and U_1 is the wind speed.

Given that the mass flow is constant and wind downstream (U_2) is slower than wind upstream (U_1) due to the wind turbine slowing it down, the area of the control volume downwind (A_2) is bigger than the area upwind (A_1).

This mass flow rate is constant throughout the control volume.

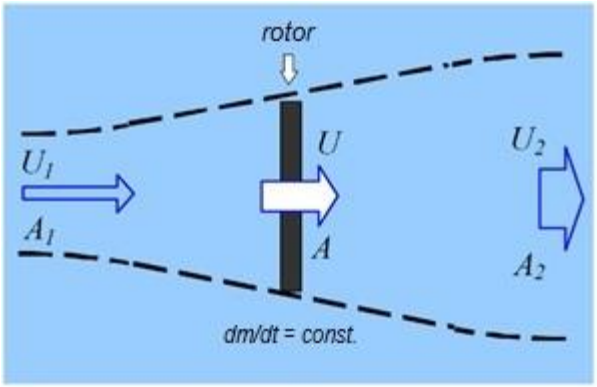

Figure 17: Wind turbine rotor control volume

The available power, which is the power of wind due to its kinetic energy, is:

$$P_d = \frac{1}{2} \cdot \rho \cdot A \cdot U_1^3$$

If a wind turbine was capable of transforming all the kinetic energy of the wind into mechanical energy, the wind particles would stop and would not allow new wind particles to reach the rotor.

Nevertheless, this ideal wind turbine does not exist. Not all the energy in the wind can be captured by the rotor blades. Cp, a coefficient that represents the fraction of power that can be transformed by the blades, is defined.

$$P_c = \frac{1}{2} \cdot \rho \cdot A \cdot U_1^3 \cdot C_p$$

The power captured by the blades is the difference between the incoming power and the power leaving the rotor.

$$P_c = P_1 - P_2 = \frac{1}{2} \cdot \dot{m} \cdot (U_1^2 - U_2^2) = \frac{1}{2} \cdot \rho \cdot A \cdot U \cdot (U_1^2 - U_2^2)$$

Assuming that wind speed decreases linearly through the wind turbine, the wind speed at the rotor is the arithmetic mean of the upstream and downstream speeds.

$$U = \frac{U_1 + U_2}{2}$$

Also, a power coefficient “a” is defined such that:

$$U = U_1 \cdot (1 - a)$$

Then:

$$U_2 = 2U - U_1 = U_1 \cdot (1 - 2a)$$

$$P_c = \frac{1}{2} \cdot \rho \cdot A \cdot U \cdot U_1^2 \cdot (1 - (1 - 2a)^2) = \frac{1}{2} \cdot \rho \cdot A \cdot U \cdot U_1^2 \cdot 4a \cdot (1 - a)$$

$$P_c = \frac{1}{2} \cdot \rho \cdot A \cdot U_1^3 \cdot 4a \cdot (1 - a)^2$$

By deriving this expression with respect to “a” and setting the result to 0, the value of “a” that gives maximum power is obtained:

$$\frac{dP_c}{da} = 0$$

$$\frac{dP_c}{da} = \frac{1}{2} \cdot \rho \cdot A \cdot U_1^3 \cdot \left(4 \cdot (1-a)^2 - 4a \cdot 2 \cdot (1-a)\right) = 0$$

$$a = {}^1/_3$$

Therefore:

$$P_{c\,max} = \frac{1}{2} \cdot \rho \cdot A \cdot U_1^3 \cdot \ 4a \cdot (1-a)^2 = \frac{1}{2} \cdot \rho \cdot A \cdot U_1^3 \cdot \frac{4}{3} \cdot \frac{4}{9}$$

$$P_{c\,max} = \frac{1}{2} \cdot \rho \cdot A \cdot U_1^3 \cdot C_{p\,max} = \frac{1}{2} \cdot \rho \cdot A \cdot U_1^3 \cdot \frac{16}{27}$$

$$C_{p\,max} = \frac{16}{27} = 0.5926$$

This value is called the Betz limit and it is the theoretical maximum efficiency of a wind turbine, 59.26%. Real wind turbines achieve peak Cp values from 0.45 to 0.50, which is about 75 to 85% of the theoretical maximum.

This coefficient depends on the rotor's characteristics and on the tip speed ratio (TSR), λ. Given R blade radius, Ω rotor speed and U_1 wind speed:

$$\lambda = \frac{\Omega \cdot R}{U_1}$$

One of the main characteristics of the wind turbine that affect the Cp is the wind turbine's number of blades.

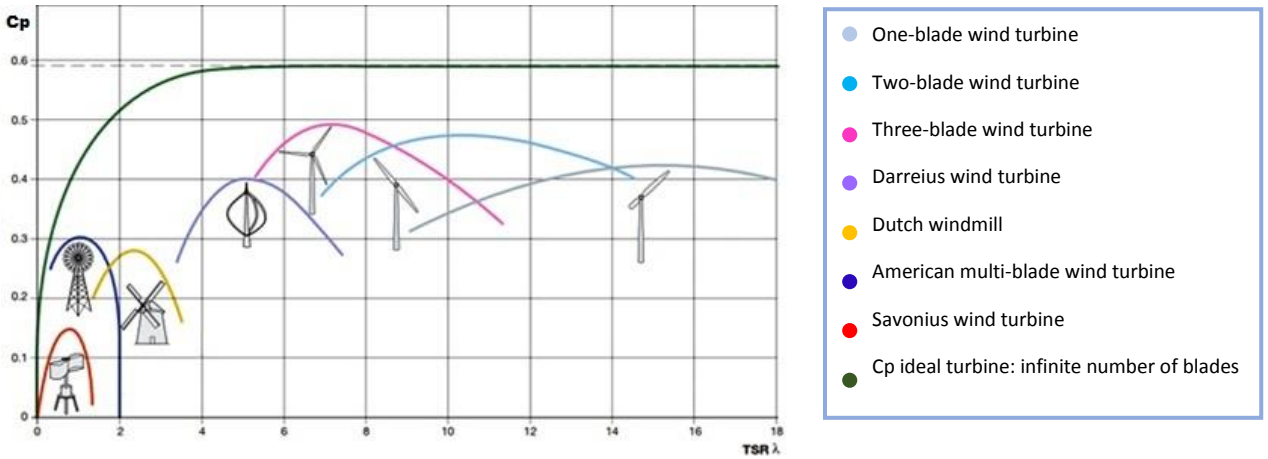

Figure 18: Cp vs tip speed ratio λ

The highest values for Cp are achieved for two and three blade wind turbines. Also, the less blades the wind turbine has, the flatter the Cp vs. λ curve is. This makes it less important for the wind turbine speed to adapt to wind's speed, which translates into a higher energy capture in a bigger range of rotor speeds.

Another parameter of the wind turbine that the Cp has a high dependence on is the blade pitch angle, because of how much the alignment of the blades affects the energy capture of the wind turbine.

Chapter 3: Modelling of the reference wind turbine

3.1. Introduction

In order to design a fitting control strategy for the specific wind turbine that is up for study, a way of analyzing its behavior is needed. Since checking the control's performance in a real wind turbine or in a prototype would be dangerous and highly expensive, a computational model of the wind turbine is needed to proceed with the study the impact of the external conditions on the wind turbine's dynamic behavior.

The aeroelastic model includes the wind turbine's aerodynamics, hydrodynamics, control and electrical system dynamic and structural dynamics and it enables coupled nonlinear simulations of the wind turbine with the control action in the time domain.

This allows the design, linearization and validation of the control model, which are the previous steps to implementing the control strategy in the real wind turbine.

3.2. Upwind 5MW wind turbine modelled in FASTv7 (Simulink Environment)

In this project, the wind turbine model that has been used is that of a 5MW onshore three-bladed wind turbine with horizontal axis. It is placed upwind, which means it has the rotor facing the wind, and it is a variable-speed, pitch-regulated wind turbine. Specifically, the Upwind 5MW baseline model developed by the National Renewable Energy Laboratory (NREL) has been used. The main characteristics of this wind turbine are explained in section 3.3 Upwind 5MW wind turbine model.

The wind turbine has been modeled with the software package FAST, which, along with GH Bladed, is the most used aeroelastic computer-aided engineering modelling tool for wind turbines.

NREL's Upwind baseline model has been chosen because FAST is a free, publicly available code that allows the modelling of the dynamic response of conventional wind turbines as well as obtaining real-time loads of each element of the wind turbine. Also, as this is a public project, it makes it easier for other projects to improve the existing model since FAST does not require a license.

Both [6] and [7] have been used to understand FAST's performance as well as NREL's pre and postprocessors.

FAST models three-bladed HAWTs with 24 degrees of freedom generated from the motions between the different elements of the wind turbine. Also, it models these elements: blades, rotor, tower, generator, drive train dynamics, etc. The wind, on the other hand, is generated by the stochastic, full-field turbulence simulator TurbSim. It is also developed by NREL and it numerically simulates a time series of three-component wind speed vectors according to the norm IEC 61400-1 [8]. To simulate deterministic winds, IEC Winds, also by NREL, is the preprocessor that generates extreme event winds according also to [8].

FAST can run simulations either as a dll (dynamic-link-library) interfaced with Simulink or using the distributed Windows executable program file. This project has been carried out in the former way, through Simulink, due to its ability to incorporate Fortran routines into its models through blocks called S-Functions.

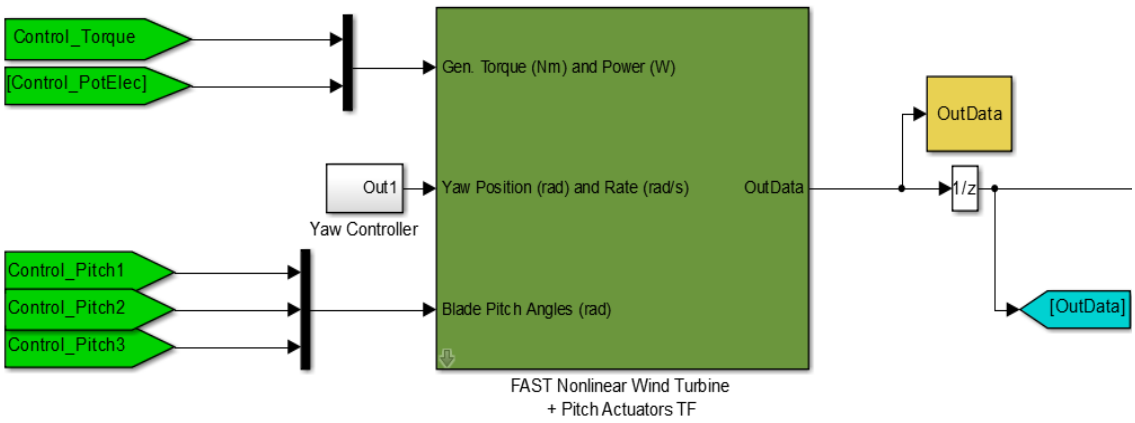

Figure 19: FAST S-Function in Simulink

Yaw, pitch and torque controls can be designed in the Simulink environment and implemented with the nonlinear aeroelastic model of the wind turbine. In the primary input file to FAST, there are several options that determine which (out of pitch, yaw and torque) are controlled by the Simulink model and which ones are not controlled at all.

The control strategy that has been designed in this project does not use yaw control, it regulates generator speed by controlling the generator torque and blade pitch angle. This is done by "measuring" the generator speed and nacelle acceleration to act on the wind turbine as is shown in the next figure.

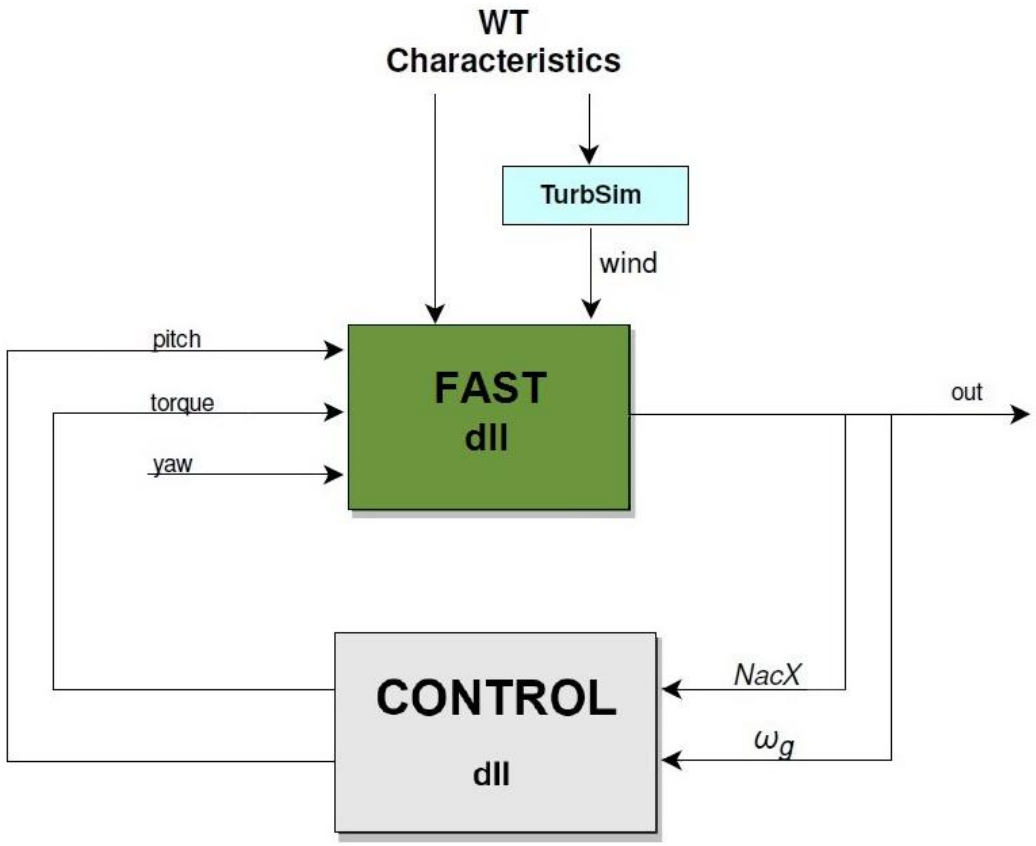

Figure 20: FAST diagram

To simulate, FAST calls for a primary input file (.fst) that includes the operating parameters of the wind turbine as well as its basic geometry. Blade, tower and aerodynamic parameters as well as wind distribution are read from separate text files (.dat, .ipt and .wnd, respectively).

When running time-marching analysis, for each primary input file, the FAST S-Function generates an ASCII output file (.out) that includes time-series data of each parameter that has been requested in the primary input file. During simulation, all of these parameters can be used in-time by Simulink.

3.3. Upwind 5MW wind turbine model

This section includes the characteristics of NREL's onshore 5MW baseline wind turbine model. These specifications are documented in [9] and they go from aerodynamic and structural to control-system properties.

3.3.1. Upwind 5MW wind turbine model characteristics

The next tables reflect the characteristics of the baseline wind turbine, which are introduced to the FAST model through text files.

General Properties	
Power Rating (MW)	5
Configuration	Upwind, 3 Blades
Control	Variable Speed & Collective Pitch
Drivetrain	High-Speed, Multiple-Stage Gearbox
Rotor diameter (m)	126
Hub diameter (m)	3
Hub height (m)	90
Cut-In Wind Speed (m/s)	3
Rated Wind Speed (m/s)	11.4
Cut-Out Wind Speed (m/s)	25
Rated Tip Speed (m/s)	6.9
Rotor mass (kg)	110,000
Nacelle mass (kg)	240,000
Tower mass (kg)	347,460

Table 1: Upwind 5MW model general properties

Blade Properties	
Length (m)	61.5
Mass (kg)	17,740
2nd Mass Moment of Inertia	11,776,047
1st Mass Moment of Inertia	363,231
Structural Damping Ratio (%)	0.477465

Table 2: Upwind 5MW model blade properties

Hub and Nacelle Properties	
Elevation of Yaw Bearing above Ground (m)	87.6
Vertical Distance along Yaw Axis from Yaw Bearing to Shaft (m)	1.96256
Distance along Shaft from Hub Center to Yaw Axis (m)	5.0191
Distance along Shaft from Hub Center to Main Bearing (m)	1.912
Hub Mass (kg)	56,780
Hub Inertia about Low-Speed Shaft ($kg \cdot m^2$)	115,926
Nacelle Mass (kg)	240,000
Nacelle Inertia about Yaw Axis ($kg \cdot m^2$)	2,607,890
Nominal Nacelle-Yaw Rate (º/s)	0.3
Yaw Actuator Natural Frequency (Hz)	3

Table 3: Upwind 5MW model hub and nacelle properties

Drivetrain Properties	
Rated Rotor Speed (rpm)	12.1
Rated Generator Speed (rpm)	1173.7
Gearbox Ratio	97:1
Electrical Generator Efficiency	94.40%
Generator Inertia about High-Speed Shaft ($kg \cdot m^2$)	534
Fully-Deployed High-Speed Shaft Brake Torque (N·m)	28,116
High-Speed Shaft Brake Tme Constant (s)	0.6

Table 5: Upwind 5MW model drive train properties

Tower Properties	
Height above Ground (m)	88
Mass (kg)	347,460
Structural-Damping Ratio of All Modes	1%

Table 4: Upwind 5MW tower properties

Description	FAST Natural Frequency (Hz)
1st Tower Fore-Aft	0.28
1st Tower Side-to-Side	0.28
1st Drivetrain Torsion	1.645
2nd Tower Fore-Aft	3.045
2nd Tower Side-to-Side	2.86
Non-structural rotational 1P	0.2
Non-structural rotational 3P	0.6
In-plane 1st collective	3.685
In-plane 2nd collective	7.605

Table 6: Upwind 5MW model natural mode frequencies

These natural frequencies are the wind turbine model's structural modes for a certain operation point. Some of these frequencies vary with the wind, which is why these frequencies are usually shown in a Campbell diagram, where the variation of the mode's frequencies is shown with respect to wind speed.

Next, the Campell diagram of the Upwind 5 MW baseline wind turbine model is shown. This diagram is extracted from [10].

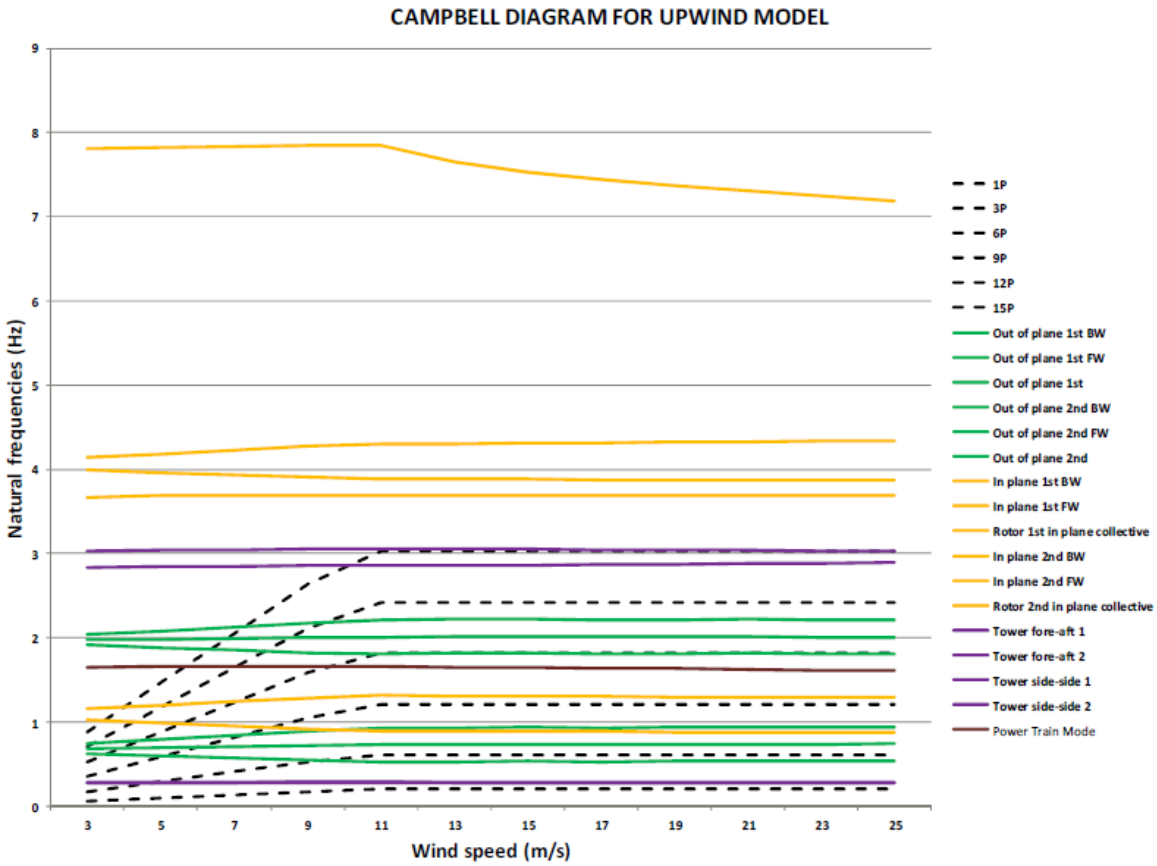

Figure 21: Campbell diagram of the 5MW Upwind baseline model

This diagram illustrates the variation of the wind turbine's modes with the wind speed. It can be observed how the non-structural rotational frequencies are the ones that vary the most at low wind speeds. This is because they depend on the rotor speed, which is why they stay constant once the wind speed exceeds the rated wind speed which, in this wind turbine, is 11.4m/s.

The frequencies that vary the most with wind speed (with generator rotational speed, actually) are the nonstructural rotational 1P and 3P frequencies, also known as blade passing frequencies. The 1P frequency corresponds to a certain blade's whole revolution, while the 3P frequency is the frequency at which any blade passes through the tower. This means that the 1P frequency matches the rotational frequency of the rotor and that the 3P frequency is three times bigger.

3.3.2.Upwind 5MW wind turbine model coordinate systems

When load or motion outputs are required from FAST, they are referred to a different coordinate system depending on what element they belong to. The next figures show the different coordinate systems that are stablished in the FAST code.

Tower-Base Coordinate System

It is fixed to the base platform. It rotates and translates with it.

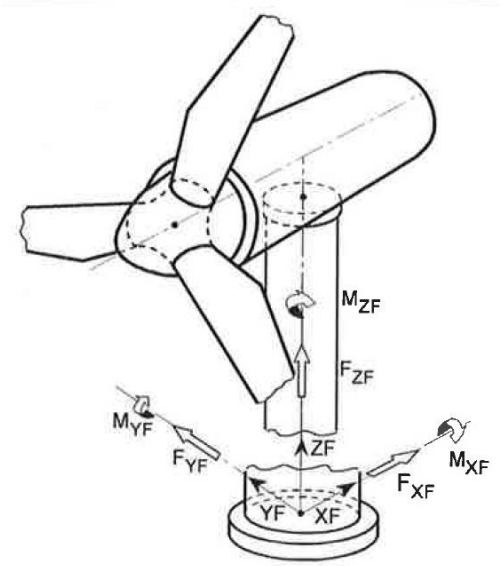

Figure 22: Tower-Base Coordinate System

Tower-Top Coordinate System

It is fixed to the top of the tower. It rotates and translates with the platform and with the tower bending. It does not yaw with the nacelle.

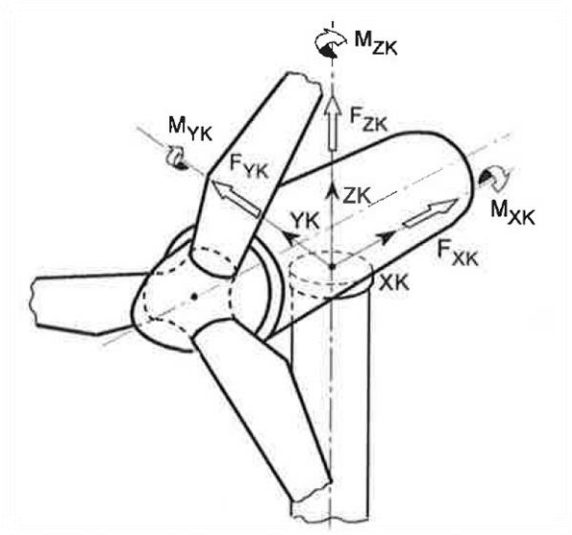

Figure 23: Tower-Top Coordinate System

Nacelle or Yaw Coordinate System

It rotates and translates with the top of the tower and it yaws with the nacelle.

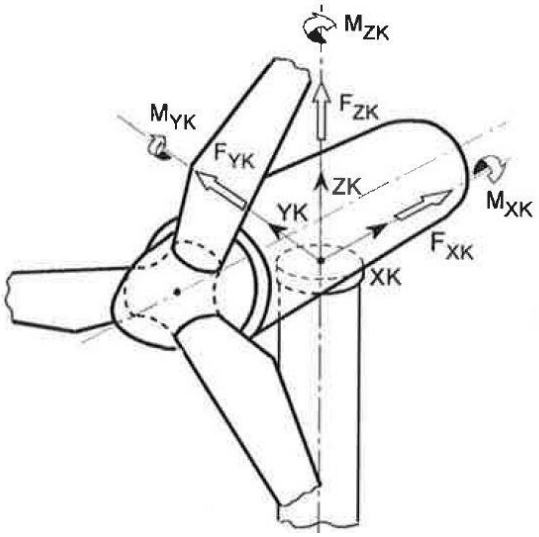

Figure 24: Nacelle or Yaw Coordinate System

Hub Coordinate System

It rotates with the rotor.

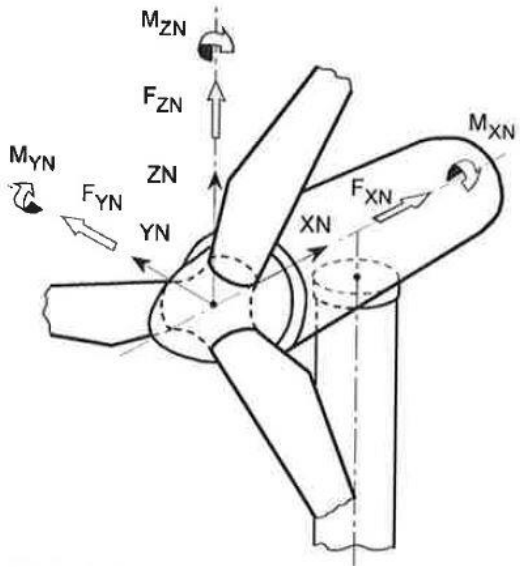

Figure 25: Hub Coordinate System

Coned Coordinate System

There is one for each blade. It rotates with the rotor. It does not pitch with the blades.

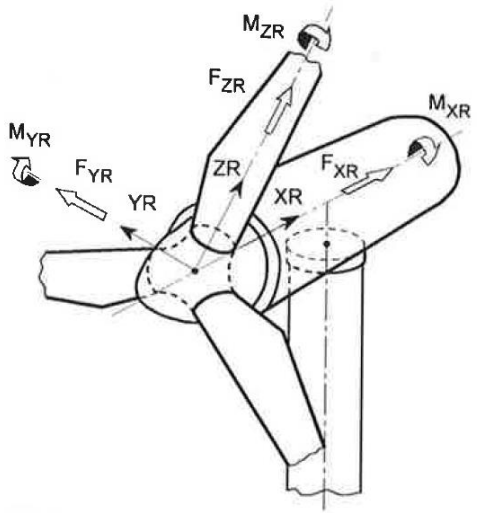

Figure 26: Coned Coordinate System

Blade Coordinate System

They are the same as the coned coordinate systems except that they pitch with the blades and have their origins at the blade root.

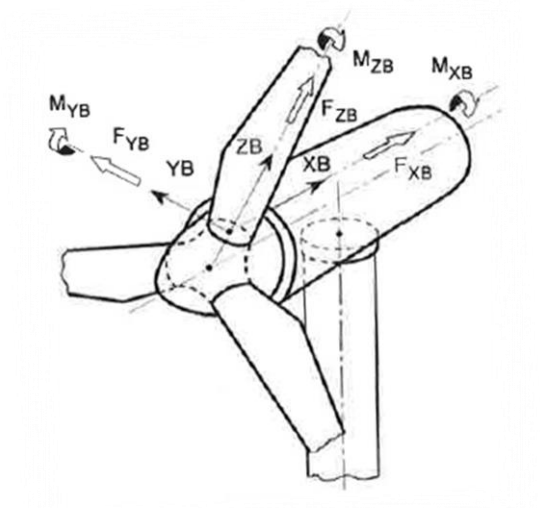

Figure 27: Blade Coordinate System

3.4. Linearization process in FASTv7

When designing and validating the control strategy, a linearized model is necessary. As well as time-series simulations, FAST is capable of performing a linearization of the aeroelastic nonlinear wind turbine model. It is done in two steps. First, a steady state operating point must be determined, this is, setting the values of the control signals, wind, the system's DOFs: displacements, velocities, accelerations, loads, etc. that conform a time invariant model. Next, output state matrices can be obtained by numeric linearization of the FAST model around this equilibrium point.

Since linearizing is done around a static operating point, the obtained state matrices are only accurate when the system is working near the values of the system's parameters that are close to that of the operation point. The further the parameters are from those of the static operating point, the worse the approximation will be.

The files FAST uses to carry out the linearization (.dat, .ipt and .fst) are the same files that FAST needs to perform time-marching analysis. The primary input file (.fst) includes a parameter that must be changed in order to call for the linearization instead of the simulation. Some other parameters need to be changed too, especially because FAST does not linearize while using Simulink, which means it is necessary to switch from Simulink's implemented control to simple internal FAST control while linearizing.

During linearization, FAST generates several output files (.fsm, .opt and .lin). The state matrices of the nonlinear plant can be computed from the latter.

In the primary input file, initial conditions of the steady state operating point can be added too, as well as the linearization parameters. This helps FAST converge to the solution when performing the numerical linearization.

When calling FAST for linearization, one DOF must be enabled to let FAST find the steady state operating point by numerical iteration. When linearizing about an operating point situated in the above rated zone (over 11.4m/s), a constant (rated) torque has been set in the primary input file to let FAST numerically find the pitch angle, the only DOF. When linearizing around a point in the below rated zone, FAST is called to linearize with a constant pitch (minimum pitch) and variable torque has been enabled to let FAST find the torque value for that operating point.

In this project, the wind turbine model has been linearized at every odd wind speed from 5m/s to 25m/s:

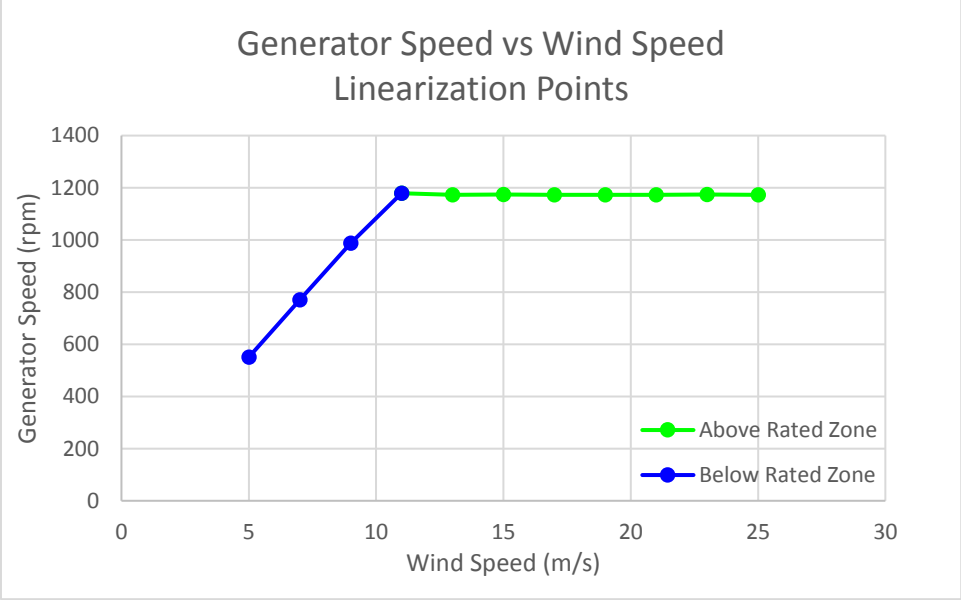

Figure 28: Generator speed vs. wind speed linearization points

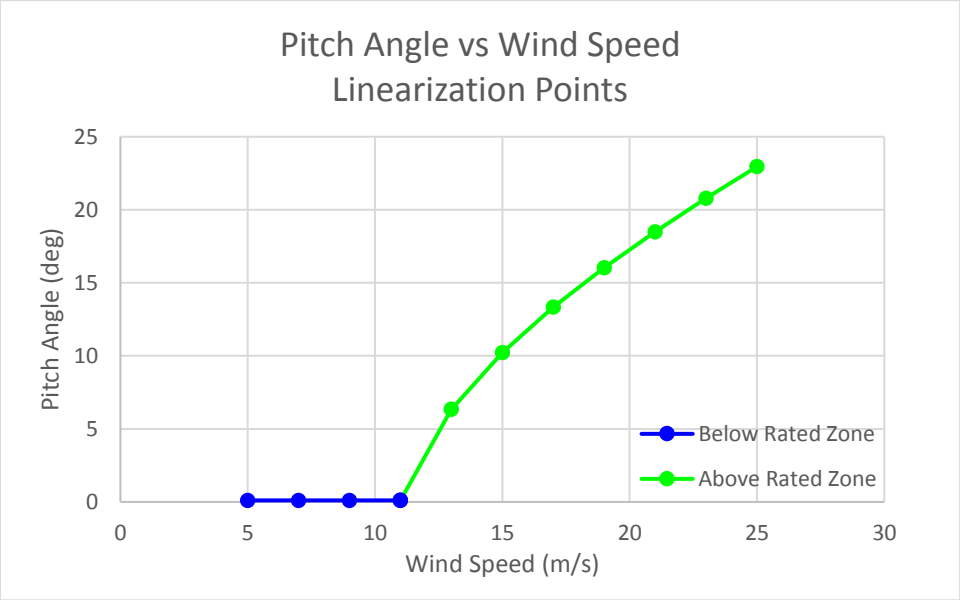

Figure 29: Pitch angle vs. wind speed linearization points

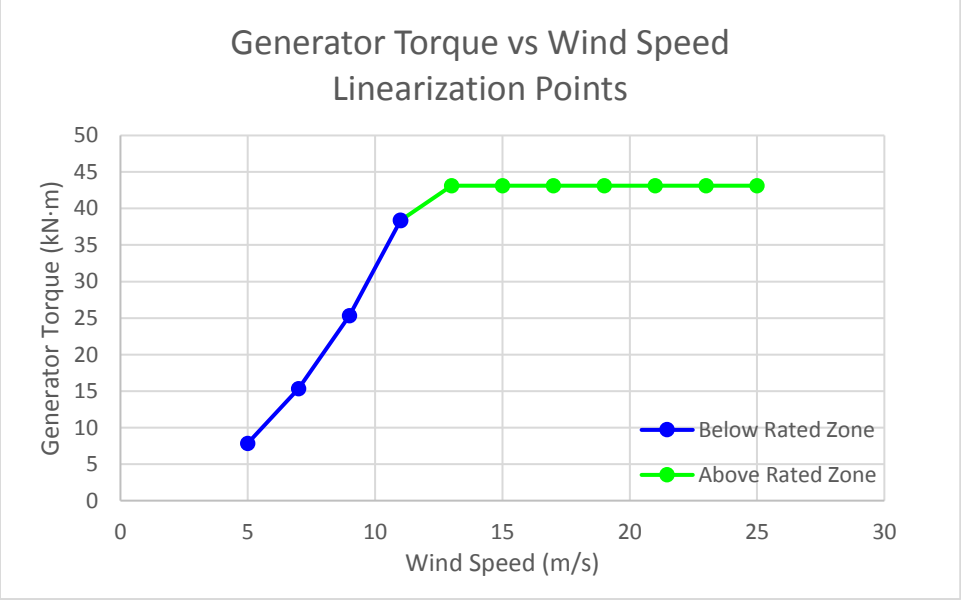

Figure 30: Generator torque vs. wind speed linearization points

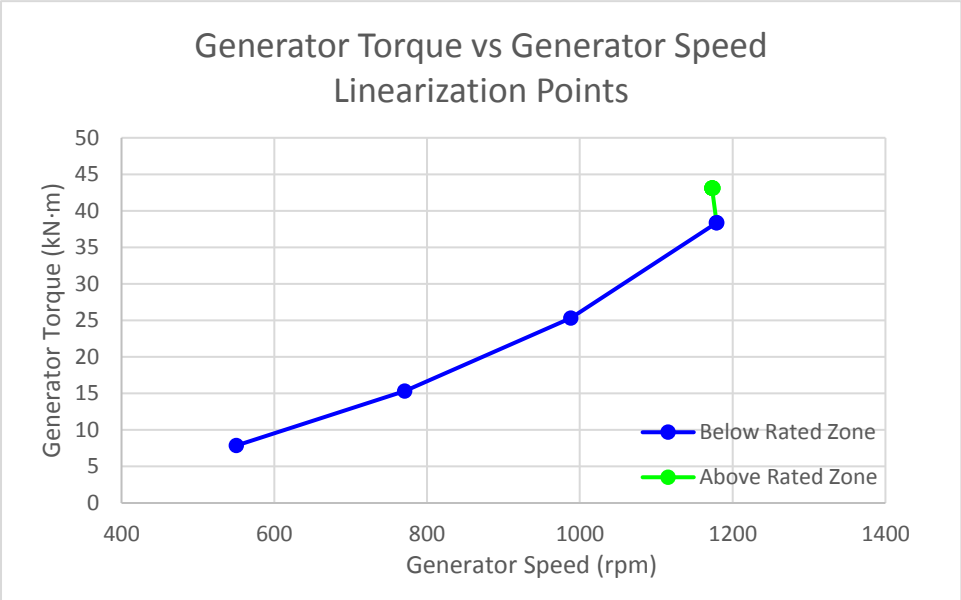

Figure 31: Generator torque vs. generator speed linearization points

At 3 m/s, FAST is unable to perform a linearization as it does not converge to a solution. This is because 3m/s is the UPWIND model's cut-in wind speed. Therefore, the linearizations have been done starting at 5m/s. The 1st torque vertical does not appear in the Generator Torque vs. Generator Speed curve because it starts at wind speeds above the cut-in speed and it goes up to 5m/s.

Chapter 4: Wind Turbine Simulink Controller Block

4.1. Introduction

In this section, the design process of the project's controller block is explained. When designing a control strategy for a wind turbine, two main objectives are pursued:

· Maximization of the energy capture at each wind speed

· Reduction of the wind turbine's structural loads

In order to achieve the first objective, **power control**, two control loops are designed:

· **Pitch control loop**

· **Torque control loop**

The second listed objective, **load reduction**, is achieved by the design of filters that give damping to those wind turbine modes that are overexcited. Two control blocks are designed with the aim of reducing structural loads:

· **DTD** (Drive Train Damping filter)

· **ATD** (Active Tower Damping)

Depending on the operating point of the wind turbine (wind speed, generator torque, generator speed…) different blocks and loops will be acting at the same time. The overall control scheme designed in this project is shown in the next figure.

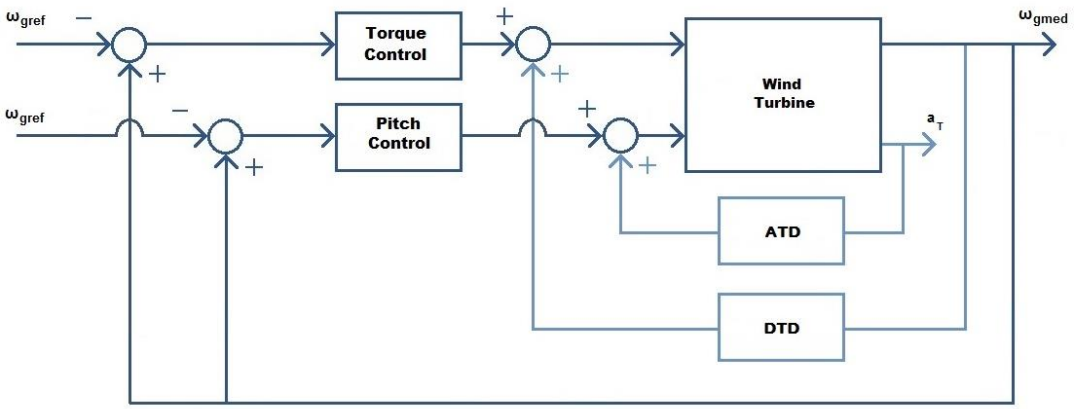

Figure 32: Scheme of the control loops and active control strategies

The control strategy of this project is based on [1] and the design has been done separately depending on the zones that appear on the 5MW Upwind turbine model's torque to generator speed curve shown next.

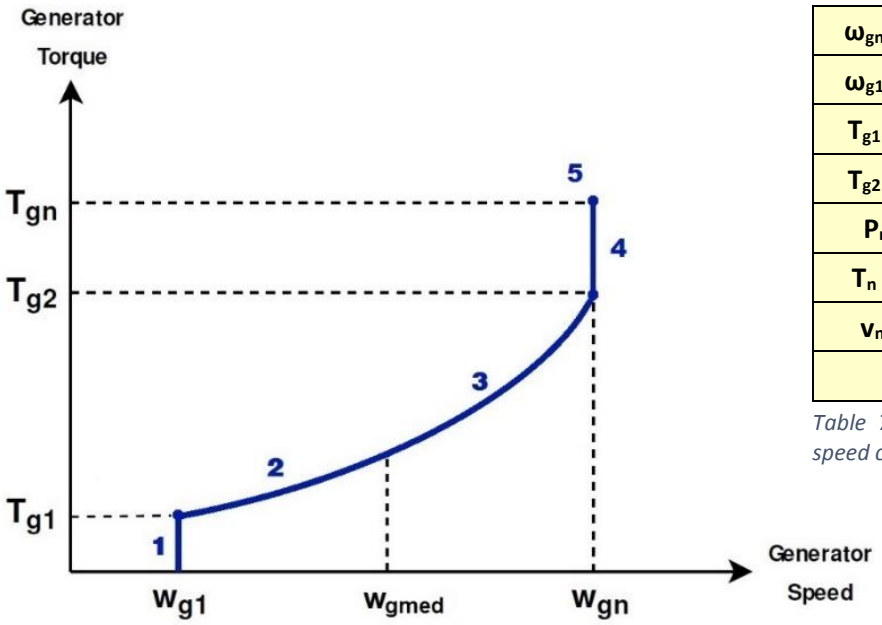

Figure 33: Generator torque to generator speed curve

ω_{gn} (rad/s)	122.9
ω_{g1} (rad/s)	41.88
T_{g1} (kN·m)	4.091
T_{g2} (kN·m)	35.23
P_n (kW)	5000
T_n (kN·m)	43.10
v_n (m/s)	11.40
K_{opt}	2.332

Table 7: Generator torque vs. speed curve parameters

4.2. Control library

4.2.1. Introduction

Before the design of the controller block, a control library is created in Simulink. This library contains all the block functions that are necessary to build the control loops. This way, every time a new block is needed, it can be copied from the library.

This library allows changing the blocks and updating them in the control model. This way, if any changes need to be made in the blocks or anything needs to be added, they will be done in the library and they will automatically update in all the existing blocks in the model.

The blocks created for the control library are: 1st order low pass filter, 2nd order low pass filter, high pass filter, band pass filter, notch filter and a PID block.

4.2.2. Discretization

Since the control block will be implemented into a computer, these blocks are taken in their continuous-time form and they are discretized to a digital, discrete-time approximation.

The continuous-time control design can be made because the system will have a small enough sample time (T_s = 0.01s). This means it can be assumed that the real discrete control will behave the same way as the continuous-time designed control does.

The requirement for this assumption to be true is for the sampling frequency (w_s) to be bigger than the fastest perceivable frequency (w_c) of the signals that appear in the system. Particularly, the sampling frequency must be bigger than twice that frequency: $w_s > 2 \cdot w_c$. This is stated in Shannon's Theorem for signal reconstruction and it is the minimum frequency that allows the correct reconstruction of the original signal.

Given this sample time (T_s = 0.01s), and starting from the continuous-time Laplace transform (s) of the blocks, different discretization methods (either Tustin or Euler) are used to reach the discrete-time Fourier transform (z) of the blocks. Then, the Fourier transform is expressed in sequential terms (k).

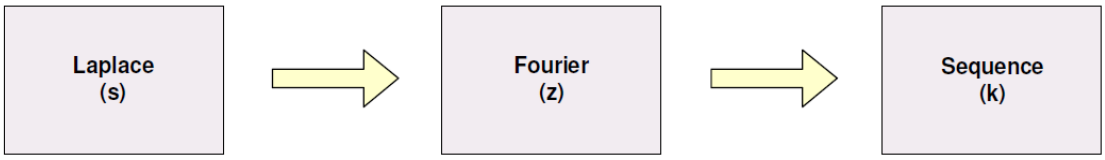

Figure 34: Discretization diagram

The discretization methods that have been used to convert the Laplace transforms into Fourier transforms are Tustin and Euler methods.

$$\textbf{\textit{Tustin}}: \quad s = \frac{2}{T} \cdot \frac{z-1}{z+1}$$

$$\textbf{\textit{Euler}}: \quad s = \frac{z-1}{z \cdot T}$$

With these methods the continuous-time Laplace transfer function,

$$\frac{Y(s)}{U(s)}$$

is transformed into a discrete-time one:

$$\frac{Y(z)}{U(z)}$$

The next step is the translation of this function into a sequential form. This is done by:

$U(z) \equiv u_k$	$Y(z) \equiv y_k$
$U(z) \cdot z^{-1} \equiv u_{k-1}$	$Y(z) \cdot z^{-1} \equiv y_{k-1}$
...	...
$U(z) \cdot z^{-n} \equiv u_{k-n}$	$Y(z) \cdot z^{-n} \equiv y_{k-n}$

u_k being the input to the block at instant k, u_{k-1} being the input at instant k-1, etc.

y_k being the output to the block at instant k, y_{k-1} being the output at instant k-1, etc.

The next sections explain each discrete-time block in the control library and their discretization.

4.2.3. 1st order Low Pass filter

$$LowPass1st\ (s) = \frac{k}{\tau \cdot s + 1}$$

This block lets input signals with frequencies under its cutoff frequency go through it and it attenuates the frequencies over this cutoff frequency. This frequency is defined as that where the filter gain is at -3dB, which corresponds to a gain of 0.7079.

As it is a 1st order filter, it attenuates the frequencies above its cutoff frequency at a smaller rate than a 2nd order filter does.

By setting the filter gain k=1 and the filter time constant τ = 1.55 seconds, the filter's cutoff frequency is set to ω_c = 0.1Hz. This filter's Bode diagram is shown next:

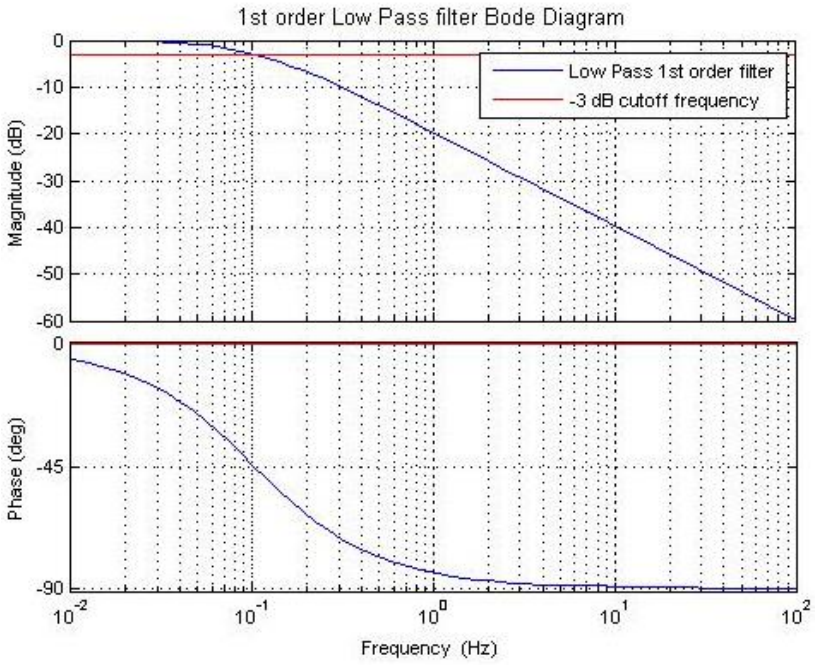

Figure 35: 1st order low pass filter Bode diagram

When entering a chirp signal (this signal increases its frequency as time increases and has unitary gain) the filter's behavior can be shown and compared to a continuous time 1st order filter:

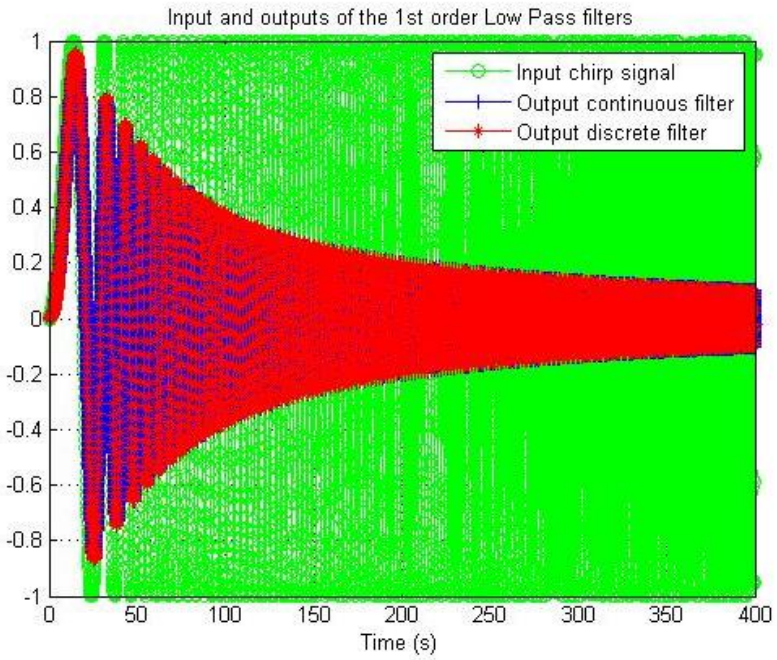

Figure 36: 1st order low pass continuous filter vs. discrete filter

The previous figure shows how the discrete-time filter behaves just like the continuous-time one as it attenuates high frequencies and lets the low ones pass through.

Next, the discretization of the filter is explained.

Laplace transform:

$$LowPass1st\ (s) = \frac{Y(s)}{U(s)} = \frac{k}{\tau \cdot s + 1}$$

Discretization method:

$$Tustin: \qquad s = \frac{2}{T} \cdot \frac{z-1}{z+1}$$

Discrete-time filter:

$$y_k = \frac{kT \cdot u_k + kT \cdot u_{k-1} - (T - 2\tau) \cdot y_{k-1}}{(2\tau + T)}$$

This is the discrete-time 1st order low pass filter that has been implemented in Simulink.

4.2.4. 2nd order Low Pass filter

$$LowPass2nd\ (s) = \ k \cdot \frac{\omega_{np}^2}{s^2 + 2\xi_p\omega_{np}s + \ \omega_{np}^2}$$

Just like the 1st order low pass filter, this filter attenuates high frequencies and lets the low frequencies pass through. This filter will attenuate at a higher rate, as it is a 2nd order filter.

By setting a unitary filter gain, unitary natural frequency and unitary damping, k=1, ξ_p=1 and ω_{np}=1, the cutoff frequency of the 2nd order filter is ω_{np} = 0.1Hz.

The Bode diagram of the filter, along with one of a 1st order filter with the same cutoff frequency is shown next:

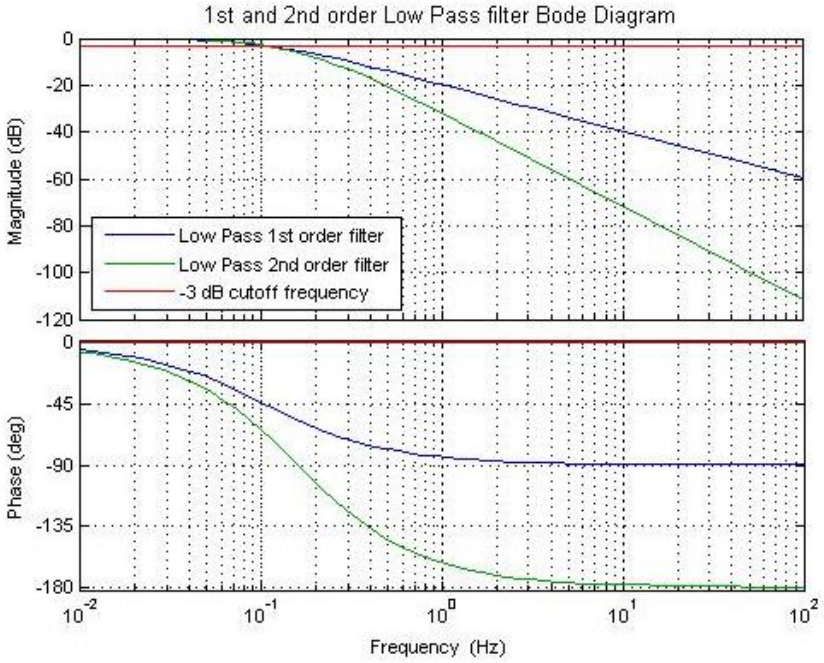

Figure 37: 1st and 2nd order filter Bode diagram

The figure displays how the 2nd order filter attenuates the input signal at -40dB/decade and the 1st order filter attenuates at -20dB/decade.

The behavior of the 2nd order filter is also compared to a continuous-time 2nd order filter by entering a chirp signal to both of them:

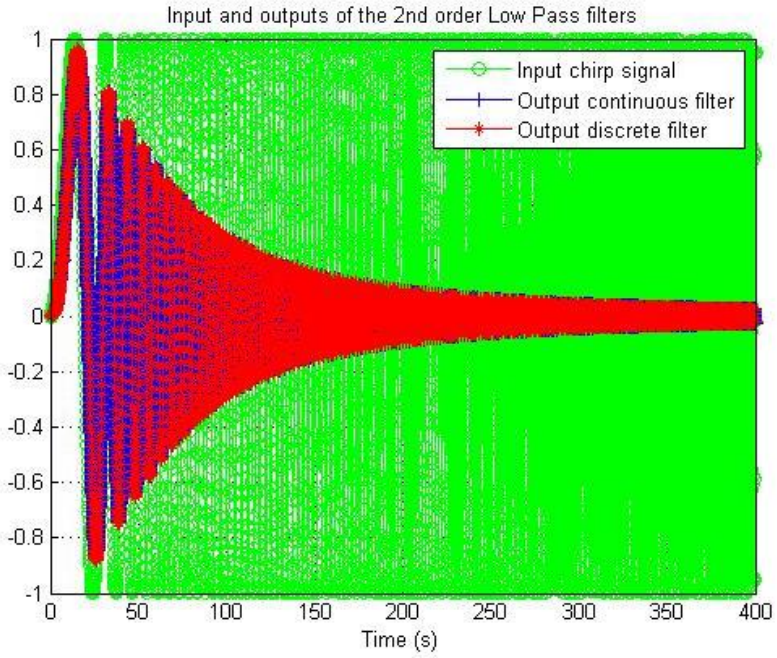

Figure 38: 2nd order low pass continuous filter vs. discrete filter

The image shows how the discrete-time filter behaves like the continuous-time one and, by comparing it to the previous chirp signal, the attenuation difference between 1st and 2nd order filters is shown next.

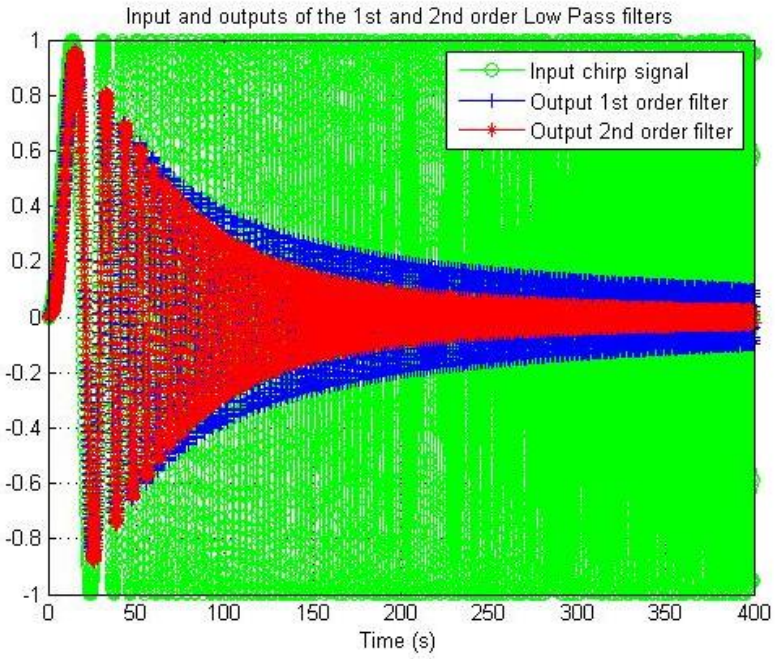

Figure 39: 1st and 2nd order low pass filter attenuation comparison

Next, the discretization of the filter is explained.

Laplace transform:

$$LowPass2nd\ (s) = \frac{Y(s)}{U(s)} = \ k \cdot \frac{\omega_{np}^2}{s^2 + 2\xi_p\omega_{np}s + \ \omega_{np}^2}$$

Discretization method:

$$Tustin: \qquad s = \frac{2}{T} \cdot \frac{z-1}{z+1}$$

Discrete-time filter:

$$y_k = \frac{(kT^2\omega_{np}^2) \cdot u_k + (2kT^2\omega_{np}^2) \cdot u_{k-1} + (kT^2\omega_{np}^2) \cdot u_{k-2}}{\left(4\xi_p\omega_{np}T + 4 + T^2\omega_{np}^2\right)}$$

$$\frac{\left(8 - 2T^2\omega_{np}^2\right) \cdot y_{k-1} + \left(4\xi_p\omega_{np}T - 4 - T^2\omega_{np}^2\right) \cdot y_{k-2}}{\left(4\xi_p\omega_{np}T + 4 + T^2\omega_{np}^2\right)}$$

This is the discrete-time 2nd order Low Pass filter that has been implemented in Simulink.

4.2.5.High Pass

$$HighPass2nd\ (s) = \ \ k \cdot \frac{s^2}{s^2 + 2\xi_p\omega_{np}s + \ \omega_{np}^2}$$

This filter allows high frequencies to pass through it and it attenuates low frequencies. It is the opposite of a low pass filter.

The Bode diagram of a high pass filter with unitary gain, unitary damping and unitary frequency is shown:

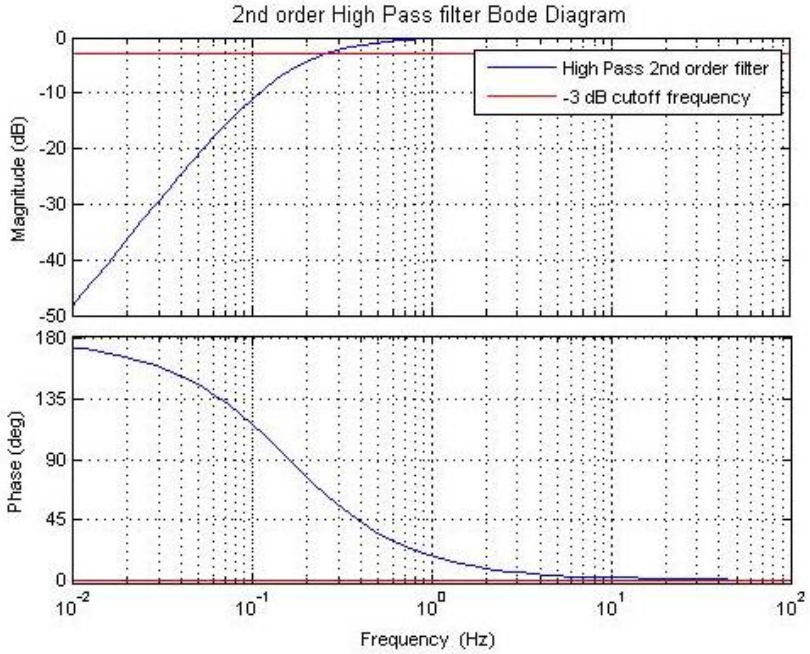

Figure 40: 2nd order high pass filter Bode diagram

The behavior of the discrete filter compared to a continuous-time high pass filter is shown with the input of a chirp function:

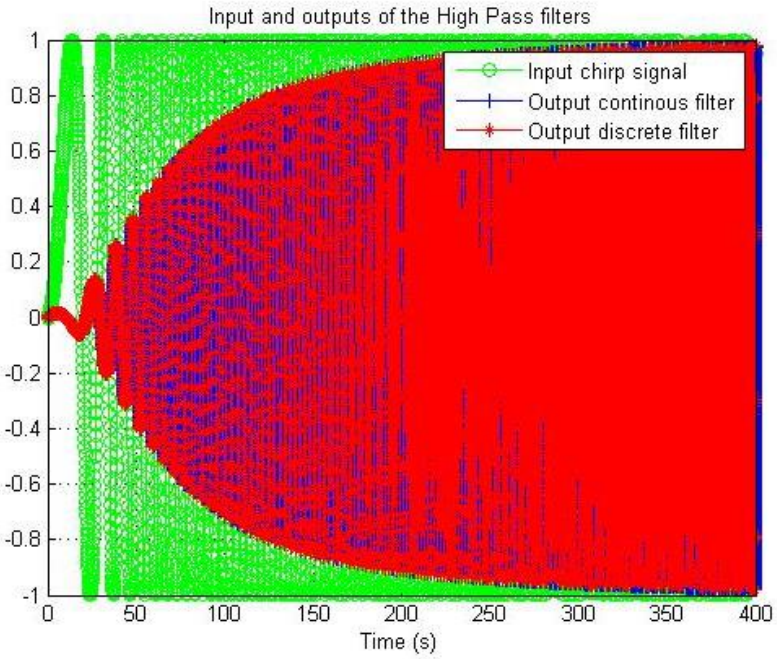

Figure 41: 2nd order high pass continuous filter vs. discrete filter

The figure shows how only the high frequencies go through the filter without getting attenuated.

Next, the discretization of the filter is explained.

Laplace transform:

$$HighPass2nd\ (s) = \frac{Y(s)}{U(s)} = \ k \cdot \frac{s^2}{s^2 + 2\xi_p \omega_{np} s + \ \omega_{np}^2}$$

Discretization method:

$$Tustin: \qquad s = \frac{2}{T} \cdot \frac{z-1}{z+1}$$

Discrete-time filter:

$$y_k = \frac{4k \cdot u_k - 8k \cdot u_{k-1} + 4k \cdot u_{k-2} + \left(8 - 2T^2\omega_{np}^2\right) \cdot y_{k-1} + \left(4\xi_p \omega_{np} T - 4 - T^2\omega_{np}^2\right) \cdot y_{k-2}}{\left(4\xi_p \omega_{np} T + 4 + T^2\omega_{np}^2\right)}$$

This is the discrete-time High Pass 2nd order filter that has been implemented in Simulink.

4.2.6.Band Pass

$$BandPass2nd\ (s) = k \cdot \frac{2\xi_p \omega_{np} s}{s^2 + 2\xi_p \omega_{np} s + \ \omega_{np}^2}$$

This filter only allows a certain band width of frequencies to go through it, and attenuates the rest of frequencies.

The Bode diagram of a unitary gain, unitary damping and unitary natural frequency 2nd order band pass filter is shown in the next figure.

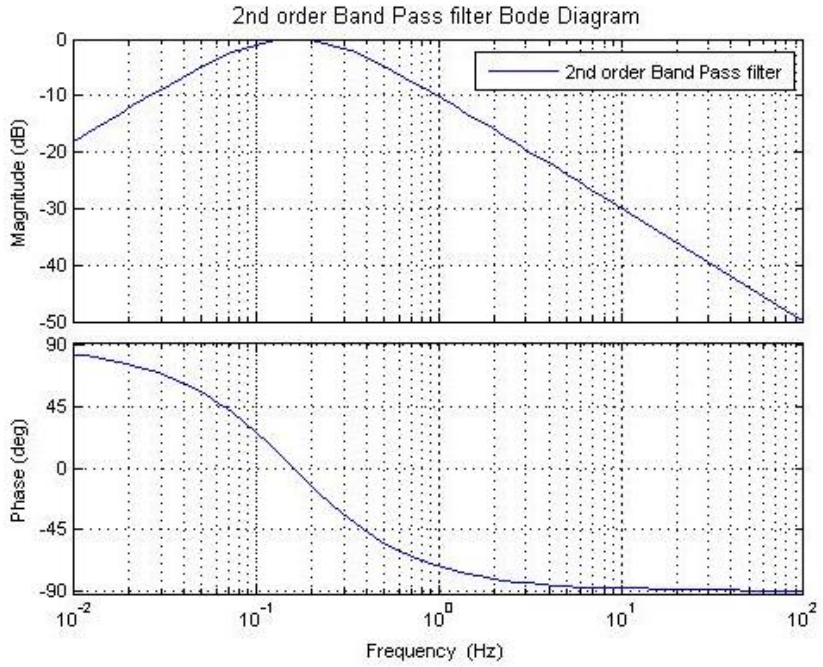

Figure 42: 2nd order band pass filter Bode diagram

The outputs when a chirp signal enters both a continuous and a discrete-time filter are shown in the next figure.

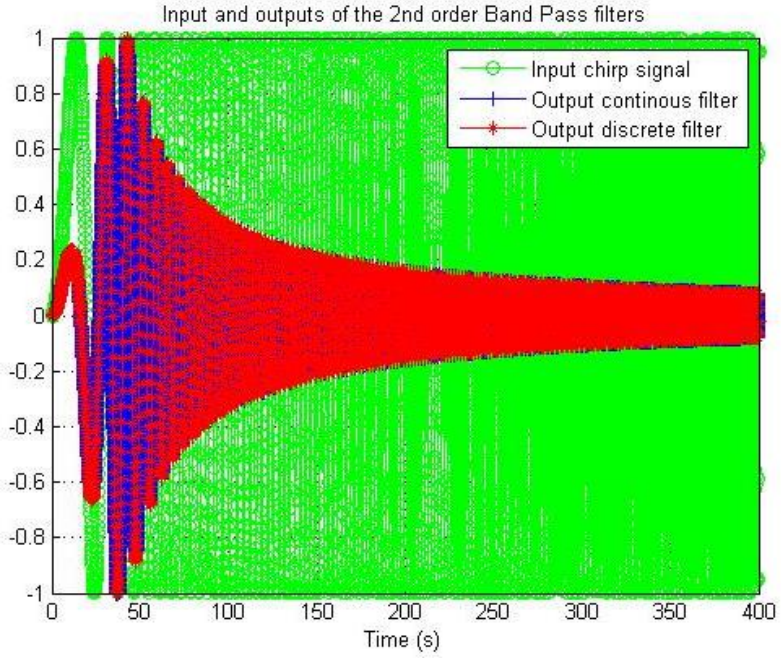

Figure 43: 2nd order band pass continuous filter vs. discrete filter

Next, the discretization of the filter is explained.

Laplace transform:

$$BandPass2nd\ (s) = \frac{Y(s)}{U(s)} = \ k \cdot \frac{2\xi_p \omega_{np} s}{s^2 + 2\xi_p \omega_{np} s + \ \omega_{np}^2}$$

Discretization method:

$$Tustin: \qquad s = \frac{2}{T} \cdot \frac{z-1}{z+1}$$

Discrete-time filter:

$$y_k = \frac{4kT\xi_p\omega_{np} \cdot u_k - 4kT\xi_p\omega_{np} \cdot u_{k-2} + \left(8 - 2T^2\omega_{np}^2\right) \cdot y_{k-1} + \left(4\xi_p\omega_{np}T - 4 - T^2\omega_{np}^2\right) \cdot y_{k-2}}{\left(4\xi_p\omega_{np}T + 4 + T^2\omega_{np}^2\right)}$$

This is the discrete-time Band Pass 2nd order filter that has been implemented in Simulink.

4.2.7.Notch filter

$$Notch\ (s) = k \cdot \frac{s^2 + 2\xi_z\omega_{nz}s + \ \omega_{nz}^2}{s^2 + 2\xi_p\omega_{np}s + \ \omega_{np}^2}$$

A notch filter attenuates a certain frequency range and lets the rest of the frequencies go through. Basically, it does the opposite to what a band pass filter does.

By setting a unitary filter gain and frequencies, and a higher damping for the pole ($\xi_p = 0.7$) than for the zero ($\xi_z = 0.07$), the next Bode diagram is obtained:

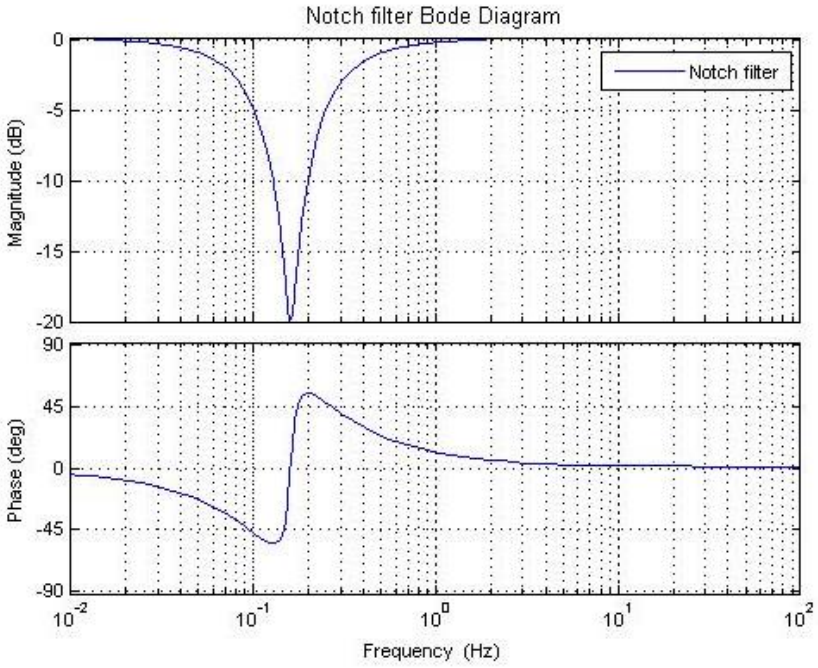

Figure 44: Notch filter Bode diagram

By inputting a chirp signal into the discrete-notch filter and to a continuous one, their behaviors are compared in the next figure.

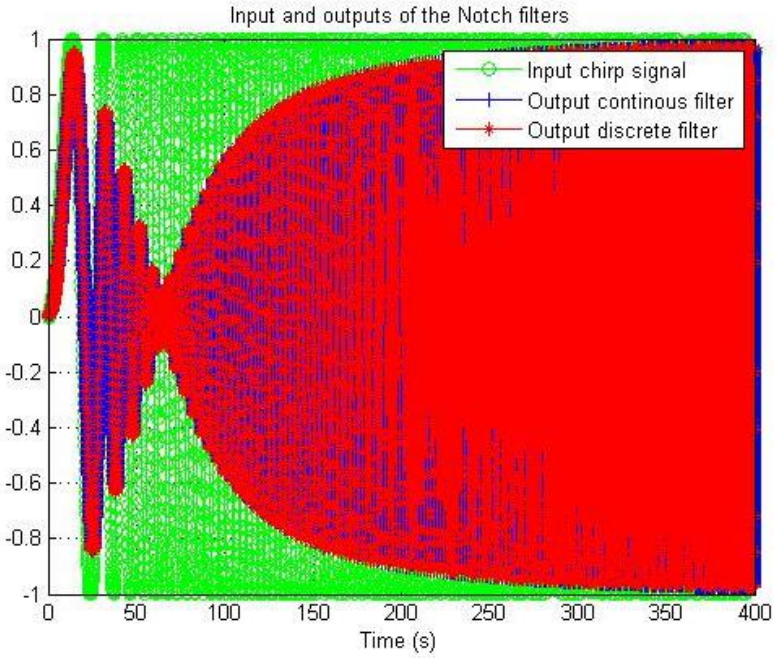

Figure 45: Notch continuous filter vs. discrete filter

Next, the discretization of the filter is explained.

Laplace transform:

$$Notch\ (s) = \frac{Y(s)}{U(s)} = \ k \cdot \frac{s^2 + 2\xi_z \omega_{nz} s + \ \omega_{nz}^2}{s^2 + 2\xi_p \omega_{np} s + \ \omega_{np}^2}$$

Discretization method:

$$Tustin: \qquad s = \frac{2}{T} \cdot \frac{z-1}{z+1}$$

Discrete-time filter:

$$y_k = \frac{k(4\xi_z \omega_{nz} T + 4 + T^2 \omega_{nz}^2) \cdot u_k + \ k(-8 + 2T^2 \omega_{nz}^2) \cdot u_{k-1}}{\left(4\xi_p \omega_{np} T + 4 + T^2 \omega_{np}^2\right)} \cdot$$

$$\cdot \frac{k(-4\xi_z \omega_{nz} T + 4 + T^2 \omega_{nz}^2) \cdot u_{k-2} + \ \left(8 - 2T^2 \omega_{np}^2\right) \cdot y_{k-1} + \left(4\xi_p \omega_{np} T - 4 - T^2 \omega_{np}^2\right) \cdot y_{k-2}}{\left(4\xi_p \omega_{np} T + 4 + T^2 \omega_{np}^2\right)}$$

This is the discrete-time Notch filter that has been implemented in Simulink.

4.2.8.PID block

$$PID(s) = k_p \left(1 + \frac{k_i}{s} + k_d \cdot s\right) = \frac{k_p \cdot s + k_i + k_d \cdot s^2}{s}$$

A PID block is composed of two zeros and a pole.

By setting unitary proportional, integral and derivative gains, $k_p = 1$, $k_i = 1$ and $k_d = 1$, the next Bode diagram is obtained:

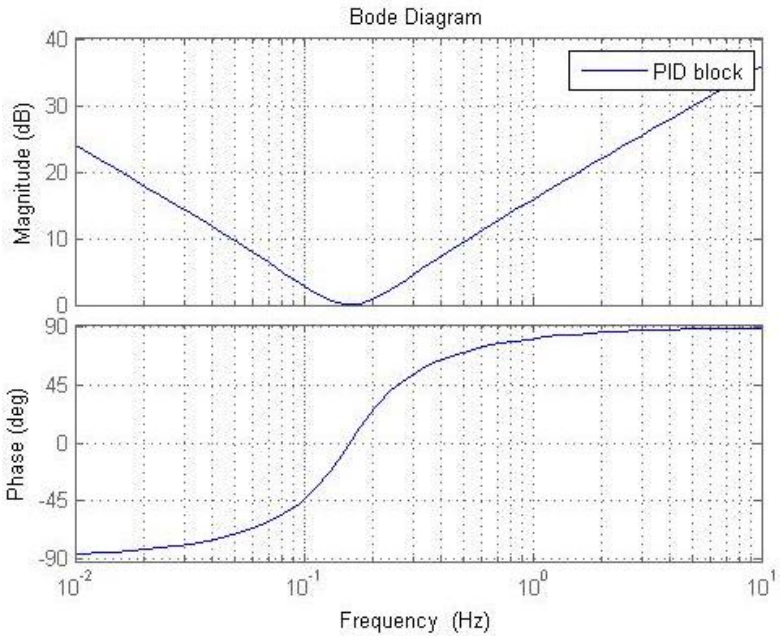

Figure 46: Bode diagram of a PID block

The integrator sets an initial slope of -20dB/dec, then, the first zero adds a slope of 20dB/dec and the magnitude graph stays constant until it reaches the frequency of the second zero, that adds another 20dB/dec resulting in a final positive 20dB/dec slope.

Control systems with more zeros than poles are not physically realizable. Therefore, another pole must be added to the original PID. This is why a filter has been introduced.

$$PID + FILTER\ (s) = k_p(1 + \frac{k_i}{s} + \frac{k_d \cdot s}{1 + \tau_d \cdot s})$$

By setting $k_p = 1$, $k_i = 0.1$, $k_d = 1$ and $\tau_d = 0.1$, the new PID block with a filter is compared to the original PID block in the next Bode diagram.

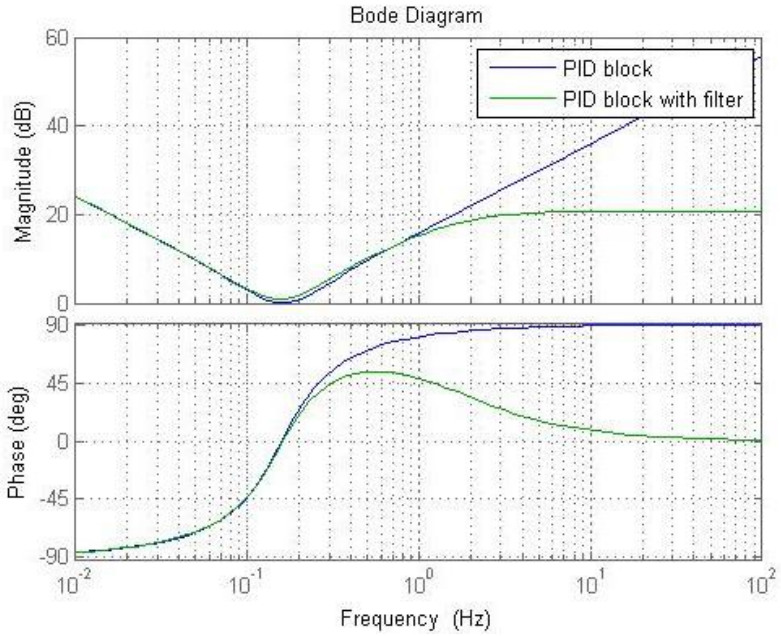

Figure 47: Bode diagram of a PID and a PID with a filter

The filter adds another 20dB/dec of slope and results in a final constant magnitude (dB).

Next, the discretization of the block is explained.

Laplace transform:

$$PID + FILTER\,(s) = \frac{U(s)}{E(s)} = k_p\left(1 + \frac{k_i}{s} + \frac{k_d \cdot s}{1 + \tau_d \cdot s}\right)$$

Discretization methods:

$$Tustin: \quad s = \frac{2}{T} \cdot \frac{z-1}{z+1}$$

$$Euler: \quad s = \frac{z-1}{z \cdot T}$$

For the PID with a filter block, the Tustin discretization method has been used for the integral term and the Euler method has been used for the derivative term and the filter.

Also, the input to this block is the error signal E(s) and the output is the control signal U(s).

Discrete-time PID:

$$u_k = \frac{k_p \cdot (2 \cdot (T + \tau_d) + k_i T \cdot (T + \tau_d) + 2k_d) \cdot e_k + k_p \cdot (-2 \cdot (T + 2\tau_d) - k_i T^2 - 4k_d) \cdot e_{k-1}}{2 \cdot (T + \tau_d)}$$

$$\frac{k_p \cdot (2\,\tau_d - k_i T \tau_d + 2k_d) \cdot e_{k-2} + 2 \cdot (T + 2\tau_d) \cdot u_{k-1} - 2\,\tau_d \cdot u_{k-2}}{2 \cdot (T + \tau_d)}$$

This is the discrete-time PID with filter block that has been implemented to the Simulink library.

4.3. Wind Turbine Control blocks

4.3.1. Main structure

The control strategy explained at the beginning of this chapter, Chapter 4: Wind Turbine Simulink Controller Block, must be supervised by a system that ensures the correct operation of all the elements in the wind turbine and control block. This system not only stops the wind turbine when a dangerous behavior is detected but it also coordinates the control blocks, allowing the correct functioning of the wind turbine.

This system is divided into two blocks: the Main Supervisory Control block and the Supervisory Control. The former is in charge of stopping the wind turbine in case an overspeed or the pressing of the alarm button occurs, and the latter coordinates the control loops.

Next, a general scheme of the control's structure is shown in a diagram.

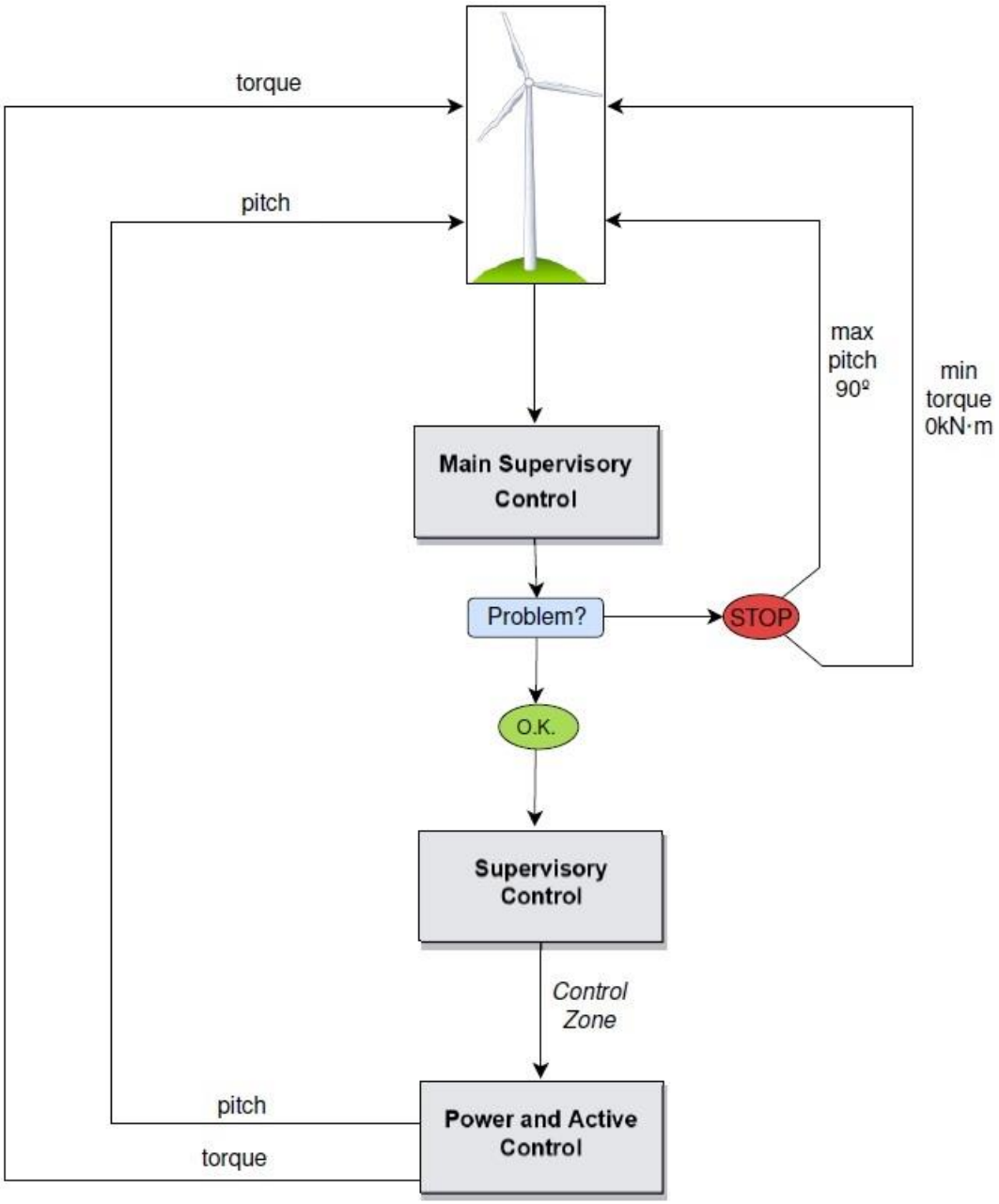

Figure 48: Diagram of the control's main structure

4.3.2.Supervisory Control

Once the Simulink library and all the blocks have been implemented, the first step in the design of the control strategy is to create a supervisory control in the Simulink model where the FAST S-Function has been placed.

The supervisory control is in charge of deciding which control loop (either pitch control or torque control) takes care of the regulation or power control. This block consists of an algorithm that, depending on the generator toque and speed that inputs the block, gives a number determining the wind turbine's operating zone.

The torque vs. generator speed curve has been divided into 5 zones that are explained next.

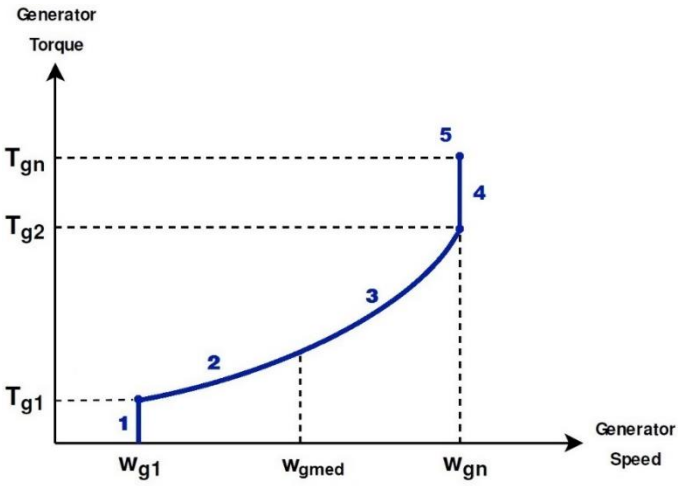

Figure 49: Supervisory control zones in generator torque vs. speed graph

1st vertical

The **1st** zone is also called the 1st vertical. It starts when the wind speed exceeds the cut-in wind speed (3m/s), which is when the electric generator is turned on. In this zone, the goal is to keep generator speed constant at ω_{g1} = 41.88 rad/s by controlling the generator torque among values below T_{g1} = 4.0907 kN·m.

In this first zone, the **torque control loop** is the one controlling the generator speed. The **DTD** works in every zone, so it is an addition to the demanded torque.

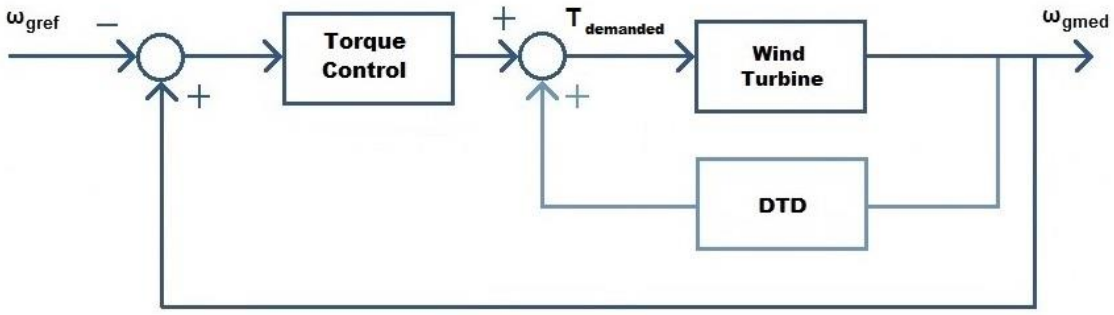

Figure 50: First vertical control scheme. Block diagram of Torque Control Loop and DTD

Quadratic curve

The **2nd** and **3rd** zone make up the optimal torque zone, the quadratic curve. Here, maximum energy capture is pursued. This is done by looking for the maximum C_p and, therefore, the optimum tip speed ratio (TSR), λ. Generator speed is not controlled in this zone, but it varies along with the wind speed. The only variable controlled here will be the generator torque, which can be set to follow the optimal torque command, open loop control.

$$P = \frac{1}{2}\rho \cdot \pi \cdot R^2 \cdot v^3 \cdot C_p = T \cdot \Omega$$

$$\lambda = \frac{\Omega_{rotor} \cdot R}{v} = \frac{\Omega_g \cdot R}{v \cdot i_g}$$

$$T_g = \frac{P_g}{\Omega_g} = \frac{\rho \cdot \pi \cdot R^3 \cdot v^3 \cdot C_p}{2 \cdot \lambda \cdot v \cdot i_g} = \frac{\rho \cdot \pi \cdot R^5 \cdot C_p}{2 \cdot \lambda^3 \cdot i_g^3} \cdot \Omega_g^2$$

$$T_{gmax} = \frac{\rho \cdot \pi \cdot R^5 \cdot C_{pmax}}{2 \cdot \lambda_{opt}^3 \cdot i_g^3} \cdot \Omega_g^2 = K_{opt} \cdot \Omega_g^2$$

Where ρ is the air density, R is the rotor radius, C_{pmax} is the maximum power coefficient of the wind turbine, i_g is the gearbox ratio, P is the generator power, v is the wind speed, Ω is the angular speed and λ_{opt} is the optimal tip speed ratio of the wind turbine.

K_{opt} is a constant since C_{pmax}, λ_{opt} and the rest of parameters are constant for each wind turbine.

As it was explained, in the quadratic zone, also known as the maximum Cp curve or maximum λ curve, there is no control of the generator speed. The torque is set to follow the optimal torque (which depends on the generator speed), which is an **open loop** control. Since the **DTD** is always activated, it is the only one that will be working in the quadratic zone.

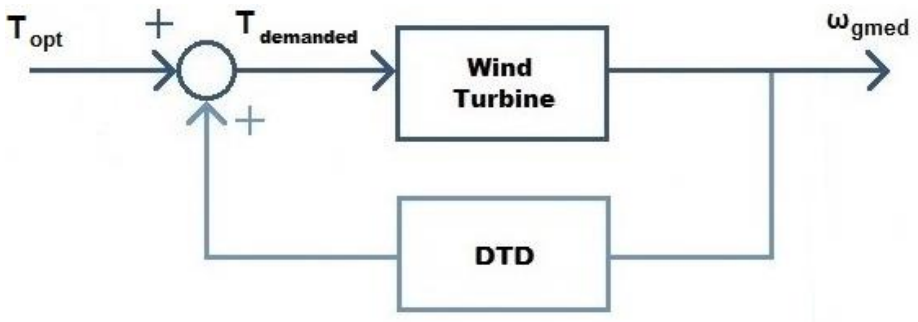

Figure 51: Quadratic curve control scheme. Block diagram of DTD

2nd vertical

The 4th zone is also called the 2nd vertical. Just like the 1st one, it consists of a torque control that pursues keeping the generator speed constant (this time at ω_{gnom} = 122.91 rad/s) by controlling generator torque between T_{g2} = 35.23 kN·m and T_{gnom} = 43.09 kN·m.

The **torque loop controls** generator speed and the **DTD** adds its demanded torque. The only difference with the control of the 1st vertical is that the objective of this 2nd vertical is to keep the generator speed at w_{gn} instead of w_{g1}.

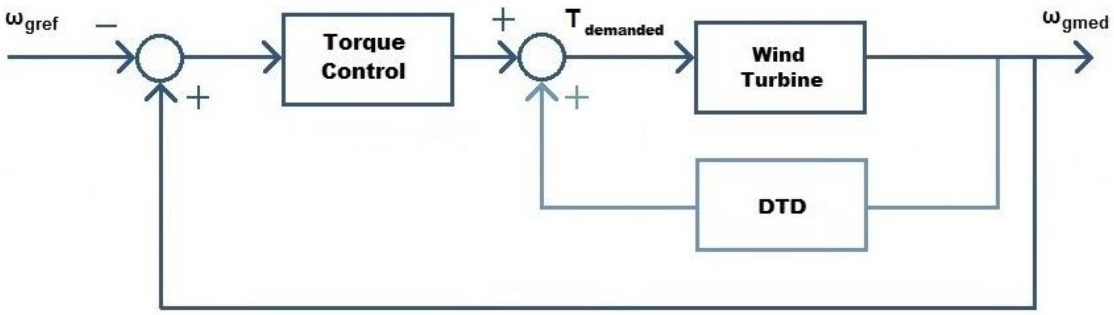

Figure 52: Second vertical control scheme. Block diagram of Torque Control Loop and DTD

Above rated

Once that wind speed has risen above 11.4 m/s (wind nominal speed), the supervisory control enters the **5th** zone. This is called the above rated zone and the goal in it is to keep the generator power from exceeding the wind turbine's rated power.

This is done because the main goal when designing a wind turbine is not maximizing the energy capture but to maximize it at the lowest cost. Choosing the size of a wind turbine according to the site's highest winds would not optimize the wind turbine's cost because the recurrence of those winds is very low compared to the increase in cost that they entail.

Wind turbines are designed for a certain rated wind speed, this is, the average wind speed in a certain site over a ten minute period. When the wind speed exceeds this rated wind speed, the supervisory control activates the pitch control loop, whose goal is to reduce the energy capture by rotating the blades. In this zone, the torque control is saturated (demanded torque is set to T_{gnom}) and only pitch control is used to keep generator speed at ω_{gnom}.

In the above rated zone, the **pitch loop** is the one that controls the generator speed. In this zone, the **ATD** gradually starts working as the pitch angle increases. The **DTD** is still activated, so the three will be working at the same time.

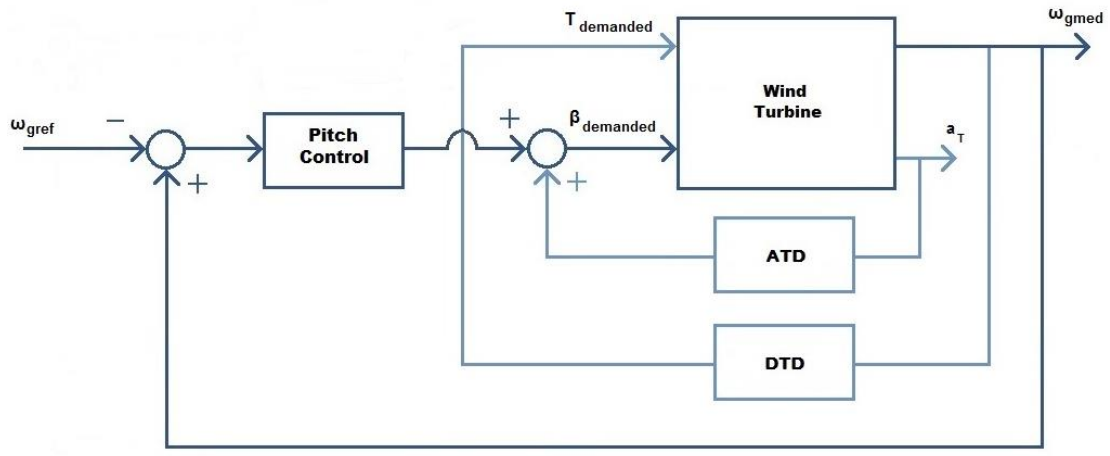

Figure 53: Above rated control scheme. Block diagram of the Pitch Control Loop, ATD and DTD

The pitch and torque control loops, as well as the active control strategies (ATD and DTD) will be explained in the next sections.

4.3.3.Torque Control

The torque control loop, as it was stated in the previous section, is a part of the regulatory control. This means that its goal is to regulate the power of the wind turbine.

The SISO scheme of this controller's torque control is shown in the next figure.

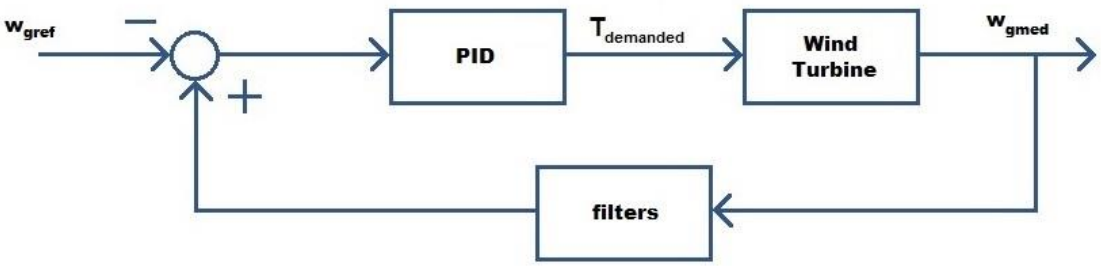

Figure 54: Torque control loop scheme

Increasing generator demanded torque decreases generator speed. To have a stable system, the loop must be a positive feedback loop. This way, an increasing torque will result in a decreasing generator speed which will reduce the generator torque, giving a stable loop.

The same applies to pitch angle. When the pitch angle increases, the blades face the wind, extracting a lower energy from it and lowering the rotor speed. The pitch control loop, therefore, is also a positive feedback control loop.

The torque control loop is composed of a PID block and different notch filters introduced to eliminate any unnecessary control action in the wind turbine's most excited frequencies. Particularly, filters that attenuate the next frequencies have been introduced: drive train torsion frequency, 1st and 2nd symmetric, 2nd tower side-to-side and 1st tower fore-aft, and the rotational 1P and 3P frequencies.

The last two frequencies, 1P and 3P, are non-structural, blade passing frequencies. The 1P frequency is the frequency at which a certain blade passes in front of the tower, it corresponds to the rotor rotating frequency. The 3P frequency is that one at which any blade passes the tower, which means it will be three times the 1P frequency. As they depend on the rotor speed, they act in a band or frequency range. As they are non-structural frequencies, something that must be taken into account is the fact that they do not appear in the linear models.

4.3.4.Pitch Control

Just like the torque control loop, the pitch control loop is a regulatory control strategy, which means its main goal is to control generated power. The difference between both loops is that the pitch control loop, as its name implies, controls generator speed by acting on the blade pitch angle instead of acting on the generator torque.

The scheme of the pitch control loop is shown in the next figure.

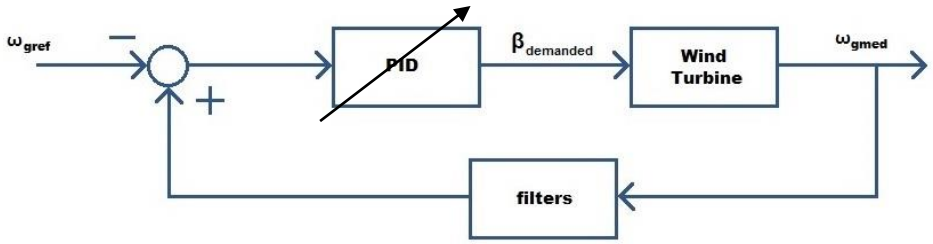

Figure 55: Pitch control loop scheme

As it is explained in the previous section, the pitch control loop is a positive feedback loop, which makes it a stable system.

The pitch loop is composed of the same elements as the torque control loop, this is, a PID and 7 notch filters to damp the excited frequencies of the wind turbine. The main difference is that the pitch loop PID's parameters are variable. This is due to the non-linearities of the pitch angle. The same angle increment results in a much higher change in the wind turbine's rotational speed at high wind speeds than at low wind speed levels. This makes it necessary to apply a gain scheduling for the PID's parameters.

Since the tuning of the PID has been carried out without a derivative term, only the gain schedulings of the PID's Kp and Ki are illustrated in the next figures.

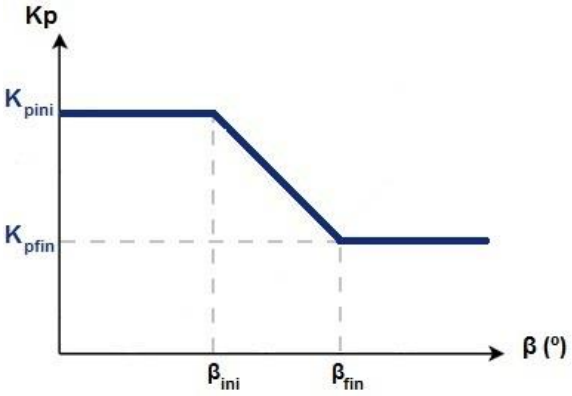

Figure 56: Kp, pitch control PID's gain scheduling

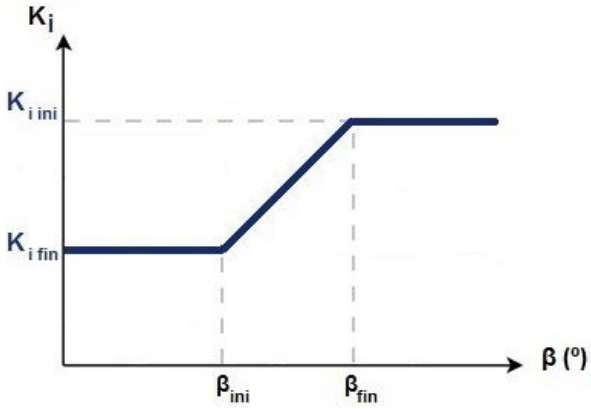

Figure 57: Ki, pitch control PID's gain scheduling

The notch filters, nevertheless, are the same ones that can be found in the torque control loop.

An additional filter has been added to the pitch control loop. It is a 1st order low pass filter and it is not activated except for load and pitch duty analysis. Its objective is to reduce pitch activity at high frequencies.

4.3.5.DTD

The drive train damping, also known as DTD, is the first one to be designed. It is part of the active control strategy, which means its objective is to act on the wind turbine's plant to obtain a desired behavior of the plant. Particularly, the DTD's objective is to give damping to the drive train mode.

It consists of a 2nd order band pass filter in series with a notch filter at the 3P rotational frequency. The input to the DTD is the wind turbine's generator speed and the output of the block (T_{DTD}) is an addition to the torque control's torque demand, only that it is active along all the control zones (both verticals, open loop and above rated), unlike the torque control loop.

$$DTD\ (s) = k_{BP} \cdot \frac{2\xi_p \omega_{np} s}{s^2 + 2\xi_p \omega_{np} s + \omega_{np}^2} \cdot k_{Notch} \cdot \frac{s^2 + 2\xi_z \omega_{nz} s + \omega_{nz}^2}{s^2 + 2\xi_p \omega_{np} s + \omega_{np}^2}$$

An example of the DTD's open loop and closed loop (DTD with the wind turbine's plant) Bode diagrams are shown next (for a wind speed of 11m/s).

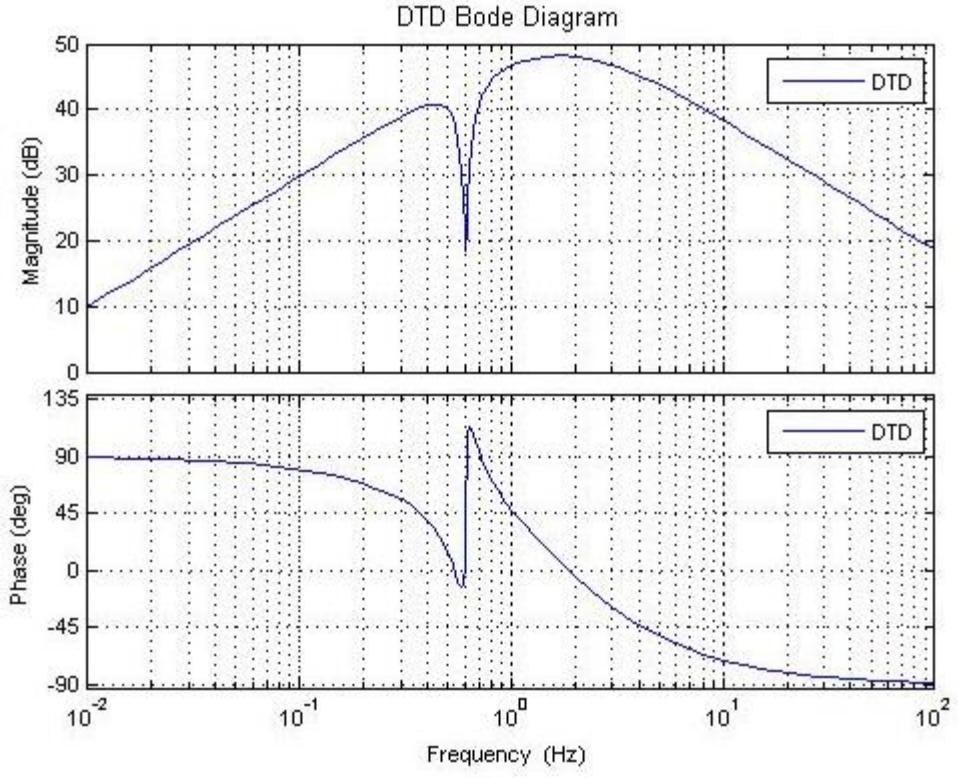

Figure 58: Open loop Bode diagram of the DTD at 11m/s

The drive train torsion mode of the Upwind 5MW wind turbine is located at 1.645 Hz, which is where the cutoff frequency of the band pass filter has been set. Also, the Bode diagram shows how the notch filter at the 3P rotational frequency (around 0.6Hz at rated speed) will filter any signal of the DTD that has a component on that frequency.

Another thing that must be checked is that, at the drive train frequency, the DTD's phase must be a little above 0 degrees. This is because, ideally, if the system did not have any delays, the DTD should have an ideal phase of exactly 0 degrees in order not to delay the signals that entered the block at that frequency. Since the system does have a certain delay due to its actuators, a little phase will be necessary. This delay depends on the converter of the electric system of the generator and in this case, this phase is around 10 degrees.

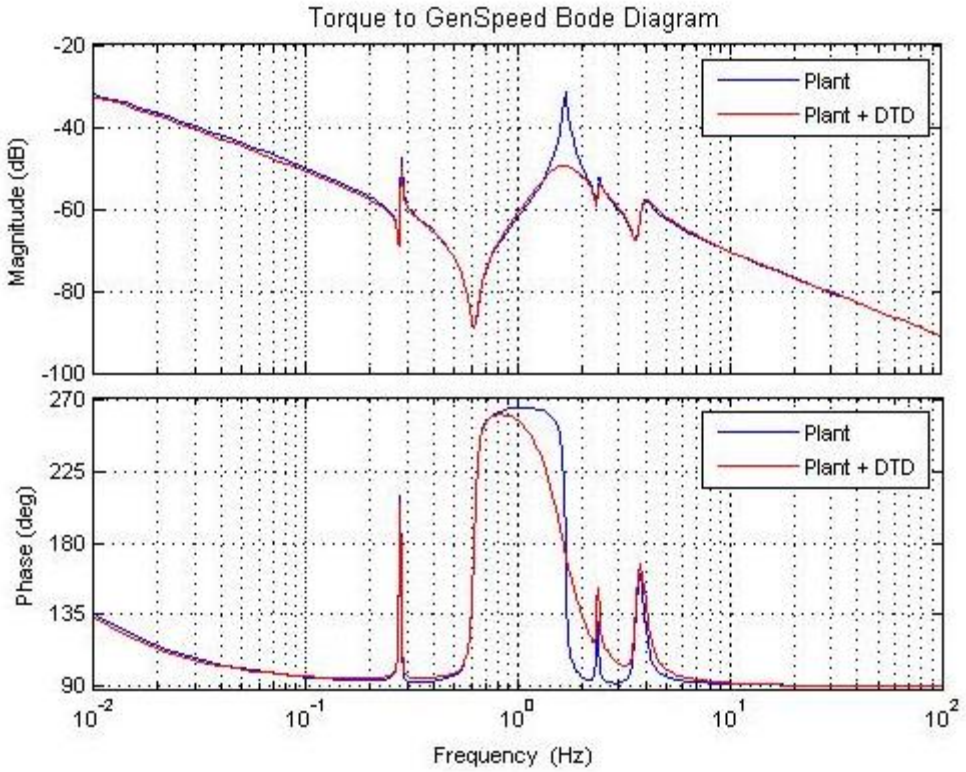

Figure 59: Bode diagram of the plant drom torque to generator speed with and without DTD at 11m/s

The figure clearly shows how the drive train damping reduces the magnitude peak the plant has at the drive train frequency. This will result in a reduction of the tower, nacelle and blade loads caused by this torsional mode.

4.3.6.ATD

The active tower damping strategy (ATD), like the DTD, is an active control strategy. This one is designed with the aim of reducing the excitement of the tower's fore-aft first mode.

The ATD consists of a 2nd order low pass filter in series with a notch filter at the rotational 3P frequency.

$$ATD\ (s) = \ k_{LP} \cdot \frac{\omega_{np}^2}{s^2 + 2\xi_p\omega_{np}s + \ \omega_{np}^2} \cdot k_{Notch} \cdot \frac{s^2 + 2\xi_z\omega_{nz}s + \ \omega_{nz}^2}{s^2 + 2\xi_p\omega_{np}s + \ \omega_{np}^2}$$

Unlike the DTD that is activated in all the control zones, the ATD only works in the above rated zone. The activation of the ATD is not instant when entering the above rated zone, it is done by gain scheduling. Therefore, the ATD includes a variable gain as well as both filters.

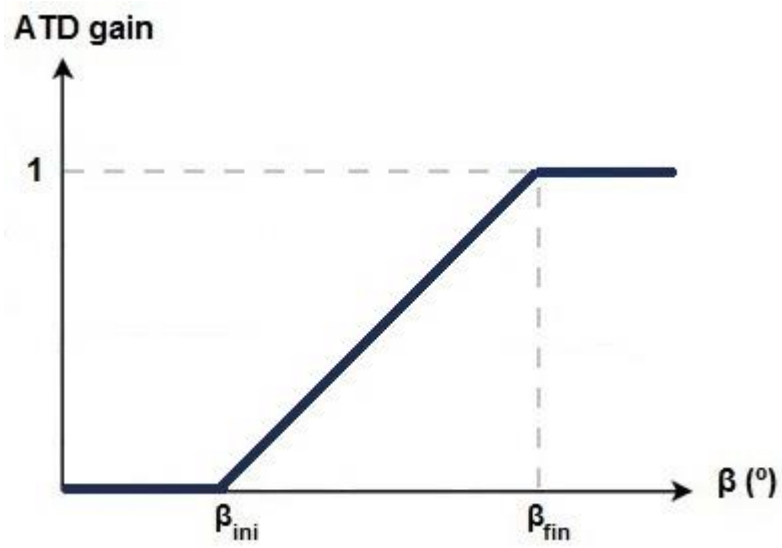

Figure 60: ATD gain scheduling

As a consequence of giving damping to the tower's 1st fore-aft mode, the nacelle's acceleration in the x axis is reduced. This acceleration is the input to the ATD and the output (β_{ATD}) is a contribution to the pitch control's demanded pitch.

An open loop Bode diagram of the ATD is shown as well as one of the closed loop of the plant with the ATD, both for a wind of 13m/s.

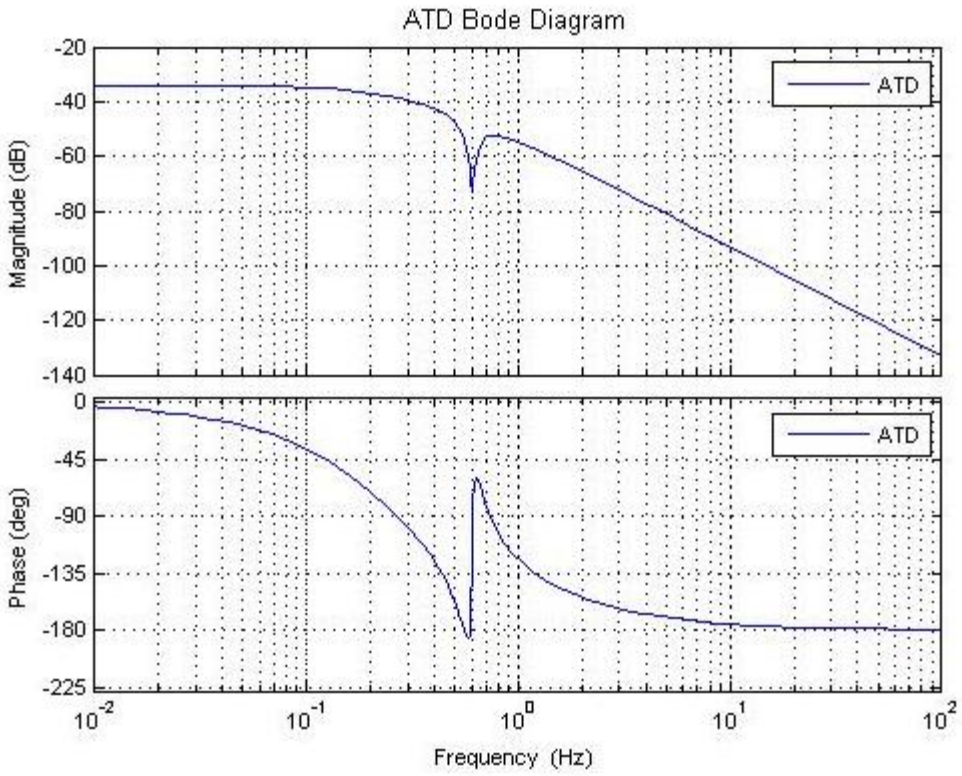

Figure 61: Open loop Bode diagram of the ATD at 13m/s

The figure shows the 2nd order low pass filter with a cutoff frequency around 0.28Hz, which is the 1st fore-aft frequency of this specific wind turbine. Also, it shows how around 0.6Hz, the 3P filter will attenuate every signal with components on that frequency.

Just like for the DTD, the phase of the ATD at the cutoff frequency (in this case 0.28Hz) must be checked. Given the actuator delay, an ATD phase of -90 degrees at the cutoff frequency is adequate.

The closed loop Bode diagram of the Plant with the ATD is shown next along with the Bode diagram of the plant from pitch angle to nacelle acceleration.

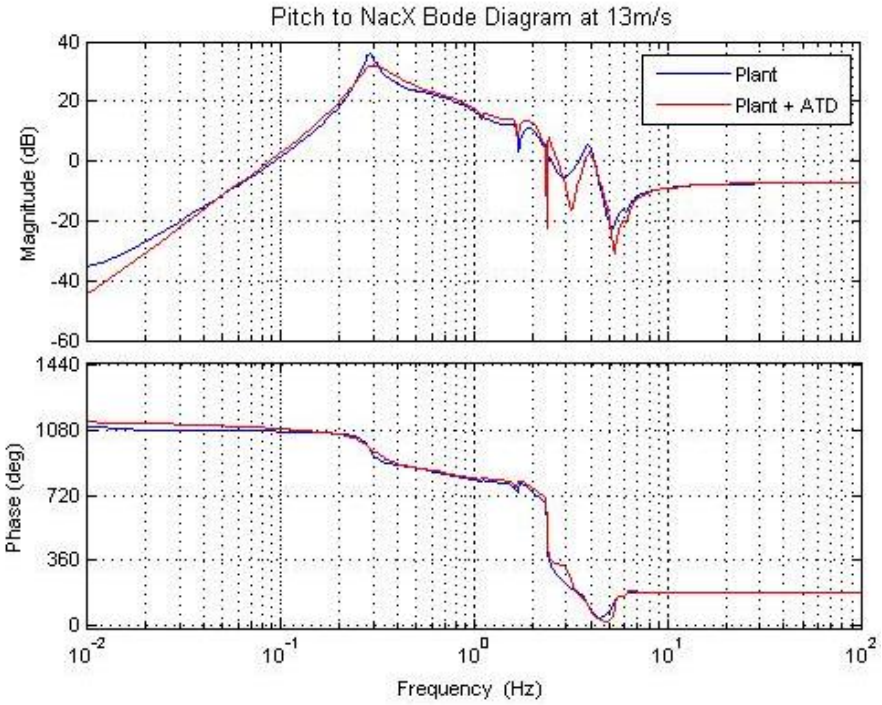

Figure 62: Bode diagram of the plant from pitch to nacelle fore-aft with and without ATD at 13m/s

The closed loop Bode diagram shows how the ATD gives damping to the tower's first fore-aft mode, at 0.28Hz. This results in a reduction of loads in the wind turbine shaft, blades… But, most importantly, it results in a reduction of longitudinal loads in the tower.

4.3.7.Main Supervisory Control

As well as the power control loops and the load reduction strategies, an emergency stop has been implemented into the Simulink model.

There are two ways of forcing the wind turbine to stop. The first one is by an emergency stop button, that can be prepared to activate at a certain moment in the simulation. The other way is when the wind turbine's rotating speed exceeds a certain value (specifically, when it exceeds a 25% of the rated speed). Then, this main supervisory control automatically forces the wind turbine to make an emergency stop by setting the control demanded torque to 0 kN·m and the pitch angle to its minimum value, 0.106 degrees.

4.4. Simulink model and parameter file

As a result of the control tuning, optimized values of the control parameters are obtained. These values are collected in a MATLAB script called the parameter file. In this section, they are shown and explained along with the blocks of the Simulink model.

4.4.1. Supervisory control

Supervisory control Simulink model

The next figure shows the supervisory control model with its inputs and outputs.

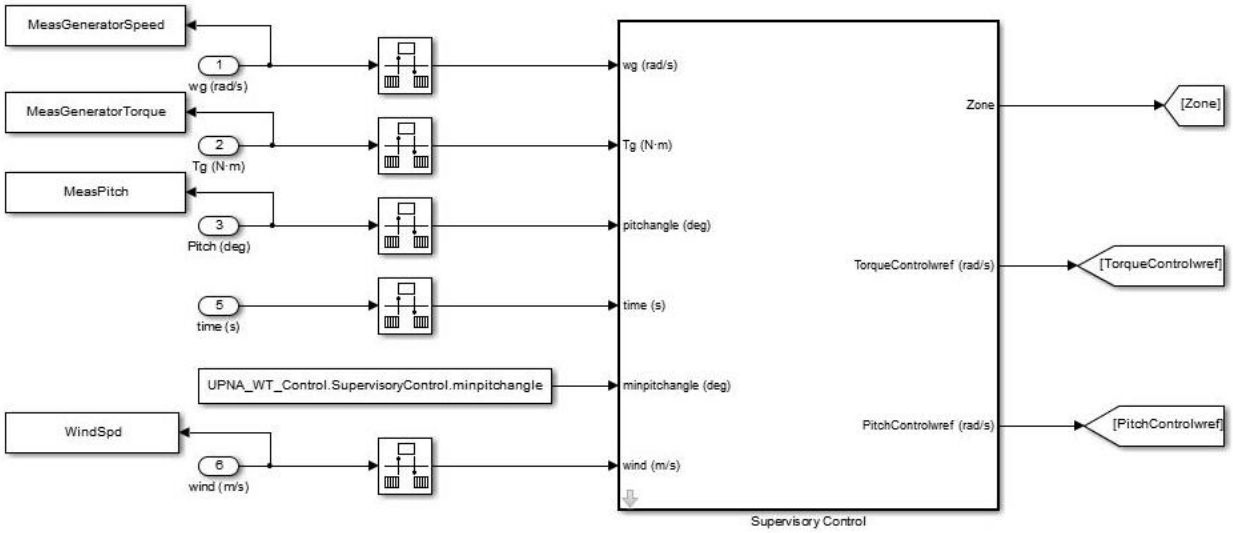

Figure 63: Simulink model of the Supervisory Control

With the measured generator speed, generator torque, pitch angle, time and wind speed, the supervisory control must generate the operation zone and the pitch and torque references for the pitch control and torque control loops, respectively. The inside of the supervisory control model is shown in the next figure.

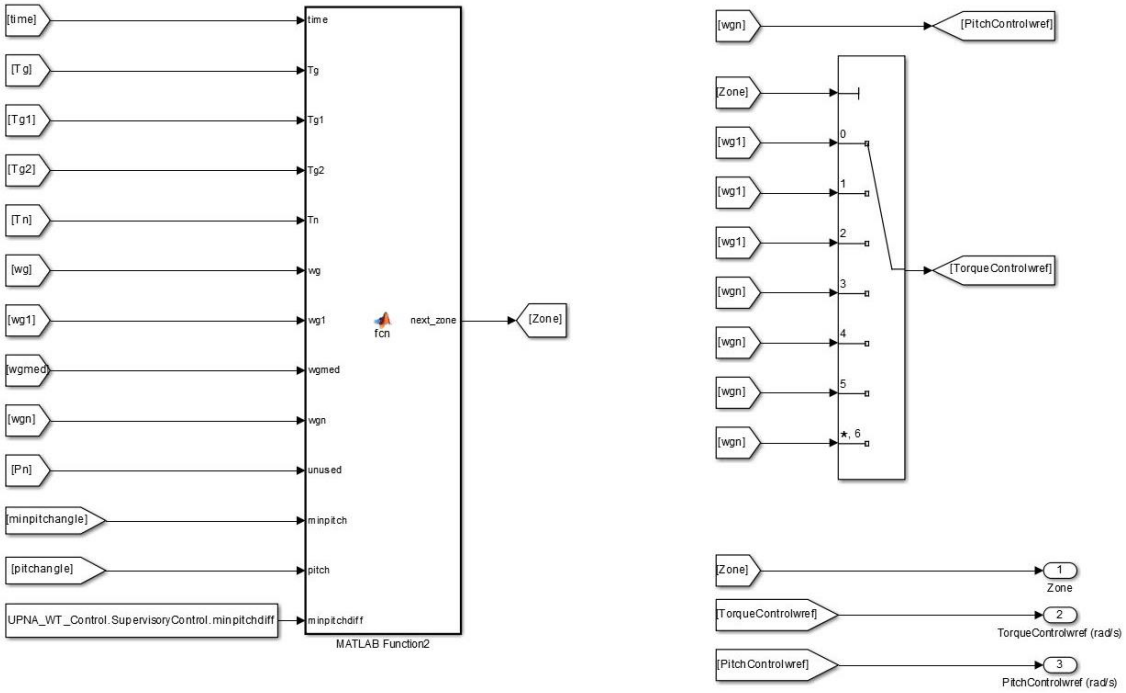

Figure 64: Internal Simulink model of the Supervisory Control

The first thing in the supervisory control block are some calculations (not shown in the previous figure) of parameters such as the mean generator speed (w_{gmed}) between w_{g1} and w_{gnom}, the

maximum torque for the first vertical (T_{g1}), or the minimum torque for the second one (T_{g2}). Then, there is also a MATLAB function that includes the algorithm that calculates the operating zone. Finally, there is a switch block, whose control signal is the zone signal. This block generates a generator speed reference for the torque control loop, which varies from w_{g1} to w_{gnom} depending on the operating zone. A switch is not necessary for the pitch reference since the pitch control loop only works in the above rated zone, it can only have a reference of w_{gnom}.

The script of the function is shown next.

```
function next_zone =
fcn(time,Tg,Tg1,Tg2,Tn,wg,wg1,wgmed,wgn,~,minpitch,pitch,minpitchdiff)


persistent zone_ant;

if isempty(zone_ant)
    zone_ant=3;
end

if ((time<5) && (pitch>minpitch*(1+minpitchdiff)))
    zone_ant=5;
    next_zone=5;
else
    next_zone=0;
end

if(time>0.2)

    actual_zone=zone_ant;

        switch actual_zone

                case 1
                    if(Tg>=Tg1)
                       next_zone = 2;
                    else
                       next_zone = 1;
                    end
                case 2
                    next_zone=2;
                    if(wg<wg1)
                        next_zone = 1;
                    end
                    if(wg>wgmed)
                        next_zone = 3;
                    end
                case 3
                    next_zone=3;
                    if(wg<=wgmed)
                        next_zone = 2;
                    end
                    if(Tg>=Tg2)
                        next_zone = 4;
                    end
                case 4
                    next_zone=4;
                    if(Tg<=Tg2)
                      next_zone = 3;
                    end
                    if(Tg>=Tn)
                      next_zone = 5;
                    end
                case 5
                    next_zone=5;
```

```
                        if((pitch<=(minpitch+minpitchdiff)) && (time>1))
                          next_zone = 4;
                        end
                        if((wg<=wgn*0.75) && (time>30))
                          next_zone = 3;
                        end
                    otherwise
                        next_zone = actual_zone;
            end

    zone_ant=next_zone;

    end
```

As it is shown, the function uses different torque, speed and pitch conditions to switch from one operating zone to another.

Supervisory control parameters

SUPERVISORY CONTROL		
Parameter	**Units**	**Explanation**
UPNA_WT_Control.SupervisoryControl.SampleTime	s	Simulink model sample time, rate at which the model samples the inputs and makes the calculations
UPNA_WT_Control.SupervisoryControl.w1	rad/s	First vertical generator rotational speed
UPNA_WT_Control.SupervisoryControl.wgn	rad/s	Nominal generator rotational speed, second vertical and above rated rotational speed
UPNA_WT_Control.SupervisoryControl.Pn	W	Rated power, reached in the above rated zone
UPNA_WT_Control.SupervisoryControl.minpitchangle	deg	Minimum blade pitch angle
UPNA_WT_Control.SupervisoryControl.maxpitchangle	deg	Maximum blade pitch angle
UPNA_WT_Control.SupervisoryControl.Kopt	$N \cdot m/(rad/s)^2$	Quadratic constant, used to set the generator torque in the quadratic zone
UPNA_WT_Control.SupervisoryControl.Tn	N·m	Nominal generator torque, set for the above rated zone
UPNA_WT_Control.SupervisoryControl.minpitchdiff	deg	Input parameter to the Supervisory Control function, used to initialize pitch
UPNA_WT_Control.SupervisoryControl.vnom	m/s	Nominal wind speed, where the above rated zone starts
UPNA_WT_Control.SupervisoryControl.GearBoxRatio	-	Gearbox ratio, from low speed shaft to high speed shaft, used in the calculation of Kopt
UPNA_WT_Control.SupervisoryControl.GeneratorSpeedMax	rad/s	Maximum generator speed, used in the overspeed mechanism to take the wind turbine to an emergency stop
UPNA_WT_Control.SupervisoryControl.GeneratorSpeedMaxIniTime	s	Initial time for emergency stop activation (deactivates it if overspeed is caused below this time, initialization issues)
UPNA_WT_Control.SupervisoryControl.maxratepitchangle	deg/s	Maximum pitch angle rate at which the blade is allowed to rotate
UPNA_WT_Control.SupervisoryControl.minratepitchangle	deg/s	Minimum pitch angle rate at which the blade is allowed to rotate, same speed but opposite direction to the maximum rate
UPNA_WT_Control.SupervisoryControl.maxratetorque	N·m/s	Maximum torque rate variations of demanded torque
UPNA_WT_Control.SupervisoryControl.minratetorque	N·m/s	Minimum torque rate variations of demanded torque, maximum demanded torque reduction rate

Table 8: Supervisory control parameter explanation

Some of these parameters will be obtained from the 5MW Upwind baseline wind turbine's characteristics and some others will be set in order to have the desired behavior of the system.

4.4.2.Pitch control loop

Next, the pitch control loop's parameters and its Simulink model are shown.

Pitch control Simulink model

Given that the pitch limitations are applied to the sum of the pitch loop demanded pitch and the ATD demanded pitch, the next figure shows what the pitch control block and the ATD block look like.

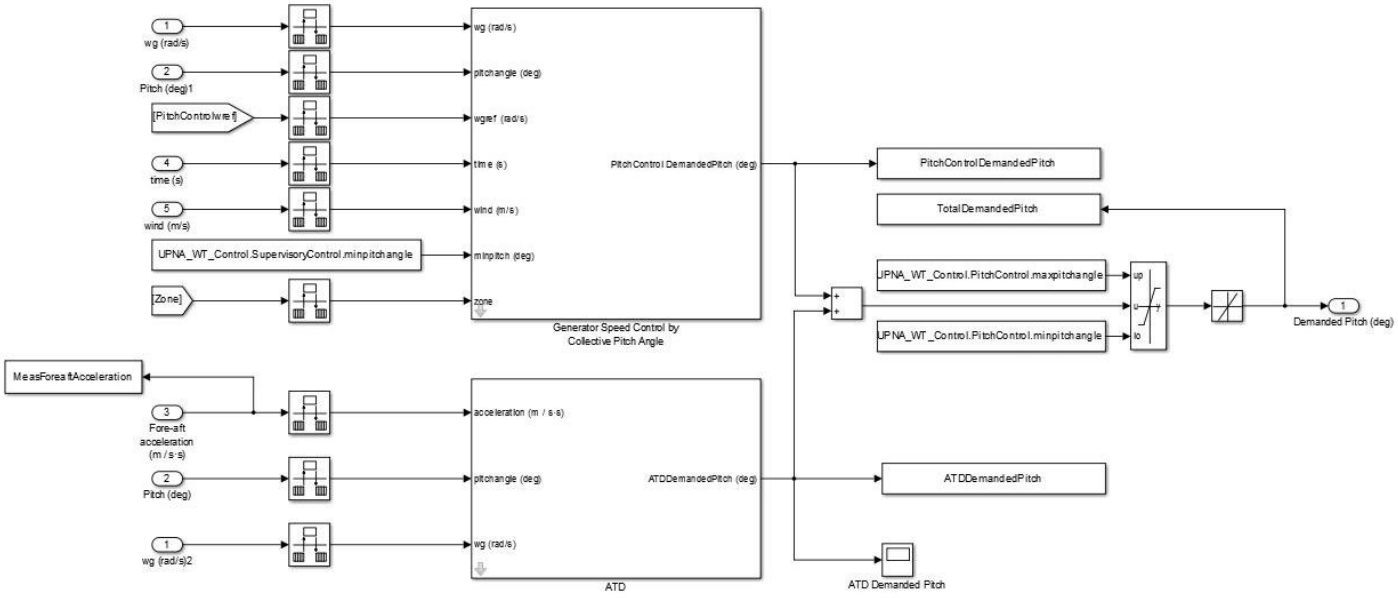

Figure 65: Simulink model of the Pitch Control Loop

The inputs to the pitch control loop are the measured generator speed, measured pitch angle, wind, time and the minimum pitch angle, as well as the reference generator speed and the zone that are calculated in the Supervisory Control.

The only output of the pitch control loop is the demanded pitch. This will add to the ATD's demanded pitch and will be limited (rate limit and saturated) before going to the FAST S-Function. The next two figures show the side the pitch control block.

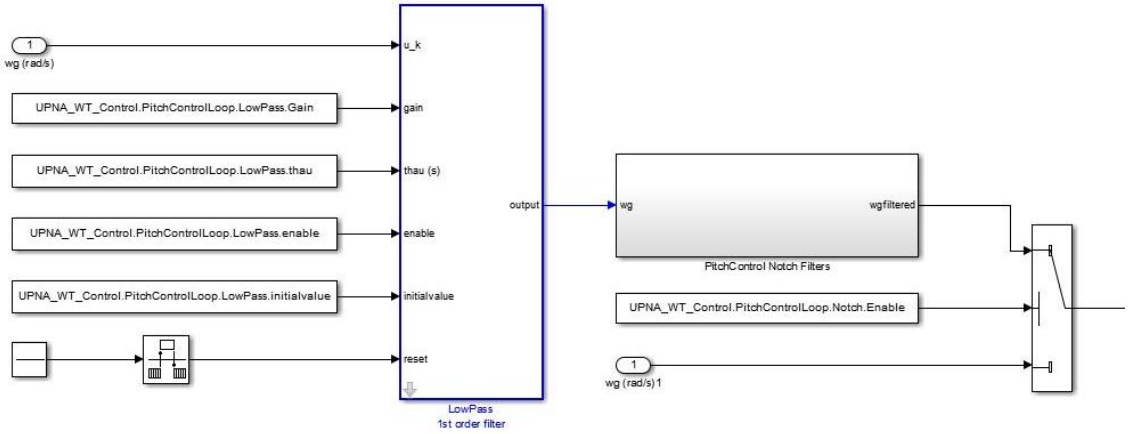

Figure 66: Internal Simulink model of the Pitch Control Loop, filters

This first figure shows the filtering of the measured generator speed. First, there is a 1st order low pass filter which is not activated in the baseline control, it is introduced for load analysis. Then, there is a block that groups all the notch filters of the pitch control loop.

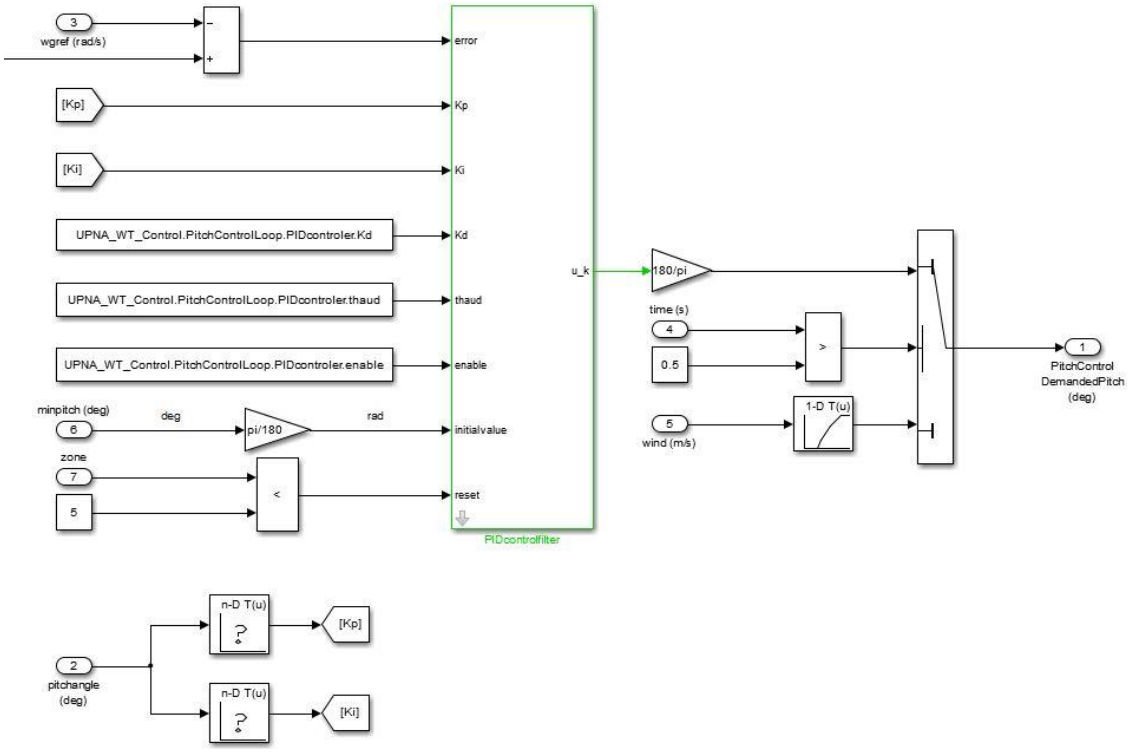

Figure 67: Internal Simulink model of the Pitch Control Loop, PID and gain schedulings

After the filtering of the generator speed signal, there is the pitch control's PID. For last, other than the variable gains of the PID, there is an initialization block that starts the pitch control demanded pitch according to the wind speed.

Pitch control control parameters

PITCH CONTROL		
Parameter	**Units**	**Explanation**
UPNA_WT_Control.PitchControlLoop.SampleTime	s	Pitch control loop sample time
UPNA_WT_Control.PitchControlLoop.Notch.Enable	-	Enabler of all the notch filters of the pitch control loop
UPNA_WT_Control.PitchControl.minpitchangle	deg	Minimum blade pitch angle
UPNA_WT_Control.PitchControl.maxpitchangle	deg	Maximum blade pitch angle
UPNA_WT_Control.PitchControl.maxratepitchangle	deg/s	Maximum pitch angle rate at which the blade is allowed to rotate
UPNA_WT_Control.PitchControl.minratepitchangle	deg/s	Minimum pitch angle rate at which the blade is allowed to rotate, same speed but opposite direction to the maximum rate
UPNA_WT_Control.PitchControlLoop.NotchDT.Gain	-	Drivetrain notch filter gain
UPNA_WT_Control.PitchControlLoop.NotchDT.Dampz	-	Drivetrain notch filter zero's damping
UPNA_WT_Control.PitchControlLoop.NotchDT.Dampp	-	Drivetrain notch filter pole's damping
UPNA_WT_Control.PitchControlLoop.NotchDT.wnz	rad/s	Drivetrain notch filter zero's natural frequency
UPNA_WT_Control.PitchControlLoop.NotchDT.wnp	rad/s	Drivetrain notch filter pole's natural frequency
UPNA_WT_Control.PitchControlLoop.NotchDT.enable	-	Drivetrain notch filter enabler
UPNA_WT_Control.PitchControlLoop.NotchDT.initialvalue	-	Drivetrain notch filter initial value
UPNA_WT_Control.PitchControlLoop.Notch1simetrica.Gain	-	First symmetric notch filter gain
UPNA_WT_Control.PitchControlLoop.Notch1simetrica.Dampz	-	First symmetric notch filter zero's damping
UPNA_WT_Control.PitchControlLoop.Notch1simetrica.Dampp	-	First symmetric notch filter pole's damping
UPNA_WT_Control.PitchControlLoop.Notch1simetrica.wnz	rad/s	First symmetric notch filter zero's natural frequency
UPNA_WT_Control.PitchControlLoop.Notch1simetrica.wnp	rad/s	First symmetric notch filter pole's natural frequency
UPNA_WT_Control.PitchControlLoop.Notch1simetrica.enable	-	First symmetric notch filter enabler
UPNA_WT_Control.PitchControlLoop.Notch1simetrica.initialvalue	-	First symmetric notch filter initial value
UPNA_WT_Control.PitchControlLoop.Notch2simetrica.Gain	-	Second symmetric notch filter gain
UPNA_WT_Control.PitchControlLoop.Notch2simetrica.Dampz	-	Second symmetric notch filter zero's damping

UPNA_WT_Control.PitchControlLoop.Notch2simetrica.Dampp	-	Second symmetric notch filter pole's damping
UPNA_WT_Control.PitchControlLoop.Notch2simetrica.wnz	rad/s	Second symmetric notch filter zero's natural frequency
UPNA_WT_Control.PitchControlLoop.Notch2simetrica.wnp	rad/s	Second symmetric notch filter pole's natural frequency
UPNA_WT_Control.PitchControlLoop.Notch2simetrica.enable	-	Second symmetric notch filter enabler
UPNA_WT_Control.PitchControlLoop.Notch2simetrica.initialvalue	-	Second symmetric notch filter initial value
UPNA_WT_Control.PitchControlLoop.Notch2sidetoside.Gain	-	Second side-to-side notch filter gain
UPNA_WT_Control.PitchControlLoop.Notch2sidetoside.Dampz	-	Second side-to-side notch filter zero's damping
UPNA_WT_Control.PitchControlLoop.Notch2sidetoside.Dampp	-	Second side-to-side notch filter pole's damping
UPNA_WT_Control.PitchControlLoop.Notch2sidetoside.wnz	rad/s	Second side-to-side notch filter zero's natural frequency
UPNA_WT_Control.PitchControlLoop.Notch2sidetoside.wnp	rad/s	Second side-to-side notch filter pole's natural frequency
UPNA_WT_Control.PitchControlLoop.Notch2sidetoside.enable	-	Second side-to-side notch filter enabler
UPNA_WT_Control.PitchControlLoop.Notch2sidetoside.initialvalue	-	Second side-to-side notch filter initial value
UPNA_WT_Control.PitchControlLoop.Notch1foreaft.Gain	-	First fore-aft notch filter gain
UPNA_WT_Control.PitchControlLoop.Notch1foreaft.Dampz	-	First fore-aft notch filter zero's damping
UPNA_WT_Control.PitchControlLoop.Notch1foreaft.Dampp	-	First fore-aft notch filter pole's damping
UPNA_WT_Control.PitchControlLoop.Notch1foreaft.wnz	rad/s	First fore-aft notch filter zero's natural frequency
UPNA_WT_Control.PitchControlLoop.Notch1foreaft.wnp	rad/s	First fore-aft notch filter pole's natural frequency
UPNA_WT_Control.PitchControlLoop.Notch1foreaft.enable	-	First fore-aft notch filter enabler
UPNA_WT_Control.PitchControlLoop.Notch1foreaft.initialvalue	-	First fore-aft notch filter initial value
UPNA_WT_Control.PitchControlLoop.Notch3P.Gain	-	3P notch filter gain
UPNA_WT_Control.PitchControlLoop.Notch3P.Dampz	-	3P notch filter zero's damping
UPNA_WT_Control.PitchControlLoop.Notch3P.Dampp	-	3P notch filter pole's damping
UPNA_WT_Control.PitchControlLoop.Notch3P.enable	-	3P notch filter enabler
UPNA_WT_Control.PitchControlLoop.Notch3P.initialvalue	-	3P notch filter initialvalue
UPNA_WT_Control.PitchControlLoop.Notch3P.NumP	-	Number of blades, used to calculate the 3P frequency with the generator speed and gearbox ratio

UPNA_WT_Control.PitchControlLoop.Notch1P.Gain	-	1P notch filter gain
UPNA_WT_Control.PitchControlLoop.Notch1P.Dampz	-	1P notch filter zero's damping
UPNA_WT_Control.PitchControlLoop.Notch1P.Dampp	-	1P notch filter pole's damping
UPNA_WT_Control.PitchControlLoop.Notch1P.enable	-	1P notch filter enabler
UPNA_WT_Control.PitchControlLoop.Notch1P.initialvalue	-	1P notch filter initialvalue
UPNA_WT_Control.PitchControlLoop.LowPass.Gain	-	First order low pass filter gain
UPNA_WT_Control.PitchControlLoop.LowPass.thau	s	Time constant of the first order low pass filter at 0.5Hz
	s	Time constant of the first order low pass filter at 1Hz
	s	Time constant of the first order low pass filter at 2Hz
UPNA_WT_Control.PitchControlLoop.LowPass.enable	-	First order low pass filter enabler
UPNA_WT_Control.PitchControlLoop.LowPass.initialvalue	-	First order low pass filter initial value
UPNA_WT_Control.PitchControlLoop.PIDcontroler.Kpini	-	Initial Kp for the pitch control loop PID's gain scheduling
UPNA_WT_Control.PitchControlLoop.PIDcontroler.Kiini	-	Initial Ki for the pitch control loop PID's gain scheduling
UPNA_WT_Control.PitchControlLoop.PIDcontroler.Kpfin	-	Final Kp for the pitch control loop PID's gain scheduling
UPNA_WT_Control.PitchControlLoop.PIDcontroler.Kifin	-	Final Ki for the pitch control loop PID's gain scheduling
UPNA_WT_Control.PitchControlLoop.PIDcontroler.Beta13	deg	Initial blade pitch angle for the pitch control loop PID's gain scheduling
UPNA_WT_Control.PitchControlLoop.PIDcontroler.Beta21	deg	Final blade pitch angle for the pitch control loop PID's gain scheduling
UPNA_WT_Control.PitchControlLoop.PIDcontroler.Kd	-	Pitch control loop PID's Kd, there is no derivative term
UPNA_WT_Control.PitchControlLoop.PIDcontroler.thaud	s	Pitch control loop PID's filter's time constant
UPNA_WT_Control.PitchControlLoop.PIDcontroler.enable	-	Pitch control loop PID's enabler
UPNA_WT_Control.PitchControlLoop.PIDcontroler.initialvalue	deg	Pitch control loop PID's initial value
UPNA_WT_Control.PitchControlLoop.PIDcontroler.minpitchangle	deg	Minimum blade pitch angle
UPNA_WT_Control.PitchControlLoop.PIDcontroler.maxpitchangle	deg	Maximum blade pitch angle

Table 9: Pitch control parameter explanation

Also, the time constant of the low pass filter depends on where the filter cutoff frequency is placed. The load analysis has been carried out with low pass filters placed at 0.5Hz, 1Hz and 2Hz, for which the time constants are shown in the table.

4.4.3. Torque control loop

The torque control loop's parameters are shown next as well as the Simulink block of the torque control.

Torque control Simulink model

The next figure shows the torque control Simulink model with its inputs and outputs.

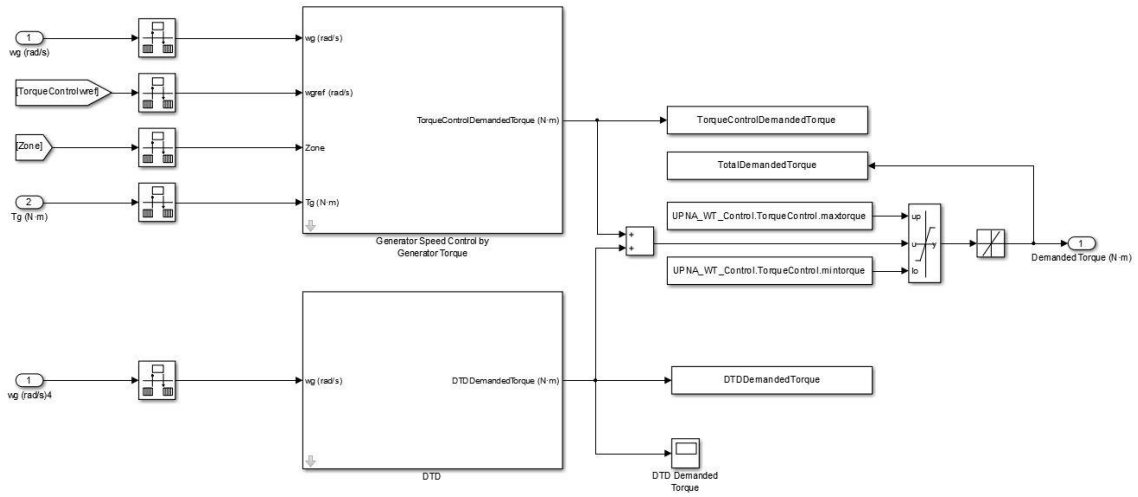

Figure 68:Simulink model of the Torque Control Loop

Given that the torque control, just like the pitch control with the ATD, is limited after the contribution of the DTD to the demanded torque, the figure also shows the DTD block.

The inputs to the torque control block are measured generator speed, measured generator torque and the generator speed reference and operating zone that exit the Supervisory Control. The only output is the torque control demanded torque, which, after being limited (by rate and saturation) and converted to FAST units, enters the S-Function.

Next, the inside of the torque control block is shown.

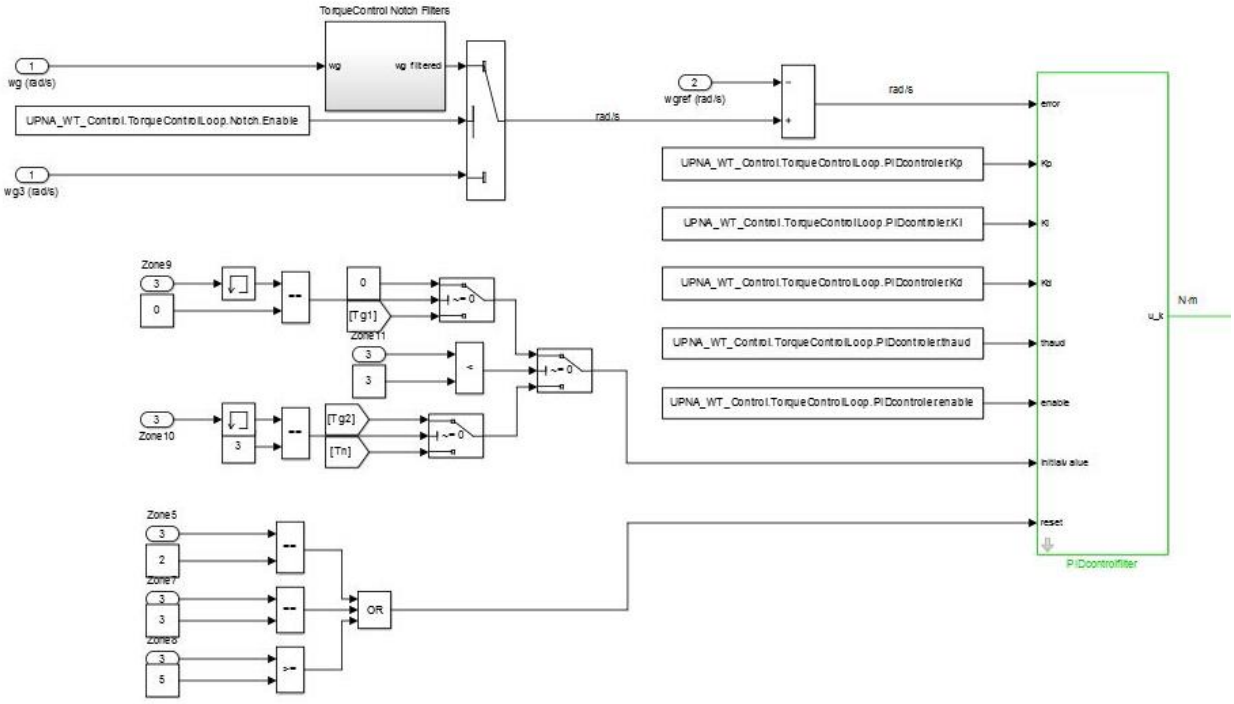

Figure 69: Internal Simulink model of the Torque Control Loop, filters and PID

The first step is the filtering of the signal. There is a block that includes all the notch filters of the torque control, that can be activated and deactivated with the notch enabler (apart from the individual enablers each filter has).

The next block in the torque control is the PID, which, unlike the pitch control, has an anti-windup strategy. This consists of a torque reset to T_{g1}, T_{g2} or T_{gn} depending on the operating zone. The reset is carried out when the operating zones are 2, 3 or 5.

This way, if the control enters the 1st vertical after operating in the quadratic curve (2nd operating zone), the torque will be reset to an initial value of T_{g1} to start controlling the demanded torque. In the same way, entering the 2nd vertical from the quadratic curve (entering operating zone 4 coming from zone 3) will reset the PID to an initial value of T_{g2}, just like when entering the 2nd vertical from the above rated zone (5th zone), would reset the PID to an initial value of T_{gnom}.

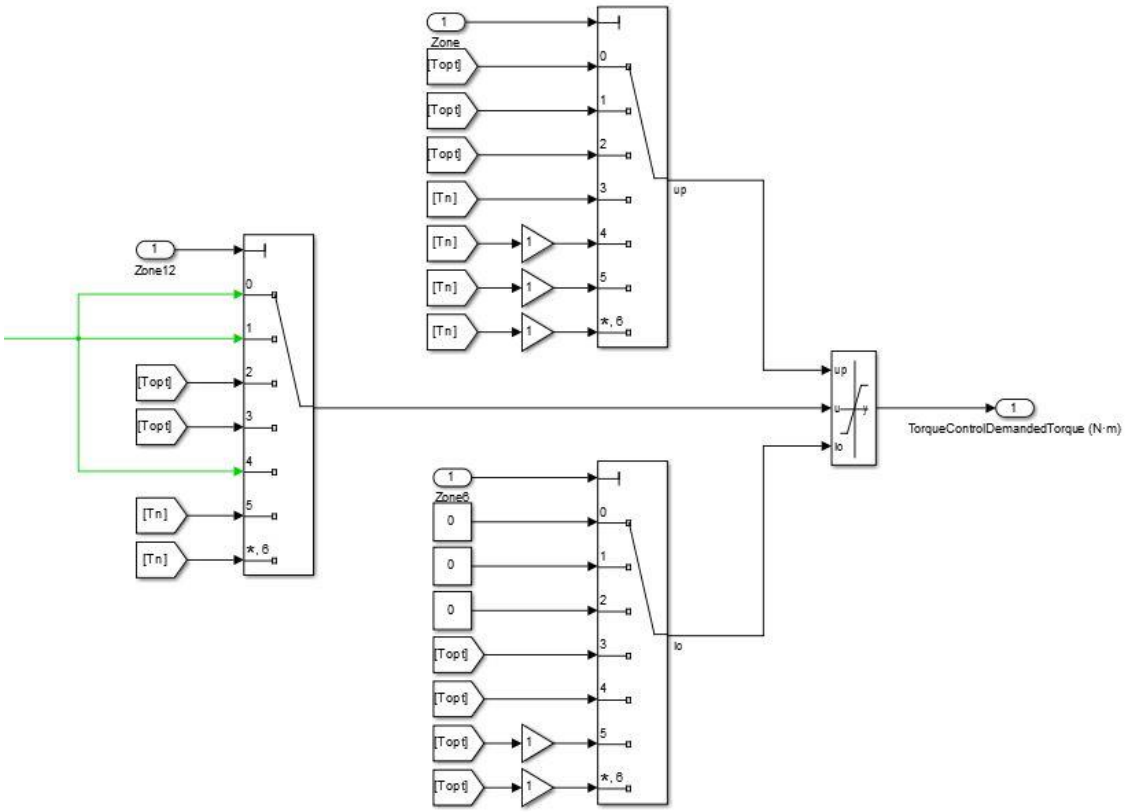

Figure 70: Internal Simulink model of the Torque Control Loop, torque limits

After the PID comes a switch block that limits the generator demanded torque in the above rated zone to T_n and also limits the torque to the optimal torque in the quadratic curve. This optimal value T_{opt} depends on the measured generator speed and it is calculated inside this torque control block.

Finally, there are a couple switches and a rate limiter that limit the torque control demanded torque.

Torque control parameters

TORQUE CONTROL		
Parameter	**Units**	**Explanation**
UPNA_WT_Control.TorqueControlLoop.SampleTime	s	Torque control loop sample time
UPNA_WT_Control.TorqueControlLoop.Notch.Enable	-	Enabler of all the notch filters of the torque control loop
UPNA_WT_Control.TorqueControl.maxtorque	N·m	Maximum torque limit set by the torque control loop
UPNA_WT_Control.TorqueControl.mintorque	N·m	Minimum torque limit set by the torque control loop
UPNA_WT_Control.TorqueControl.maxratetorque	N·m/s	Maximum torque rate variations of demanded torque
UPNA_WT_Control.TorqueControl.minratetorque	N·m/s	Minimum torque rate variations of demanded torque, maximum demanded torque reduction rate
UPNA_WT_Control.TorqueControlLoop.NotchDT.Gain	-	Drivetrain notch filter gain
UPNA_WT_Control.TorqueControlLoop.NotchDT.Dampz	-	Drivetrain notch filter zero's damping
UPNA_WT_Control.TorqueControlLoop.NotchDT.Dampp	-	Drivetrain notch filter pole's damping
UPNA_WT_Control.TorqueControlLoop.NotchDT.wnz	rad/s	Drivetrain notch filter zero's natural frequency
UPNA_WT_Control.TorqueControlLoop.NotchDT.wnp	rad/s	Drivetrain notch filter pole's natural frequency
UPNA_WT_Control.TorqueControlLoop.NotchDT.enable	-	Drivetrain notch filter enabler
UPNA_WT_Control.TorqueControlLoop.NotchDT.initialvalue	-	Drivetrain notch filter initial value
UPNA_WT_Control.TorqueControlLoop.Notch1simetrica.Gain	-	First symmetric notch filter gain
UPNA_WT_Control.TorqueControlLoop.Notch1simetrica.Dampz	-	First symmetric notch filter zero's damping
UPNA_WT_Control.TorqueControlLoop.Notch1simetrica.Dampp	-	First symmetric notch filter pole's damping
UPNA_WT_Control.TorqueControlLoop.Notch1simetrica.wnz	rad/s	First symmetric notch filter zero's natural frequency
UPNA_WT_Control.TorqueControlLoop.Notch1simetrica.wnp	rad/s	First symmetric notch filter pole's natural frequency
UPNA_WT_Control.TorqueControlLoop.Notch1simetrica.enable	-	First symmetric notch filter enabler
UPNA_WT_Control.TorqueControlLoop.Notch1simetrica.initialvalue	-	First symmetric notch filter initial value
UPNA_WT_Control.TorqueControlLoop.Notch2simetrica.Gain	-	Second symmetric notch filter gain
UPNA_WT_Control.TorqueControlLoop.Notch2simetrica.Dampz	-	Second symmetric notch filter zero's damping

UPNA_WT_Control.TorqueControlLoop.Notch2simetrica.Dampp	-	Second symmetric notch filter pole's damping
UPNA_WT_Control.TorqueControlLoop.Notch2simetrica.wnz	rad/s	Second symmetric notch filter zero's natural frequency
UPNA_WT_Control.TorqueControlLoop.Notch2simetrica.wnp	rad/s	Second symmetric notch filter pole's natural frequency
UPNA_WT_Control.TorqueControlLoop.Notch2simetrica.enable	-	Second symmetric notch filter enabler
UPNA_WT_Control.TorqueControlLoop.Notch2simetrica.initialvalue	-	Second symmetric notch filter initial value
UPNA_WT_Control.TorqueControlLoop.Notch2sidetoside.Gain	-	Second side-to-side notch filter gain
UPNA_WT_Control.TorqueControlLoop.Notch2sidetoside.Dampz	-	Second side-to-side notch filter zero's damping
UPNA_WT_Control.TorqueControlLoop.Notch2sidetoside.Dampp	-	Second side-to-side notch filter pole's damping
UPNA_WT_Control.TorqueControlLoop.Notch2sidetoside.wnz	rad/s	Second side-to-side notch filter zero's natural frequency
UPNA_WT_Control.TorqueControlLoop.Notch2sidetoside.wnp	rad/s	Second side-to-side notch filter pole's natural frequency
UPNA_WT_Control.TorqueControlLoop.Notch2sidetoside.enable	-	Second side-to-side notch filter enabler
UPNA_WT_Control.TorqueControlLoop.Notch2sidetoside.initialvalue	-	Second side-to-side notch filter initial value
UPNA_WT_Control.TorqueControlLoop.Notch1foreaft.Gain	-	First fore-aft notch filter gain
UPNA_WT_Control.TorqueControlLoop.Notch1foreaft.Dampz	-	First fore-aft notch filter zero's damping
UPNA_WT_Control.TorqueControlLoop.Notch1foreaft.Dampp	-	First fore-aft notch filter pole's damping
UPNA_WT_Control.TorqueControlLoop.Notch1foreaft.wnz	rad/s	First fore-aft notch filter zero's natural frequency
UPNA_WT_Control.TorqueControlLoop.Notch1foreaft.wnp	rad/s	First fore-aft notch filter pole's natural frequency
UPNA_WT_Control.TorqueControlLoop.Notch1foreaft.enable	-	First fore-aft notch filter enabler
UPNA_WT_Control.TorqueControlLoop.Notch1foreaft.initialvalue	-	First fore-aft notch filter initial value
UPNA_WT_Control.TorqueControlLoop.Notch3P.Gain	-	3P notch filter gain
UPNA_WT_Control.TorqueControlLoop.Notch3P.Dampz	-	3P notch filter zero's damping
UPNA_WT_Control.TorqueControlLoop.Notch3P.Dampp	-	3P notch filter pole's damping
UPNA_WT_Control.TorqueControlLoop.Notch3P.enable	-	3P notch filter enabler
UPNA_WT_Control.TorqueControlLoop.Notch3P.initialvalue	-	3P notch filter initialvalue

UPNA_WT_Control.TorqueControlLoop.Notch3P.NumP	-	Number of blades, used to calculate the 3P frequency with the generator speed and gearbox ratio
UPNA_WT_Control.TorqueControlLoop.Notch1P.Gain	-	1P notch filter gain
UPNA_WT_Control.TorqueControlLoop.Notch1P.Dampz	-	1P notch filter zero's damping
UPNA_WT_Control.TorqueControlLoop.Notch1P.Dampp	-	1P notch filter pole's damping
UPNA_WT_Control.TorqueControlLoop.Notch1P.enable	-	1P notch filter enabler
UPNA_WT_Control.TorqueControlLoop.Notch1P.initialvalue	-	1P notch filter initialvalue
UPNA_WT_Control.TorqueControlLoop.PIDcontroler.Kp	-	Torque control loop PID's Kp
UPNA_WT_Control.TorqueControlLoop.PIDcontroler.Ki	-	Torque control loop PID's Ki
UPNA_WT_Control.TorqueControlLoop.PIDcontroler.Kd	-	Torque control loop PID's Kd, there is no derivative term
UPNA_WT_Control.TorqueControlLoop.PIDcontroler.thaud	s	Torque control loop PID's filter's time constant
UPNA_WT_Control.TorqueControlLoop.PIDcontroler.enable	-	Torque control loop PID's enabler
UPNA_WT_Control.TorqueControlLoop.PIDcontroler.initialvalue	N·m	Torque control loop PID's initial value

Table 10: Torque control parameter explanation

4.4.4.DTD

DTD Simulink model

Just like it was explained in the previous section, the DTD's torque demand is added to that of the torque control before the limitations are made. This is shown in the next figure.

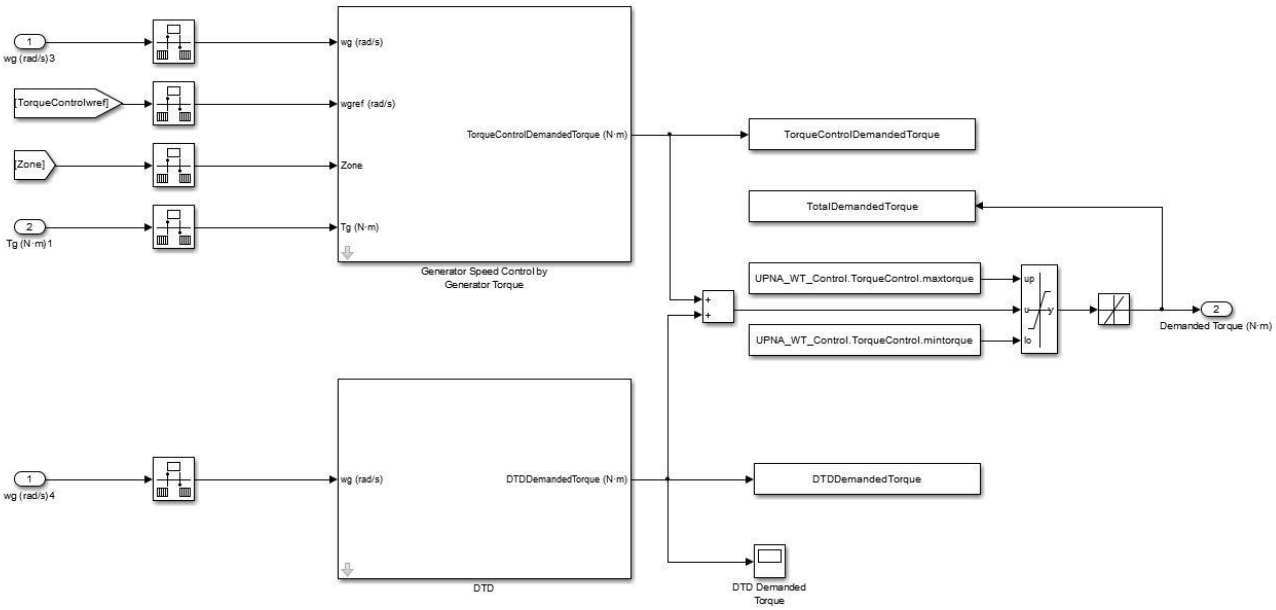

Figure 71: Simulink model of the DTD

The previous figure shows the only input the DTD has is the measured generator speed and the only output is the DTD demanded torque T_{DTD}. Next, the inside of the DTD block is shown.

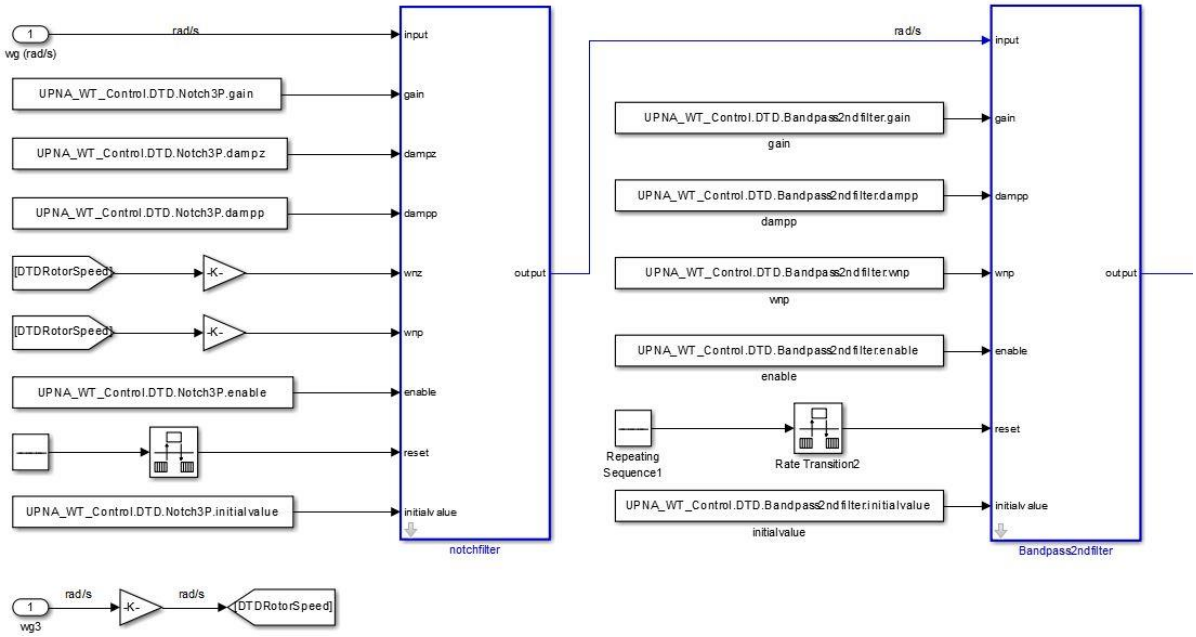

Figure 72: Internal Simulink model of the DTD, filters

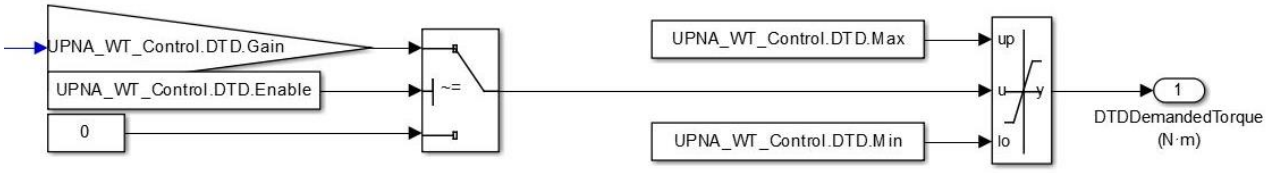

Figure 73: Internal Simulink model of the DTD, DTD gains and limits

The previous two figures show how the DTD is composed of a 3P notch filter, a 2nd order band pass filter, the DTD enabler, external gain and its limitations.

DTD control parameters

DTD		
Parameter	**Units**	**Explanation**
UPNA_WT_Control.DTD.SampleTime	s	DTD block's sample time
UPNA_WT_Control.DTD.Gain	-	DTD external gain
UPNA_WT_Control.DTD.Enable	-	DTD enabler
UPNA_WT_Control.DTD.Max	N·m	Maximum DTD torque limitation
UPNA_WT_Control.DTD.Min	N·m	Minimum DTD torque limitation, it is the maximum torque the DTD can substract from the demanded torque
UPNA_WT_Control.DTD.Bandpass2ndfilter.gain	-	DTD band pass filter gain
UPNA_WT_Control.DTD.Bandpass2ndfilter.dampp	-	DTD band pass filter dampp
UPNA_WT_Control.DTD.Bandpass2ndfilter.wnp	rad/s	DTD band pass filter pole's natural frequency
UPNA_WT_Control.DTD.Bandpass2ndfilter.enable	-	DTD band pass filter enabler
UPNA_WT_Control.DTD.Bandpass2ndfilter.initialvalue	-	DTD band pass filter initial value
UPNA_WT_Control.DTD.Notch3P.gain	-	DTD 3P notch gain
UPNA_WT_Control.DTD.Notch3P.dampz	-	DTD 3P notch zero's damping
UPNA_WT_Control.DTD.Notch3P.dampp	-	DTD 3P notch pole's damping
UPNA_WT_Control.DTD.Notch3P.enable	-	DTD 3P notch filter enabler
UPNA_WT_Control.DTD.Notch3P.initialvalue	-	DTD 3P notch filter initial value
UPNA_WT_Control.DTD.Notch3P.NumP	-	Number of blades, used to calculate the 3P frequency with the generator speed and gearbox ratio

Table 11: DTD parameter explanation

4.4.5.ATD

ATD Simulink model

The ATD demanded pitch, just like the DTD torque, is added to the pitch control demanded pitch before the rate and saturation limitations. This is shown in the next figure.

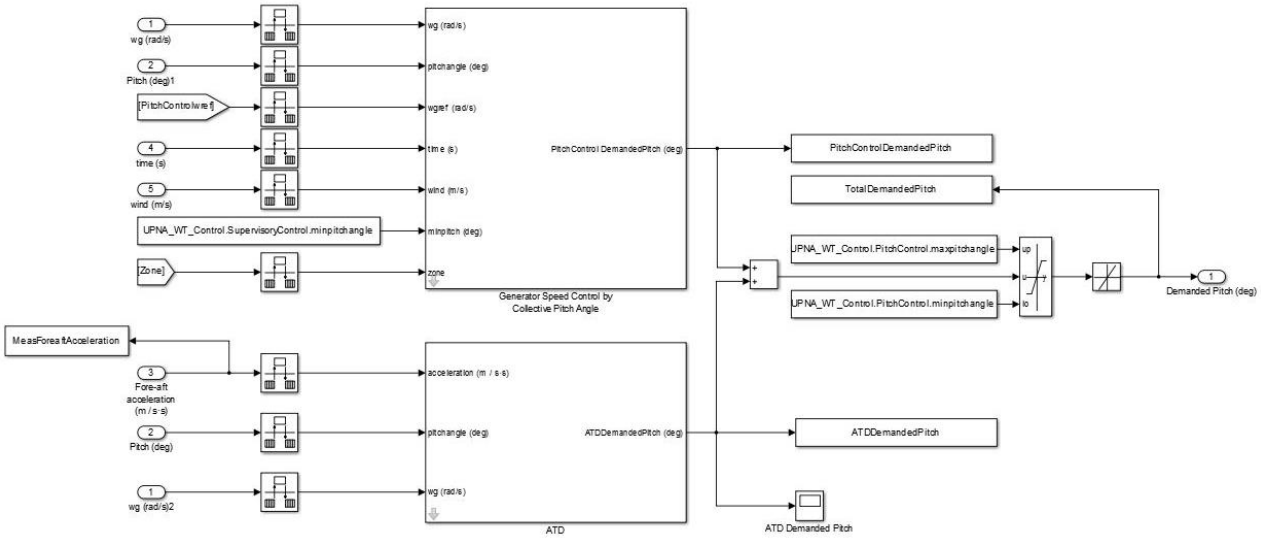

Figure 74: Simulink model of the ATD

The inputs to the ATD block are measured tower top fore-aft acceleration, the measured pitch angle, and the measured generator speed, with the only output of the ATD demanded pitch. The inside of the ATD block is shown in the next figure.

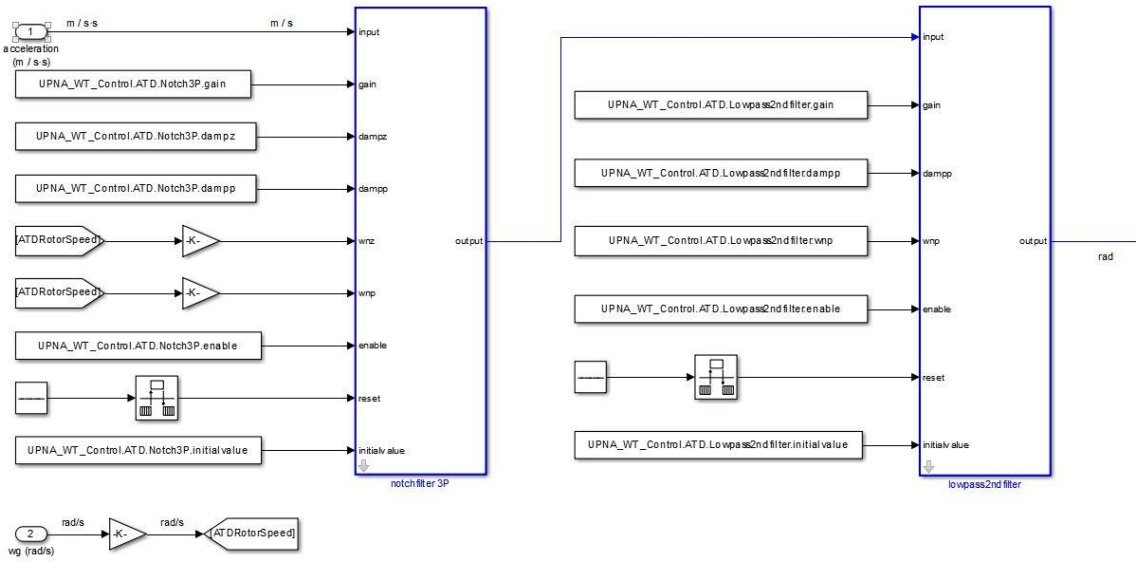

Figure 75: Internal Simulink model of the ATD, filters

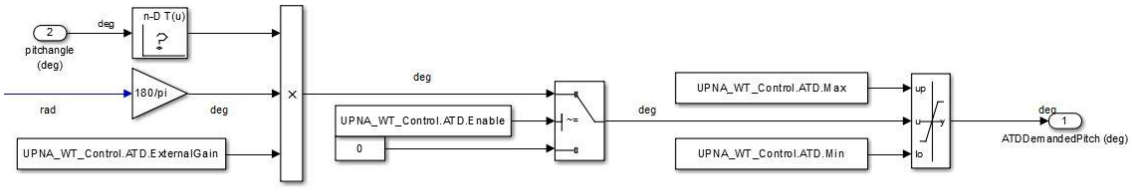

Figure 76: Internal Simulink model of the ATD, ATD gain scheduling and limits

The two previous figures show that the ATD is composed of a notch filter at the 3P frequency, a low pass 2nd order filter, the gain scheduling that introduces the ATD gradually as pitch increases, an ATD enabler and the ATD pitch upper and lower limitations.

ATD control parameters

ATD		
Parameter	**Units**	**Explanation**
UPNA_WT_Control.ATD.SampleTime	s	ATD block's sample time
UPNA_WT_Control.ATD.ExternalGain	-	ATD external gain
UPNA_WT_Control.ATD.Enable	-	ATD enabler
UPNA_WT_Control.ATD.Max	deg	Maximium ATD pitch angle limitation
UPNA_WT_Control.ATD.Min	deg	Minimum ATD pitch angle limitation
UPNA_WT_Control.ATD.Gain.Kini	-	ATD gain scheduling initial gain
UPNA_WT_Control.ATD.Gain.Kfin	-	ATD gain scheduling final gain
UPNA_WT_Control.ATD.Gain.Betaini	deg	ATD gain scheduling initial pitch angle
UPNA_WT_Control.ATD.Gain.Betafin	deg	ATD gain scheduling final pitch angle
UPNA_WT_Control.ATD.Gain.minpitchangle	deg	ATD gain scheduling x minimum limit
UPNA_WT_Control.ATD.Gain.maxpitchangle	deg	ATD gain scheduling x maximum limit
UPNA_WT_Control.ATD.Lowpass2ndfilter.gain	-	ATD second order low pass filter gain
UPNA_WT_Control.ATD.Lowpass2ndfilter.dampp	-	ATD second order low pass filter pole's damping
UPNA_WT_Control.ATD.Lowpass2ndfilter.wnp	rad/s	ATD second order low pass filter pole's natural frequency
UPNA_WT_Control.ATD.Lowpass2ndfilter.enable	-	ATD second order low pass filter enabler
UPNA_WT_Control.ATD.Lowpass2ndfilter.initialvalue	-	ATD second order low pass filter initial value
UPNA_WT_Control.ATD.Notch3P.Gain	-	ATD 3P notch filter gain
UPNA_WT_Control.ATD.Notch3P.Dampz	-	ATD 3P notch filter zero's damping
UPNA_WT_Control.ATD.Notch3P.Dampp	-	ATD 3P notch filter pole's damping
UPNA_WT_Control.ATD.Notch3P.enable	-	ATD 3P notch filter enabler
UPNA_WT_Control.ATD.Notch3P.initialvalue	-	ATD 3P notch filter initial value
UPNA_WT_Control.ATD.Notch3P.NumP	-	Number of blades, used to calculate the 3P frequency with the generator speed and gearbox ratio

Table 12: ATD parameter explanation

Chapter 5: Baseline Control Tuning for 5MW Upwind model in FASTv7

5.1. Introduction

The next step in the design of the control strategy is the control tuning. This is, adjusting the values of the PIDs' and filters' parameters to achieve the desired performance of the control system.

The first requirement of the control is always the system's stability. Some values of the PID's or the filters' parameters can make the system unstable. When checking stability, the first step is to introduce the DTD to ensure a good damping value in the drive train mode. Then, phase and gain margins must be checked in an open loop Bode diagram of the pitch and torque control loops used to regulate the generator speed in different control zones. The last step is to check that, when introducing the ATD, the system's stability does not get jeopardized and that the ATD provides the correct damping value in the tower's fore-aft 1st mode.

The second requirement varies from one system to another. Depending on the application, a system can require a faster response, a lower overshoot, etc. The main two control objectives that determine this second requirement are whether the control is designed to reject disturbance (control regulation) or to follow the reference (reference tracking).

Reference tracking refers to how well the control system implements a change in reference. The requirements that a control with this objective must fulfill are both low rise time and low settling time.

Control regulation, on the other side, is focused on rejecting the disturbance and remaining as close as possible to the operating point despite a disturbance input. The objective of wind turbine control and therefore the objective of the control scheme designed in this project is to reject its main disturbance, the wind.

To adjust the control's parameters, the linear models previously obtained by FAST linearizations are necessary. From these linear models, the state matrices of the wind turbine's plants can be developed. This means the single-input single-output plants can be obtained and used together with the continuous-time Laplace forms of the control blocks in order to check, adjust and optimize the system's behavior.

As the linearizations are carried out in several linearization points, the control tuning can only be done at those operating points. Particularly, it has been carried out at 5m/s, 11m/s, 13m/s, 19m/s and 25m/s. With the values of the parameters at those operating points, the optimal values for the parameters (including the ones that have gain scheduling) are obtained.

It is known, at each operating point, which elements of the control are active. This, together with the wind turbine's linear plants results in a continuous-time Laplace representation of the whole system at that point.

By a single-input single-output control design method and the MATLAB GUI (Graphical User Inteface) tool sisotool, the optimal values of the parameters for that system are obtained. This tool allows a quick, online response of how changing the parameters affects the system's performance. A lot of different aspects of the system such as open loop stability, closed loop behavior, root locus zero and pole positions or the system's step response can be checked with this tool.

The resulting parameter values of the control tuning are shown and explained in the next sections.

5.2. Supervisory Control

5.2.1.Parameters

SUPERVISORY CONTROL		
Parameter	**Value**	**Units**
UPNA_WT_Control.SupervisoryControl.SampleTime	0.1	s
UPNA_WT_Control.SupervisoryControl.w1	41.88	rad/s
UPNA_WT_Control.SupervisoryControl.wgn	122.91	rad/s
UPNA_WT_Control.SupervisoryControl.Pn	5000000	W
UPNA_WT_Control.SupervisoryControl.minpitchangle	0.106	deg
UPNA_WT_Control.SupervisoryControl.maxpitchangle	90	deg
UPNA_WT_Control.SupervisoryControl.Kopt	2.3323	$N \cdot m/(rad/s)^2$
UPNA_WT_Control.SupervisoryControl.Tn	43121	N·m
UPNA_WT_Control.SupervisoryControl.minpitchdiff	0.1	deg
UPNA_WT_Control.SupervisoryControl.vnom	11.4	m/s
UPNA_WT_Control.SupervisoryControl.GearBoxRatio	97	-
UPNA_WT_Control.SupervisoryControl.GeneratorSpeedMax	153.64	rad/s
UPNA_WT_Control.SupervisoryControl.GeneratorSpeedMaxIniTime	100	s
UPNA_WT_Control.SupervisoryControl.maxratepitchangle	8	deg/s
UPNA_WT_Control.SupervisoryControl.minratepitchangle	-8	deg/s
UPNA_WT_Control.SupervisoryControl.maxratetorque	20000	N·m/s
UPNA_WT_Control.SupervisoryControl.minratetorque	-20000	N·m/s

Table 13: Supervisory control parameter values

Most of these values, such as nominal generator speed, rated power, etc. come straight from the specifications of the wind turbine. Others, such as Kopt, are calculated from those specifications. The rest, are obtained either from security hardware limits of operation (as in blade pitch angle rate or maximum torque rate) or because with those values, the desired behavior is obtained during simulation.

For example, the maximum generator speed has been set to a 25% over the nominal speed (w_{gn}) so that if the generator speed increases above 1.25 times the desired speed, the emergency stop would activate. Also, the emergency stop has an activation time, in this case, 100s. This is done to avoid having the wind turbine stop if the generator speed is too high at the beginning of the simulation due to initialization issues.

5.3. DTD

5.3.1.Control performance

The drive train mode is coupled with other modes of the wind turbine. This can cause instability of the system, so the first task when designing the control strategy of a wind turbine is to give damping to the drive train mode. Therefore, the DTD is the first control block to be designed.

Given that the DTD is always activated, the behavior of the system at different wind speeds in every operating zone will be shown.

The operating zones are the ones indicated in Figure 33 in Chapter 4: Wind Turbine Simulink Controller Block.

Zone 1: 1st vertical (5m/s)

In this zone, both the DTD and the torque control are active. Several Bode diagrams are graphed to show different aspects of the system's behavior due to the DTD.

The DTD is an element of the wind turbine's active control, it is placed in order to "affect" the plant's behavior. The performance of the plant alone and the plant when the DTD is added is shown in the next Bode diagram.

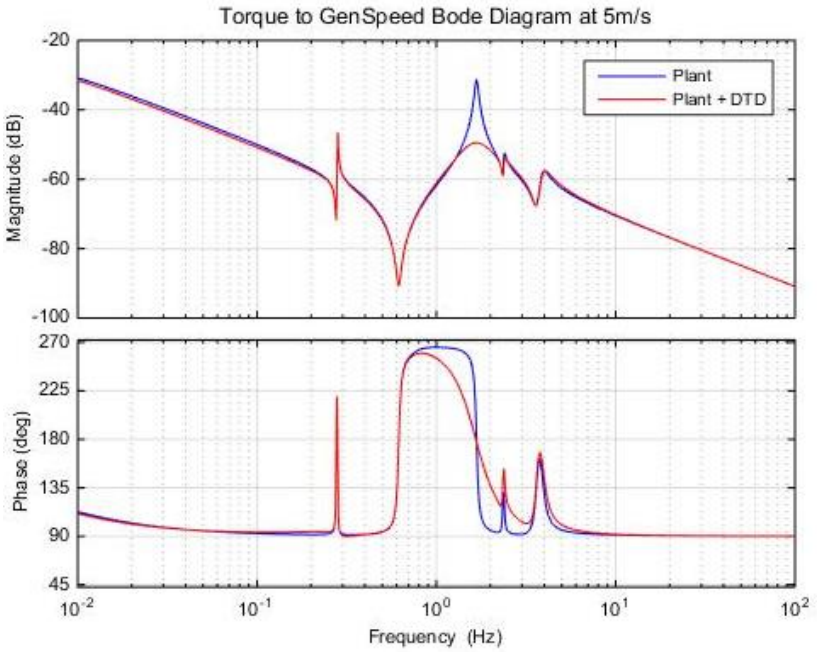

Figure 77: Bode diagram of the plant from torque to generator speed with and without DTD at 5m/s

The previous figure shows how, by adding the DTD, the drive train mode frequency is a lot less excited. This is because the DTD gives damping to this mode.

For some wind turbines, a variable DTD gain is required depending on the operating point. For this wind turbine model, introducing a DTD gain scheduling is not necessary.

Also, the disturbance sensibility (relation between the generator speed and the disturbance) of the DTD is shown in the next figure.

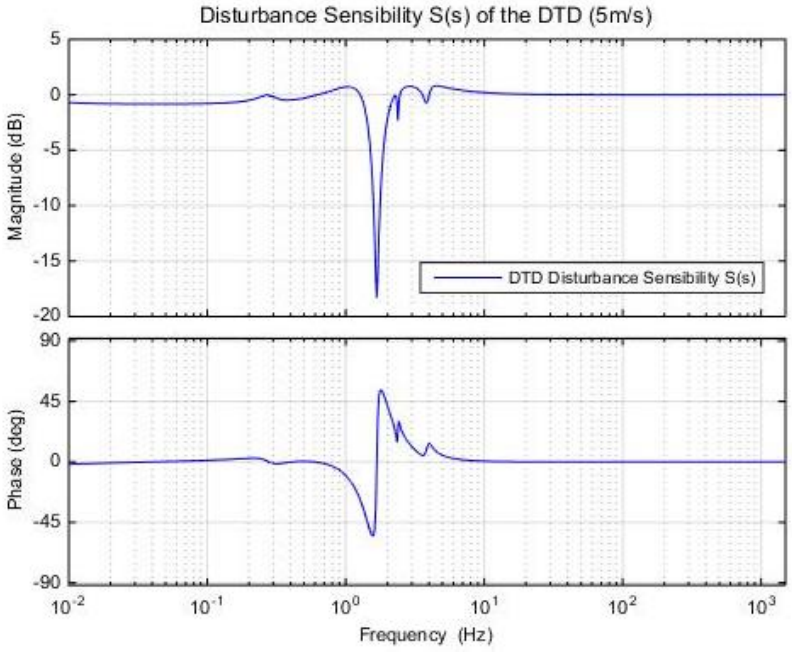

Figure 78: Bode diagram of the DTD's disturbance sensibility S(s) at 5m/s

The previous closed loop Bode diagram shows how any disturbance that enters the system at the drive train frequency will be highly attenuated by the DTD.

Zones 2 & 3: Quadratic curve (9 m/s)

In this zone there is no generator speed control, there is an open loop control. The only control element that will be active is the DTD.

The comparison between the plant's behavior with and without the DTD is shown again next, this time at a wind speed of 9m/s.

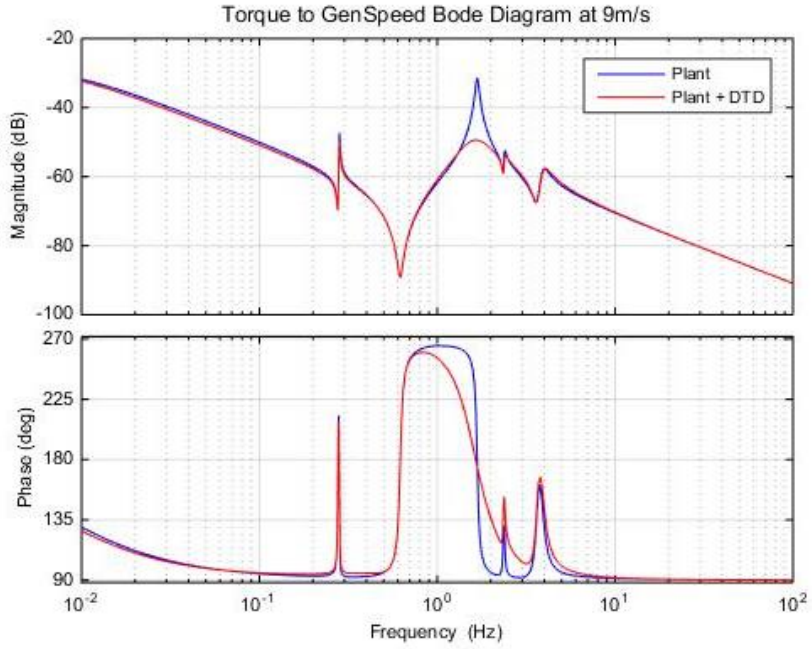

Figure 79: Bode diagram of the plant from torque to generator speed with and without DTD at 9m/s

In the next figure, the DTD's disturbance sensibility is also shown for a 9m/s wind speed.

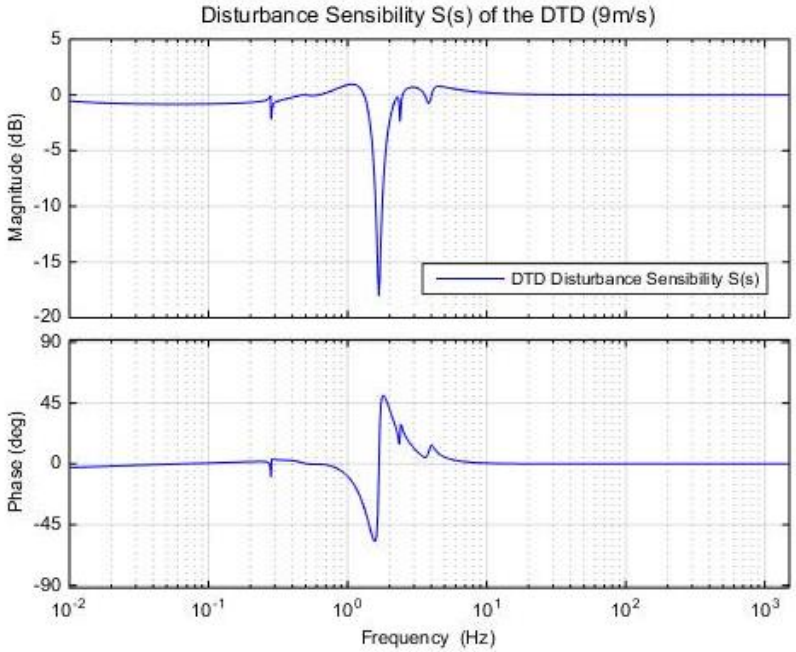

Figure 80: Bode diagram of the DTD's disturbance sensibility S(s) at 9m/s

Zone 4: 2nd vertical (11m/s)

In the 2nd vertical, just like in the 1st one, both the torque control loop and the DTD are active. Next, several Bode diagrams show the different behaviors of the control with and without the DTD. The next figure shows the difference in the performance of the plant with the addition of the DTD.

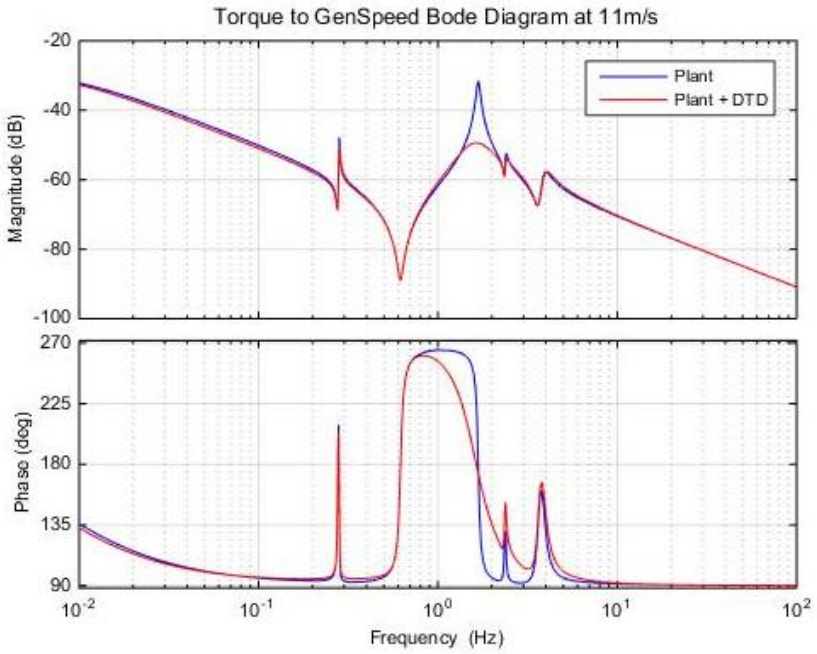

Figure 81: Bode diagram of the plant from torque to generator speed with and without DTD at 11m/s

The next Bode diagram shows the disturbance sensibility of the DTD in the second vertical, at 11m/s.

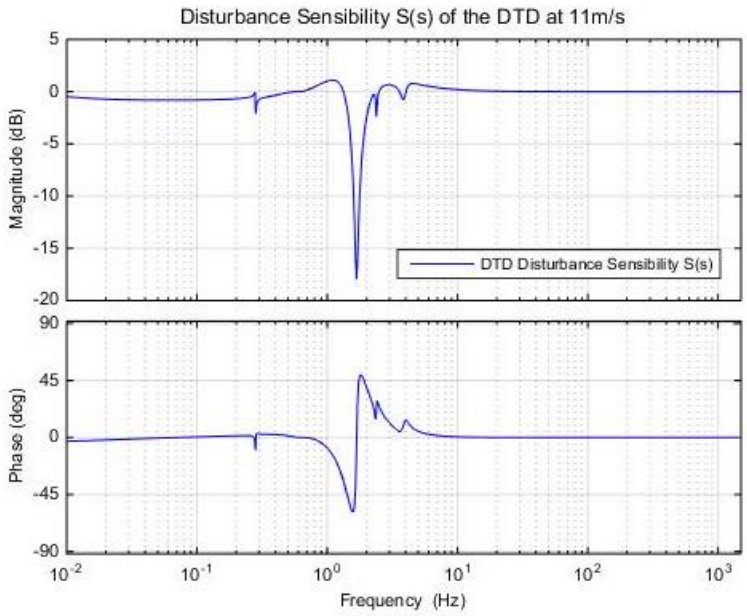

Figure 82: Bode diagram of the DTD's disturbance sensibility S(s) at 11m/s

The previous figure shows, just like at other operating points, that any disturbance entering the system at the drive train frequency will result highly attenuated by the DTD.

Zone 5: Above rated

As it was said, the DTD is activated along all the operating zones, including the above rated zone. For this reason, the behavior of the system due to the DTD's actuation will be shown in above rated wind speeds too.

The next figure shows the different behavior of the torque vs. generator speed plant due to the addition of the DTD at 19m/s.

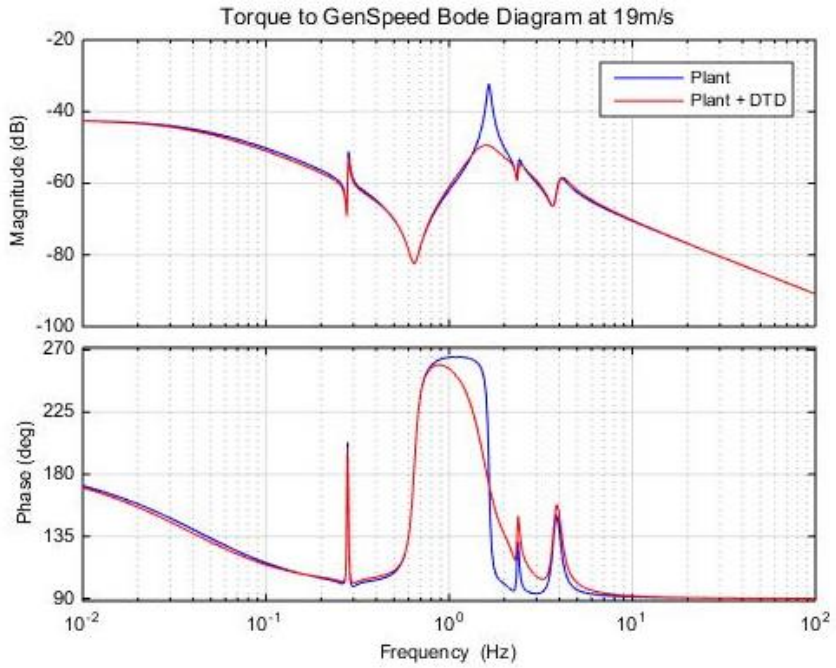

Figure 83: Bode diagram of the plant from torque to generator speed with and without DTD at 19m/s

Just like at lower wind speeds, the DTD gives damping to the excited drive train mode of the plant.

The next figure illustrates the closed loop disturbance rejection of the DTD at 19m/s.

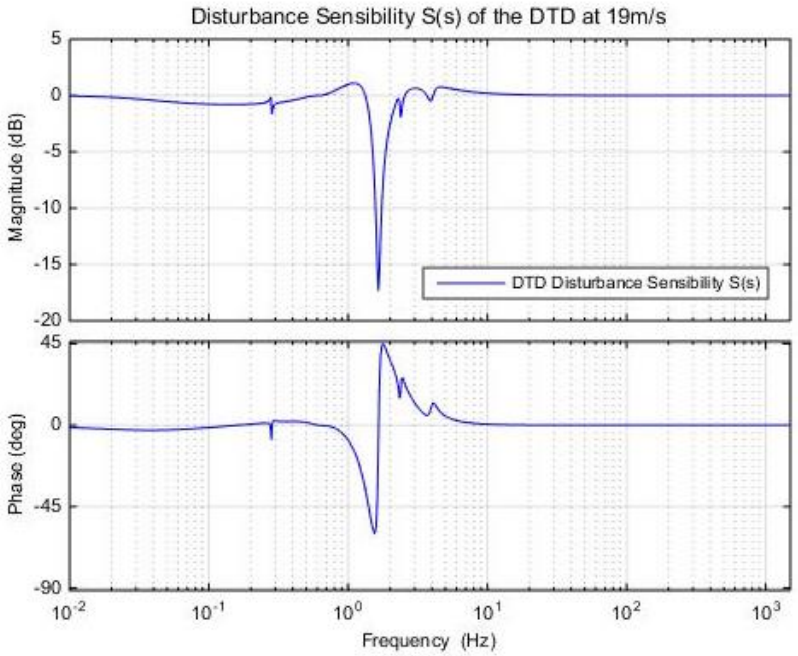

Figure 84: Bode diagram of the DTD's disturbance sensibility S(s) at 19m/s

The figure shows the attenuation that the DTD gives to any disturbance entering the system at the drive train frequency.

5.3.2.Parameters

DTD		
Parameter	**Value**	**Units**
UPNA_WT_Control.DTD.SampleTime	0.01	s
UPNA_WT_Control.DTD.Gain	2500	-
UPNA_WT_Control.DTD.Enable	1	-
UPNA_WT_Control.DTD.Max	2500	N·m
UPNA_WT_Control.DTD.Min	-2500	N·m
UPNA_WT_Control.DTD.Bandpass2ndfilter.gain	1	-
UPNA_WT_Control.DTD.Bandpass2ndfilter.dampp	0.984	-
UPNA_WT_Control.DTD.Bandpass2ndfilter.wnp	10.33	rad/s
UPNA_WT_Control.DTD.Bandpass2ndfilter.enable	1	-
UPNA_WT_Control.DTD.Bandpass2ndfilter.initialvalue	0	-
UPNA_WT_Control.DTD.Notch3P.gain	1	-
UPNA_WT_Control.DTD.Notch3P.dampz	0.01	-
UPNA_WT_Control.DTD.Notch3P.dampp	0.2	-
UPNA_WT_Control.DTD.Notch3P.enable	1	-
UPNA_WT_Control.DTD.Notch3P.initialvalue	0	-
UPNA_WT_Control.DTD.Notch3P.NumP	3	-

Table 14: DTD parameter values

These values are obtained by observing the effect that changing the DTD parameters has on the behavior of the Bode diagrams shown in the previous section. By using sisotool, the relation between the parameter and the system's behavior is more easily found.

In the MATLAB script, once again, the minimum and maximum torque values have been referred to the ones in the Supervisory Control so that, in case they need to be changed, changing them once is enough.

5.4. Torque Control

5.4.1.Control performance

Once the DTD has been designed, the next step is to design the torque control, which is designed with the main objective of rejecting disturbances. The capacity of a system for disturbance rejection can be seen in its disturbance sensibility graph. Two requirements in this graph must be met: a minimum band width and a maximum peak.

Depending on the application, different limits are set. For the torque control, the next limits are stablished for this specific wind turbine when doing the control tuning:

Torque Control Loop Disturbance Sensibility		
1st vertical	Band Width	≈ 0.04 Hz
	Peak	< 6 dB
2nd vertical	Band Width	≈ 0.08 Hz
	Peak	< 6 dB

Table 15: Torque Control disturbance sensibility requirements

The band width is the frequency at which the Bode crosses the cutoff frequency, -3dB. The bigger the band width, the better the system will reject low frequency disturbances.

The values of the parameters that make the system fulfill these requirements are found as a result of the control tuning. Also, as the band width gets bigger, higher frequencies are rejected, which makes the system faster. The drawback to this is that, as the band width increases, the magnitude peak of the disturbance rejection gets higher, which causes more oscillations in the time response. Since the maximum suitable peak is set to 6dB, a compromise between both requirements must be met. Nevertheless, a band width bigger than 0.1Hz is not desired either.

The behavior of the torque control loop is going to be explained in every operating zone. These zones correspond to the ones explained in Figure 85 in Chapter 4: Wind Turbine Simulink Controller Block.

Zone 1: 1st vertical

Before pursuing the design objective, the first aspect that must be checked when tuning the torque control loop is the system's stability, which can be seen in the open loop response of the system.

The behavior of the torque control, the DTD alone, the plant with the DTD and the open loop are shown in the next Bode diagram.

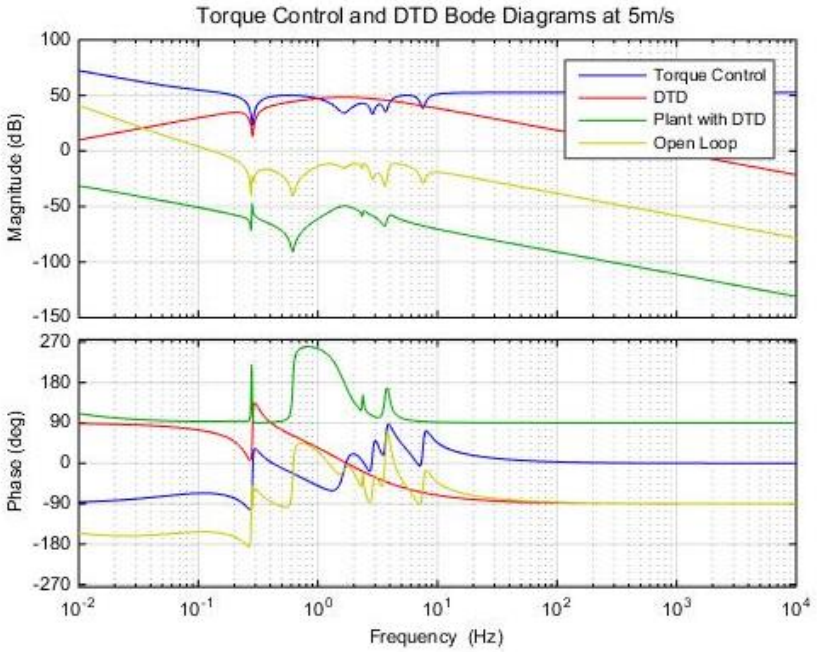

Figure 86: Bode diagram of the torque control, DTD, plant with DTD and open loop at 5m/s

While the open loop is looked at in order to check stability margins, the behavior is only checked in the closed loop. The next Bode diagram shows the stability margins of the open loop at a wind speed of 5m/s.

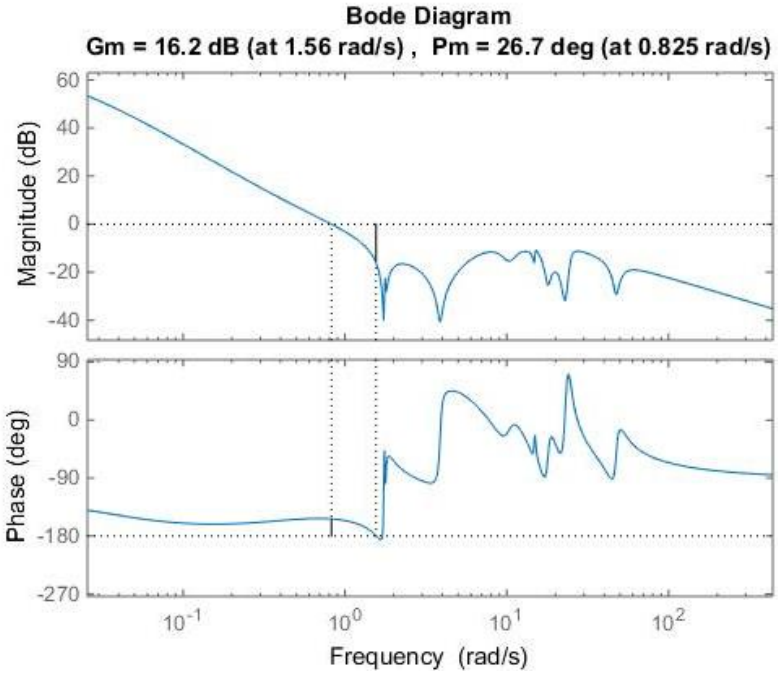

Figure 87: Gain and phase margins of the torque control at 5m/s

Some theoretical stability margins are a gain margin greater than 6dB and a phase margin between 30 and 60 degrees. The phase margin of this system is a little smaller but it is a suitable phase margin.

Once the system's stability has been checked, the parameters must be further adjusted in order to meet the torque control's main objective, the rejection of the system's disturbance. The main performance aspect that must be checked is the loop's disturbance sensibility.

As it was stated in table Table 15, the performance requirement for the torque control loop is to have a disturbance rejection response with a minimum band width of 0.04Hz and a maximum peak of 6dB.

The next figure shows the disturbance sensibility response of the torque control at 5m/s.

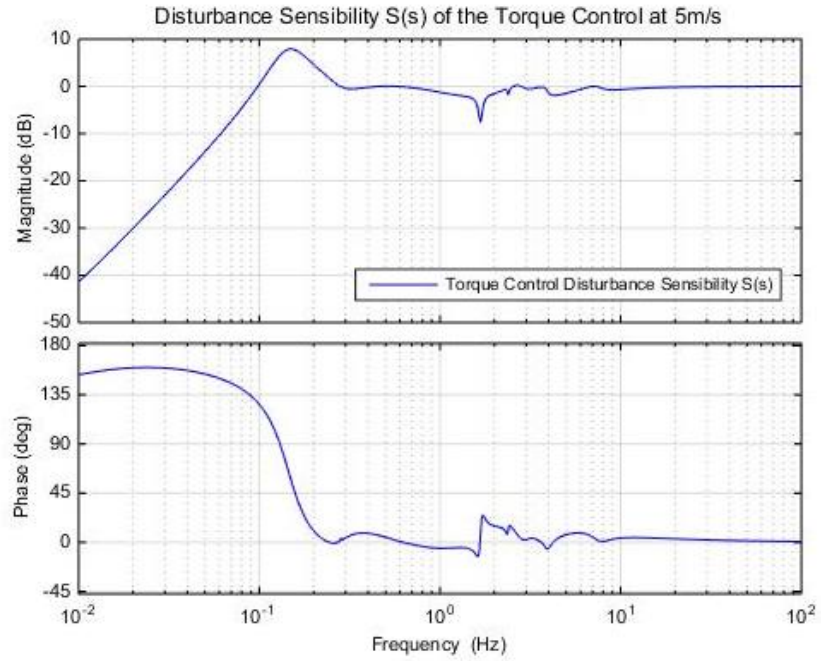

Figure 88: Bode diagram of torque control's disturbance sensibility S(s) at 5m/s

The exact BW and peak magnitude of the previous Bode diagram are shown in the next figure.

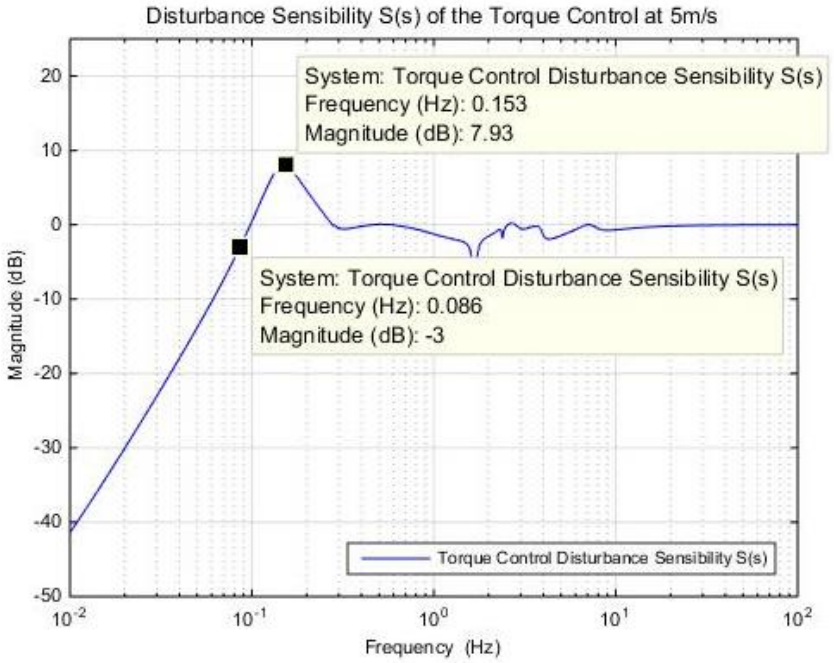

Figure 89: Band width and magnitude peak of the torque control's S(s) at 5m/s

In this case, a faster system has been chosen and the peak requirement has slightly been exceeded (7.93 dB instead of 6dB). This only happens in the first vertical and simulations have been checked to ensure that the peak does not affect the system's stability. The system is faster

because of the high band width (0.086Hz), which helps improve the generator speed tracking at the 1st vertical (coupling generator speed).

Zone 4: 2nd vertical

Since the torque control loop is not activated in the quadratic curve nor in the above rated zone, the performance of the system due to the torque control is shown in the 2nd vertical too.

The next bode shows the torque control, DTD only, plant with DTD and the open loop behavior of the plant with DTD and the torque control, where we can see the stability margins.

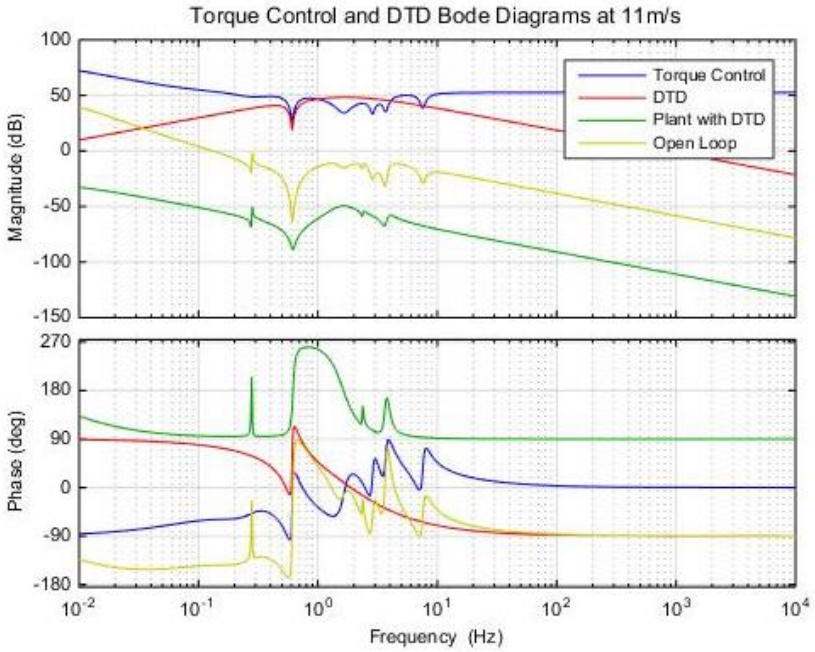

Figure 90: Bode diagram of the torque control, DTD, plant with DTD and open loop at 11m/s

Again, the open loop is graphed to check stability margins. The next Bode diagram shows the exact gain and phase margins of the system.

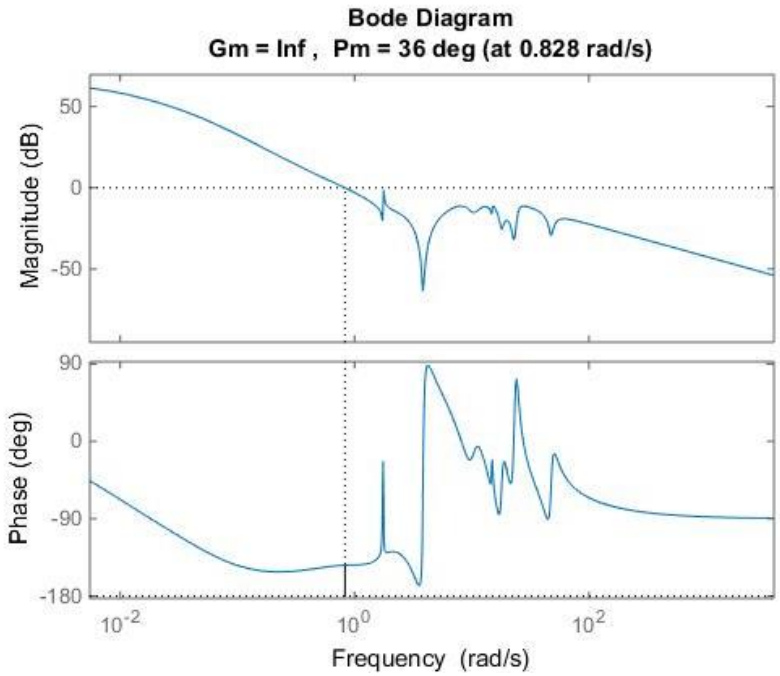

Figure 91: Gain and phase margins of the torque control at 11m/s

An infinite gain margin means that the phase of the system always remains above -180º, which means that is a stable system. Also, a phase margin of 36 degrees is a good phase margin, as it is in the range of suitable phase margins (between 30 and 60 degrees).

Next, the disturbance rejection behavior of the loop must be checked. This is done in the Bode diagram of the torque control's disturbance sensibility at 11m/s.

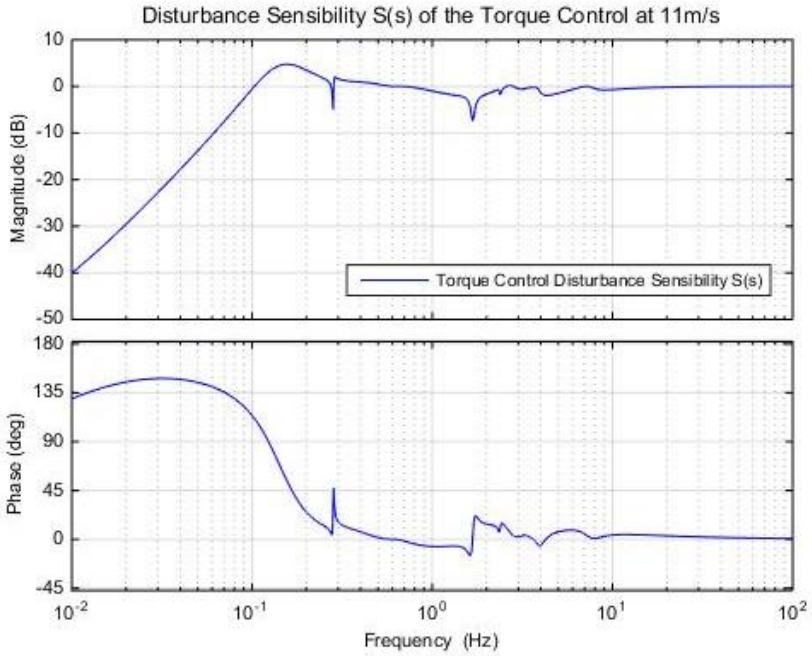

Figure 92: Bode diagram of torque control's disturbance sensibility S(s) at 11m/s

The exact values of the band width and peak of the previous Bode diagram are shown in the next figure.

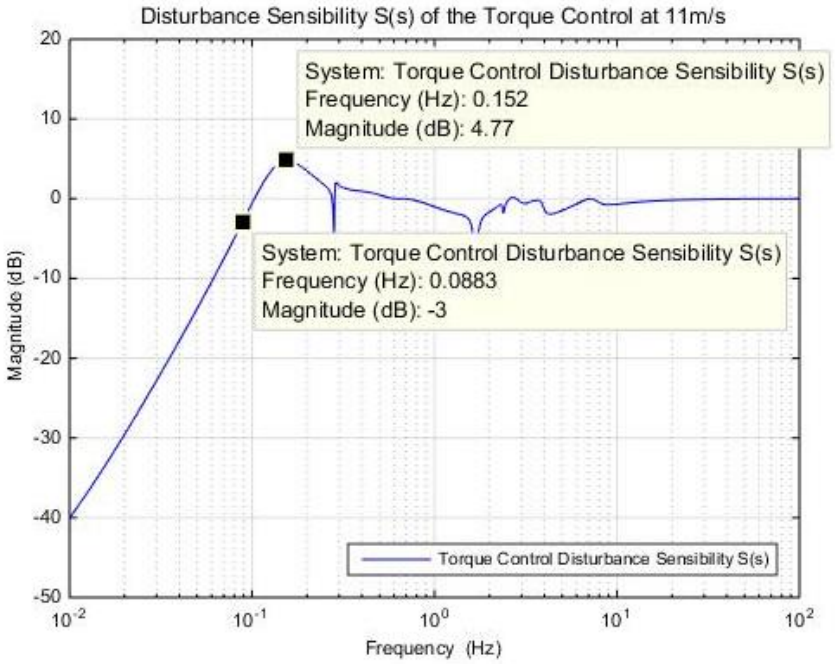

Figure 93: Band width and magnitude peak of the torque control's S(s) at 11m/s

In the 2nd vertical, both band width and peak requirements are met, a band width of 0.0883Hz, and a peak of 4.77dB (smaller than 6dB).

5.4.2.Parameters

The torque control parameters resulting from the control tuning are shown in the next tables. The values of these parameters stay the same for the 1st and for the 2nd vertical, that is why the 1st vertical has compromised the magnitude of the peak in the disturbance sensibility response and a faster performance has been chosen in this operating zone, to fit both vertical's parameters.

TORQUE CONTROL		
Parameter	**Value**	**Units**
UPNA_WT_Control.TorqueControlLoop.SampleTime	0.01	s
UPNA_WT_Control.TorqueControlLoop.Notch.Enable	1	-
UPNA_WT_Control.TorqueControl.maxtorque	49589	N·m
UPNA_WT_Control.TorqueControl.mintorque	0	N·m
UPNA_WT_Control.TorqueControl.maxratetorque	20000	N·m/s
UPNA_WT_Control.TorqueControl.minratetorque	-20000	N·m/s
UPNA_WT_Control.TorqueControlLoop.NotchDT.Gain	1	-
UPNA_WT_Control.TorqueControlLoop.NotchDT.Dampz	0.1	-
UPNA_WT_Control.TorqueControlLoop.NotchDT.Dampp	0.8	-
UPNA_WT_Control.TorqueControlLoop.NotchDT.wnz	10.34	rad/s

UPNA_WT_Control.TorqueControlLoop.NotchDT.wnp	10.34	rad/s
UPNA_WT_Control.TorqueControlLoop.NotchDT.enable	1	-
UPNA_WT_Control.TorqueControlLoop.NotchDT.initialvalue	0	-
UPNA_WT_Control.TorqueControlLoop.Notch1simetrica.Gain	1	-
UPNA_WT_Control.TorqueControlLoop.Notch1simetrica.Dampz	0.03	-
UPNA_WT_Control.TorqueControlLoop.Notch1simetrica.Dampp	0.15	-
UPNA_WT_Control.TorqueControlLoop.Notch1simetrica.wnz	23.15	rad/s
UPNA_WT_Control.TorqueControlLoop.Notch1simetrica.wnp	23.15	rad/s
UPNA_WT_Control.TorqueControlLoop.Notch1simetrica.enable	1	-
UPNA_WT_Control.TorqueControlLoop.Notch1simetrica.initialvalue	0	-
UPNA_WT_Control.TorqueControlLoop.Notch2simetrica.Gain	1	-
UPNA_WT_Control.TorqueControlLoop.Notch2simetrica.Dampz	0.03	-
UPNA_WT_Control.TorqueControlLoop.Notch2simetrica.Dampp	0.15	-
UPNA_WT_Control.TorqueControlLoop.Notch2simetrica.wnz	47.48	rad/s
UPNA_WT_Control.TorqueControlLoop.Notch2simetrica.wnp	47.48	rad/s
UPNA_WT_Control.TorqueControlLoop.Notch2simetrica.enable	1	-
UPNA_WT_Control.TorqueControlLoop.Notch2simetrica.initialvalue	0	-
UPNA_WT_Control.TorqueControlLoop.Notch2sidetoside.Gain	1	-
UPNA_WT_Control.TorqueControlLoop.Notch2sidetoside.Dampz	0.03	-
UPNA_WT_Control.TorqueControlLoop.Notch2sidetoside.Dampp	0.15	-
UPNA_WT_Control.TorqueControlLoop.Notch2sidetoside.wnz	17.97	rad/s
UPNA_WT_Control.TorqueControlLoop.Notch2sidetoside.wnp	17.97	rad/s
UPNA_WT_Control.TorqueControlLoop.Notch2sidetoside.enable	1	-
UPNA_WT_Control.TorqueControlLoop.Notch2sidetoside.initialvalue	0	-
UPNA_WT_Control.TorqueControlLoop.Notch1foreaft.Gain	1	-
UPNA_WT_Control.TorqueControlLoop.Notch1foreaft.Dampz	0.35	-
UPNA_WT_Control.TorqueControlLoop.Notch1foreaft.Dampp	0.55	-
UPNA_WT_Control.TorqueControlLoop.Notch1foreaft.wnz	1.76	rad/s
UPNA_WT_Control.TorqueControlLoop.Notch1foreaft.wnp	1.76	rad/s
UPNA_WT_Control.TorqueControlLoop.Notch1foreaft.enable	1	-
UPNA_WT_Control.TorqueControlLoop.Notch1foreaft.initialvalue	0	-
UPNA_WT_Control.TorqueControlLoop.Notch3P.Gain	1	-
UPNA_WT_Control.TorqueControlLoop.Notch3P.Dampz	0.01	-
UPNA_WT_Control.TorqueControlLoop.Notch3P.Dampp	0.2	-
UPNA_WT_Control.TorqueControlLoop.Notch3P.enable	1	-
UPNA_WT_Control.TorqueControlLoop.Notch3P.initialvalue	0	-
UPNA_WT_Control.TorqueControlLoop.Notch3P.NumP	3	-
UPNA_WT_Control.TorqueControlLoop.Notch1P.Gain	1	-
UPNA_WT_Control.TorqueControlLoop.Notch1P.Dampz	0.01	-
UPNA_WT_Control.TorqueControlLoop.Notch1P.Dampp	0.2	-
UPNA_WT_Control.TorqueControlLoop.Notch1P.enable	0	-
UPNA_WT_Control.TorqueControlLoop.Notch1P.initialvalue	0	-
UPNA_WT_Control.TorqueControlLoop.PIDcontroler.Kp	0.0075	-
UPNA_WT_Control.TorqueControlLoop.PIDcontroler.Ki	0.04	-
UPNA_WT_Control.TorqueControlLoop.PIDcontroler.Kd	0	-
UPNA_WT_Control.TorqueControlLoop.PIDcontroler.thaud	10	s
UPNA_WT_Control.TorqueControlLoop.PIDcontroler.enable	1	-
UPNA_WT_Control.TorqueControlLoop.PIDcontroler.initialvalue	0	N·m

Table 16: Torque control parameter values

Here, the values of maximum and minimum torque rates have been referred to those in the Supervisory Control. This way, if they need to be changed, once in the Supervisory Control will be enough.

The maximum torque that limits the torque control has been calculated to be a 15% over the rated generator torque to ensure that the torque does not exceed this limit. There is also a lower limit that avoids the torque from having negative values.

5.5. Pitch Control

5.5.1.Control performance

After the control tuning of the torque control, comes the pitch control loop. Its objective is the same, disturbance rejection in the generator speed output, only that the pitch control loop acts on the blade pitch angle instead of on the generator torque.

The requirements of the disturbance rejection closed loop graph such as a required band width or a maximum peak vary depending on the wind speed. The requirements the pitch control loop must fulfill are shown in the next table.

Pitch Control Loop Disturbance Sensibility		
Low wind speeds	Band Width	≈ 0.04 Hz
	Peak	< 6 dB
Medium wind speeds	Band Width	≈ 0.075 Hz
	Peak	< 6 dB
High wind speeds	Band Width	≈ 0.1 Hz
	Peak	< 6 dB

Figure 94: Pitch Control disturbance sensibility requirements

These band width requirements are set due to load limits. At low above rated wind speeds, the generator speed should not be as tightly controlled as at high above rated wind speeds.

At the same time, a high band width at low above rated wind speeds lowers the gain margin due to plant behavior at those operating points. This means that achieving a high band width at low wind speeds will not be as easy.

If too much band width is demanded at low wind speeds, the pitch angle activity highly increases and the control is not feasible because of the pitch actuators, that cannot take that much activity. Indeed, a fast control (big band width) is often not even possible because it becomes unstable.

Just like for the torque control, a compromise between a bigger band width (faster response) and a lower peak (lower oscillations) must be reached.

The pitch control loop is only activated in the above rated zone. In this section, the behavior of the system in that zone due to the pitch control is going to be analyzed.

Just like for the torque control loop, the first thing that must be checked when performing the control tuning is the system's stability. This will be checked in the open loop response of the system.

The next figure shows a Bode diagram of the pitch control, the ATD, the plant with the ATD and the open loop.

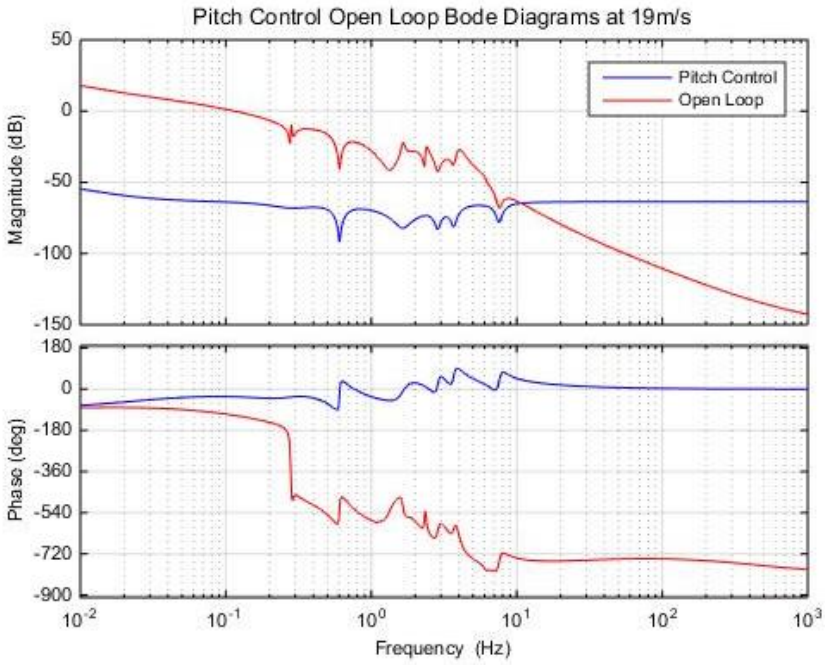

Figure 95: Bode diagram of the pitch control, ATD, plant with ATD and open loop at 19m/s

In the previous figure, the open loop stability can be observed.

Next, the gain and phase margins are shown in a new Bode diagram of the open loop response of the system at the above rated zone.

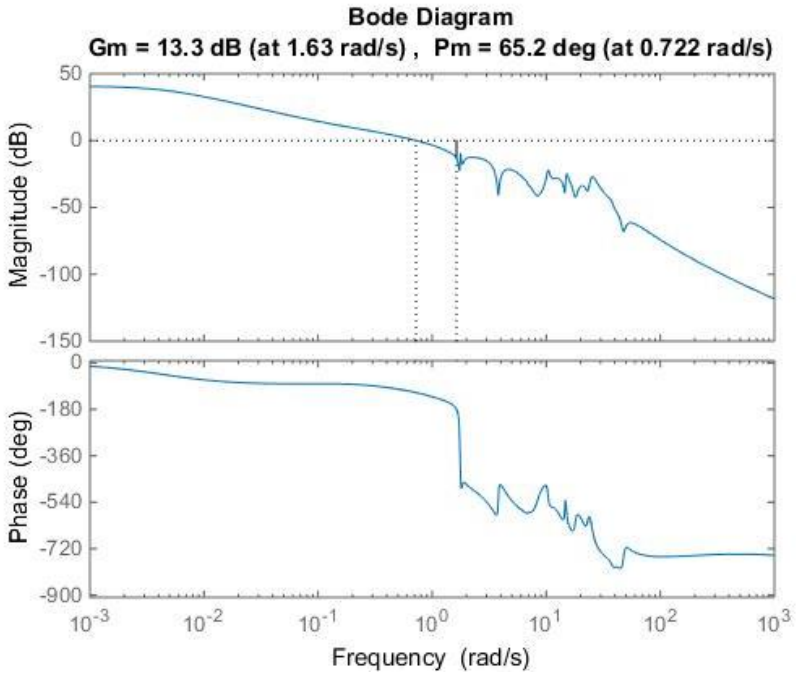

Figure 96: Gain and phase margins of the pitch control at 19m/s

An open loop gain margin of 13.3dB and a phase margin of 65.2 degrees mean the system has a stable closed loop.

The next thing to check when performing the control tuning of the pitch control loop is the rejection of the disturbances, which is the main design objective of the loop. Just like for the torque control loop, it can be checked in the disturbance sensibility Bode graph of the system.

Since different band width requirements are set for different above rated wind speeds, the disturbance sensibility of the pitch control is shown at 13 m/s, 19m/s and 25m/s.

The next graph shows the pitch control disturbance sensibility graph at 13m/s.

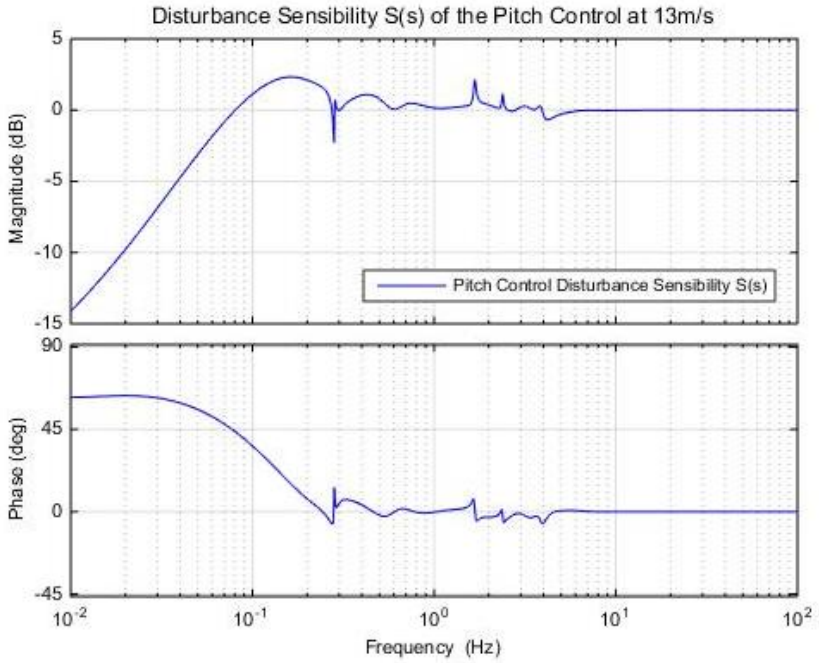

Figure 97: Bode diagram of pitch control's disturbance sensibility S(s) at 13m/s

In the S(s) and T(s) sensibilities, the effect of the DTD strategy is not shown in the pitch control graphs. This is because the disturbance that enters the output only afects the pitch control (PID and filters) and it does not take into account the influence of the DTD. The pitch control loop plant does have the closed DTD and it does contribute to disturbance rejection but, as the only accesible disturbance is the one that goes straight to the generator speed (output), this relationship can not be shown.

The exact band width and peak magnitudes at 13m/s are shown in the next graph.

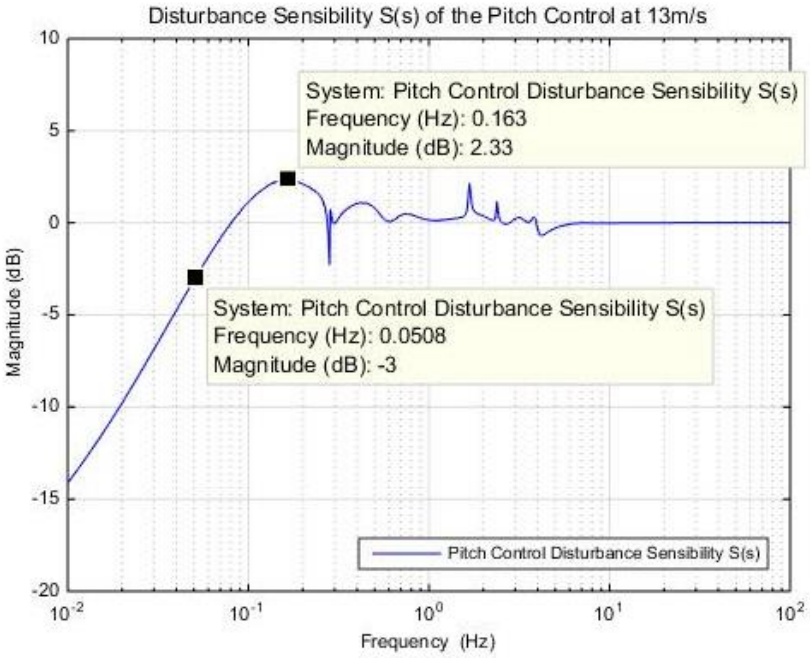

Figure 98: Band width and magnitude peak of the pitch control's S(s) at 13m/s

At low speeds, the pitch control loop must have a minimum band width of 0.04Hz, which is accomplished by the control tuning because the disturbance sensibility band width at 13m/s is 0.0508Hz. Also, the magnitude peak, 2.33dB, is lower than the maximum limit, 6dB.

Now, the disturbance sensibility S(s) of the loop is shown at 19m/s.

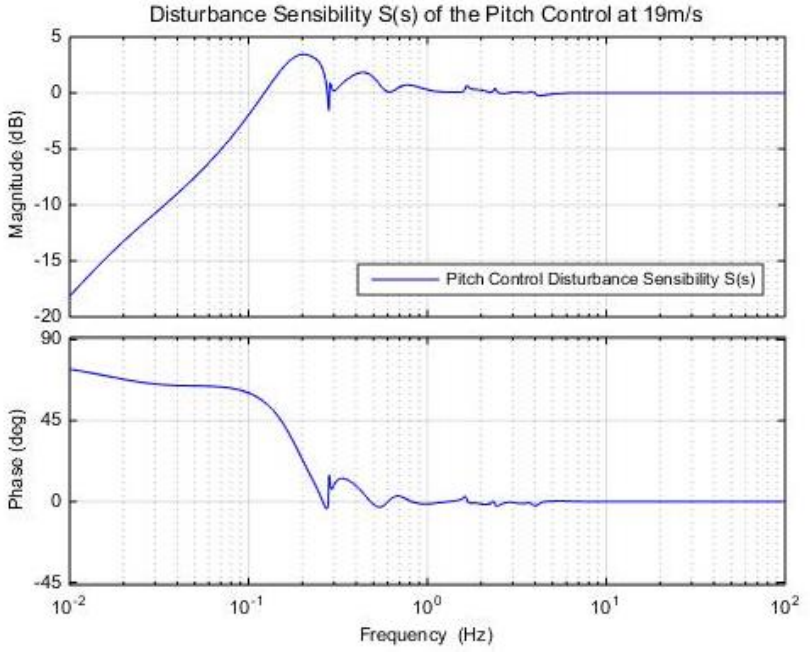

Figure 99: Bode diagram of pitch control's disturbance sensibility S(s) at 19m/s

In the previous figure, the behavior of the system with respect to disturbances is illustrated. Low frequency disturbances will be attenuated while higher frequency ones will go through the system with little amplification or attenuation.

The exact BW and peak values are shown in the next figure.

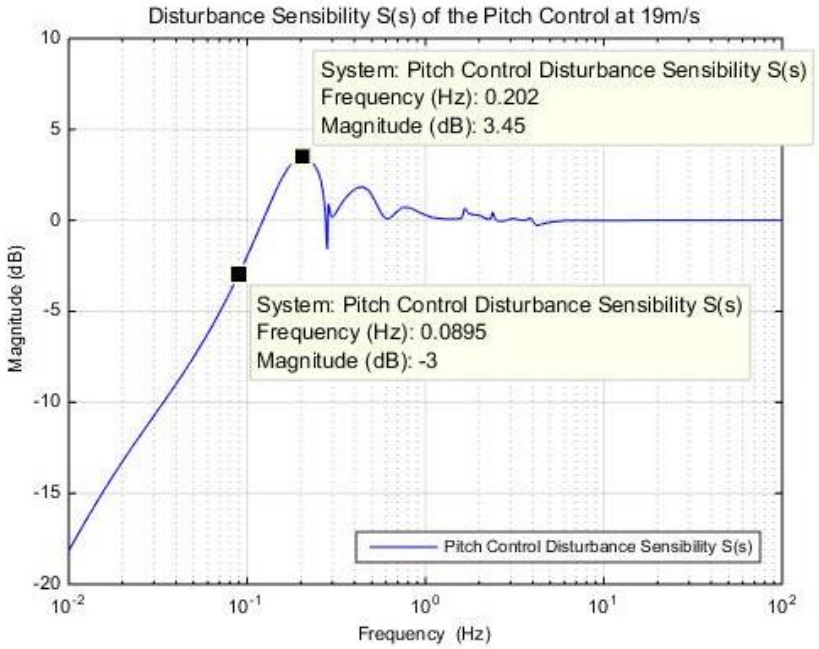

Figure 100: Band width and magnitude peak of the pitch control's S(s) at 19m/s

Both peak maximum (6dB) and minimum band width (0.075Hz) requirements are met at 19m/s because the resulting band width and peak magnitude are 0.0895Hz and 3.45dB, respectively.

The last wind speed at which the closed loop behavior is going to be shown is at 25m/s. Next there is a graph of the disturbance sensibility S(s) at this wind speed.

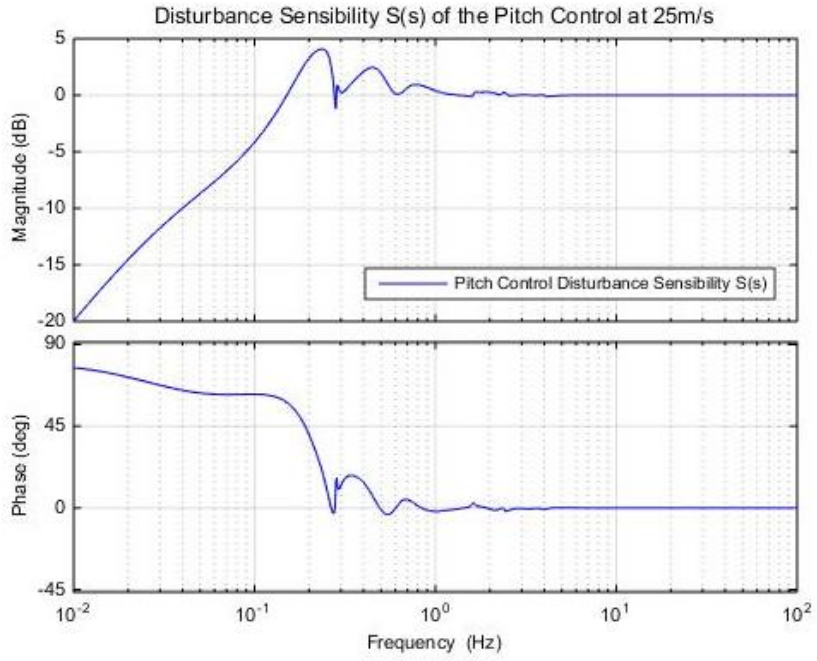

Figure 101: Bode diagram of pitch control's disturbance sensibility S(s) at 25m/s

The next figure shows the exact values of the system's band width and peak magnitude at 25m/s.

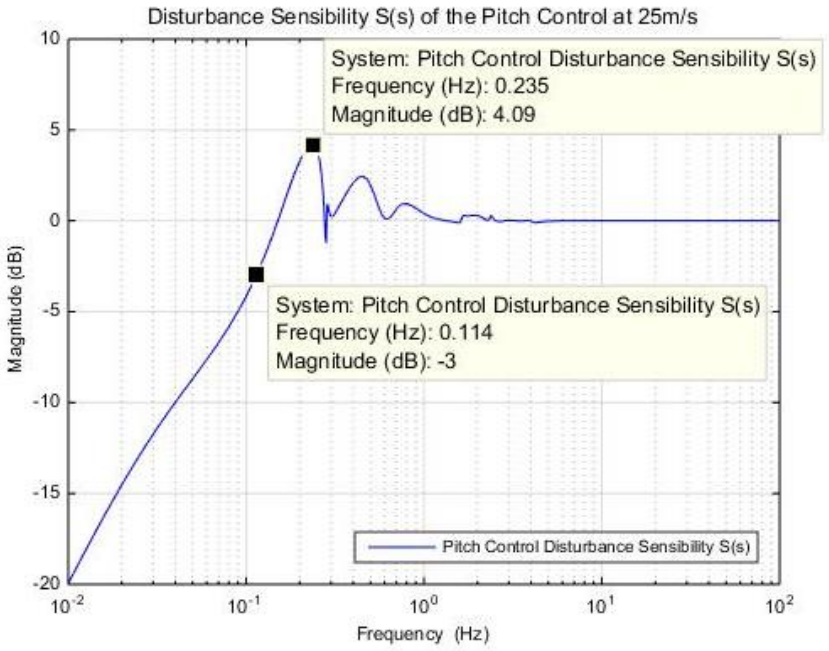

Figure 102: Band width and magnitude peak of the pitch control's S(s) at 25m/s

At high winds, the pitch control is required to be faster. Therefore, a bigger band width is required (0.1Hz). This requirement is fulfilled with a band width of 0.114Hz as well as the peak requirement, with a peak of 4.09dB (under 6dB).

5.5.2.Parameters

Given that the pitch control's PID contains variable gains, the pitch control can be designed to reach the specifications better at each operating point. The result of the control tuning of the pitch control loop is shown in the next tables.

PITCH CONTROL		
Parameter	**Value**	**Units**
UPNA_WT_Control.PitchControlLoop.SampleTime	0.01	s
UPNA_WT_Control.PitchControlLoop.Notch.Enable	1	-
UPNA_WT_Control.PitchControl.minpitchangle	0.106	deg
UPNA_WT_Control.PitchControl.maxpitchangle	90	deg
UPNA_WT_Control.PitchControl.maxratepitchangle	8	deg/s
UPNA_WT_Control.PitchControl.minratepitchangle	-8	deg/s
UPNA_WT_Control.PitchControlLoop.NotchDT.Gain	1	-
UPNA_WT_Control.PitchControlLoop.NotchDT.Dampz	0.1	-
UPNA_WT_Control.PitchControlLoop.NotchDT.Dampp	0.8	-
UPNA_WT_Control.PitchControlLoop.NotchDT.wnz	10.34	rad/s
UPNA_WT_Control.PitchControlLoop.NotchDT.wnp	10.34	rad/s
UPNA_WT_Control.PitchControlLoop.NotchDT.enable	1	-
UPNA_WT_Control.PitchControlLoop.NotchDT.initialvalue	0	-

UPNA_WT_Control.PitchControlLoop.Notch1simetrica.Gain	1	-
UPNA_WT_Control.PitchControlLoop.Notch1simetrica.Dampz	0.03	-
UPNA_WT_Control.PitchControlLoop.Notch1simetrica.Dampp	0.15	-
UPNA_WT_Control.PitchControlLoop.Notch1simetrica.wnz	23.15	rad/s
UPNA_WT_Control.PitchControlLoop.Notch1simetrica.wnp	23.15	rad/s
UPNA_WT_Control.PitchControlLoop.Notch1simetrica.enable	1	-
UPNA_WT_Control.PitchControlLoop.Notch1simetrica.initialvalue	0	-
UPNA_WT_Control.PitchControlLoop.Notch2simetrica.Gain	1	-
UPNA_WT_Control.PitchControlLoop.Notch2simetrica.Dampz	0.03	-
UPNA_WT_Control.PitchControlLoop.Notch2simetrica.Dampp	0.15	-
UPNA_WT_Control.PitchControlLoop.Notch2simetrica.wnz	47.48	rad/s
UPNA_WT_Control.PitchControlLoop.Notch2simetrica.wnp	47.48	rad/s
UPNA_WT_Control.PitchControlLoop.Notch2simetrica.enable	1	-
UPNA_WT_Control.PitchControlLoop.Notch2simetrica.initialvalue	0	-
UPNA_WT_Control.PitchControlLoop.Notch2sidetoside.Gain	1	-
UPNA_WT_Control.PitchControlLoop.Notch2sidetoside.Dampz	0.03	-
UPNA_WT_Control.PitchControlLoop.Notch2sidetoside.Dampp	0.15	-
UPNA_WT_Control.PitchControlLoop.Notch2sidetoside.wnz	17.97	rad/s
UPNA_WT_Control.PitchControlLoop.Notch2sidetoside.wnp	17.97	rad/s
UPNA_WT_Control.PitchControlLoop.Notch2sidetoside.enable	1	-
UPNA_WT_Control.PitchControlLoop.Notch2sidetoside.initialvalue	0	-
UPNA_WT_Control.PitchControlLoop.Notch1foreaft.Gain	1	-
UPNA_WT_Control.PitchControlLoop.Notch1foreaft.Dampz	0.35	-
UPNA_WT_Control.PitchControlLoop.Notch1foreaft.Dampp	0.55	-
UPNA_WT_Control.PitchControlLoop.Notch1foreaft.wnz	1.76	rad/s
UPNA_WT_Control.PitchControlLoop.Notch1foreaft.wnp	1.76	rad/s
UPNA_WT_Control.PitchControlLoop.Notch1foreaft.enable	1	-
UPNA_WT_Control.PitchControlLoop.Notch1foreaft.initialvalue	0	-
UPNA_WT_Control.PitchControlLoop.Notch3P.Gain	1	-
UPNA_WT_Control.PitchControlLoop.Notch3P.Dampz	0.01	-
UPNA_WT_Control.PitchControlLoop.Notch3P.Dampp	0.2	-
UPNA_WT_Control.PitchControlLoop.Notch3P.enable	1	-
UPNA_WT_Control.PitchControlLoop.Notch3P.initialvalue	0	-
UPNA_WT_Control.PitchControlLoop.Notch3P.NumP	3	-
UPNA_WT_Control.PitchControlLoop.Notch1P.Gain	1	-
UPNA_WT_Control.PitchControlLoop.Notch1P.Dampz	0.01	-
UPNA_WT_Control.PitchControlLoop.Notch1P.Dampp	0.2	-
UPNA_WT_Control.PitchControlLoop.Notch1P.enable	0	-
UPNA_WT_Control.PitchControlLoop.Notch1P.initialvalue	0	-
UPNA_WT_Control.PitchControlLoop.LowPass.Gain	1	-
UPNA_WT_Control.PitchControlLoop.LowPass.thau	0.316	s
	0.158	s
	0.079	s
UPNA_WT_Control.PitchControlLoop.LowPass.enable	0	-
UPNA_WT_Control.PitchControlLoop.LowPass.initialvalue	0	-
UPNA_WT_Control.PitchControlLoop.PIDcontroler.Kpini	0.0075	-
UPNA_WT_Control.PitchControlLoop.PIDcontroler.Kiini	0.04	-
UPNA_WT_Control.PitchControlLoop.PIDcontroler.Kpfin	0.0058	-

UPNA_WT_Control.PitchControlLoop.PIDcontroler.Kifin	0.22	-
UPNA_WT_Control.PitchControlLoop.PIDcontroler.Beta13	6.42	deg
UPNA_WT_Control.PitchControlLoop.PIDcontroler.Beta21	18.53	deg
UPNA_WT_Control.PitchControlLoop.PIDcontroler.Kd	0	-
UPNA_WT_Control.PitchControlLoop.PIDcontroler.thaud	100	s
UPNA_WT_Control.PitchControlLoop.PIDcontroler.enable	1	-
UPNA_WT_Control.PitchControlLoop.PIDcontroler.initialvalue	0.106	deg
UPNA_WT_Control.PitchControlLoop.PIDcontroler.minpitchangle	0.106	deg
UPNA_WT_Control.PitchControlLoop.PIDcontroler.maxpitchangle	90	deg

Table 17: Pitch control parameter values

The maximum and minimum pitch angles and angle rates are also referred to the ones in the Supervisory Control parameters, just like in the torque control. This way, if the value of these limits changes, they only need to be changed once.

5.6. ATD

5.6.1.Control performance

The final step when performing the wind turbine's control tuning is the adjustment of the ATD's parameters. Its objective, just like the DTD, is to give damping to one of the wind turbine's most excited structural modes. The ATD is designed in order to damp the 1st tower fore-aft mode.

The ATD is also only activated in the above rated zone. Therefore, the behavior due to the ATD's contribution will be shown for the above rated wind speeds of 13m/s, 19m/s and 25m/s.

Next, a Bode diagram of the plant with and without the ATD contribution is shown.

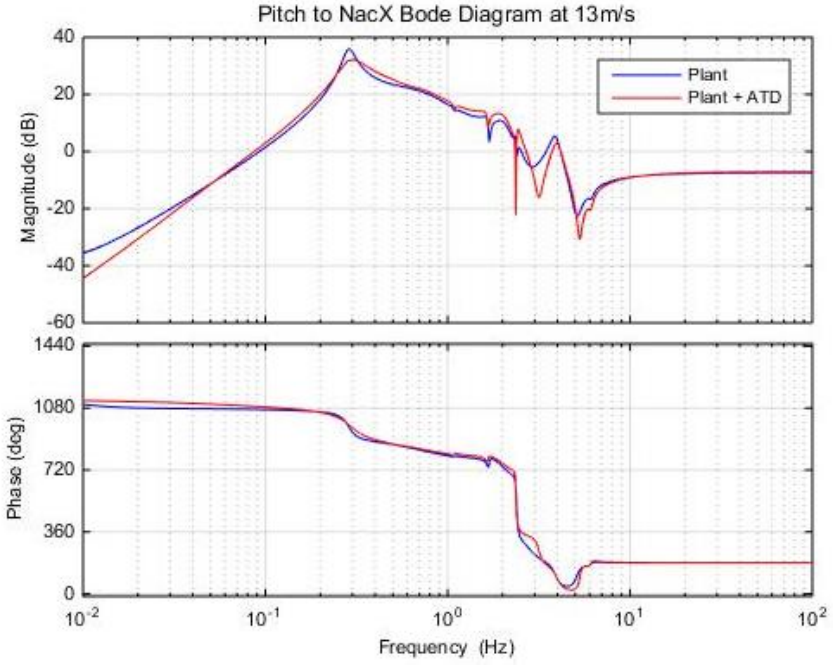

Figure 103: Bode diagram of the plant from pitch to nacelle fore-aft with and without ATD at 13m/s

It can be appreciated from the figure how the ATD reduces the 1st fore-aft mode of the plant. Next, the same graph is shown for a wind speed of 19m/s.

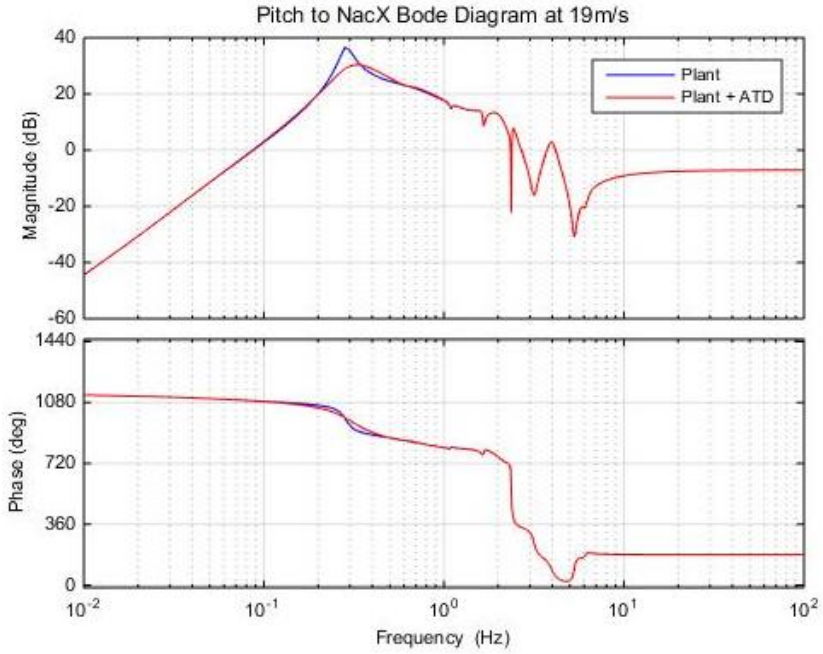

Figure 104: Bode diagram of the plant from pitch to nacelle fore-aft with and without ATD at 19m/s

The ATD damps the excited fore-aft mode of the plant, to a higher level than at low wind speeds. The next figure shows the same plant configurations but for a 25m/s wind speed.

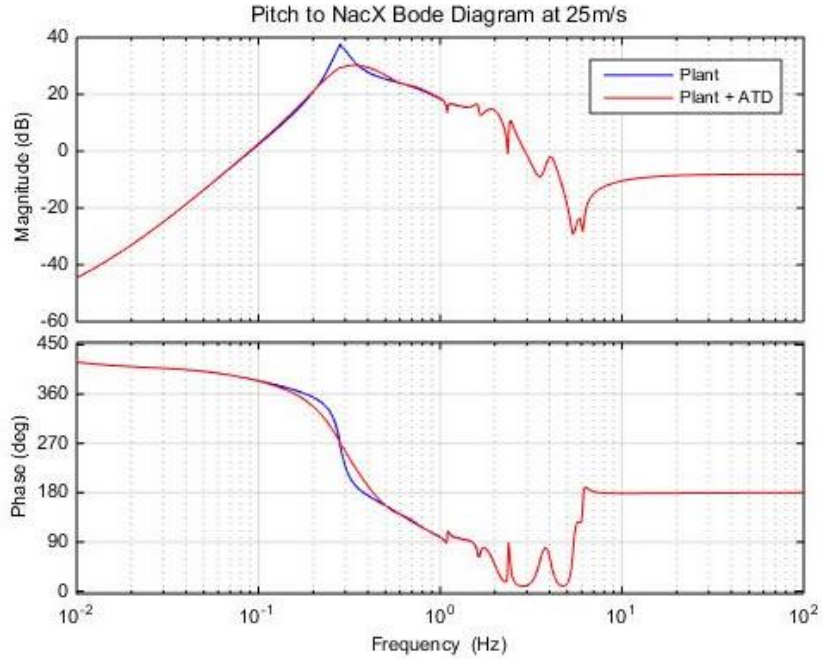

Figure 105: Bode diagram of the plant from pitch to nacelle fore-aft with and without ATD at 25m/s

The previous figure illustrates how the ATD gives damping to the plant's 1st fore-aft frequency. The effect of the ATD at 25m/s is bigger than at lower above rated wind speeds.

The ATD's disturbance rejection behavior is goint to be checked too. The Bode diagram of the ATD's disturbance sensibility is going to be shown next with that purpose.

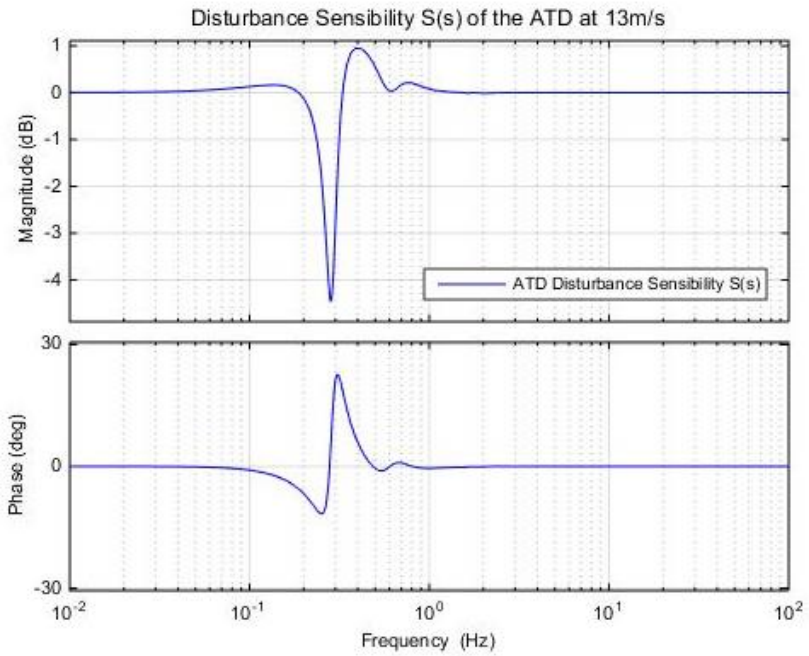

Figure 106: Bode diagram of the ATD's disturbance sensibility S(s) at 13m/s

In the previous figure, the disturbance sensibility of the ATD is shown at a wind speed of 13m/s. It illustrates how any disturbance entering the system at the 1st fore-aft mode frequency will be highly attenuated by the ATD. The drawback is that frequencies entering the system at a frequency a little over 0.28Hz will be amplified. The load analysis will determine if the overall ATD strategy is worth introducing and if the amplification of those frequencies is not as harmful for the loads as the excited fore-aft frequency, which is the target frequency in this strategy.

Since the ATD has a variable gain depending on the blade pitch angle, the ATD will have a higher contribution above certain wind speeds. The disturbance sensibility is therefore shown at 25m/s too.

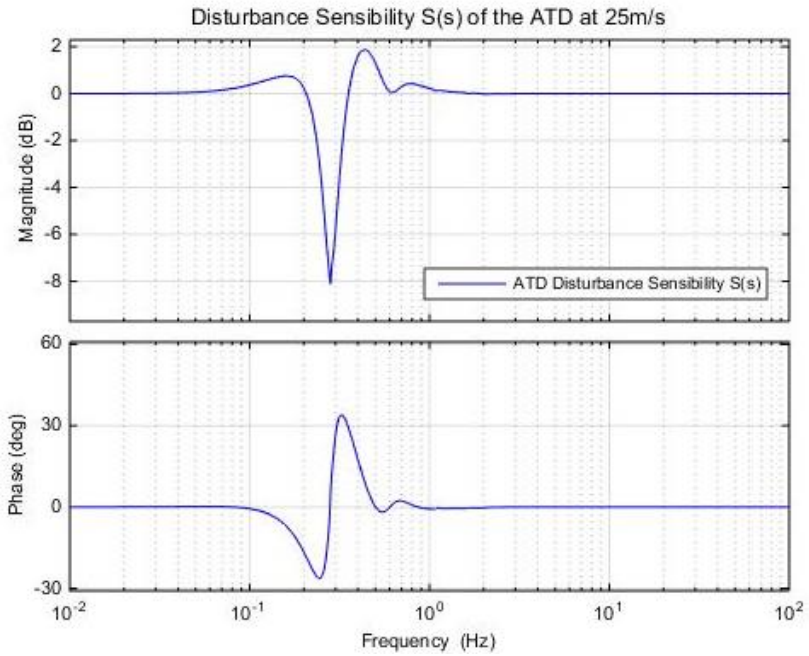

Figure 107: Bode diagram of the ATD's disturbance sensibility S(s) at m/s

The attenuating effect of the ATD is higher at higher wind speeds, attenuating at -8dB, which is an attenuation 1.61 times higher than at low above rated wind speeds.

5.6.2.Parameters

The next table shows the results of the control tuning for the ATD, which has been carried out at 13m/s, 19m/s and 25m/s in order to adjust the values of the parameters that are variable depending on the operating point.

ATD		
Parameter	**Value**	**Units**
UPNA_WT_Control.ATD.SampleTime	0.01	s
UPNA_WT_Control.ATD.ExternalGain	0.036	-
UPNA_WT_Control.ATD.Enable	1	-
UPNA_WT_Control.ATD.Max	1	deg
UPNA_WT_Control.ATD.Min	-1	deg
UPNA_WT_Control.ATD.Gain.Kini	0	-
UPNA_WT_Control.ATD.Gain.Kfin	1	-
UPNA_WT_Control.ATD.Gain.Betaini	0.116	deg
UPNA_WT_Control.ATD.Gain.Betafin	5	deg
UPNA_WT_Control.ATD.Gain.minpitchangle	0.106	deg
UPNA_WT_Control.ATD.Gain.maxpitchangle	90	deg
UPNA_WT_Control.ATD.Lowpass2ndfilter.gain	1	-

UPNA_WT_Control.ATD.Lowpass2ndfilter.dampp	1	-
UPNA_WT_Control.ATD.Lowpass2ndfilter.wnp	2.07	rad/s
UPNA_WT_Control.ATD.Lowpass2ndfilter.enable	1	-
UPNA_WT_Control.ATD.Lowpass2ndfilter.initialvalue	0	-
UPNA_WT_Control.ATD.Notch3P.Gain	1	-
UPNA_WT_Control.ATD.Notch3P.Dampz	0.01	-
UPNA_WT_Control.ATD.Notch3P.Dampp	0.2	-
UPNA_WT_Control.ATD.Notch3P.enable	1	-
UPNA_WT_Control.ATD.Notch3P.initialvalue	0	-
UPNA_WT_Control.ATD.Notch3P.NumP	3	-

Table 18: ATD parameter values

The initial angle (βini) of the gain scheduling is the minimum pitch angle (0.106 degrees) plus a minimum pitch difference (0.01 degrees) defined in the Supervisory control. This angle, as well as the values corresponding to minimum or maximum pitch angles are referred to the Supervisory control's parameters so that, in case they need to be changed, changing the Supervisory control values is enough.

Chapter 6: Validation of baseline Control Tuning for 5MW Upwind model in FASTv7

6.1. Introduction

Once the control tuning has been carried out, the next step is to validate the designed control strategy. A statistical analysis of the system's simulation must be carried out, along with a fatigue load analysis.

When validating the control strategy, two different aspects must be checked separately. First, the **power control** must be checked. This can be done by simulation (by ramp or step responses), the regulation capacity of the system can be observed. Once the regulation control has been validated and the tracing of the torque vs. generator speed curve has been ensured, the **active control** strategies must be validated too. To determine the improvement in the wind turbine's performance due to the active control strategies (DTD and ATD), different control configurations will be simulated:

· **Scenario A:** Baseline control, only power control will be activated

· **Scenario B:** Baseline + DTD: power control and DTD block will be activated

· **Scenario C:** Baseline + DTD + ATD: power control and both DTD and ATD active control blocks will be activated

As it was stated in the abstract of this project, an extra validation situation has been added. Delft University's control [2] has also been used to validate the control strategy designed in this project. Therefore, the last configuration is:

· **Scenario D:** Delft University's control strategy

6.2. Time-series simulation analysis

First, the system's response to a ramp wind input is illustrated. This way, the regulation control behavior is checked.

The next figure is a graph of the actual torque vs. generator speed curve resulting when simulating the system (both regulation control and active control remain active in this simulation) with a ramp wind input. The wind input starts at 2m/s and it has an increasing slope up to 15m/s. Then, it decreases down to 2m/s. This way both behaviors (with increasing and with decreasing wind) can be observed.

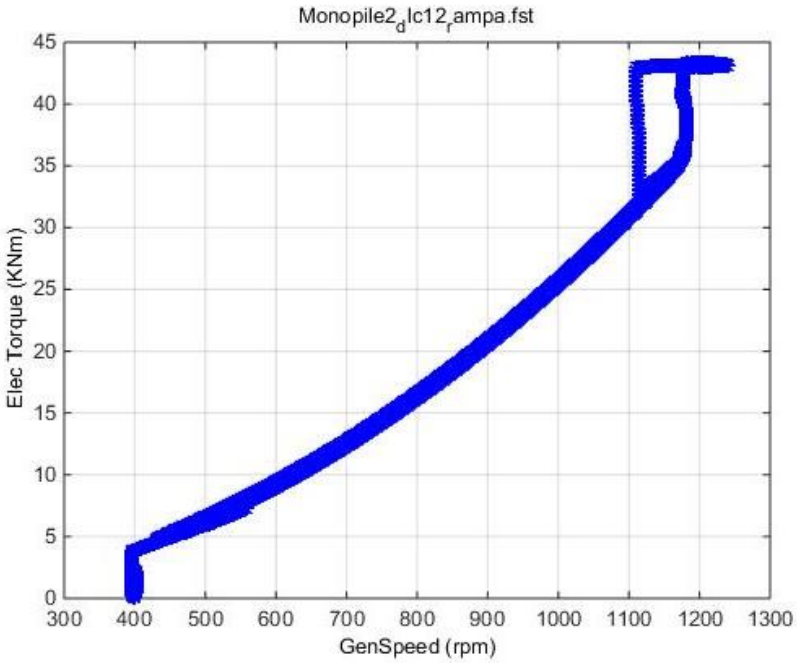

Figure 108: Generator torque vs. generator speed with a ramp input

The previous figure clearly shows how the regulation control is set to follow the torque vs. generator speed graph. Both the 1st and the 2nd verticals can be observed as well as the optimal torque curve.

The supervisory control zone has been designed to stay in the above rated zone for as long as possible. This way, whenever the wind turbine is operating in the above rated zone and the wind decreases, the supervisory control will not let the control switch to the 2nd vertical until the wind speed decreases enough so that the generator speed reaches a 75% of the nominal wind speed. This is why when the wind speed is decreasing, the supervisory control takes the torque straight from nominal torque to optimal torque (optimal torque curve) without going through the 2nd vertical.

Next, a figure with the electric generated power vs. generator speed is shown.

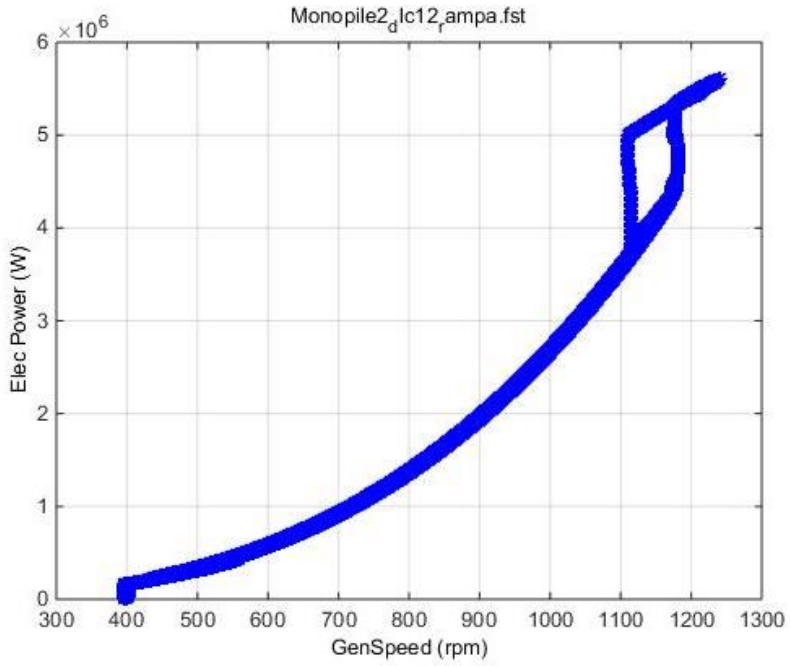

Figure 109: Generator power vs. generator speed with a ramp input

This graph shows the same behavior as the previous graph, only that it illustrates how, when working in the above rated zone, since the generator demanded torque is set to its nominal value and the generator is a little overspeed, the generated power is over the rated value.

The next figure shows different time-series graphs of several significant variables of the system, such as wind, generator torque, generator speed and blade pitch angle.

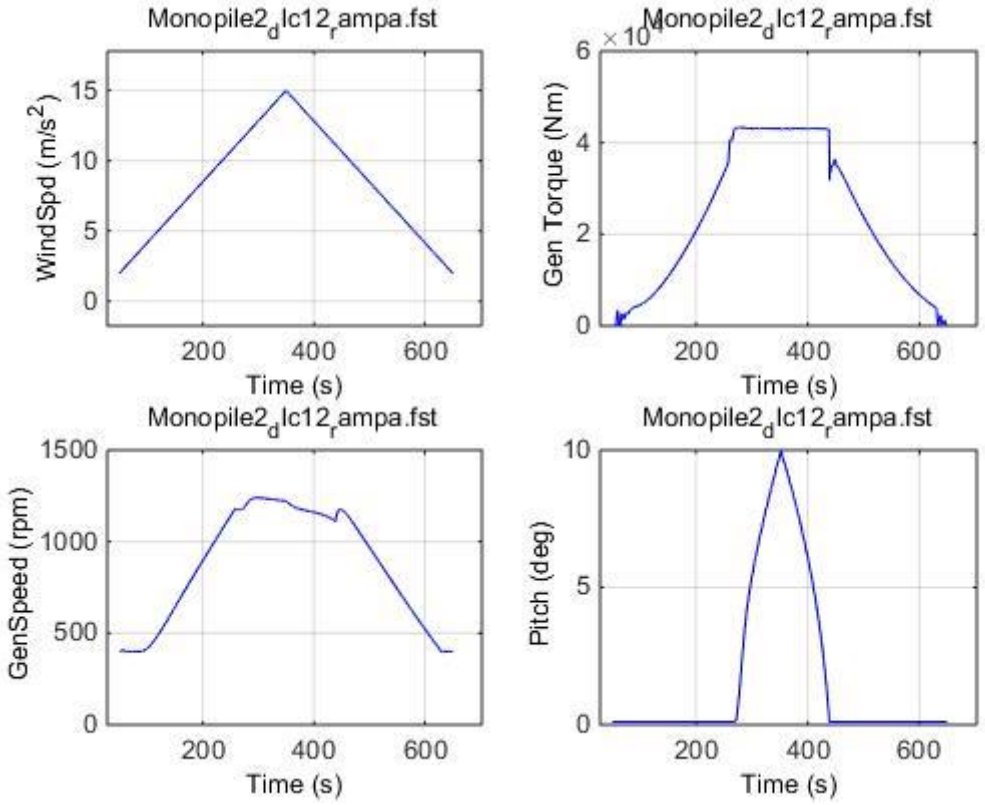

Figure 110: Wind, generator speed, torque and pitch angle vs. time with a ramp input

Just like for the previous two graphs, the first 50 seconds have been removed from the graphs due to initialization issues.

Also, to further show the disturbance rejection capacity of the control system, a step response of the system at every wind speed is shown too. For this simulation, a wind speed that goes from 2m/s up to 25m/s by increasing 1m/s every 50 seconds is used.

The next figure is the torque vs. generator speed graph.

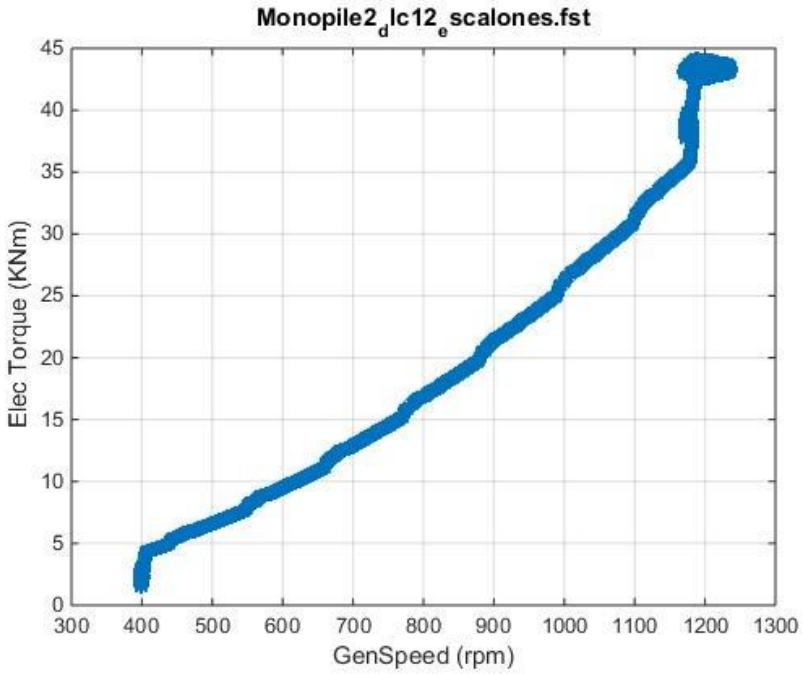

Figure 111: Generator torque vs. generator speed with unitary step inputs

This time, we can observe a little oscillation in the transition from one wind speed to the other.

Next, a figure of the generated power vs. generator speed is shown.

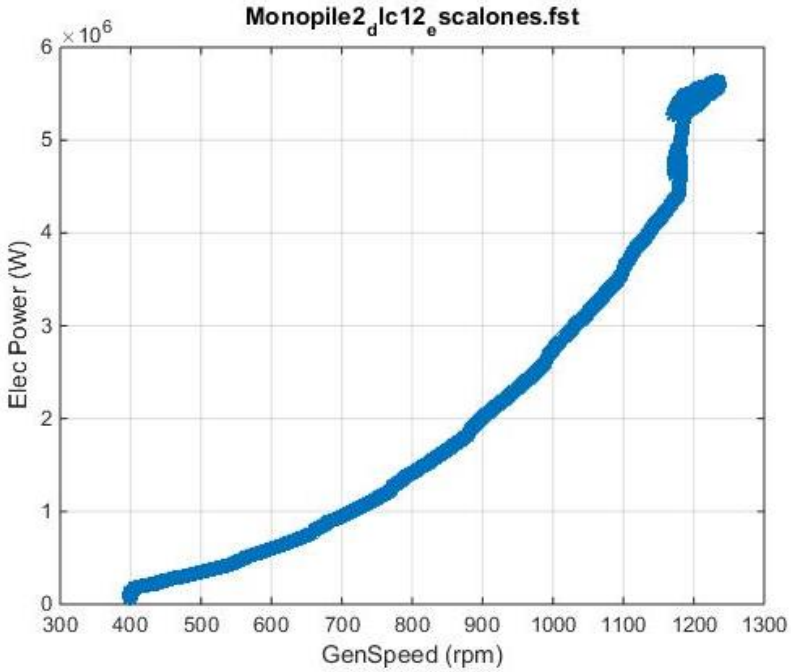

Figure 112: Generator power vs. generator speed with unitary step inputs

Just like for the generator torque, very small oscillations can be observed in the moment that the wind speed increases.

Next, a figure with the time-series graphs of the wind speed, generator torque, generator speed and blade pitch angle is shown.

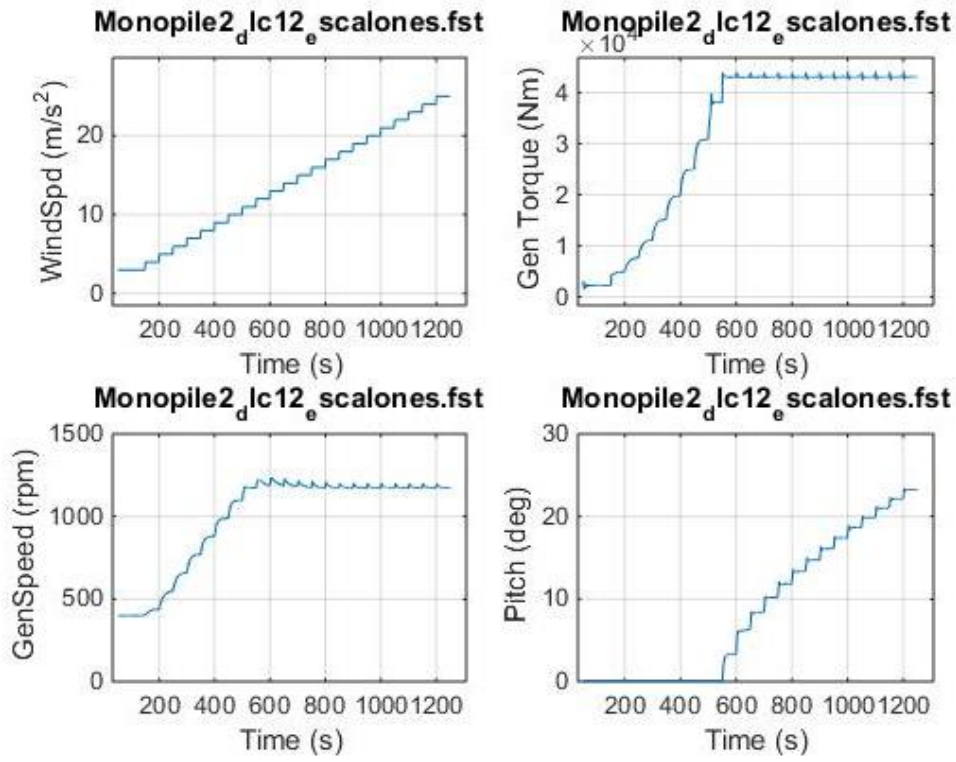

Figure 113: Wind, generator speed, torque and pitch angle vs. time with unitary step inputs

observe the system's behavior better, a bigger generator speed graph is shown again in the next figure.

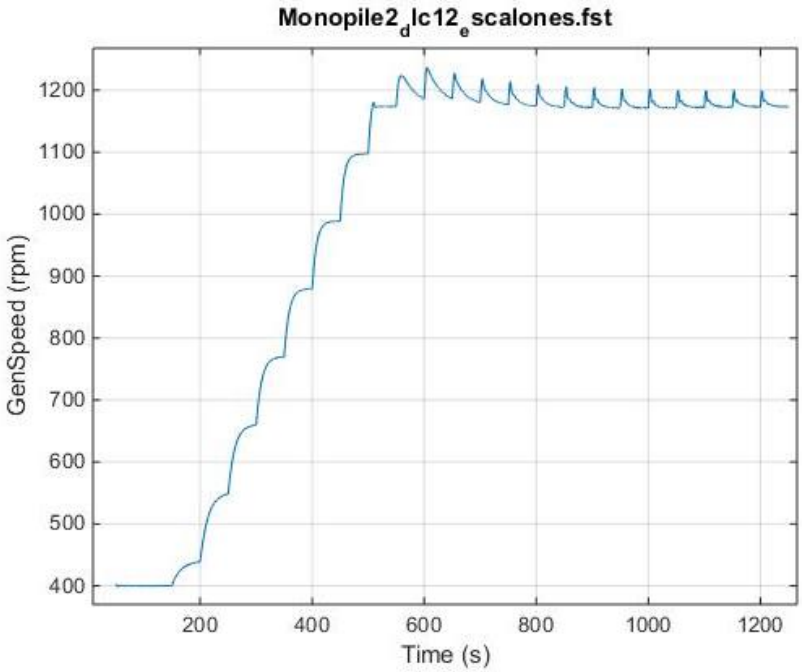

Figure 114: Generator speed vs. time with unitary step inputs

From the graph, it can be observed how the same wind speed increase, 1m/s, results in a higher perturbation for the generator speed at low above rated speeds than at high above rated speeds. This has been a design requirement. As it has been explained in section 5.5.1 Control performance, the pitch control has been set to have a faster response at high wind speeds.

6.3. Statistical analysis

In this section, the simulation data is going to be analyzed for the different scenarios proposed at the beginning of this chapter:

· **Scenario A: baseline control**

· **Scenario B: baseline + DTD**

· **Scenario C: baseline + DTD + ATD**

· **Scenario D: Delft's control**

These four different configurations have been simulated for a total time of 600s and for different power production winds with a mean speed of 3, 5 7 9 11 13 15 17 19 21 23 and 25m/s. The selected wind bins are generated using TurbSim, a stochastic, full-field wind generator that creates turbulent winds according to [8].

In the next section, different graphs of significant wind turbine variables are represented with respect to wind speed.

The first graph is a representation of the generated power vs. wind speed for the four different configurations.

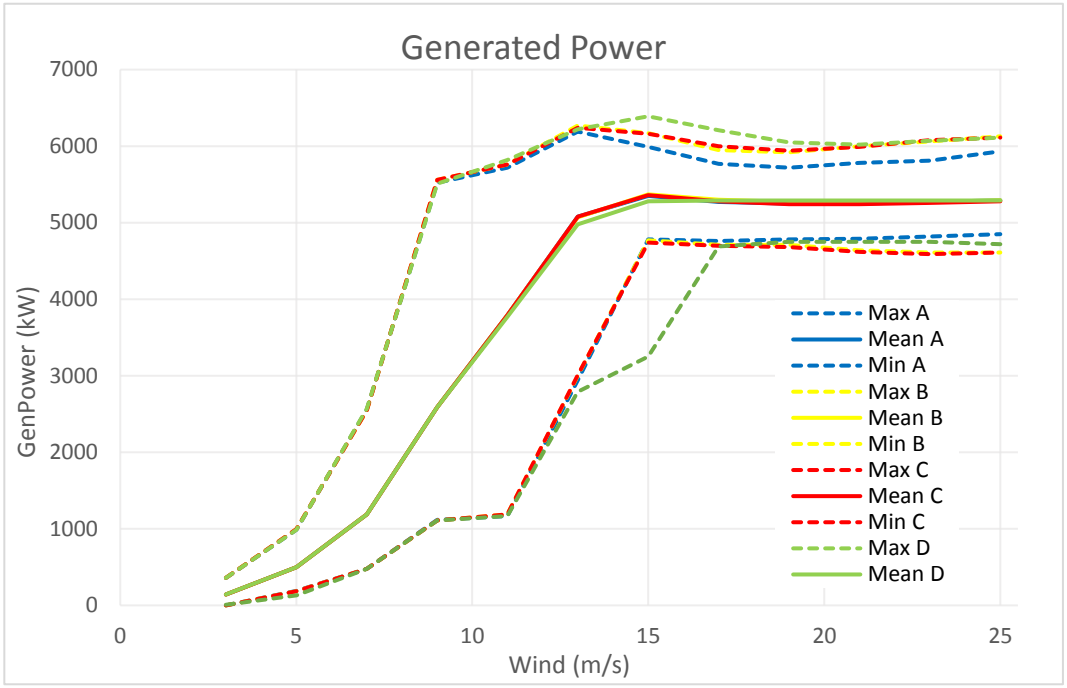

Figure 115: Generated power statistics for 600s simulations

The previous graph illustrates how the mean power is practically the same for the four configurations, only that in the transition zone from the below rated to the above rated zone, any of the configurations of the control strategy of this project (Scenarios A, B and C) extract a little bit more power than the one from Delft's University (Scenario D).

It can also be observed from the previous figure that the control scheme in Scenario D has a worse regulation at 15m/s, because it has a smaller minimum and a bigger maximum than the control Scenarios A, B and C.

Next, a graph of the standard deviation of the pitch angle at each wind speed is shown.

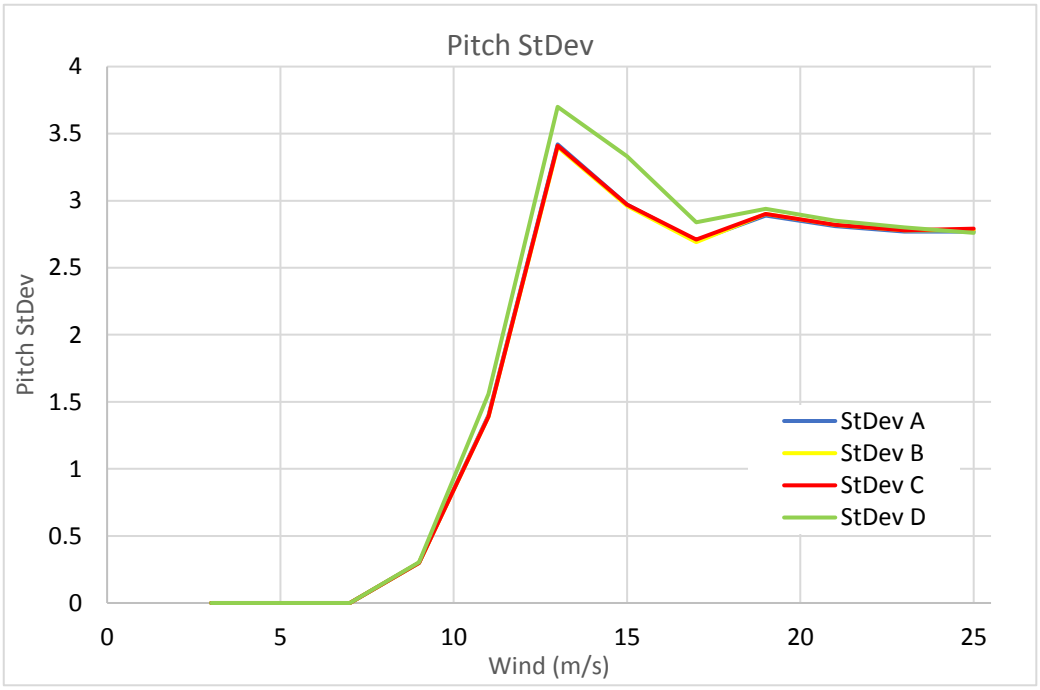

Figure 116: Pitch standard deviation for 600s simulations

This graph is a representation of the pitch duty, this is, the pitch activity. The goal is to achieve the most (either power regulation or ATD effect) with the least pitch activity. It can be observed how the Scenario D has a bigger pitch duty at small above rated speeds than any configuration of the proposed control configuration, Scenarios A, B and C.

Next, a graph of the tower base momentum in the "y" direction is shown. It is the maximum load the tower must withstand, which means it is the one that determines the tower's characteristics. Therefore, reducing this load will be significant for the tower design.

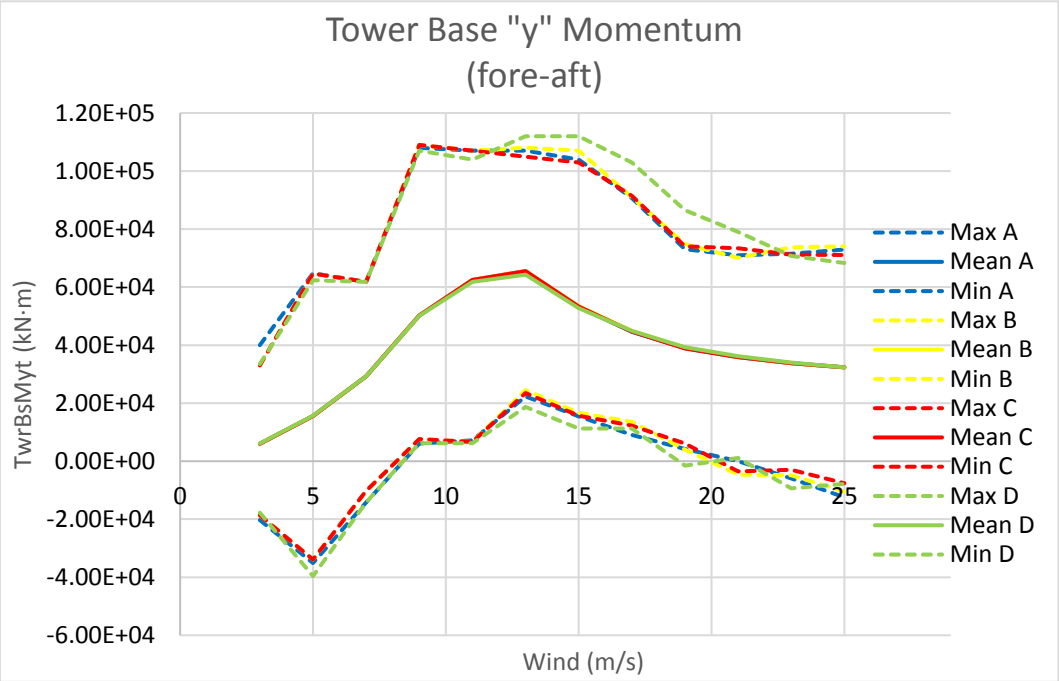

Figure 117: Tower base "y" momentum statistics for 600s simulations

The previous graph shows the tower base load in the "y" direction at each wind speed. The maximum mean load is obtained at 13m/s, which is right after entering the above rated zone. Practically the same mean load is obtained with all the control configurations, although a higher maximum load can be observed from 13m/s to 23m/s with the Scenario D control configuration.

Finally, the low speed shaft momentum in the "x" axis is represented with respect to wind speed in the next figure.

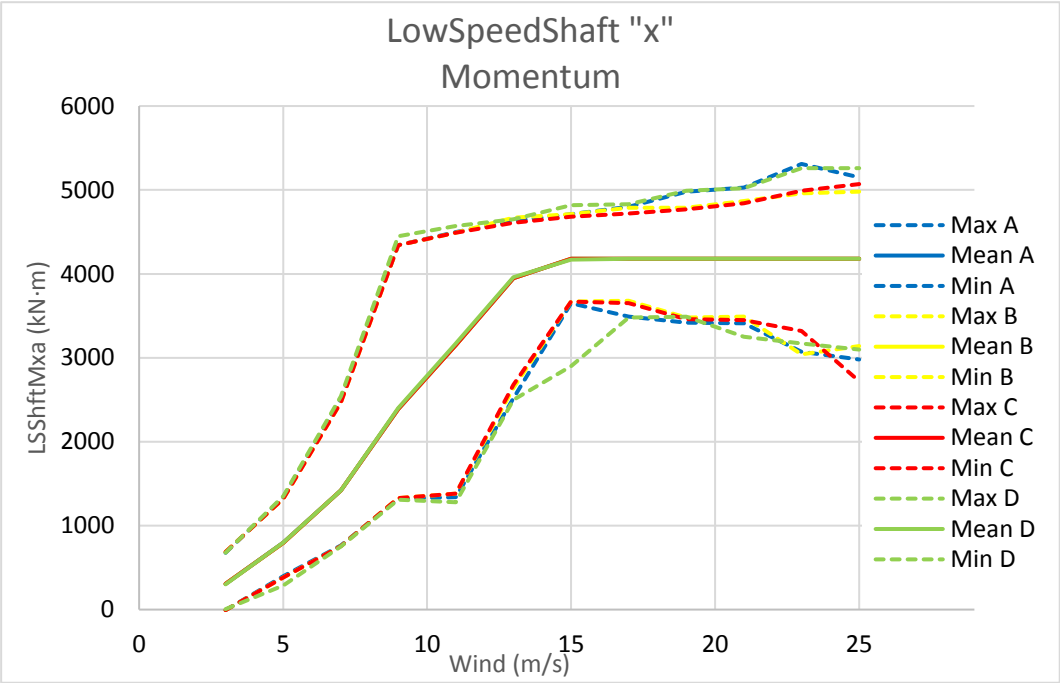

Figure 118: Low speed shaft "x" momentum statistics for 600s simulations

In the previous figure, it is shown how the four control configurations have the same mean load. The figure also illustrates how the maximum loads appear at 23 and 25m/s for the Scenario configurations A and D.

When entering the DTD, Scenarios B and C, a reduction of the load maximums at high speeds is observed. This is because the drive train mode causes a high momentum in the "x" direction in the low speed shaft and, when activating the DTD, the damping of that mode results in the reduction of this load.

6.4. Frequency analysis in power production wind of 25m/s

In this section, a frequency analysis of the four control configurations is going to be carried out. Particularly, the four situations are going to be simulated for a wind speed of 19m/s.

Next, the time-series and frequency decompositions of several variables are going to be shown.

The first analyzed variable is the generator speed.

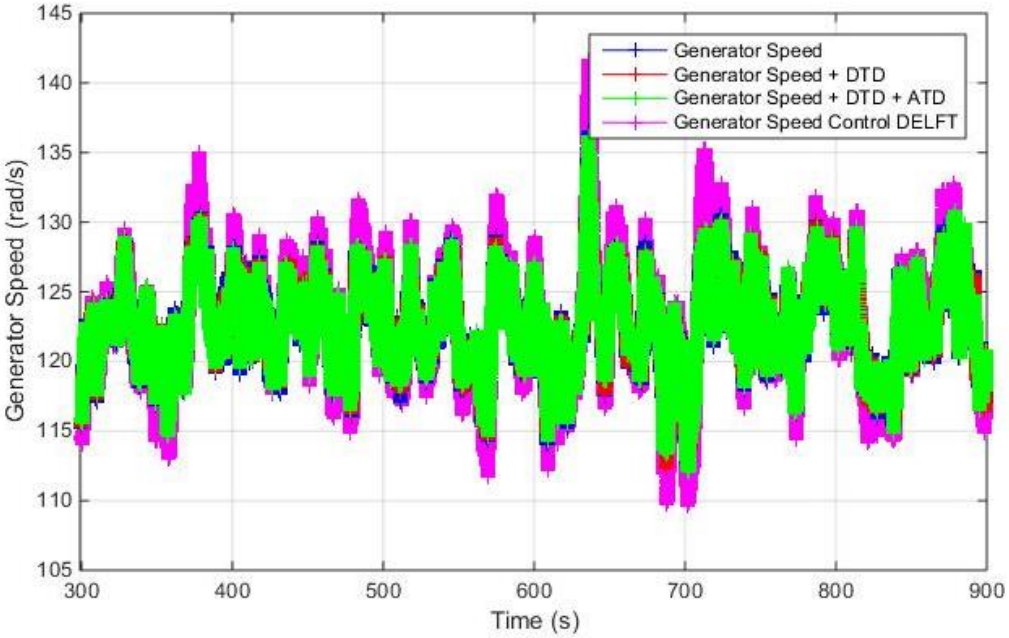

Figure 119: Generator speed vs. time in 60s simulations

The previous figure shows a graph of the generator speed vs. time. Both this project's and Delft's control strategy give the same average speed (rated generator speed), but the figure illustrates how the latter does not keep the generator speed as tight to the desired value as the former does.

The inconvenience of keeping the generator speed too tight to the reference value is that any disturbance will not result in a change in the generator speed but it will be transmitted straight to the mechanical system of the wind turbine, which increases the loads and efforts in the structure.

Next, the Fast Fourier Transform (FFT) of the generator speed is shown in the figure below. The FFT of a signal is the result of an algorithm that computes the frequency representation of a time domain signal. This way, the components of the signal at each frequency are shown, which makes its frequency analysis much easier.

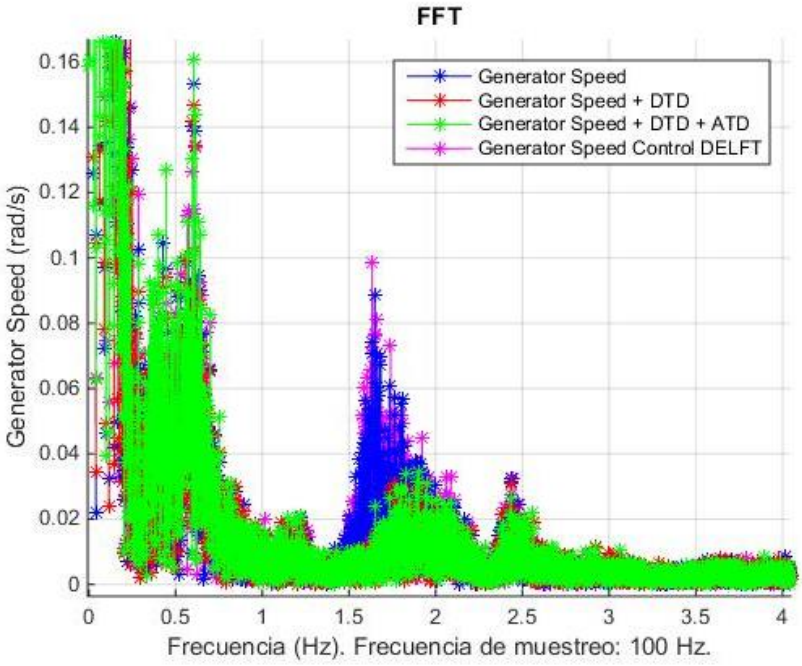

Figure 120: Generator speed FFT in 600s simulations

The figure shows how, for Delft's control strategy as well as for the strategy without DTD, there is a much higher activity at the drive train frequency (1.645 Hz). When entering the DTD, the damping of the drive train mode makes reduces the generator speed activity at that frequency.

Next, the blade pitch angle is going to be analyzed.

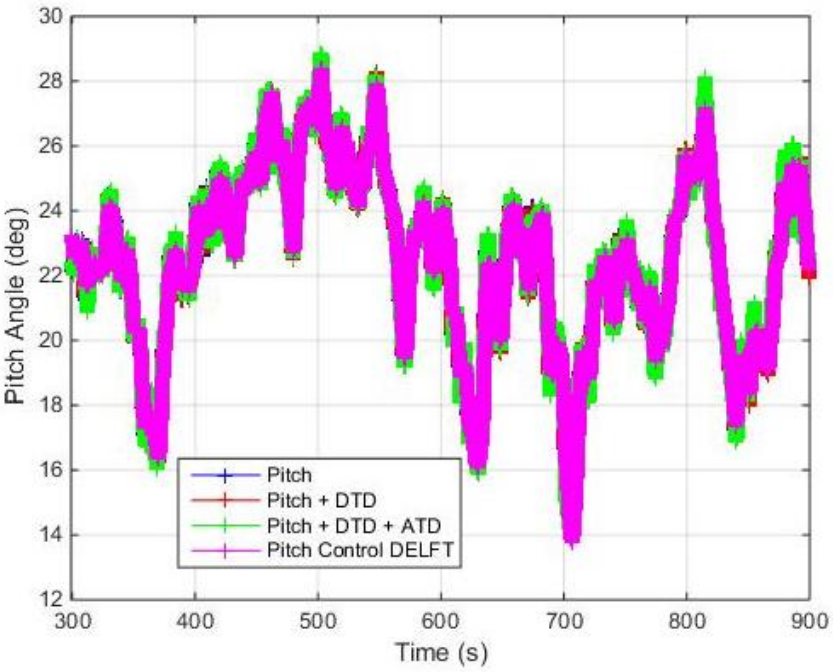

Figure 121: Blade pitch angle vs. time for 600s simulations

The previous figure shows the pitch angle vs. simulation time, it illustrates that this project's control strategy has a little more activity than Delft University's.

Next, the FFT of the pitch signal is graphed.

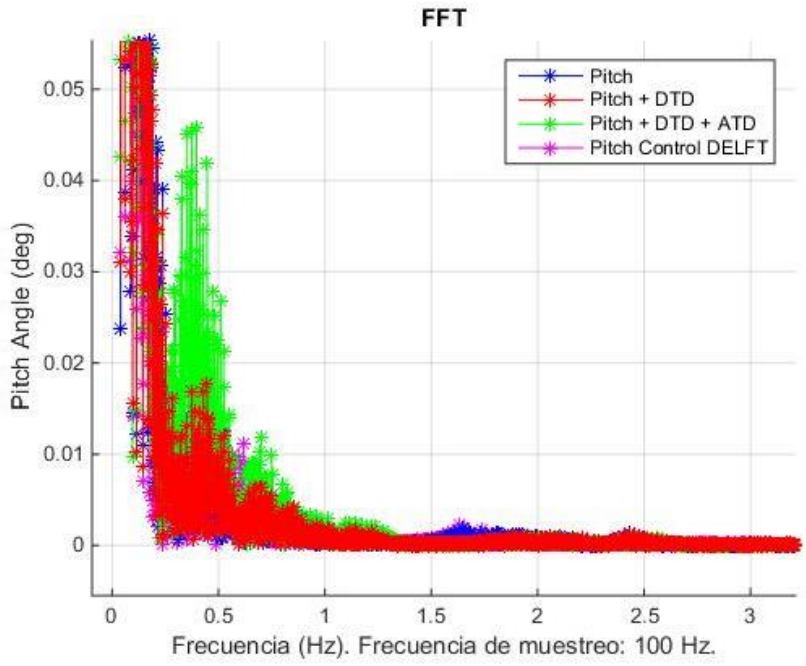

Figure 122: Blade pitch angle FFT in 600s simulations

The figure shows how the complete control strategy of this project (the one that includes the ATD) has a lot of activity at the 1st tower fore-aft frequency. This is because of the ATD's contribution to the blade pitch angle, which is focused at that frequency.

The figure also shows how the pitch angle is also affected by the DTD, which contributes to reducing pitch activity at the drive train frequency.

Now, the generated power is going to be analyzed. The following figure shows the time-series of the electric power produced by the generator.

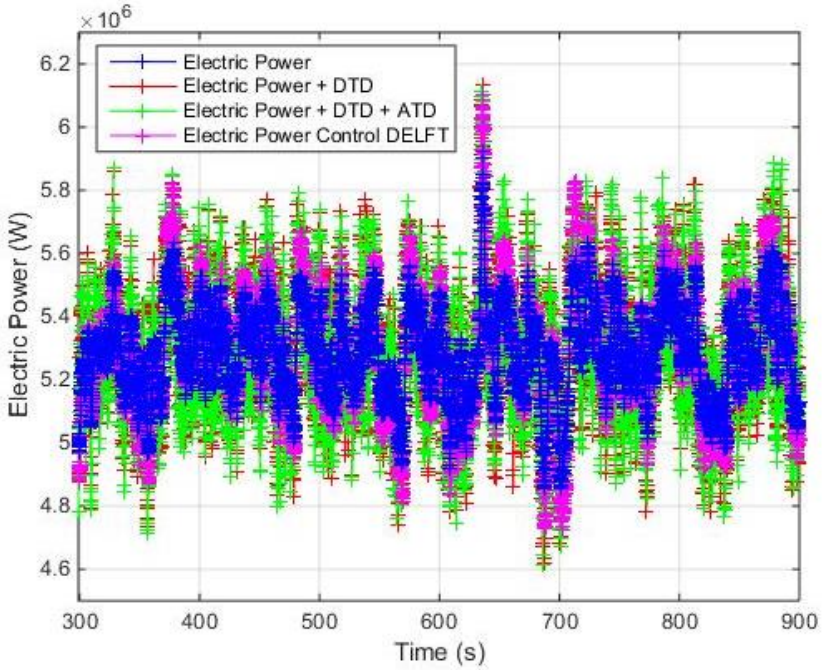

Figure 123: Generator power vs. time in 600s simulations

Next, the FFT of the power signal is graphed.

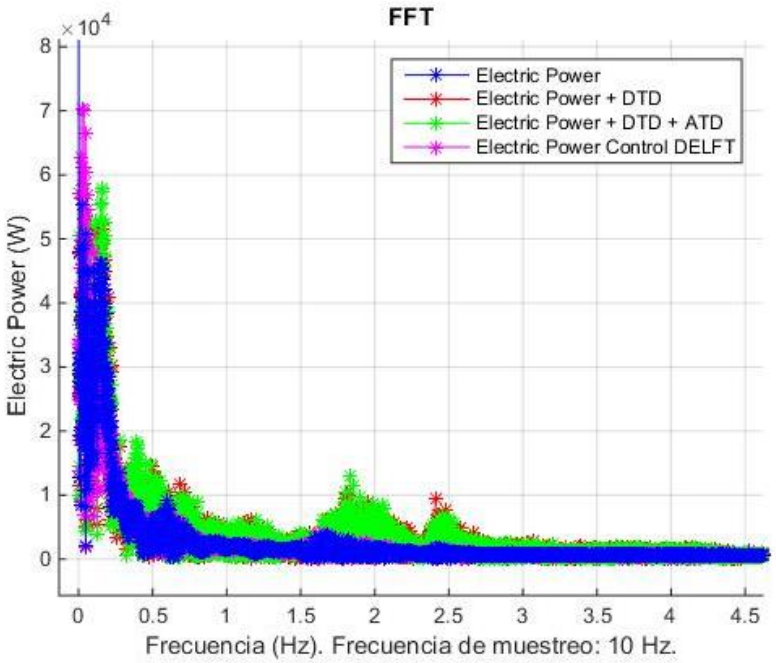

Figure 124: Generator power FFT in 600s simulations

It can be observed from the previous graph how the electric power of the Scenario C control has a much higher component at the drive train frequency (1.645 Hz) than the Scenario D, which does not have a DTD strategy. The same thing happens at the 1st fore-aft mode frequency, where the only strategy with ATD (Scenario C) has a much higher component.

Next, the nacelle's fore-aft acceleration is analyzed.

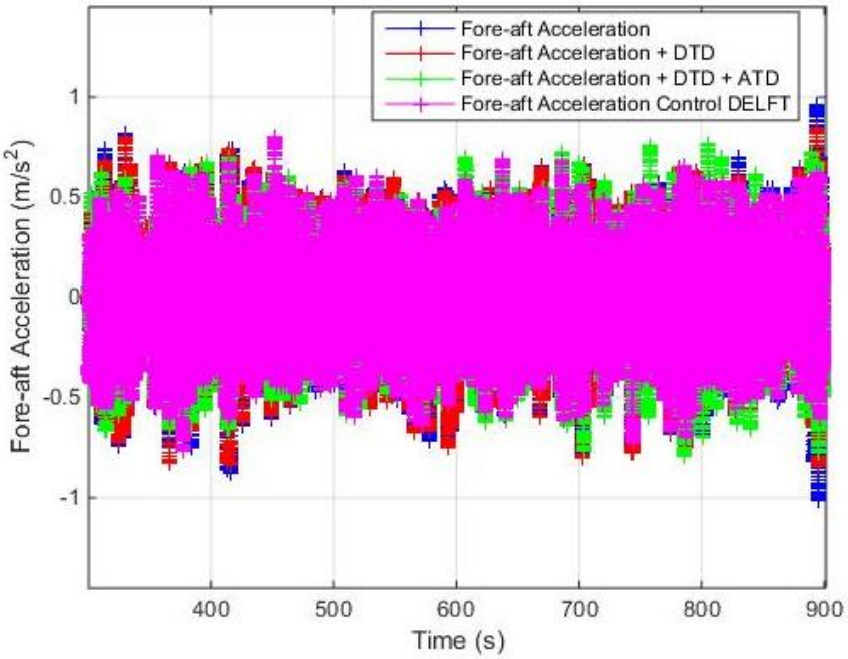

Figure 125: Nacelle fore-aft acceleration vs. time in 600s simulations

The previous figure shows the time series of the nacelle's fore-aft acceleration and next, the FFT of the same signal is graphed.

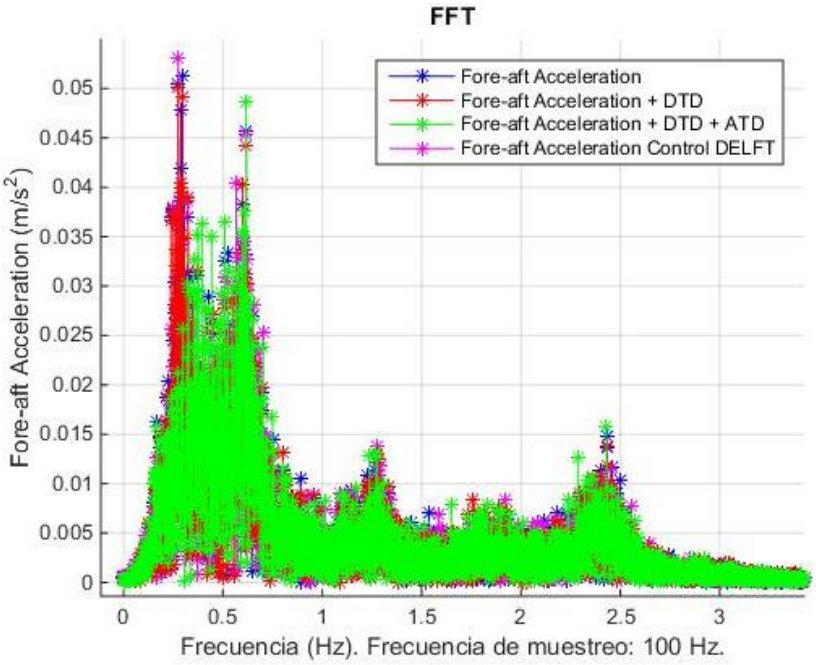

Figure 126: Nacelle fore-aft acceleration FFT in 600s simulations

The previous graph shows how the activity at the 1st tower fore-aft frequency is drastically reduced when the ATD is introduced in the control strategy of this project. The figure also shows that, when introducing the ATD strategy, the component of the fore-aft acceleration at the 3P

rotational frequency (0.6 Hz) increases its amplitude. The load analysis will be the one to determine if removing that fore-aft frequency activity is worth it even though the ATD introduces some 3P frequency amplification.

Next, the ATD's pitch contribution is analyzed.

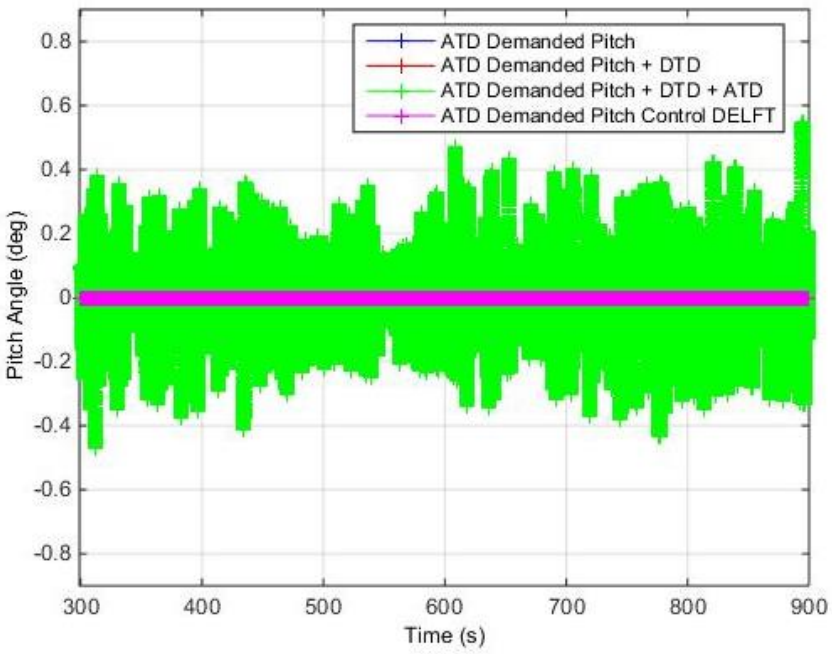

Figure 127: ATD Demanded pitch angle vs. time in 600s simulations

Now, the FFT graph of the pitch demanded by the ATD is shown for each control configuration

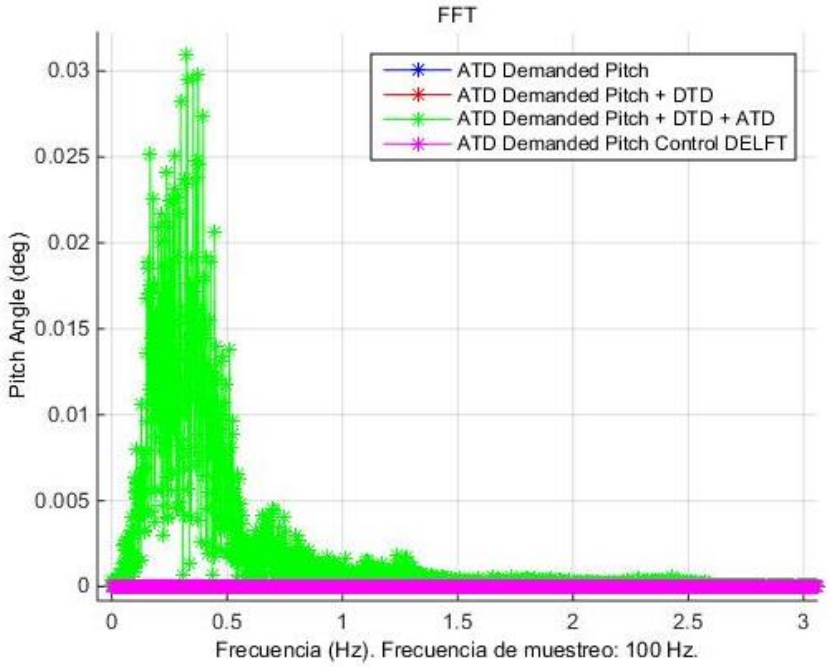

Figure 128: ATD Demanded pitch vs. time in 600s simulations

The only configuration that has an ATD strategy and that therefore has an ATD pitch signal is the Scenario C. The FFT graph shows how most activity focuses at the 1st tower fore-aft mode frequency.

6.5. Fatigue Load analysis (minirainflows)

6.5.1. Fatigue load analysis process

When validating a control strategy, carrying out a load analysis is essential. Any improvement introduced in the controller block should be reflected positively in the wind turbine's structural loads.

To carry out the fatigue load analysis, **standardized wind** distributions must be used. As it was explained in section 3.2 Upwind 5MW wind turbine modelled in FASTv7 (Simulink Environment), these winds are generated by the stochastic, full-field wind simulator TurbSim, developed by NREL. They are generated according to the norm IEC 61400-1 [8].

Once these standard winds have been generated, the different control configurations must be simulated with those winds. Next, the simulation output files must be postprocessed by the MATLAB-based fatigue life estimator **MLife**. If extreme loads needed to be analyzed, the postprocessor MCrunch would be used.

The MLife tool needs three types of files in order to carry out not only the fatigue load analysis, but also a statistical analysis of the simulations. These files are: the simulation output files (**.out**), the main MLife input file (**.mlif**) and a MATLAB script (**.m**) that calls for the MLife main file therefore executing the postprocessor. The analysis settings and parameters are read from the MLife input file, also referred to as the settings file. Mlife allows including more than one simulation output (.out) in the same main input (.mlif) file, which gives the possibility to analyze several wind distributions in the same run.

The variables that want to be analyzed must be indicated first in the main simulation input file (.fst) so that the data appears in the simulation output file (.out) and second in the (.mlif) file, so that only the desired variables get analyzed.

Some of the most important settings that must be indicated at the .mlife file are the Wöhler curve of the different components' material and the Weibull distribution of the emplacement's winds.

The **Wöhler** curve of a material, also termed S-N curve, is a plot that represents the alternating stress (S) vs. cycles to failure (N) for that material. This way, knowing either the number of cycles to failure or the fatigue stress applied, the other one can be obtained.

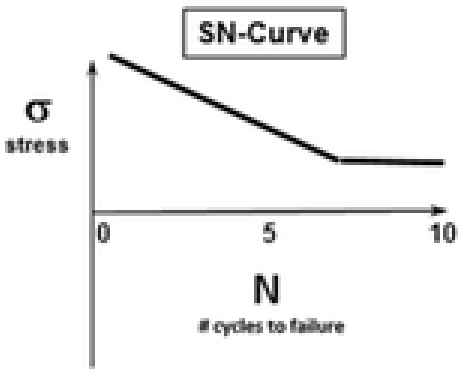

Figure 129: Typical S-N or Wöhler curve

To indicate the component's material, a Wöhler associated slope "m" must be introduced to MLife: 3 to 5 for modular steel; 7 to 9 for iron and 12 to 14 for fiber. Each component can be tested with more than one material. The next S-N curve slopes have been introduced for the different components in the .mlif file to carry out the load analysis of this project: **m = 12** for the **blades**, **m = 8** for the **tower and yaw** and **m = 4** for the **shaft**

To carry out the load analysis, the probability density distribution of the wind speed must be known. This is called the **Weibull** distribution of wind at a certain site. Not only it is important for the load calculation but also for the wind turbine's AEP (Annual Energy Production). The wind distribution used for the load and statistic analysis of this project has been extracted from [11] and it is shown next. It is defined in MLife with the curve's shape factor, 2, and mean wind speed, 11 m/s.

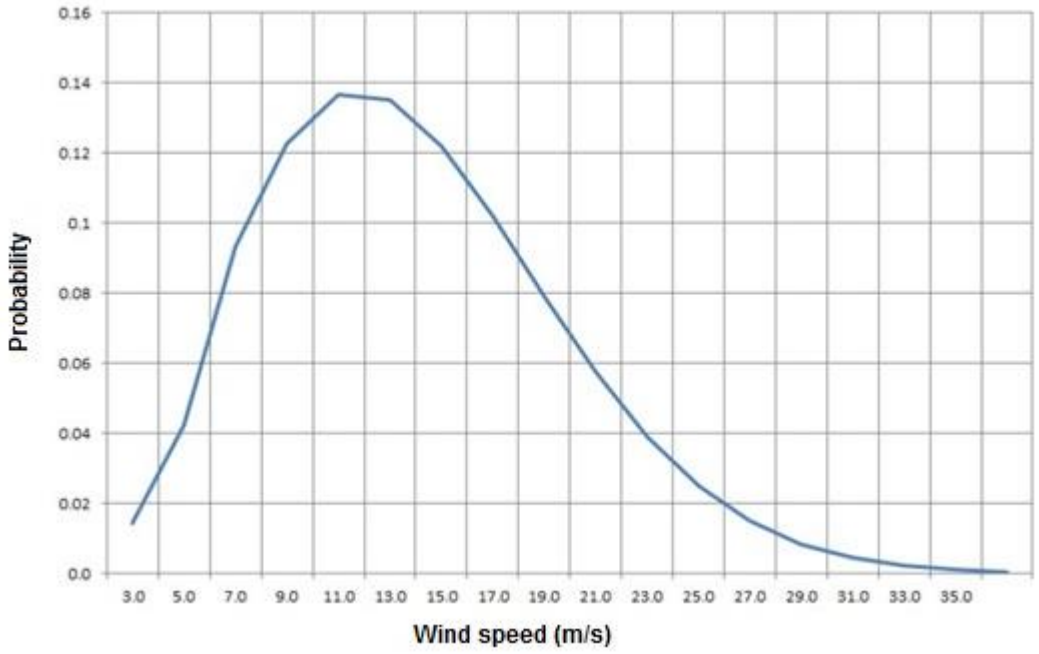

Figure 130: Weibull distribution used for load and statistical analysis

The .mlif file also includes the option to write down the analysis results to text files, to Excel workbooks or to a combination of both. These files include the different components' lifetime and short-term damage, lifetime and short-term damage equivalent loads, etc.

In this project, the different control configurations are compared in terms of **Damage Equivalent Loads (DEL)**. This equivalent load is the constant frequency and amplitude load that woud provoque the same damage in the components as the real irregular loads do.

Finally, the variables that are going to be analyzed to see the improvement of each control scenario are the following:

BLADE

· **RootMxb1**: blade edgewise moment at the blade root (kN·m)

· **RootMyb1**: blade flapwise moment at the blade root (kN·m)

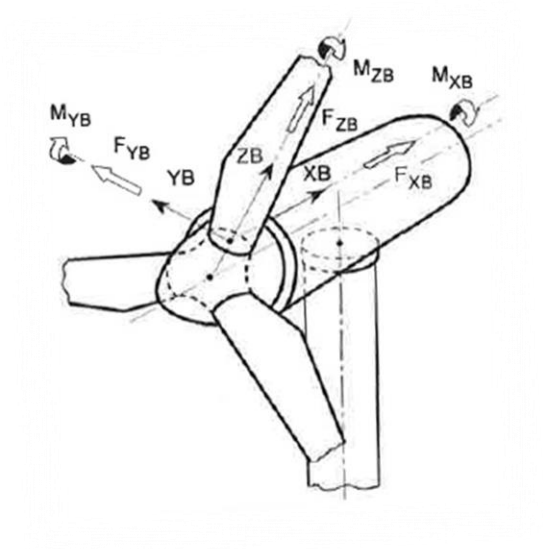

Figure 131: Blade coordinate system for blade root loads

TOWER

· **TwrBsMxt**: tower base side-to-side moment (kN·m)

· **TwrBsMyt**: tower base fore-aft moment (kN·m)

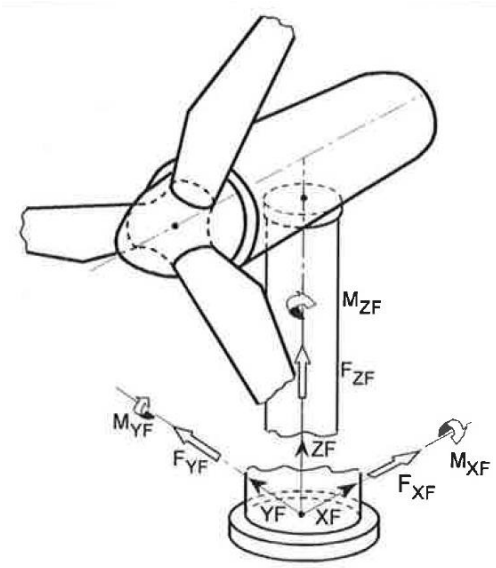

Figure 132: Tower coordinate system for tower base loads

YAW, TOWER TOP

· **YawBrFxn**: rotating yaw bearing shear force (kN)

· **YawBrMxn**: rotating yaw bearing roll moment (kN·m)

· **YawBrMyn**: rotating yaw bearing pitch moment (kN·m)

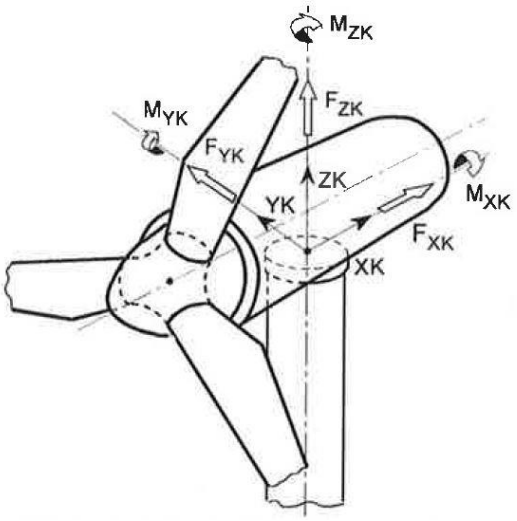

Figure 133: Yaw coordinate system for yaw bearing loads

SHAFT

· **LSShftMxa**: low speed shaft torque (rotating low speed shaft torsional moment in the "x" axis) (kN·m)

· **LSShftMys**: nonrotating low speed shaft bending moment in the "y" axis (kN·m)

· **LSSGagMzs**: nonrotating low speed shaft bending moment in the "z" axis (kN·m)

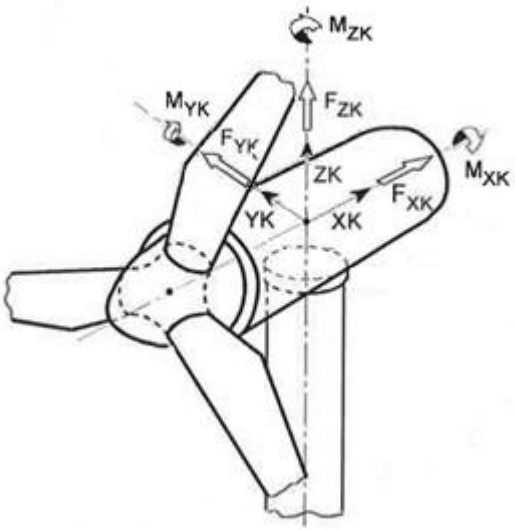

Figure 134: Shaft coordinate system for low speed shaft loads

6.5.2.Fatigue load analysis results

This section is dedicated to analyzing the fatigue load results obtained from Mlife. The study has been carried out with the same four scenarios from section 6.1.

The obtained damage equivalent loads are compared in the spider chart below.

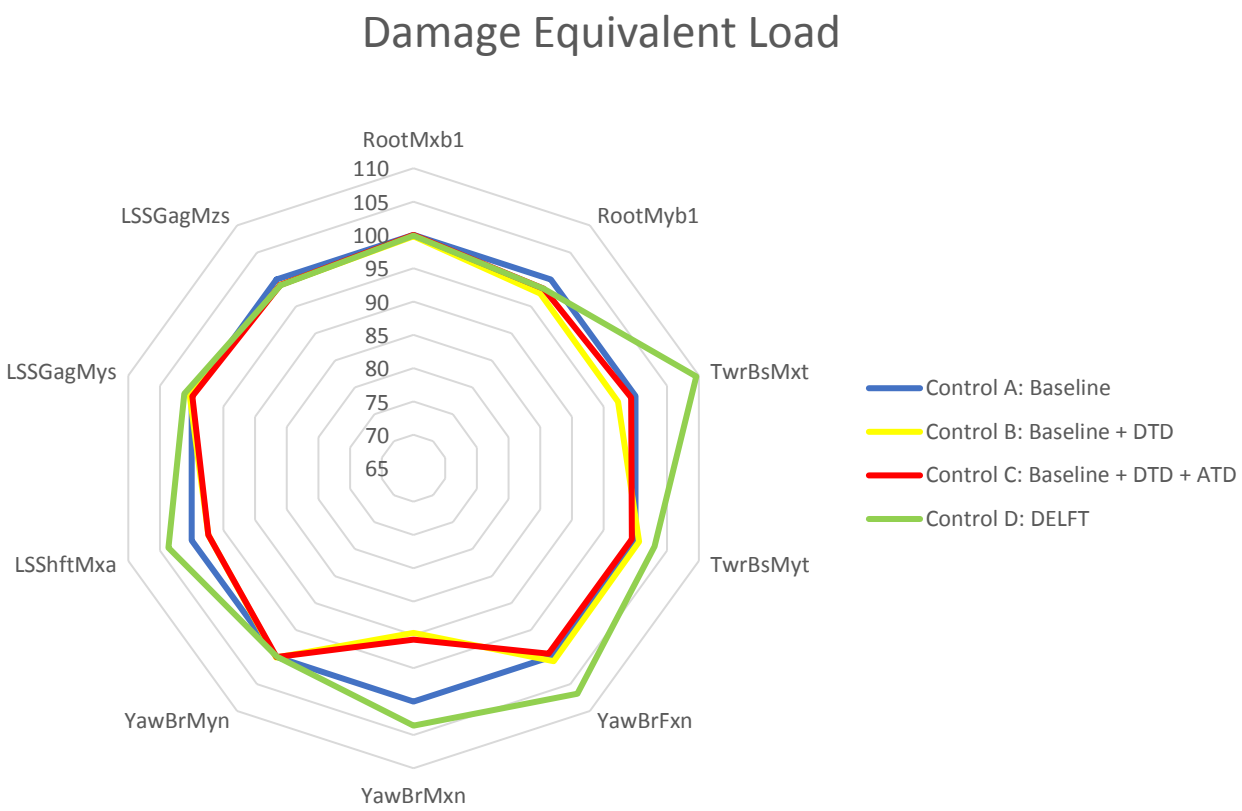

Figure 135: Fatigue load analysis spider chart for 600s simulations

The reference scenario is the Scenario A, which only has the power control proposed in this project. It can be observed that, for Scenario B, which corresponds to the activation of the DTD, an important reduction of the yaw bearing moment in the "x" axis (10% load reduction) can be observed. This is due to the damping of the drive train mode. When reducing the vibrations of the DTD in the "x" axis, the ones transmitted to the yaw bearing are reduced. For the same reasons, the tower base momentum in the x axis lightly decreases too. A 3% load reduction is obtained too for the rotating moment of the shaft, which makes sense due to the reduction of the shaft's vibrations.

When introducing the ATD strategy, Scenario C, the tower base "y" momentum slightly decreases. This is due to the damping of the tower's 1st fore-aft mode. By reducing the nacelle's acceleration in that frequency, the moment transmitted to the tower base in the "y" axis is reduced. The yaw bearing shear force in the "x" axis decreases a little bit too, due to the same reasons.

For last, it can be observed that the Scenario D, Delft's control strategy has a 10% higher tower base momentum in the "x" axis than Scenario A, which means that that control strategy is worse for the excitement of the drive train mode than the one proposed in this project. In consecuence, the yaw bearing moment in the "x" axis is bigger too (4% bigger than strategy A), as well as the low speed shaft rotating moment (4% higher loads). Also, something similar happens, to a lower

level (3% higher load with Scenario D), with the tower base's momentum in the "y" axis. The D strategy itself gives less damping to the 1st fore-aft mode than the Scenario A does. This is very significant for the load analysis because the tower base "y" load is a lot bigger than the "x" load in absolute terms, which means the "y" load is the one that sets the design requirements of the tower.

6.6. Conclusions

It can be concluded that the A, B and C strategies introduced in this project's control strategy, are beneficial and they reduce the wind turbine's structural loads. It can be concluded that strategy D, Delft's control strategy, could be better adjusted for this specific model and simulating conditions. Under these circumstances, the control strategy proposed in this project gives better results.

It was observed in the frequential analysis of the nacelle's fore-aft acceleration that the ATD reduced the component of the acceleration at the 1st tower fore-aft mode frequency, 0.28 Hz, but that it amplified the acceleration at the 3P frequency, 0.6 Hz. As it can be observed in the spider chart of the previous section, section 6.5.2, the ATD strategy is worth introducing, because even though it amplifies the 3P frequency, the reduction of the acceleration at the 1st tower fore-aft frequency reduces the structural loads more than the amplification of the other frequency increases them.

Since the three, A, B and C strategies have been validated, the new control baseline for future analysis will be Scenario C, which includes power control as well as the active control DTD and ATD strategies.

Chapter 7: Analysis of generator speed filtering process in Pitch Control Loop vs baseline

7.1. Introduction

In this chapter, the analysis of the generator speed filtering process in the pitch control is going to be carried out. To do this, the baseline control strategy will be the control strategy proposed in this project including the active control strategy, this is, the pitch and torque loops will be activated as well as the DTD and ATD strategies.

This study consists of a statistical and load analysis, as well as a closed loop performance analysis.

The main parameters that are going to be varied are the pitch control's notch filters' width and depth. Next, the relationship between the parameters of the notch filters appearing in the Simulink control library and the filters width and depth is explained.

The filters in the control library have been built with the next formula and parameters:

$$Notch\ (s) = k \cdot \frac{s^2 + 2\xi_z\omega_{nz}s + \omega_{nz}^2}{s^2 + 2\xi_p\omega_{np}s + \omega_{np}^2}$$

And another way of expressing a notch filter is:

$$N\ (s) = \frac{s^2 + 2 \cdot g_{min} \cdot damp \cdot freq \cdot s + freq^2}{s^2 + 2 \cdot damp \cdot freq \cdot s + freq^2}$$

And from [12] it is obtained that:

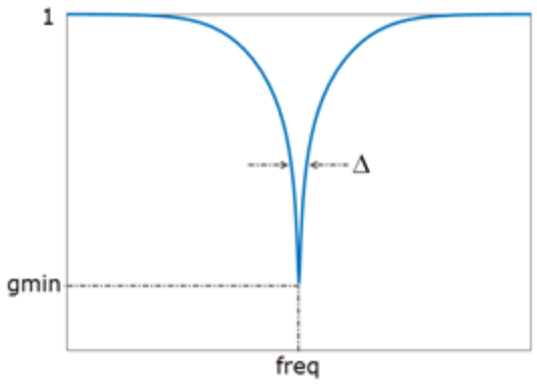

Figure 136: Notch filter parameter interpretation

Where the damping ratio *damp* controls the notch width Δ, larger *damp* means larger Δ.

The relationship between this filter's parameters and the parameters of the filter in the Simulink library are:

$$\omega_{nz} = \omega_{np} = freq$$

$$\xi_p = damp$$

$$\xi_z = g_{min} \cdot \xi_p$$

By moving the pole (ω_{nz}) and the zero (ω_{np}), which are placed at the same frequency, the notch filter is moved.

By **increasing ξ_z**, the absolute value of **g_{min} decreases** proportionally and vice versa.

By **increasing ξ_p, Δ increases** proportionally and vice versa.

Once the relationship between the different parameters and their effect on the filter's shape and location has been explained, the following scenarios are proposed to carry this study out.

The filters that are going to be modified during this analysis are the pitch control loop's 1st order low pass filter and the notch filters placed at the drive train mode (Notch DT), at the 1st symmetric (Notch Sym), at the 2nd tower side-to-side (Notch 2Tss) and at the 1P and 3P frequencies.

Control		PitchControl					
		LowPass	NotchDT	NotchSym	Notch2Tss	Notch1P	Notch3P
Baseline	**0**	OFF	baseline	baseline	baseline	OFF	baseline
Scenario 1	**0**	0.5 Hz	baseline	baseline	baseline	OFF	baseline
	1	1 Hz	baseline	baseline	baseline	OFF	baseline
	2	2 Hz	baseline	baseline	baseline	OFF	baseline
Scenario 2	**3**	OFF	gmin↑	baseline	baseline	OFF	baseline
	4	OFF	gmin↓	baseline	baseline	OFF	baseline
	5	OFF	damp↑	baseline	baseline	OFF	baseline
	6	OFF	damp↓	baseline	baseline	OFF	baseline
	7	OFF	OFF	baseline	baseline	OFF	baseline
Scenario 3	**8**	OFF	baseline	gmin↑	baseline	OFF	baseline
	9	OFF	baseline	gmin↓	baseline	OFF	baseline
	10	OFF	baseline	damp↑	baseline	OFF	baseline
	11	OFF	baseline	damp↓	baseline	OFF	baseline
	12	OFF	baseline	OFF	baseline	OFF	baseline
Scenario 4	**13**	OFF	baseline	baseline	gmin↑	OFF	baseline
	14	OFF	baseline	baseline	gmin↓	OFF	baseline
	15	OFF	baseline	baseline	damp↑	OFF	baseline
	16	OFF	baseline	baseline	damp↓	OFF	baseline
	17	OFF	baseline	baseline	OFF	OFF	baseline
Scenario5	**18**	OFF	baseline	baseline	baseline	ON	baseline
Scenario 6	**19**	OFF	baseline	baseline	baseline	OFF	gmin↑
	20	OFF	baseline	baseline	baseline	OFF	gmin↓
	21	OFF	baseline	baseline	baseline	OFF	damp↑
	22	OFF	baseline	baseline	baseline	OFF	damp↓
	23	OFF	baseline	baseline	baseline	OFF	OFF

Table 19: Pitch control filtering process study Scenarios

In these studies, except for the 1st order low pass filter and the notch filter at the 1P, variations of the filter's damp (notch filter width Δ) and gmin of a **10%** are going to be studied. The next table includes the new values of the parameters for each configuration.

Scenario 1: LowPass	Baseline	Case 0 (0.5Hz)	Case 1 (1Hz)	Case 2 (2Hz)
UPNA_WT_Control.PitchControlLoop.LowPass.enable	0	1	1	1
UPNA_WT_Control.PitchControlLoop.LowPass.thau (s)	-	0.316	0.158	0.079

Scenario 2: Notch DT	Baseline	Case 3 (gmin↑)	Case 4 (gmin↓)	Case 5 (damp↑)	Case 6 (damp↓)	Case 7 (OFF)
UPNA_WT_Control.PitchControlLoop.NotchDT.Dampz	0.1	0.0909	0.11	0.1	0.1	0.1
UPNA_WT_Control.PitchControlLoop.NotchDT.Dampp	0.8	0.8	0.8	0.88	0.7273	0.8
UPNA_WT_Control.PitchControlLoop.NotchDT.enable	1	1	1	1	1	0

Scenario 3: Notch Sym	Baseline	Case 8 (gmin↑)	Case 9 (gmin↓)	Case 10 (damp↑)	Case 11 (damp↓)	Case 12 (OFF)
UPNA_WT_Control.PitchControlLoop.Notch1simetrica.Dampz	0.03	0.0273	0.033	0.03	0.03	0.03
UPNA_WT_Control.PitchControlLoop.Notch1simetrica.Dampp	0.15	0.15	0.15	0.165	0.1364	0.15
UPNA_WT_Control.PitchControlLoop.Notch1simetrica.enable	1	1	1	1	1	0

Scenario 3: Notch 2Tss	Baseline	Case 13 (gmin↑)	Case 14 (gmin↓)	Case 15 (damp↑)	Case 16 (damp↓)	Case 17 (OFF)
UPNA_WT_Control.PitchControlLoop.Notch1simetrica.Dampz	0.03	0.0273	0.033	0.03	0.03	0.03
UPNA_WT_Control.PitchControlLoop.Notch1simetrica.Dampp	0.15	0.15	0.15	0.165	0.1364	0.15
UPNA_WT_Control.PitchControlLoop.Notch1simetrica.enable	1	1	1	1	1	0

Scenario5: Notch 1P	Baseline	Case 18 (ON)
UPNA_WT_Control.PitchControlLoop.Notch1P.enable	0	1

Scenario6: Notch 3P	Baseline	Case 19 (gmin↑)	Case 20 (gmin↓)	Case 21 (damp↑)	Case 22 (damp↓)	Case 23 (OFF)
UPNA_WT_Control.PitchControlLoop.NotchDT.Dampz	0.01	0.0091	0.011	0.01	0.01	0.01
UPNA_WT_Control.PitchControlLoop.NotchDT.Dampp	0.2	0.2	0.2	0.22	0.22	0.2
UPNA_WT_Control.PitchControlLoop.NotchDT.enable	1	1	1	1	1	0

Table 20: Pitch control filtering process study Scenarios' parameters

7.2. Control scenario 1, 1st order Low Pass filter

7.2.1.Control performance (open loop, sensitivities) vs baseline

In this first scenario, the addition of a 1st order low pass filter in the pitch control loop is going to be studied. There will be four different configurations: the filter is going to be OFF, placed at 0.5Hz, 1Hz and 2Hz in order to compare the control behavior with the different filters.

First, the open loop behavior of the pitch control is shown for the four configurations.

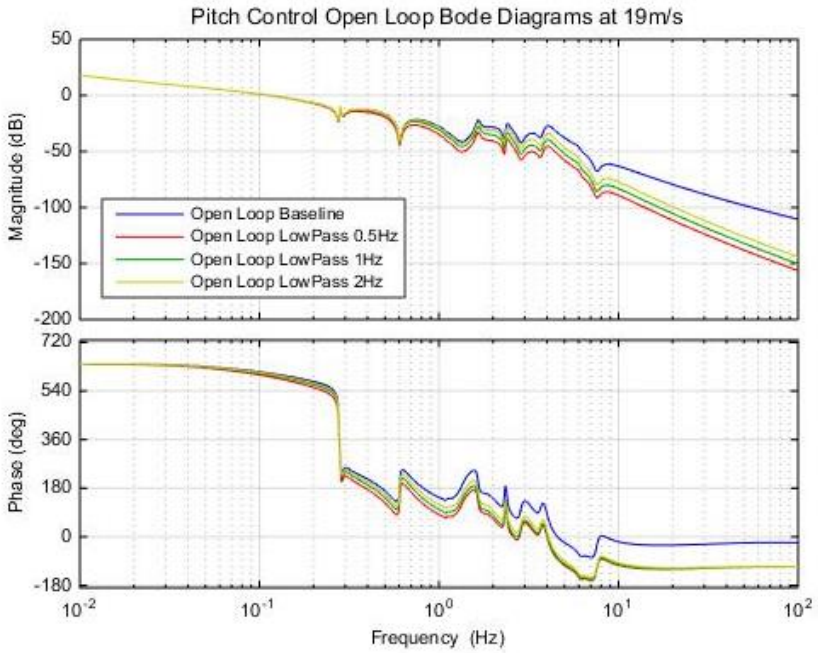

Figure 137: Bode diagram of the pitch control open loop for Scenario 1 at 19m/s

From the previous figure, it can be observed that the neither the gain nor the phase margin vary a lot with the modification of the 1st order low pass filter. Nevertheless, the configuration with the biggest gain and phase margins is the Baseline configuration (13.3dB and 65.2 deg, respectively). It can also be observed how the one with the low pass filter placed at 0.5Hz (Case 1) is the one with the smallest margins (9.72dB and 53.6deg).

Next, the closed loop disturbance sensibility S(s) of the pitch control is going to be checked for the four configurations.

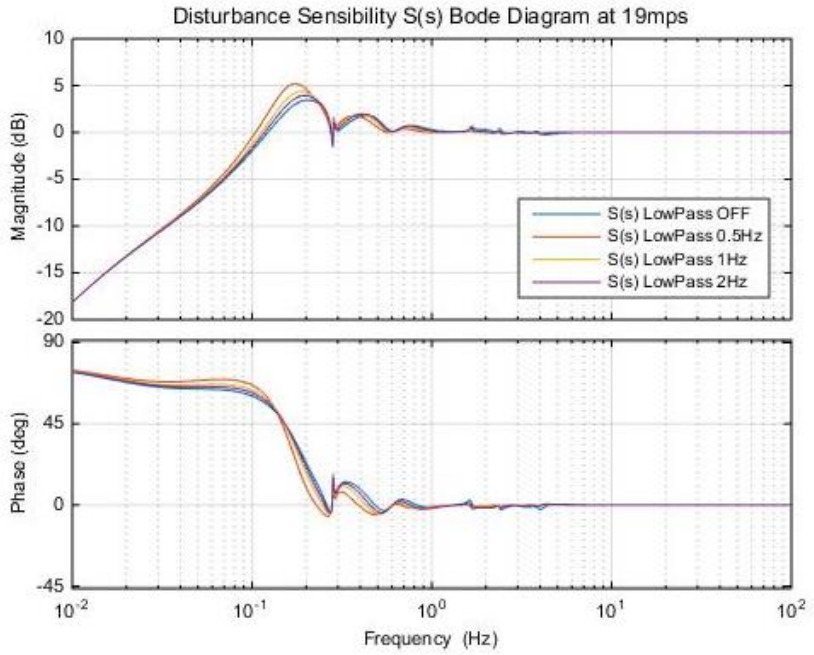

Figure 138: Bode diagram of the closed loop pitch control's S(s) for Scenario 1 at 19m/s

From the previous graph, it can be observed how the best disturbance rejection behavior in the closed loop is with the Baseline configuration. The one that is the furthest from the desired behavior is Case 0, with the filter placed at 0.5Hz, because it has the biggest peak, bigger than 6dB.

Next, the tracking sensibility T(s) of the configurations at 25m/s is shown.

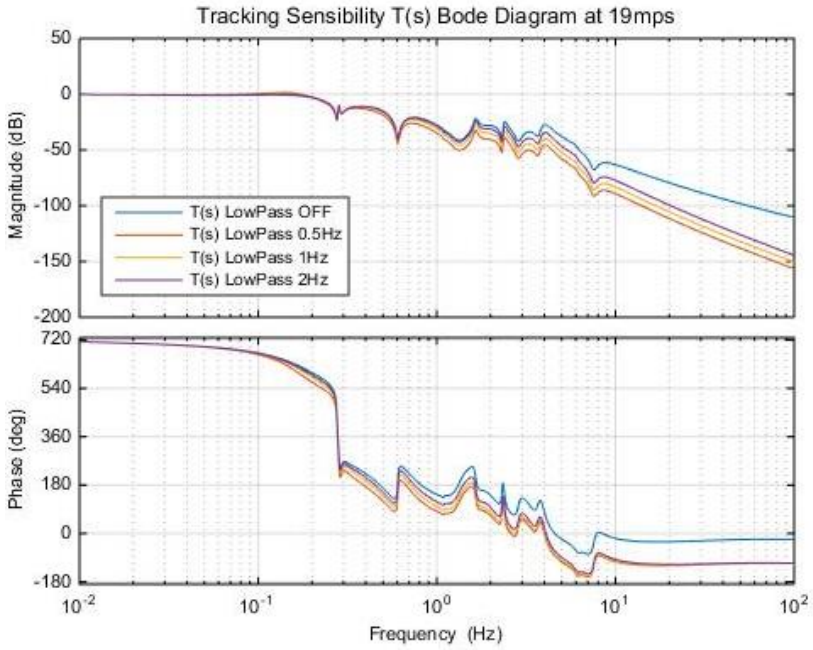

Figure 139: Bode diagram of the closed loop pitch control's T(s) for Scenario 1 at 19m/s

The previous graph shows how the configurations with the low pass filter activated have a small amplification of the tracking response at certain frequencies (between 0.14Hz and 0.2Hz), which is not the desired behavior. The desired closed loop tracking response is a response with 0dB at low frequencies so that the reference is followed and tracking rejection at high frequencies, with additional attenuation of the frequencies where the notch filters have been placed. Again, the Baseline configuration behavior is the closest to the desired behavior and Case 0 is the furthest.

Next, the control sensibility U(s) is going to be shown for the four different configurations.

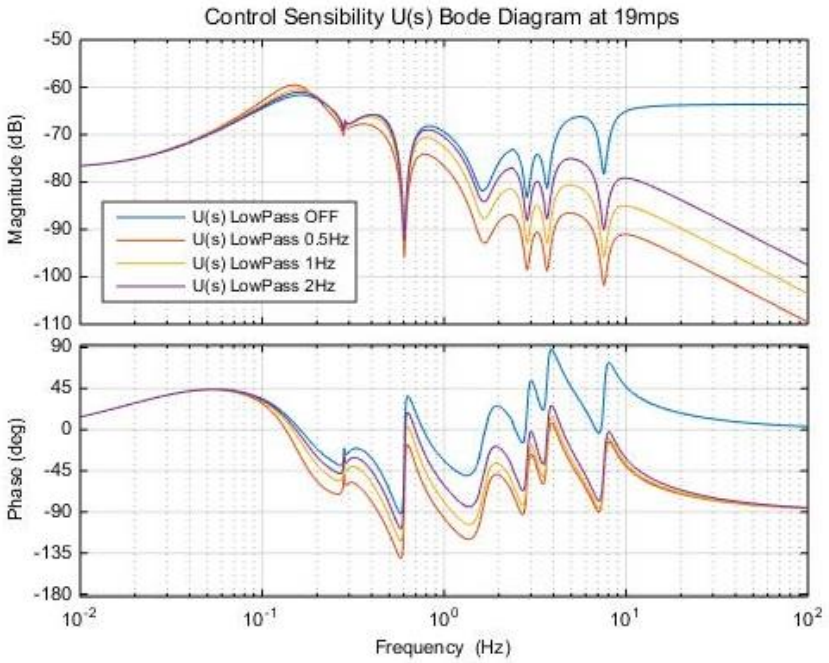

Figure 140: Bode diagram of the closed loop pitch control's U(s) for Scenario 1 at 19m/s

The control sensibility is the relationship between the disturbance and the control action. At low frequencies, which is where the wind disturbance will be, a constant control action is sought. Then, at the frequencies where the notch filters are placed, a very low control action is necessary so that the activity at those frequencies is as small as possible. Finally, a low magnitude would be best at high frequencies in order to reject disturbance noise. This is where the low pass filter configurations have the best behavior, because they filter high frequencies. The configuration with the best closed loop control sensibility U(s) behavior is Case 2. This configuration has a low pass filter at 2Hz. It rejects noise at high frequencies and it has the 2nd closest desired behavior at other frequencies because it has the second smallest peak at lower frequencies.

7.2.2.Statistical analysis

In this section, the statistical analysis of the four configurations is going to be carried out.

First, the generator speed vs. wind maximums, minimums and means are shown in the next figure.

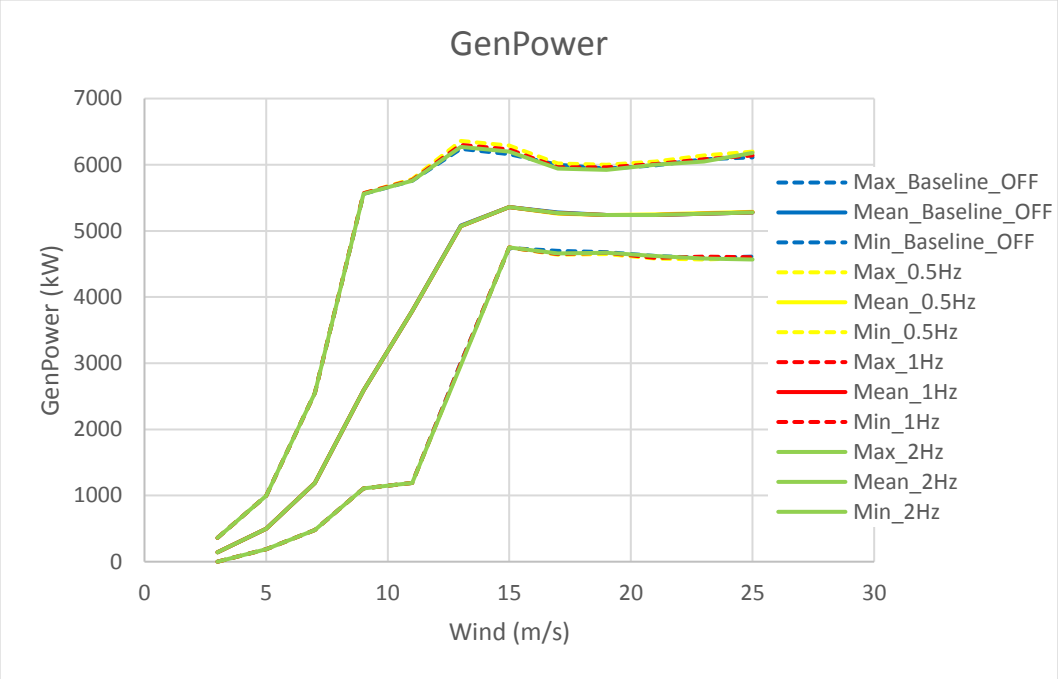

Figure 141: Generated power statistics for Scenario 1

It can be observed how the mean generated power is the same for the four configurations, only that Case 1, with the first order filter, is the one with the maximum generated power. Since they all have the same mean, the one with the minimum maximum will be selected, which is the Baseline configuration.

Next, the standard deviation graph of the pitch is shown vs. wind.

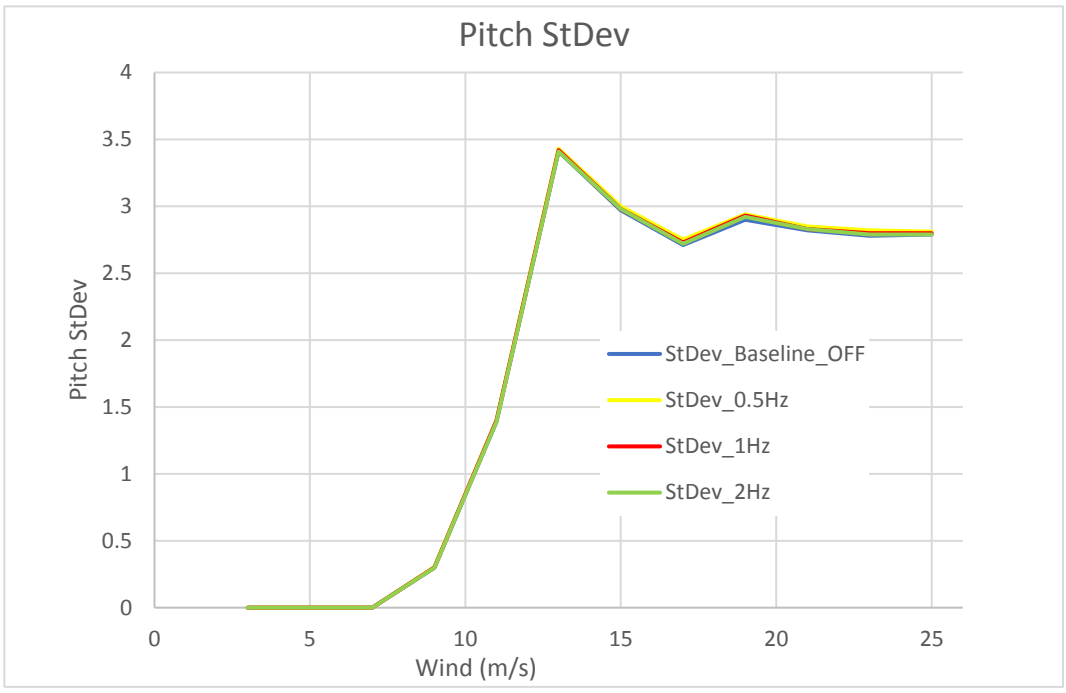

Figure 142: Pitch standard deviation for Scenario 1

It can be observed from the previous figure that the pitch activity, reflected in the pitch standard deviation, is very similar with the four configurations. Indeed, the Baseline configuration seems to be the one with the lowest pitch duty, with a minimum difference.

The very little difference that can be observed in the open and closed loop behavior as well as in the statistics when introducing the low pass 1st order filter could be due to the fact that the pitch actuator is a 1st order filter with a cutoff frequency of 1 Hz. The actuator itself is capable of filtering the high frequencies of the pitch signal by its own dynamics and therefore introducing this filter barely has any effect on the system.

Next, the tower base “y” momentum is shown with respect to wind.

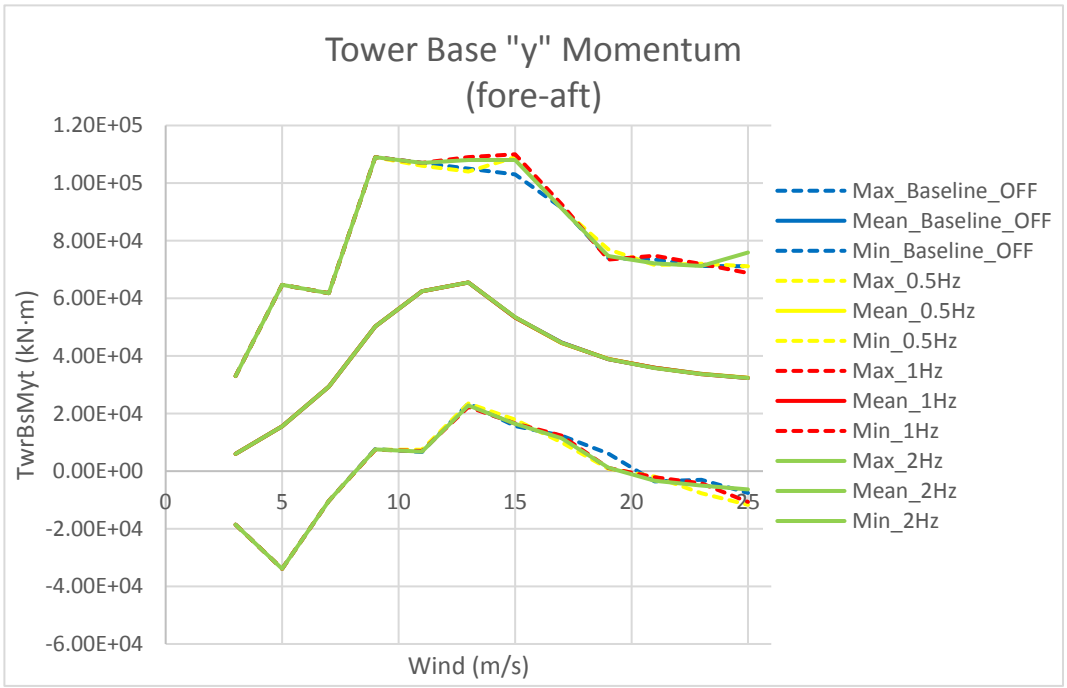

Figure 143: Tower base "y" momentum statistics for Scenario 1

The previous figure shows how the four configurations have the same mean momentum. Therefore, the one with the smallest maximums will be the best. Even though the load at 21m/s is a little above the Case 2 configuration (low pass filter at 2 Hz), the configuration with smallest overall maximums is the Baseline configuration, no low pass filter.

Next, the low speed shaft momentum in the "x" axis is graphed with respect to wind.

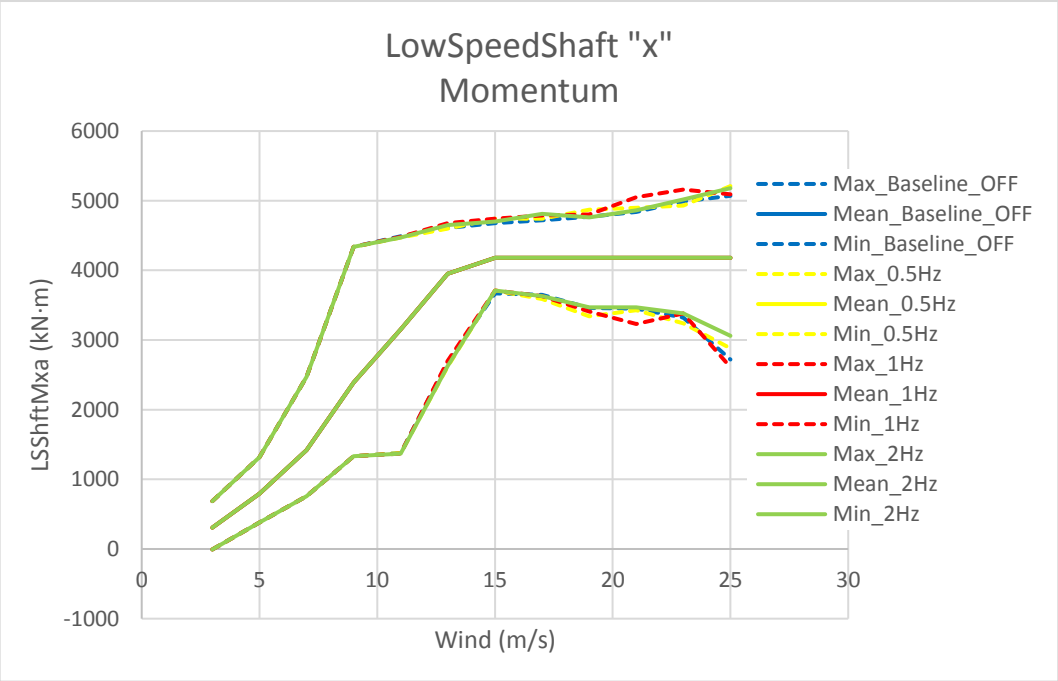

Figure 144: Low speed shaft "x" momentum statistics for Scenario 1

Just like for the graph before, the previous graph shows the same load mean for all four configurations. The best strategy regarding low speed shaft momentum in the "x" axis is therefore the Baseline configurations because it has the smallest load maximums.

7.2.3.Fatigue load analysis

Next, a fatigue load analysis is going to be carried out for the four configurations of the Scenario 1. The same settings and variables as the ones explained in section 6.5.1 are used.

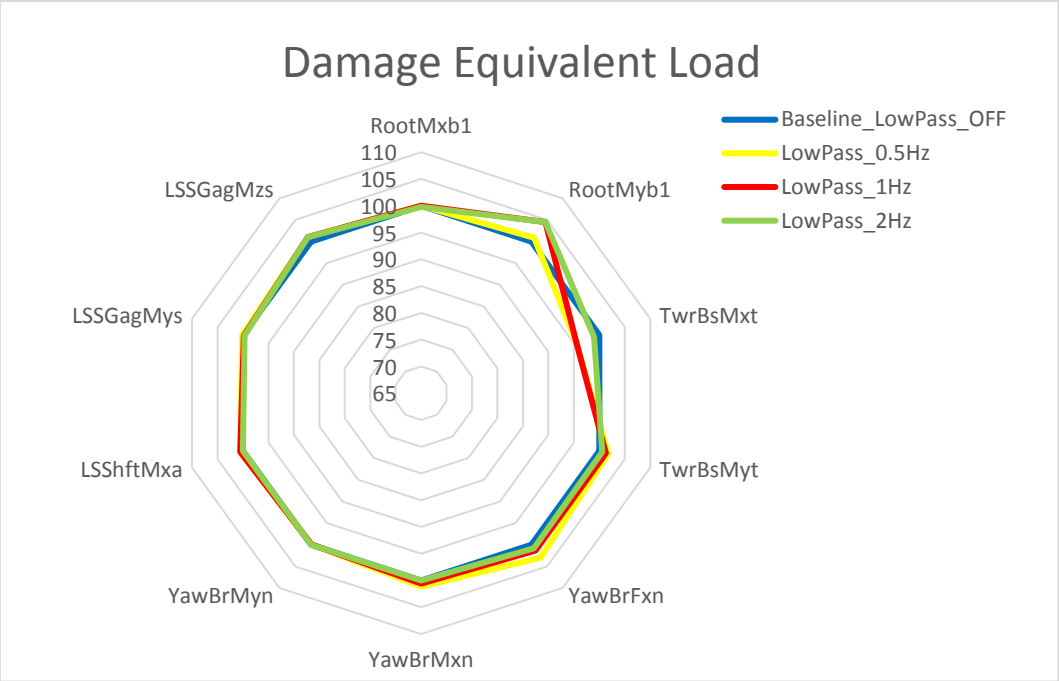

Figure 145: Fatigue load analysis spider chart for Scenario 1

From the previous spider chart it can be observed how the blade root momentum increases in the "y" axis when introducing any filter, especially when placing it at 1Hz and 2Hz.

It can also be observed how, when introducing the 0.5Hz and the 1Hz filter, the tower base momentum in the "x" axes is reduced.

Overall, the Case 1 configuration and the Baseline configuration are the ones with the smallest loads.

7.3. Control scenario 2, Notch DT filter

7.3.1. Control performance (open loop, sensitivities) vs baseline

Next, the closed loop behavior of the different scenarios when varying the parameters of the notch placed at the drive train mode frequency are shown.

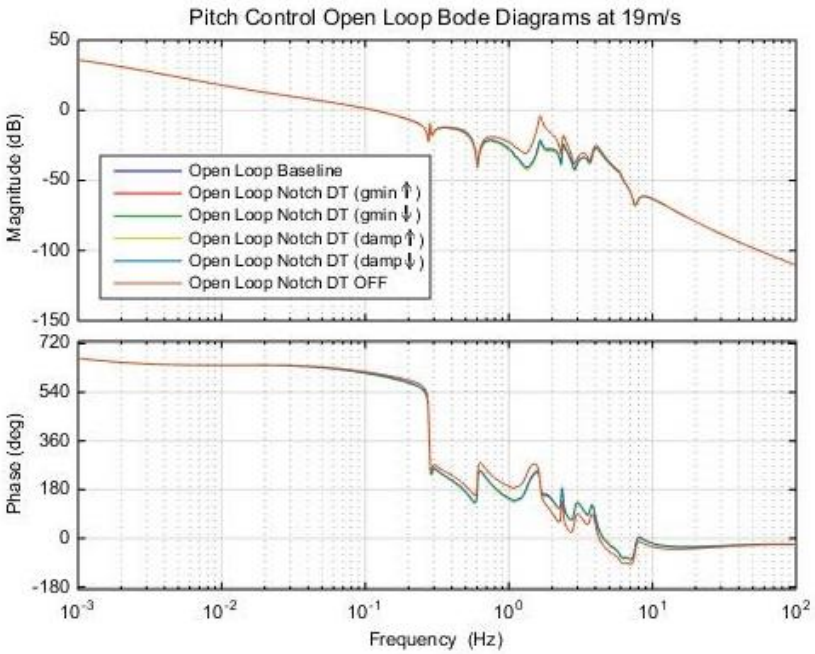

Figure 146: Bode diagram of the pitch control open loop for Scenario 2 at 19m/s

The open loop diagram shows little margin difference, even though it can be checked if zoomed in the graph that the least stable option is Case 7, where the notch filter at the drive train mode frequency is turned OFF (gain and phase margins 4.3dB and 70.6 deg, respectively). The most stable option is Case 6 (13.4dB GM and 65.7deg PM), with a lower damp (notch filter width Δ), very close to the Baseline scenario.

The disturbance sensibility S(s) of the drive train notch cases is shown in the next figure.

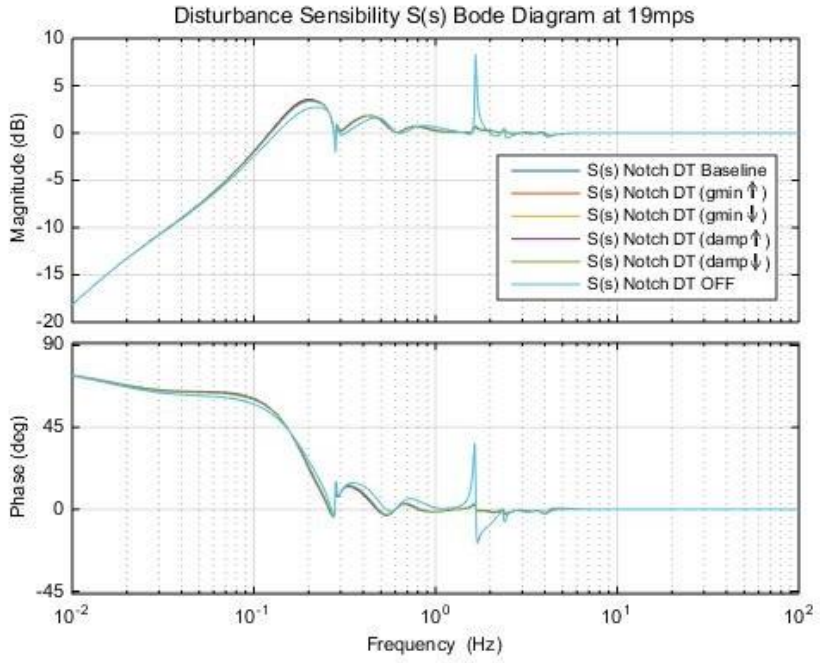

Figure 147: Bode diagram of the closed loop pitch control's S(s) for Scenario 2 at 19m/s

The figure clearly shows how the closed disturbance rejection loop would amplify any frequency entering the system at the drive train frequency if the filter was OFF. Therefore, it can be concluded that the worst configuration in this Scenario is Case 7, which does not have the notch drive train filter.

The tracking sensibility of the six cases is graphed next.

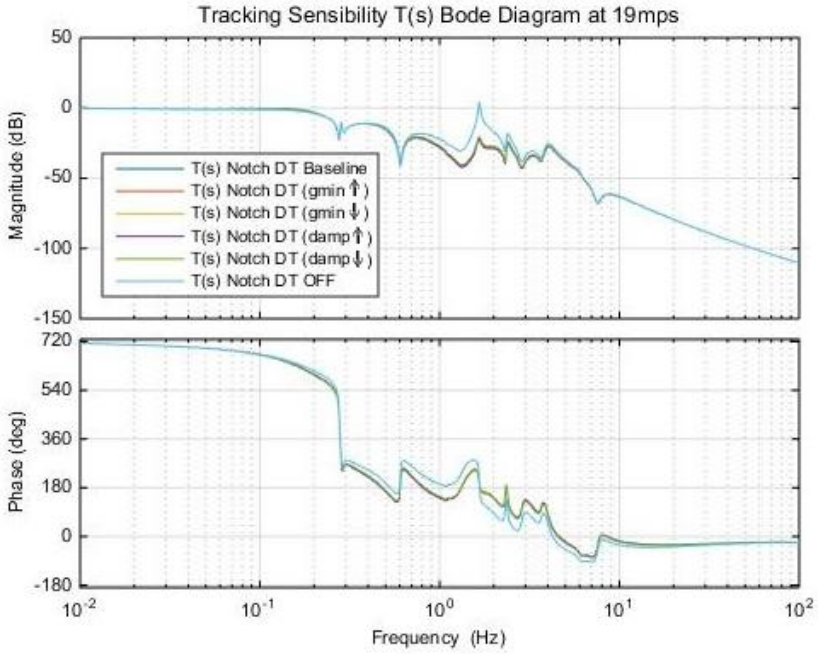

Figure 148: Bode diagram of the closed loop pitch control's T(s) for Scenario 2 at 19m/s

Again, the figure shows how removing the notch filter at the drive train frequency would result in the amplification of any signal entering the system at a frequency around 1.645 Hz, which is the opposite of the desired behavior.

The control sensibility U(s) of the configurations is shown in the figure below.

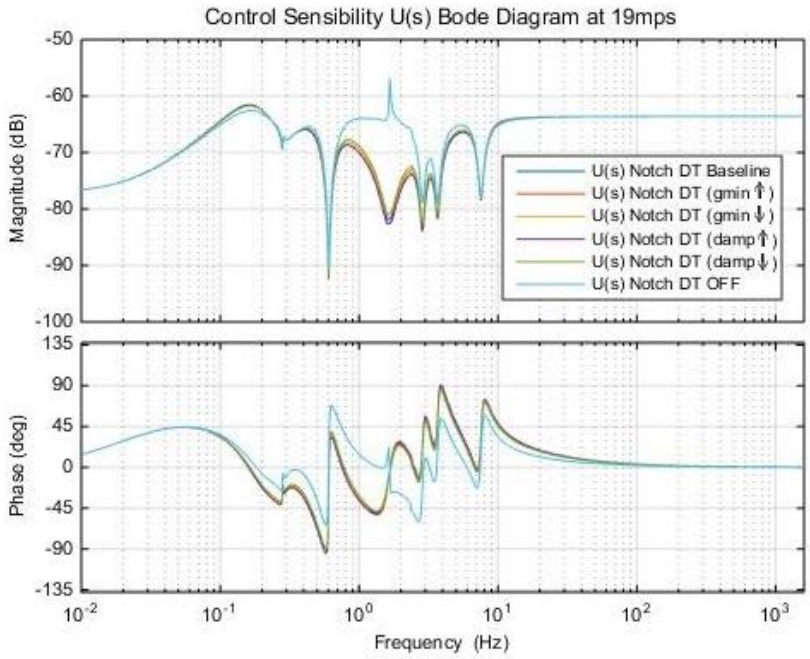

Figure 149: Bode diagram of the closed loop pitch control's U(s) for Scenario 2 at 19m/s

If the notch filter at the DT frequency was removed, a lot of control action would exist at that frequency, since one of the design objectives is to avoid activity at excited frequencies such as the drive train mode frequency, this would be the worst case scenario.

7.3.2. Statistical analysis

This section is dedicated to the analysis of several variables with respect to wind for the six configurations in Scenario 2.

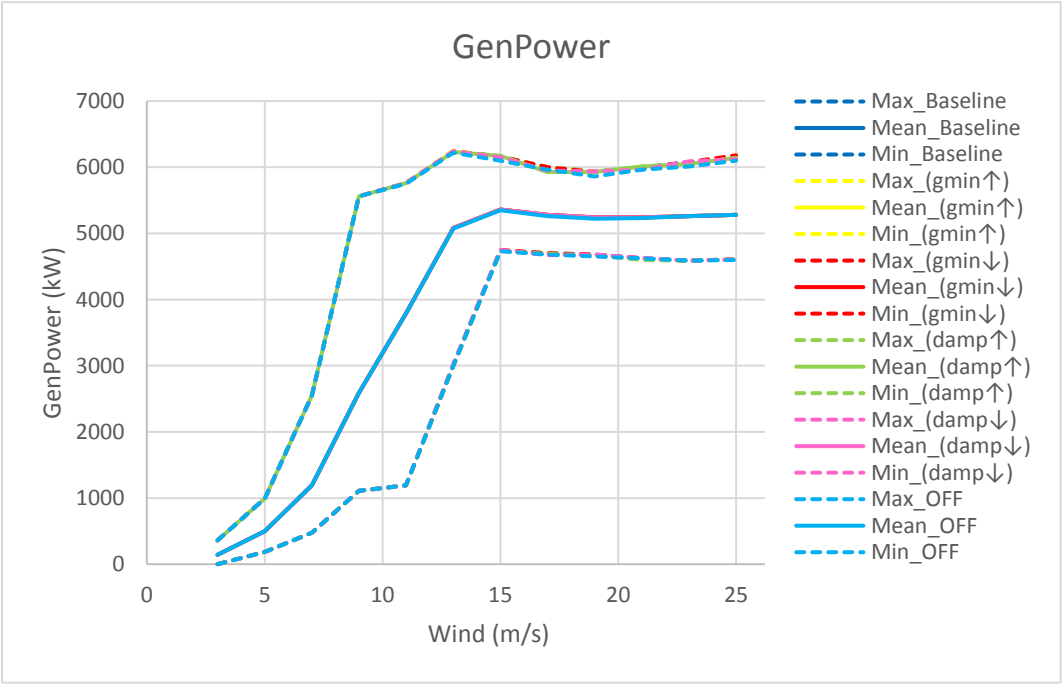

Figure 150: Generated power statistics for Scenario 2

The previous figure shows how varying the parameters of the notch filter barely affects the wind turbine's power production.

The next figure represents the standard deviation of the pitch angle for the different configurations.

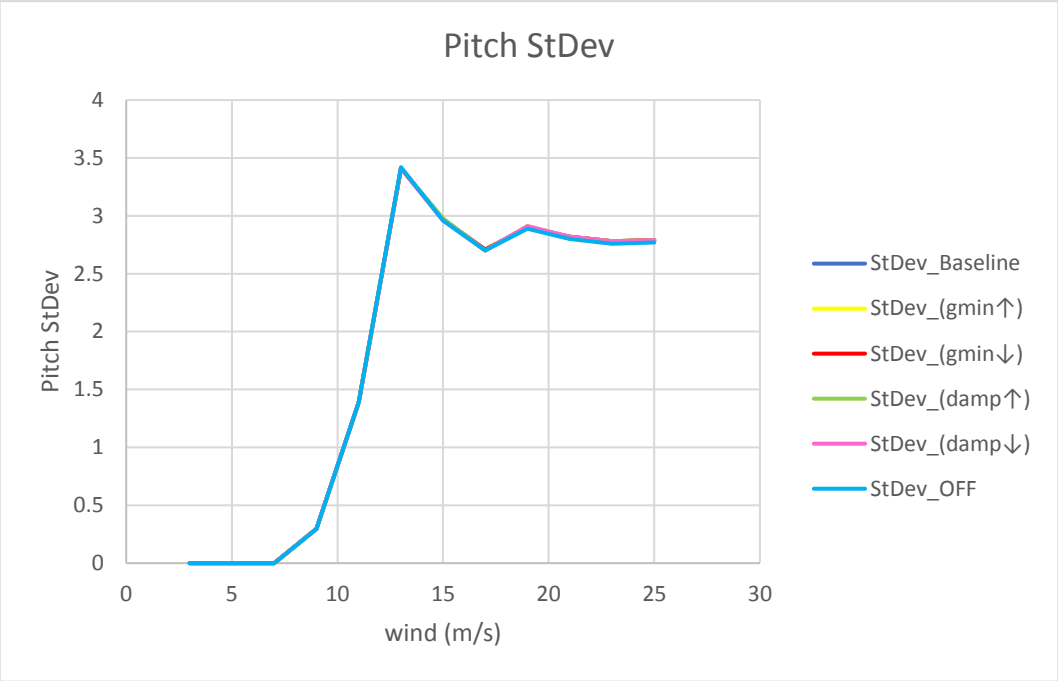

Figure 151: Pitch standard deviation for Scenario 2

Just like for the power production, the notch filter at the drive train mode frequency does not have too much effect on the pitch duty either.

In the next figure, the tower base momentum in the "y" axis is shown with respect to wind.

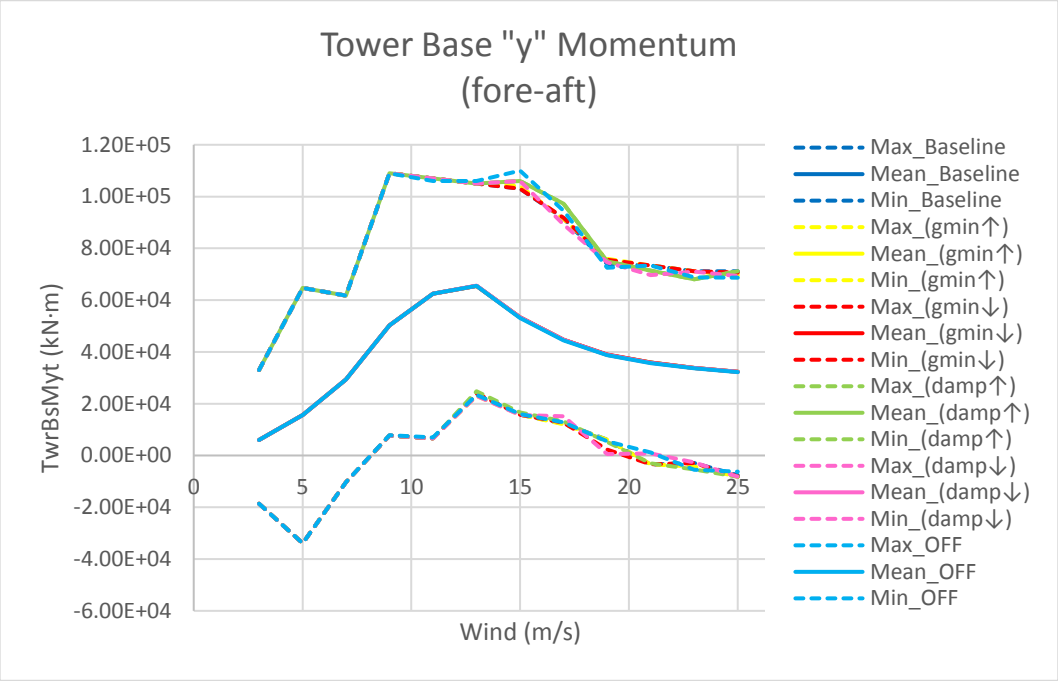

Figure 152: Tower base "y" momentum statistics for Scenario 2

The previous graph shows that the six configurations give the same tower base mean momentum, but, for a wind speed of 15m/s, the graph shows how turning off the filter at the drive train, the maximum load increases.

The next graph is a representation of the low speed shaft momentum in the “x” axis with respect to wind.

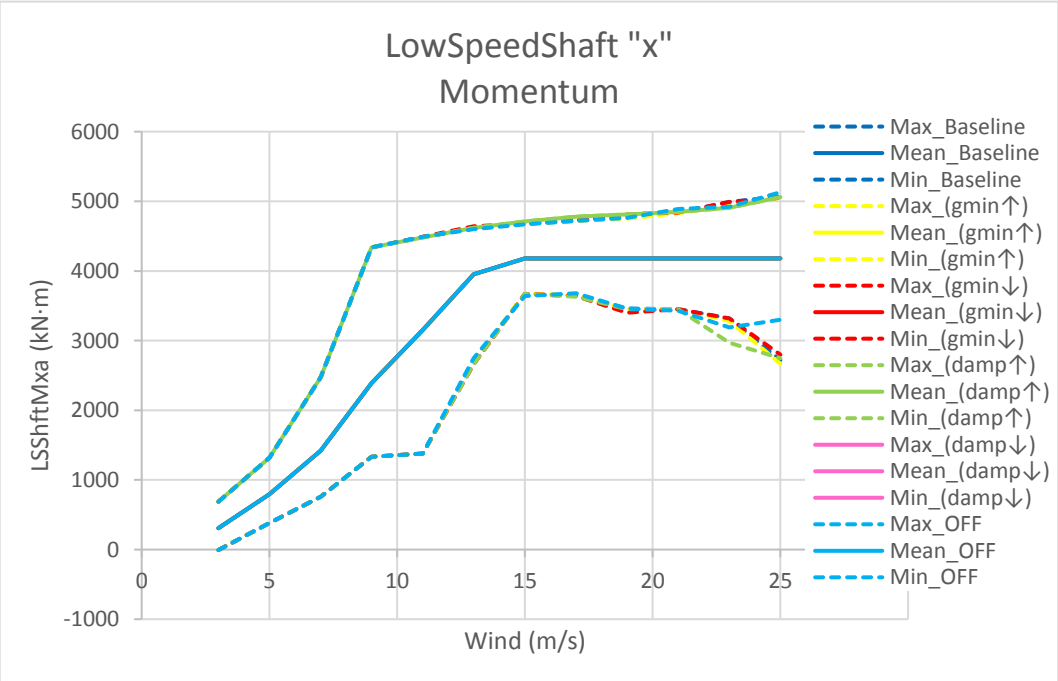

Figure 153: Low speed shaft "x" momentum statistics for Scenario 2

Even though it was expected to see more change in the low speed shaft momentum in the rotational axis, the figure shows the same mean and maximum loads for every configuration.

7.3.3. Fatigue load analysis

In this section, the Damage Equivalent Load of several components is going to be analyzed for the 6 configurations of the notch filter placed at the drive train mode frequency.

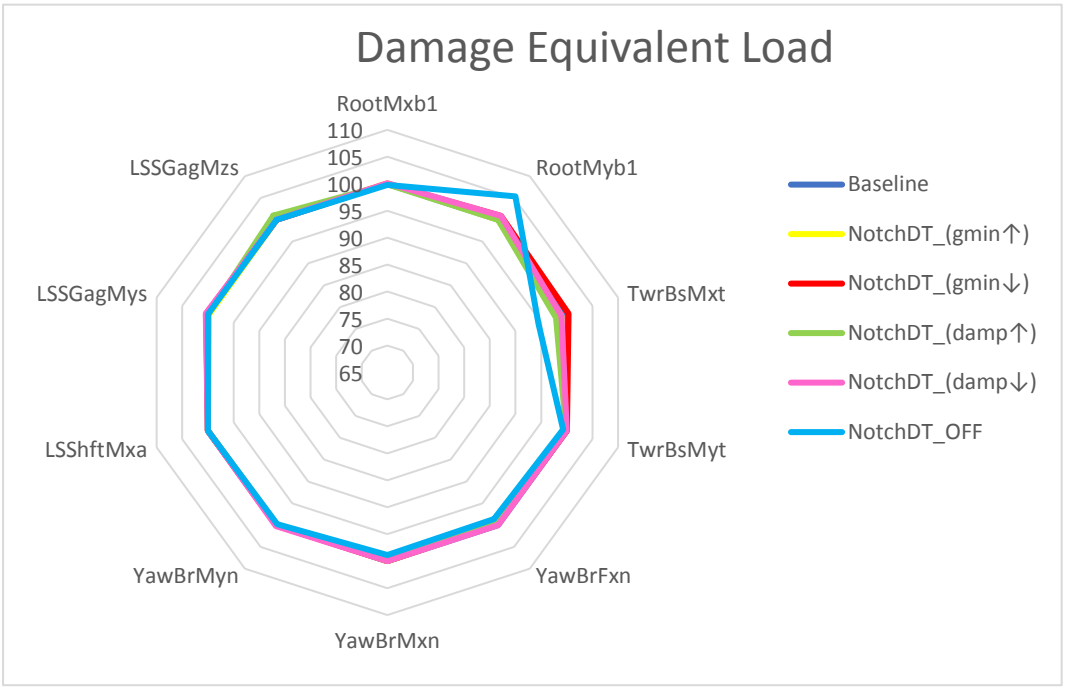

Figure 154: Fatigue load analysis spider chart for Scenario 2

The figure shows a 5% increase in blade root loads in the "y" axis and, unexpectedly, loads in the tower base "x" momentum decrease when the filter is turned off. The rest of configurations barely affect the loads in the elements that have been studied.

7.4. Control scenario 3, Notch Symmetric filter

7.4.1. Control performance (open loop, sensitivities) vs baseline

Next, different closed loop behaviors are going to be analyzed for another 6 different configurations, this time by varying the notch filter placed at the 1st symmetric frequency.

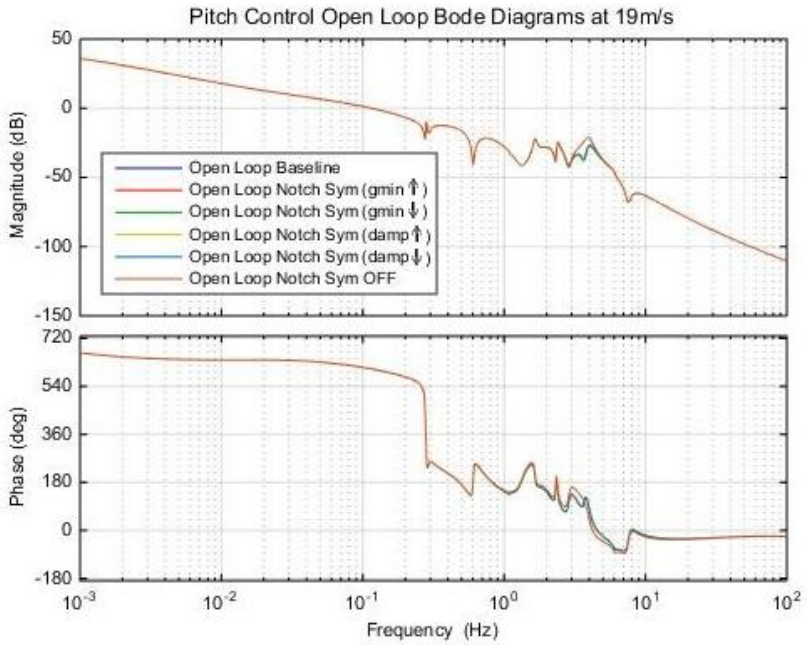

Figure 155: Bode diagram of the pitch control open loop for Scenario 3 at 19m/s

As it can be observed from the previous graph, introducing changes in the notch filter placed at the 1st symmetric frequency, barely changes open loop stability. Despite of this, the configuration with a slightly bigger gain margin is Case 12 (GM 13.4dB and PM 65.6deg), at which the filter is turned OFF. The rest have a GM of 13.2dB and a PM of 65.1deg.

The disturbance sensibility S(s) graph of the different configurations is shown next at a wind speed of 19 m/s.

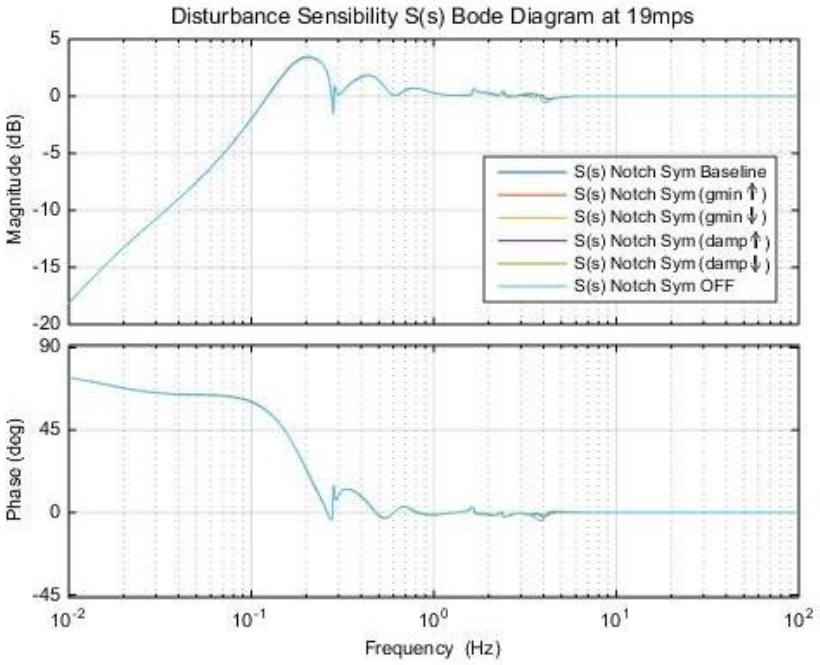

Figure 156: Bode diagram of the closed loop pitch control's S(s) for Scenario 3 at 19m/s

The previous figure shows how the variation of the filter placed at the 1st symmetric barely affects the closed loop disturbance rejection response of the system.

Next, the tracking sensibility graph T(s) is represented.

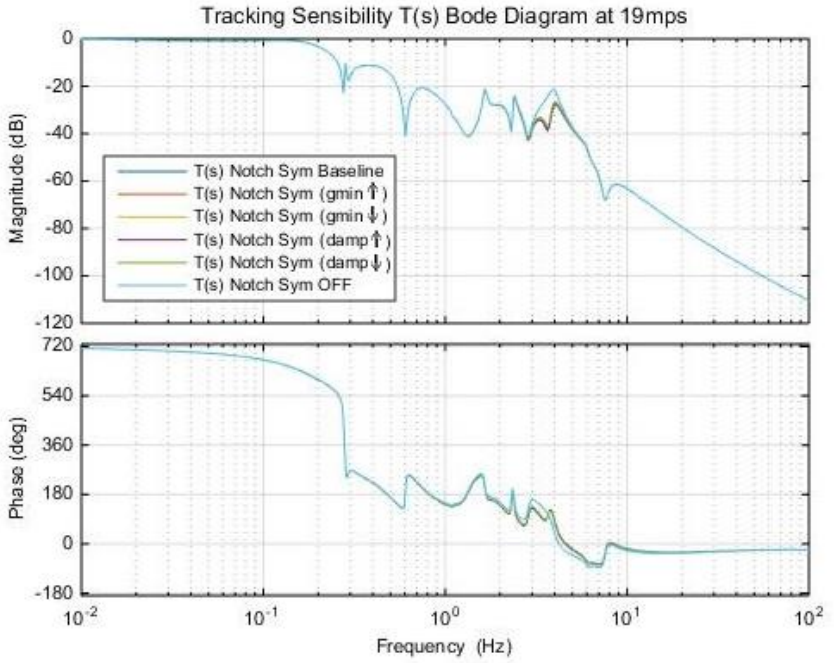

Figure 157: Bode diagram of the closed loop pitch control's T(s) for Scenario 3 at 19m/s

The tracking sensibility response shows how, when deactivating the filter, any frequency entering the system at that frequency will not be as attenuated as with the filter. The less activity there is at the wind turbine's excited structural mode frequencies, the better.

The next graph shows the control sensibility of the different configurations.

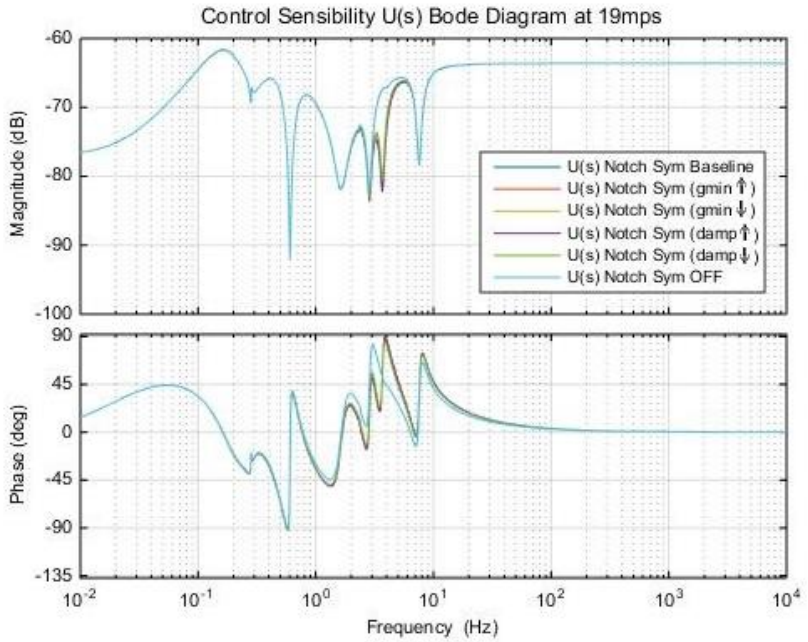

Figure 158: Bode diagram of the closed loop pitch control's U(s) for Scenario 3 at 19m/s

Again, just like for the graph before, the previous graph shows how the frequencies entering the system at the 1st symmetric frequency (this time as a disturbance) will not be attenuated.

7.4.2. Statistical analysis

This section is dedicated to the statistical analysis of the different simulation variables.

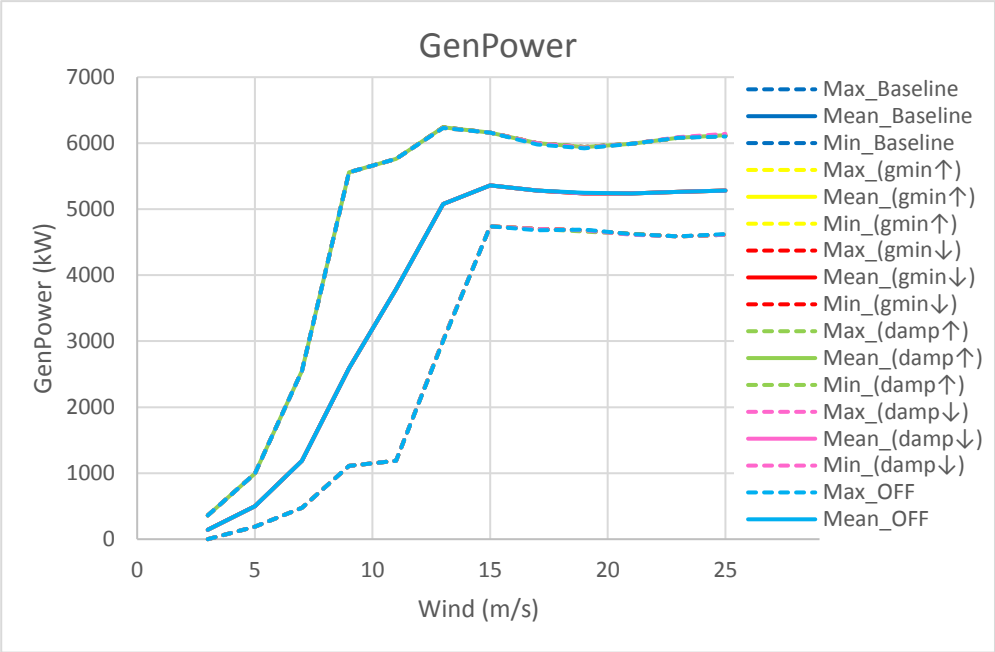

Figure 159: Generated power statistics for Scenario 3

The previous figure shows how the notch filter at the 1st symmetric mode frequency does not affect the power production too much.

Next, the standard deviation of the pitch with respect to wind is graphed.

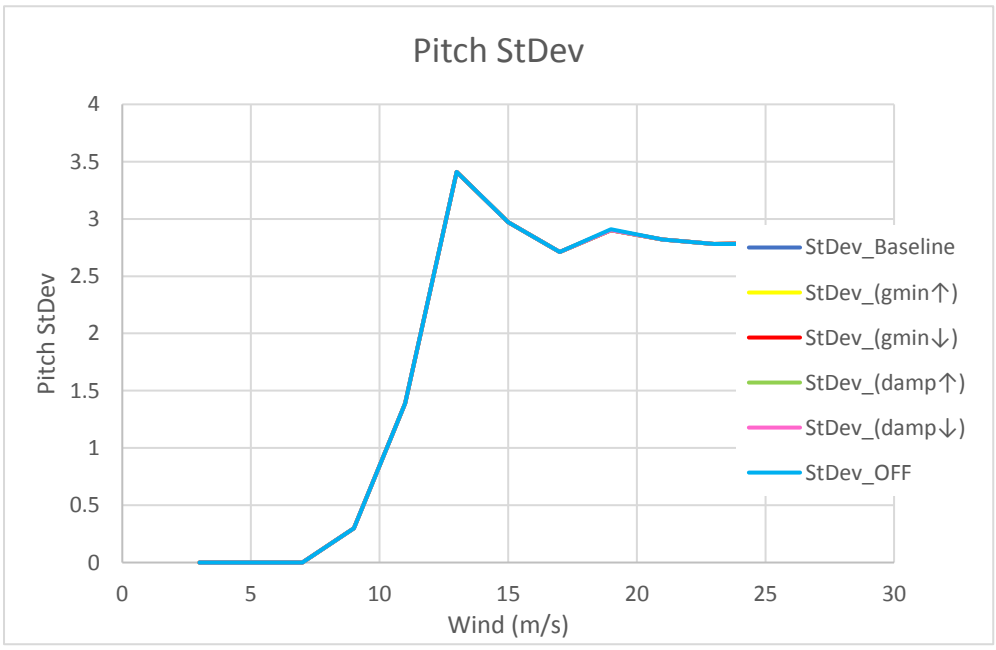

Figure 160: Pitch standard deviation for Scenario 3

The previous graph does not show any variations of the pitch duty for the variations of the notch filter at the 1st symmetric mode frequency.

Next, the tower base momentum in the "y" axis is represented with respect to wind.

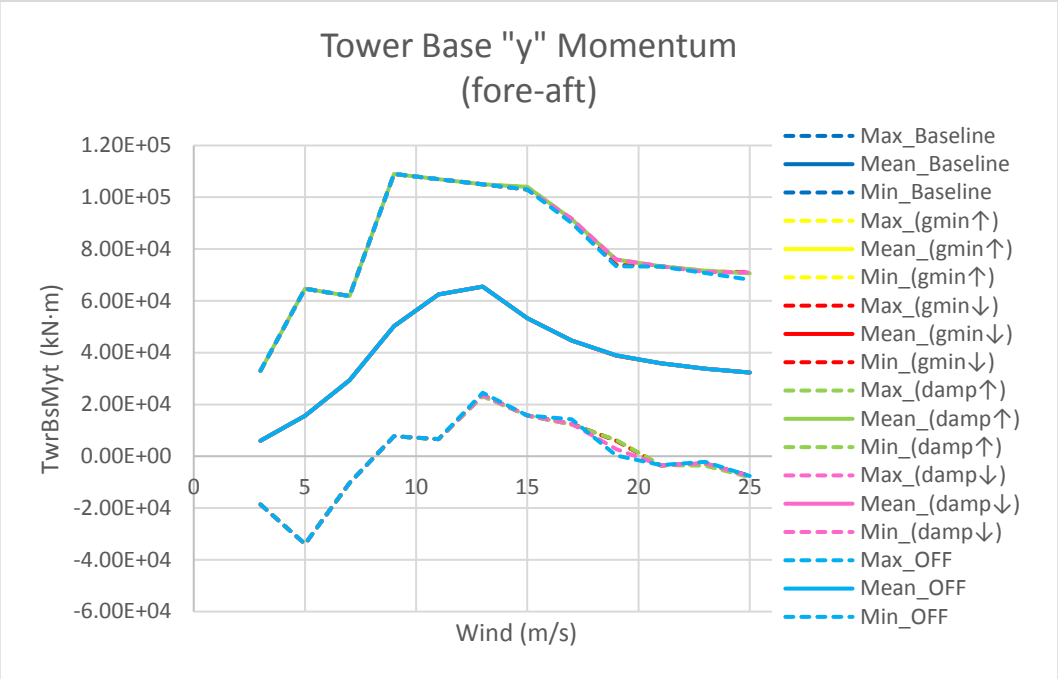

Figure 161: Tower base "y" momentum statistics for Scenario 3

In the previous graph, it can be observed how modifying the notch's parameters the mean tower base load stays the same. The figure also shows how the maximum load is a little lower at 25m/s for Case 12, which is the one with the filter deactivated.

The next figure shows the maximum, mean and minimum values of the low speed shaft momentum in the "x" axis for the six different configurations.

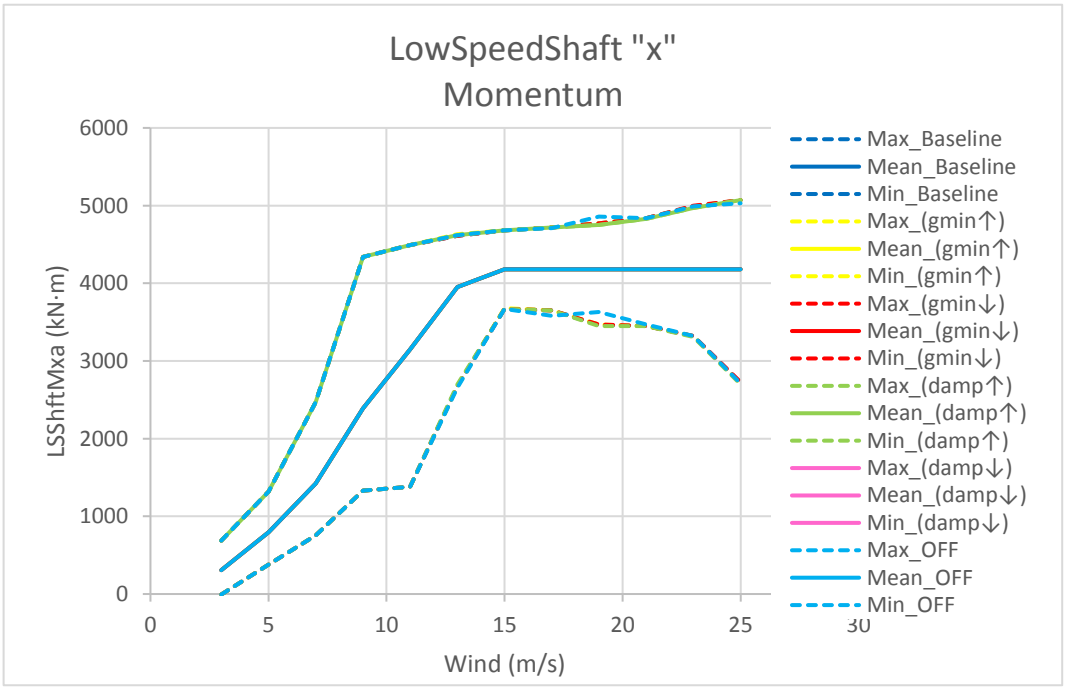

Figure 162: Low speed shaft "x" momentum statistics for Scenario 3

The figure shows that even though the load mean is the same for all the configurations, at 19 m/s the load is a little higher when the notch filter is OFF.

7.4.3. Fatigue load analysis

The next spider chart shows some of the wind turbine component loads for the different configurations in Scenario 3.

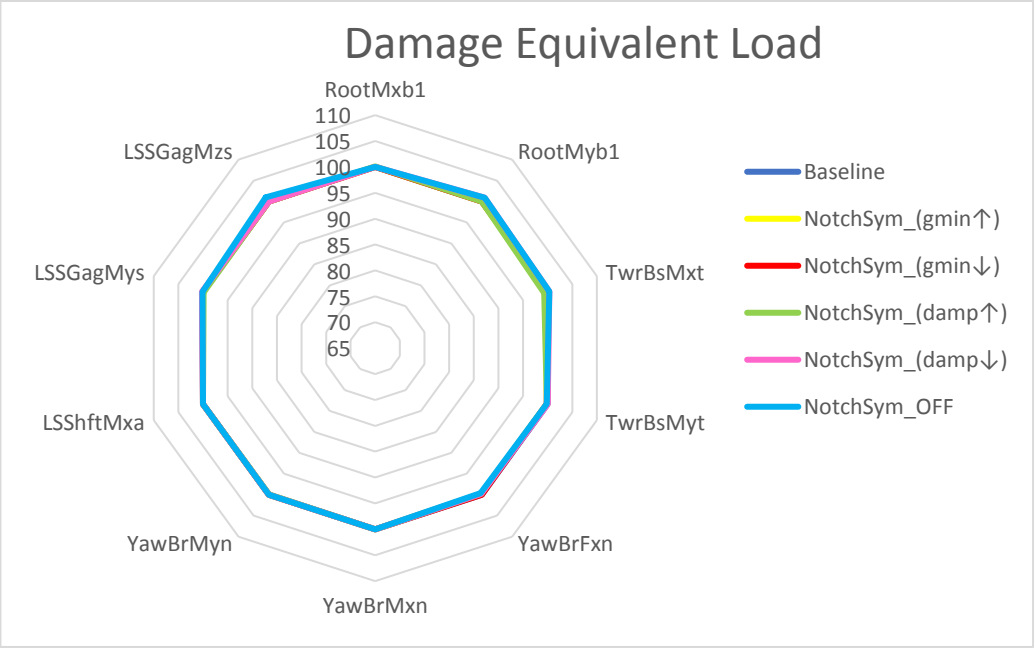

Figure 163: Fatigue load analysis spider chart for Scenario 3

When varying the notch filter at the 1st symmetric mode frequency, the loads in the wind turbine elements barely change a 1%.

7.5. Control scenario 4, Notch Side-to-side filter

7.5.1. Control performance (open loop, sensitivities) vs baseline

The next figure shows the open loop performance of the pitch control loop when varying the parameters of the notch filter placed at the 2nd tower side-to-side mode frequency.

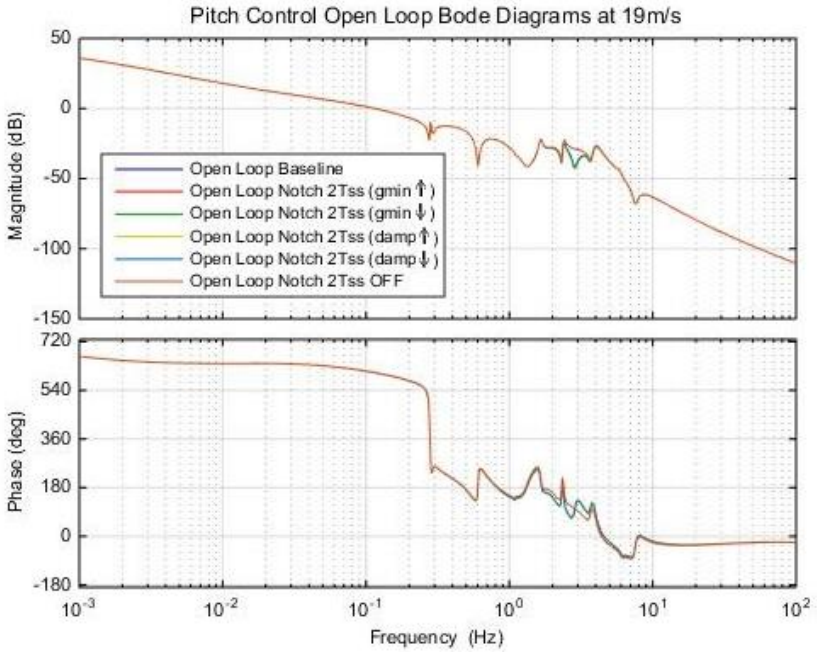

Figure 164: Bode diagram of the pitch control open loop for Scenario 4 at 19m/s

The graph shows how there open loop stability does not change much with the changes introduced at the 2nd tower side-to-side mode frequency. Nevertheless, the scenario that would give slightly bigger stability margins is Case 17 (13.5dB and 65.7deg gain and phase margins, respectively), where the notch filter is turned OFF. The case with a little lower stability is Case 15 (13.2dB and 65.1deg).

Next, the disturbance sensibility S(s) is graphed for the different configurations.

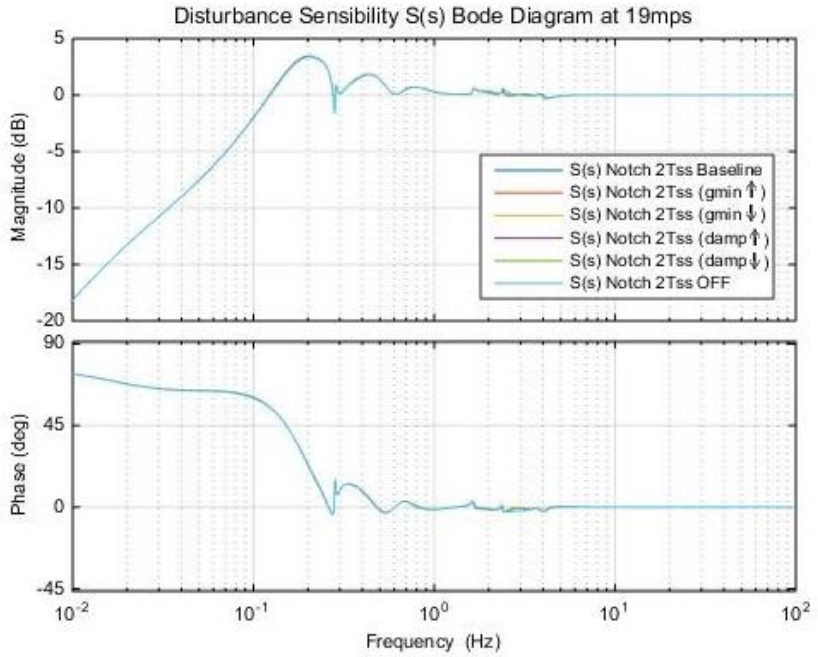

Figure 165: Bode diagram of the closed loop pitch control's S(s) for Scenario 4 at 19m/s

As it can be seen in the previous figure, there are barely any changes in the disturbance sensibility response when varying this notch filter.

The closed loop tracking response for Scenario 4 is shown in the next figure.

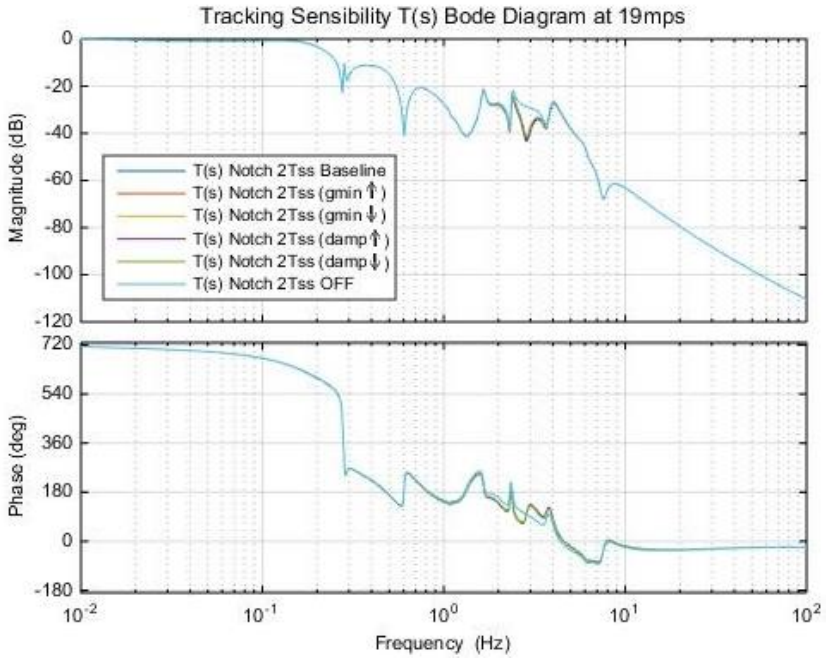

Figure 166: Bode diagram of the closed loop pitch control's T(s) for Scenario 4 at 19m/s

When turning off the filter, any reference entering the system at that frequency will not be attenuated. This is reflected in the previous figure.

The next figure represents the control sensibility U(s), the relationship between the disturbance and the control action.

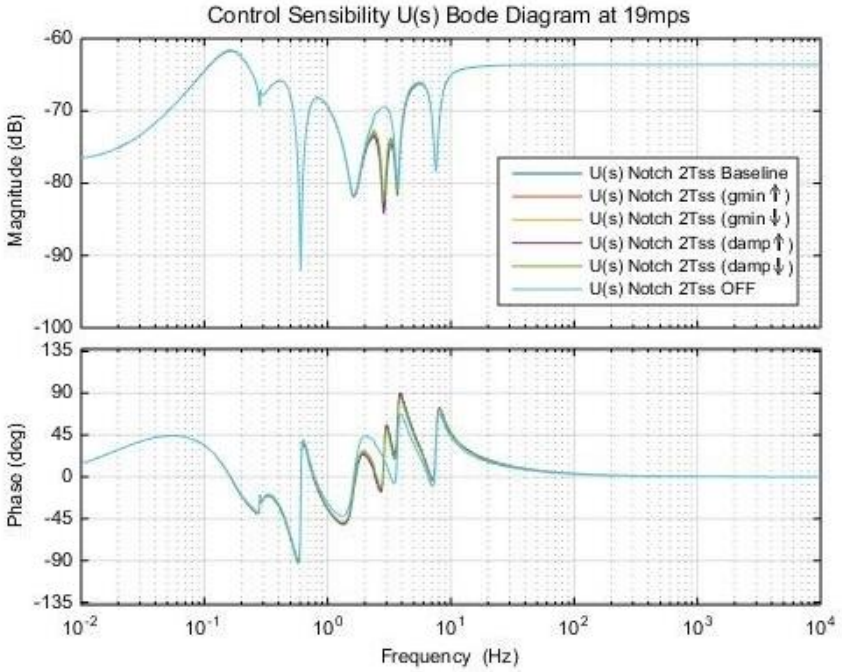

Figure 167: Bode diagram of the closed loop pitch control's U(s) for Scenario 4 at 19m/s

Again, when turning off the filter, any frequency entering the system, this time as a disturbance, will not be as attenuated as with the filter. Since any control action at those frequencies wants to be avoided, the filter should stay ON.

7.5.2. Statistical analysis

In this section, the statistics of the cases in Scenario 4 are going to be analyzed.

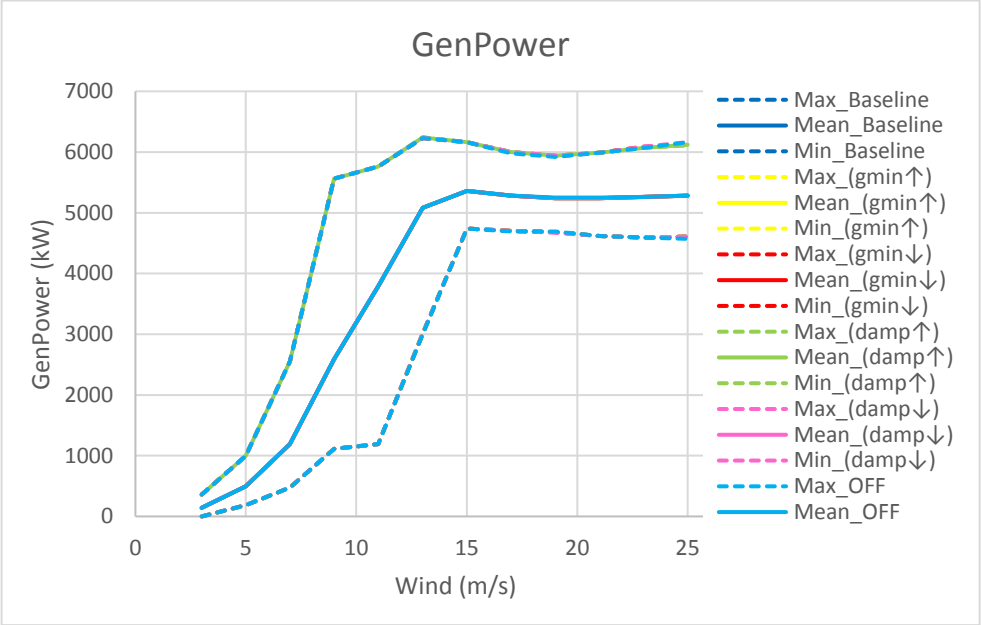

Figure 168: Generated power statistics for Scenario 4

The figure shows very little variation in the generated power between all the notch 2nd tower-side-to-side mode configurations.

The next graph shows pitch standard deviation with respect to wind.

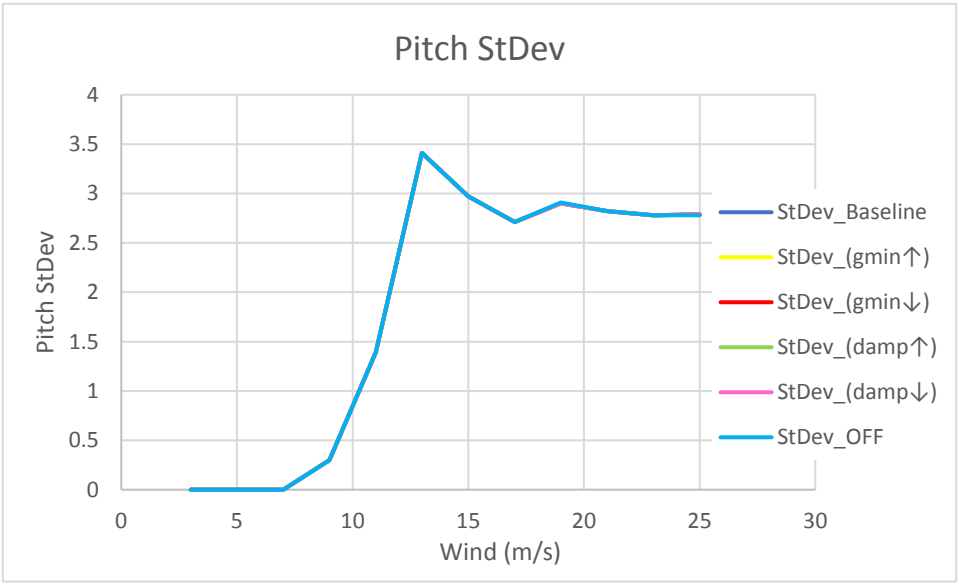

Figure 169: Pitch standard deviation for Scenario 4

Pitch duty is not too affected by the 2nd tower side-to-side filter parameters according to the previous graph.

Next, tower base momentum in the “y” axis is graphed.

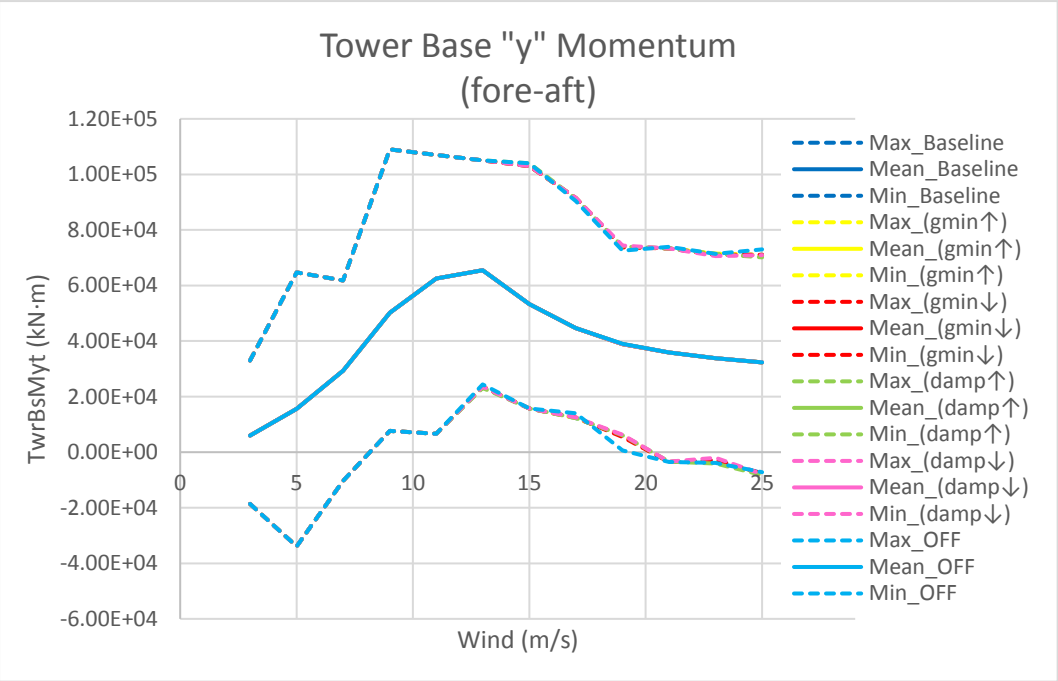

Figure 170: Tower base "y" momentum statistics for Scenario 4

It can be seen in the previous figure that the modification of the 2nd tower side-to-side filter does not vary the load mean and it barely changes its maximums.

Next, there is a graph that represents the low speed shaft’s momentum in the “x” axis with respect to wind.

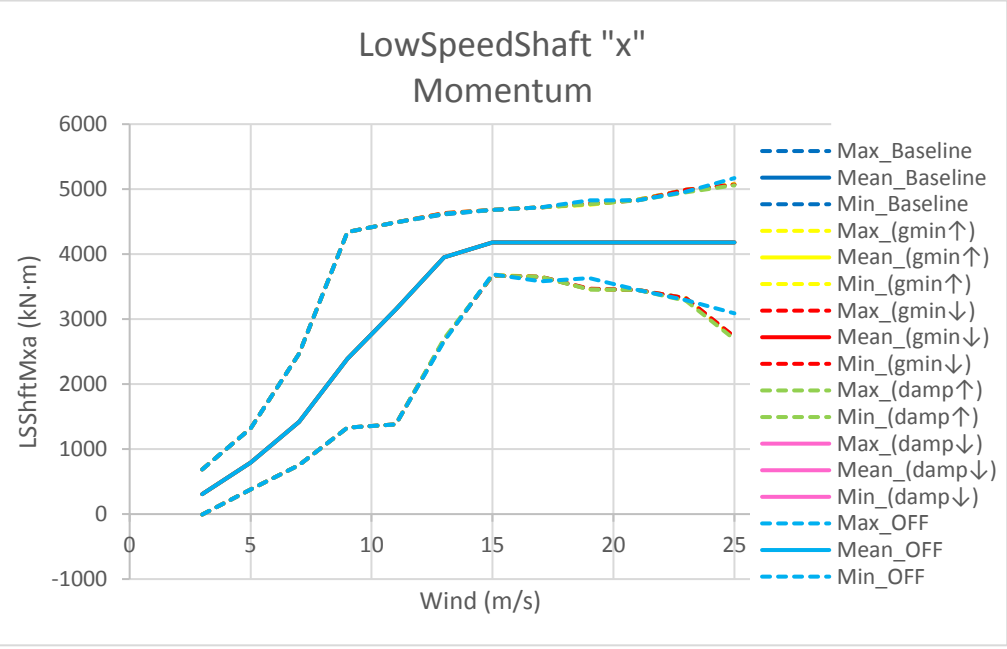

Figure 171: Low speed shaft "x" momentum statistics for Scenario 4

Again, the figure does not show too much variation of the mean nor maximum loads of the low speed shaft with none of the different filter configurations.

7.5.3. Fatigue load analysis

The next spider chart shows damage equivalent load for several wind turbine components that are being studied for different configurations of the notch filter placed at the 2nd tower side-to-side mode frequency.

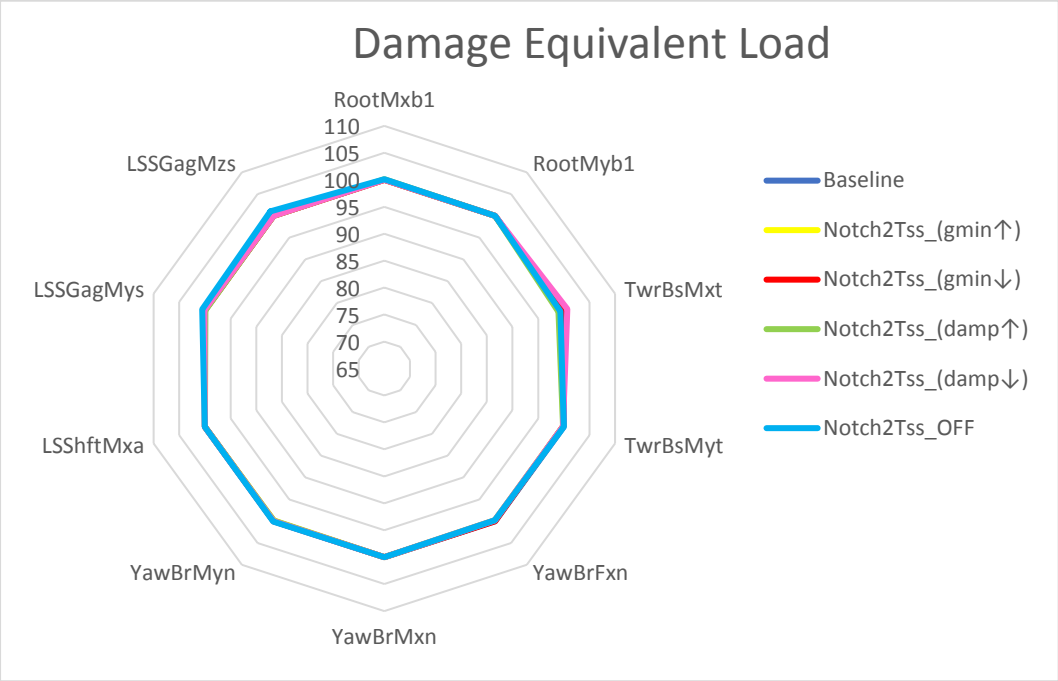

Figure 172: Fatigue load analysis spider chart for Scenario 4

The previous spider chart shows very little variation of the loads when varying the width and depth of this filter.

7.6. Control scenario 5, Notch 1P filter

7.6.1. Control performance (open loop, sensitivities) vs baseline

In this section, the effect of activating and deactivating the filter placed at the rotational 1P frequency is studied.

The next graph shows the open loop behavior of the system with and without the notch filter placed at the nonstructural 1P rotational frequency.

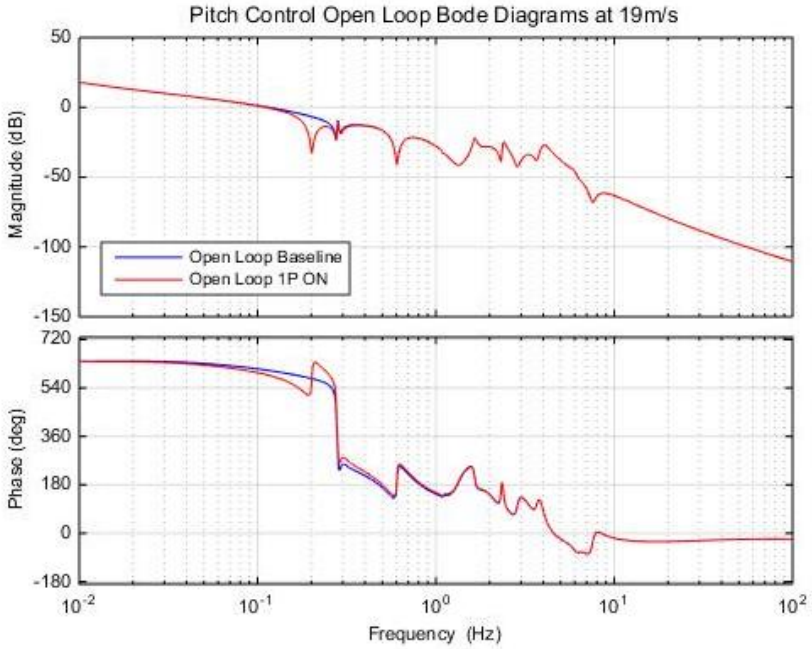

Figure 173: Bode diagram of the pitch control open loop for Scenario 5 at 19m/s

The graph shows how both the gain and the phase margins go down (from 13.3dB to 7.86dB and from 65.2deg to 50.6deg) as the filter is turned ON. Initially, this filter was included among the notch filters introduced in the pitch control loop. Later, when checking open loop margins, the filter was removed for stability reasons.

Next, the disturbance sensibility S(s) graph of the closed loop system is shown for both configurations.

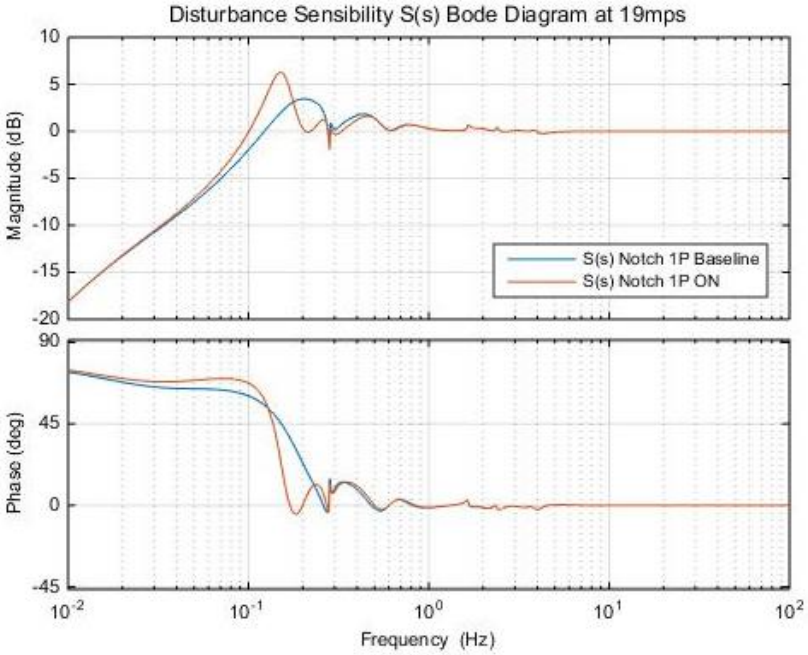

Figure 174: Bode diagram of the closed loop pitch control's S(s) for Scenario 5 at 19m/s

The previous figure shows not only how the Baseline configuration (1P notch filter OFF) has a higher band width, which makes it a faster system, but it also presents a smaller peak, which will result in fewer oscillations in the time response of the system.

Next, the tracking sensibility T(s) is graphed for both configurations at 19 m/s.

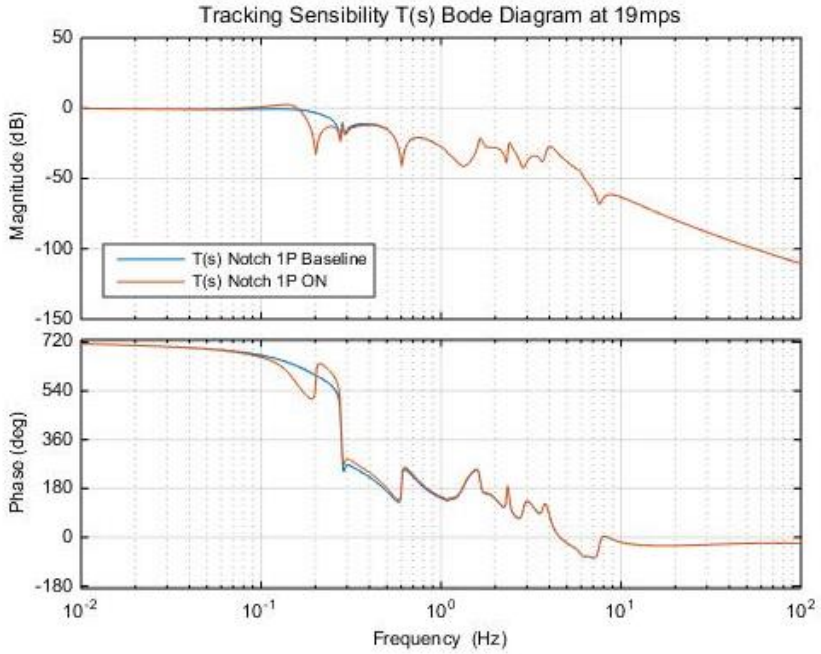

Figure 175: Bode diagram of the closed loop pitch control's T(s) for Scenario 5 at 19m/s

The figure shows that activating the filter will attenuate the 1P frequency, which is beneficial since the attenuation of these frequencies (rotational frequencies too, not only structural modes) is an additional design requirement of the pitch control loop.

Next, the control sensibility U(s) of the Scenario 5 configurations is graphed.

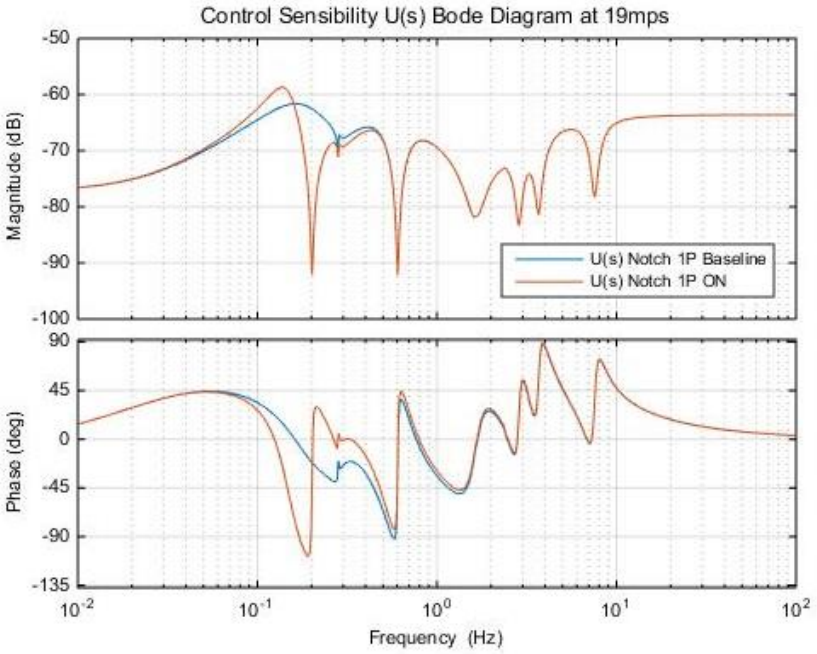

Figure 176: Bode diagram of the closed loop pitch control's U(s) for Scenario 5 at 19m/s

It can be observed from the figure how the Baseline scenario does not attenuate the 1P frequency. Therefore, if a disturbance enters the system at the 1P frequency, there will be more control action than the desired one.

7.6.2. Statistical analysis

This section is dedicated to the statistical analysis of several simulation variables with respect to wind.

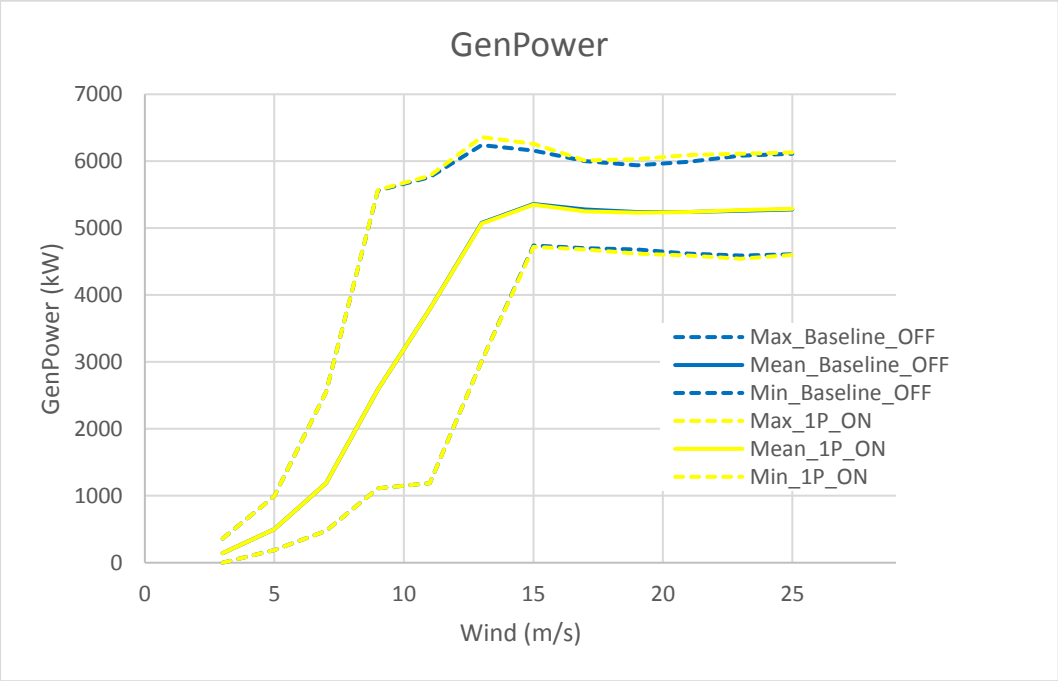

Figure 177: Generated power statistics for Scenario 5

The introduction of the 1P notch filter increases the generator power maximums, but it keeps the same power mean.

Next, the standard deviation of the pitch is graphed with respect to time.

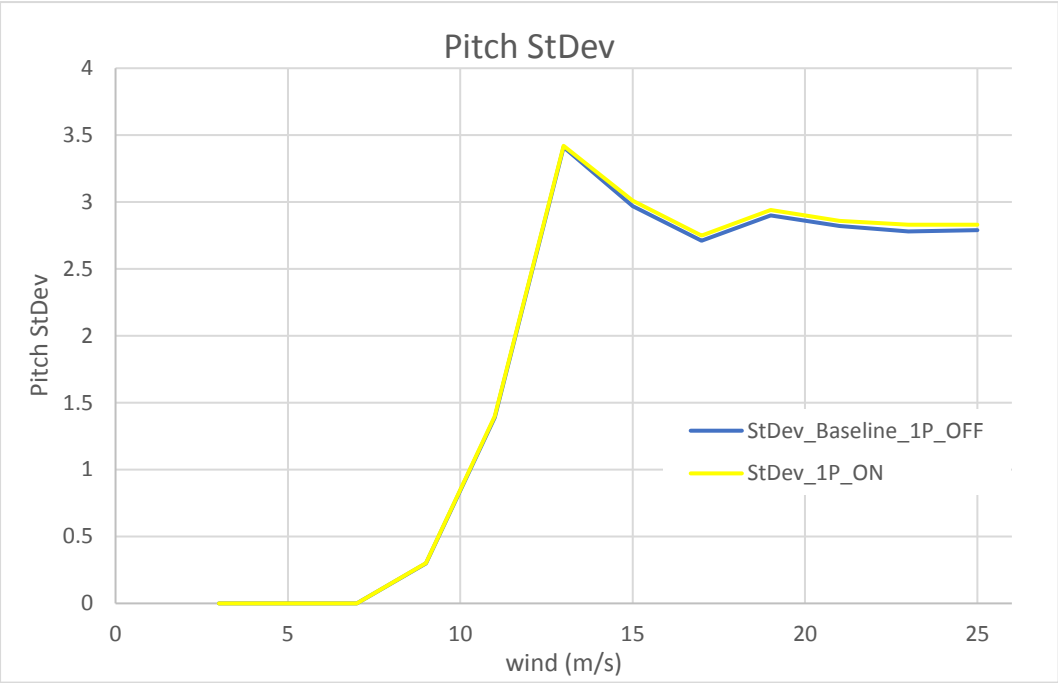

Figure 178: Pitch standard deviation for Scenario 5

The figure shows how pitch duty is slightly smaller when the notch filter at the 1P frequency is OFF.

Next, tower base momentum in the “y” axis is analyzed with respect to wind.

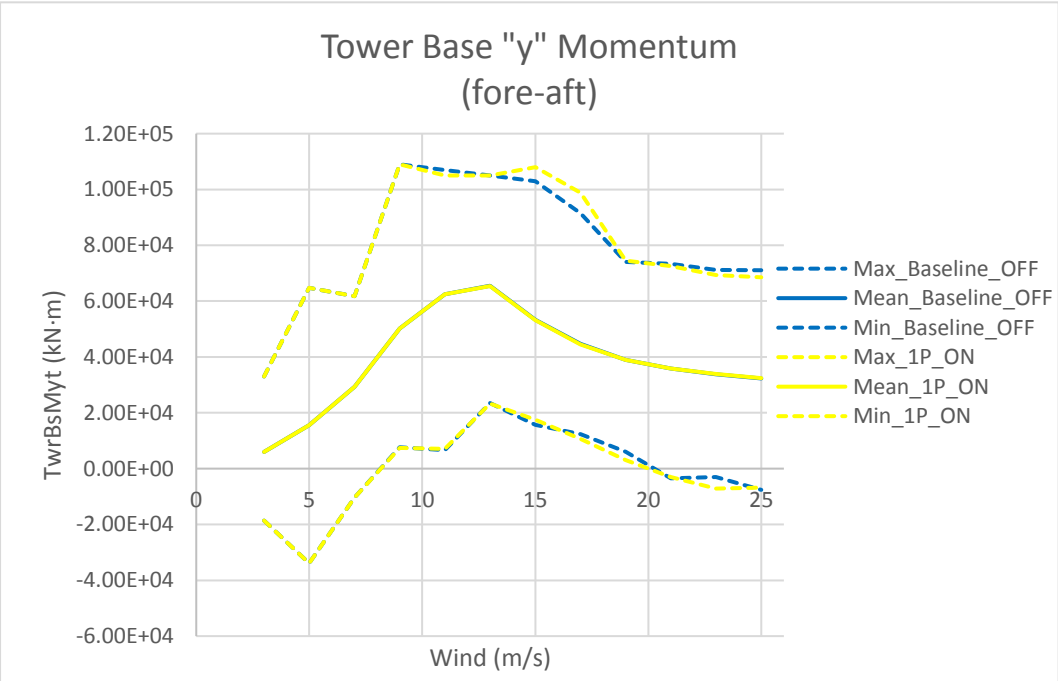

Figure 179: Tower base "y" momentum statistics for Scenario 5

It can be observed from the figure that, at a wind speed of 15m/s, turning on the filter placed at the nonstructural 1P frequency increases maximum tower base loads in the “y” axis.

In the next figure, low speed shaft rotational momentum in the “x” axis is graphed.

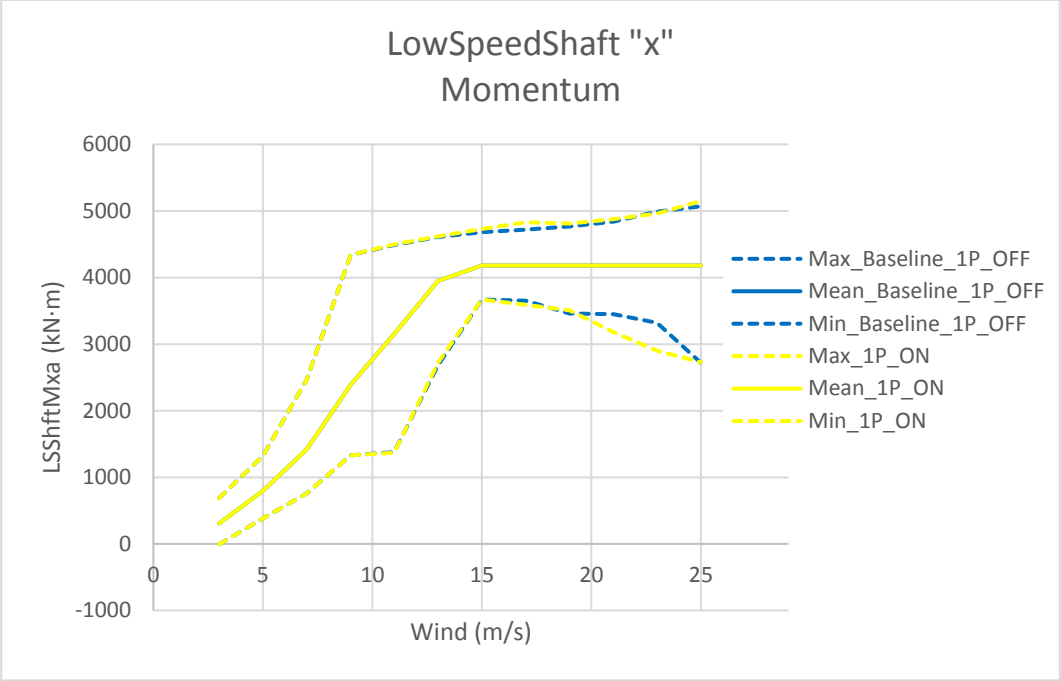

Figure 180: Low speed shaft "x" momentum statistics for Scenario 5

The previous graph illustrates how the same load mean and practically the same maximums when introducing the notch filter at the 1P rotational frequency.

7.6.3. Fatigue load analysis

To fully validate the activation or deactivation of the notch filter placed at the 1P frequency, the damage equivalent load must be studied.

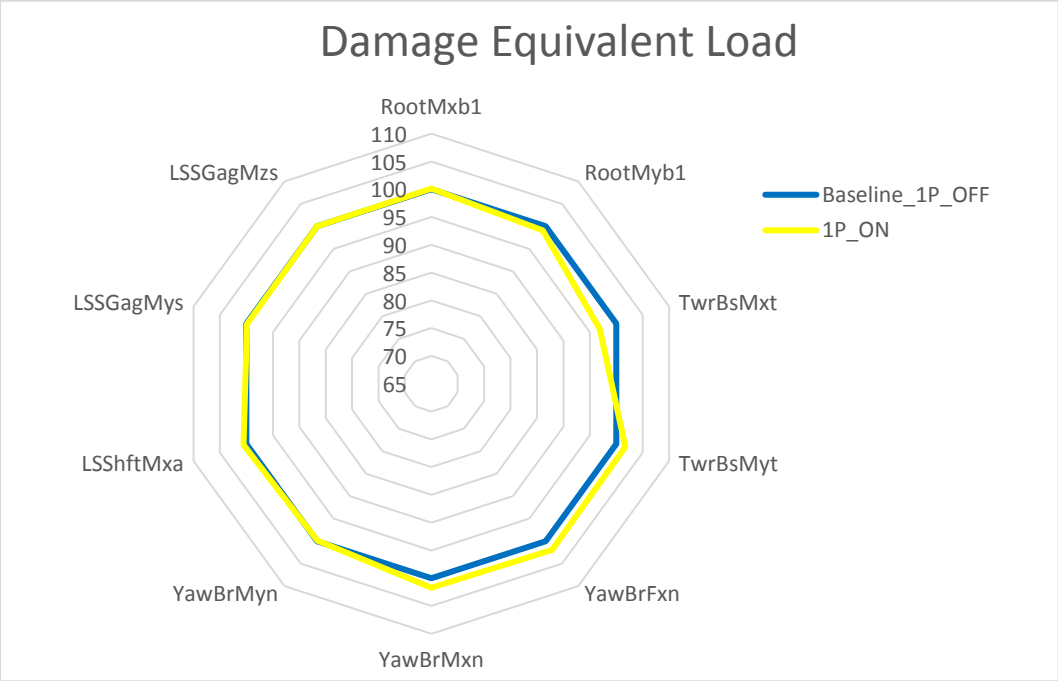

Figure 181: Fatigue load analysis spider chart for Scenario 5

The spider chart illustrates a 3% reduction in the tower base momentum in the "x" direction (side-to-side). It also shows a 2% increase in the tower base momentum in the "y" direction (fore-aft). As it was explained in previous analysis, the fore-aft momentum is the maximum load the tower must withstand, which means the load reduction in the "x" axis is not worth it. The notch filter should be turned off.

7.7. Control scenario 6, Notch 3P filter

7.7.1. Control performance (open loop, sensitivities) vs baseline

The final Scenario consists of changing the parameters of the notch filter placed at the 3P nonstructural frequency.

First, the open loop margins are going to be checked in the next Bode plot.

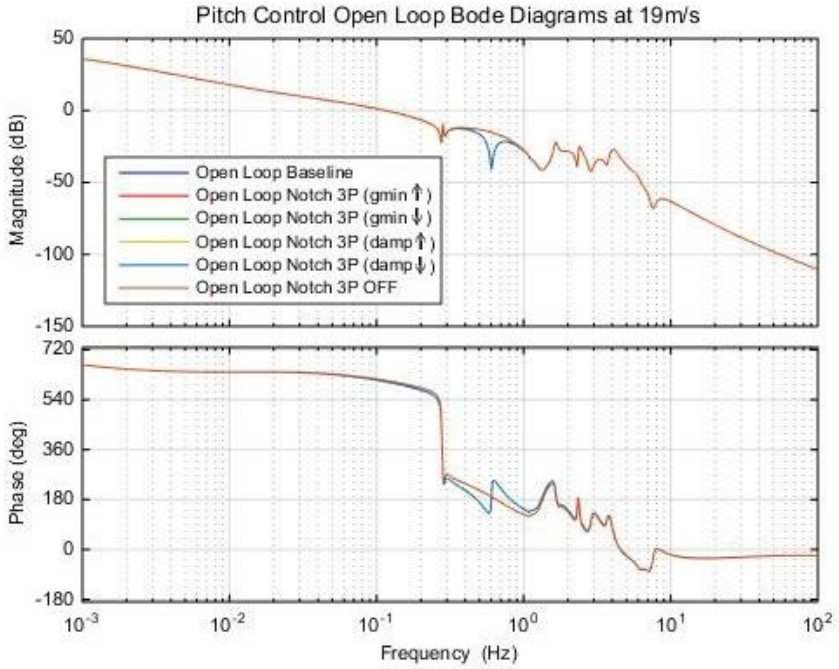

Figure 182: Bode diagram of the pitch control open loop for Scenario 6 at 19m/s

When zooming into the previous figure, it can be observed that the open loop gain and phase margins increase (from 13.3dB to 15.2dB and from 65.2deg to 69.4deg) when deactivating the notch filter at the 3P rotational frequency.

Next, the closed loop disturbance sensibility behavior is graphed for a wind speed of 19 m/s.

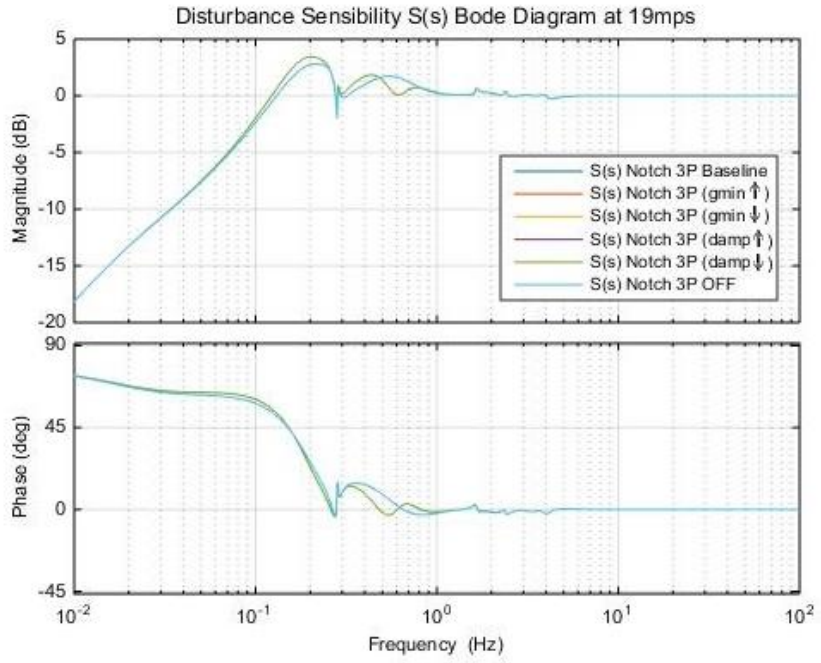

Figure 183: Bode diagram of the closed loop pitch control's S(s) for Scenario 6 at 19m/s

The previous Bode plot shows a better band width and peak response performance for the configuration without the 3P filter. Nevertheless, a high amplification of the 3P frequency can

also be observed in the disturbance sensibility response. Any disturbance entering the system around the 3P frequency (≈ 0.6 Hz), will be amplified and this is not admissible.

The next Bode plot shows the closed loop tracking sensibility T(s) of the system at 19 m/s.

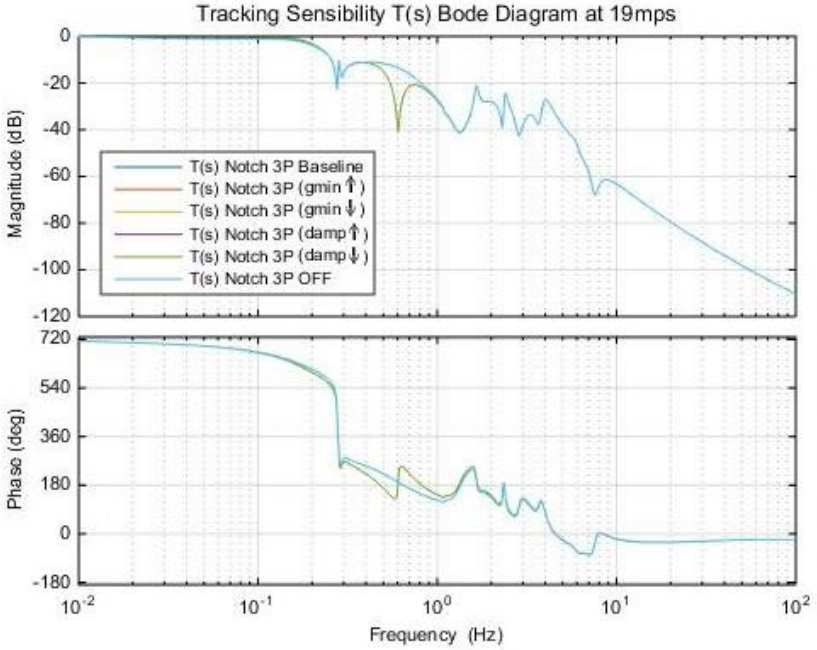

Figure 184: Bode diagram of the closed loop pitch control's T(s) for Scenario 6 at 19m/s

According to the previous figure, any disturbance entering the system at the 3P rotational frequency will be a lot less attenuated if the filter is turned off. The rest of configurations have almost the same tracking sensibility behavior.

Next, a Bode diagram of the control sensibility U(s) is graphed.

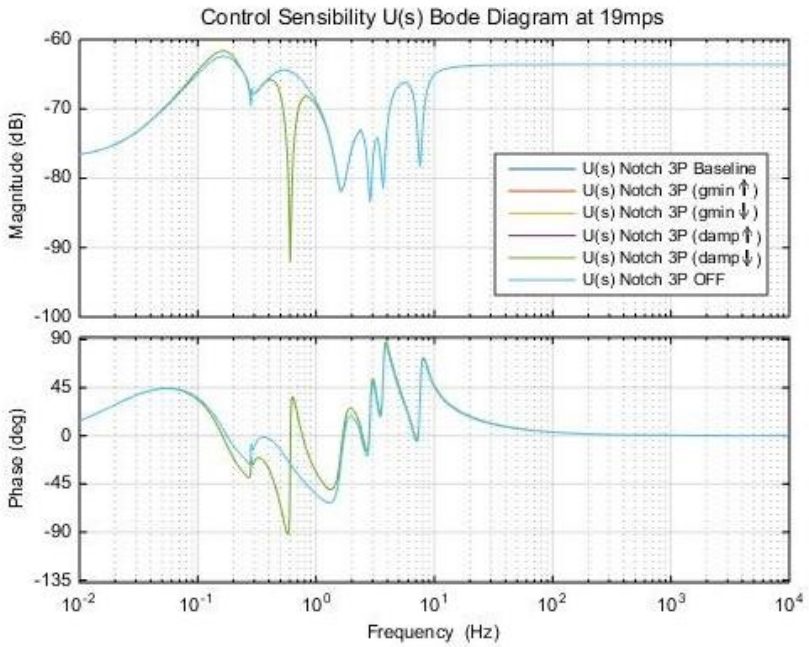

Figure 185: Bode diagram of the closed loop pitch control's U(s) for Scenario 6 at 19m/s

Again, turning off the filter is prejudicial for the closed loop behavior. In this case, the control action will be a lot higher at those frequencies, which must be avoided.

7.7.2. Statistical analysis

Next, the statistical analysis for the sixth Scenario is carried out.

The next figure shows minimum, maximum and mean power generated with respect to the wind speed.

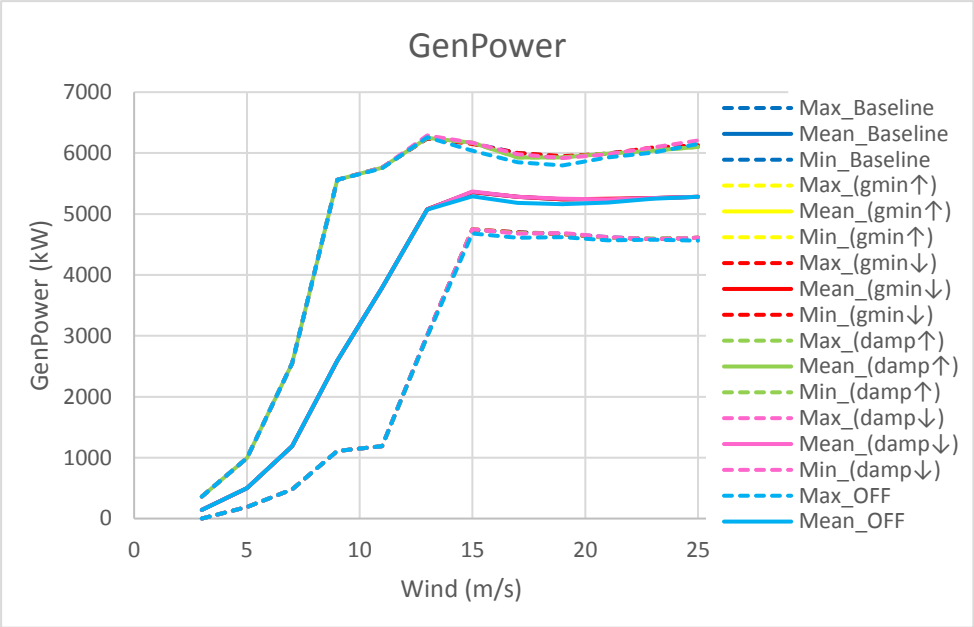

Figure 186: Generated power statistics for Scenario 6

The figure shows a reduction of the power mean when turning off the 3P notch filter, as well as a reduction of the power maximums.

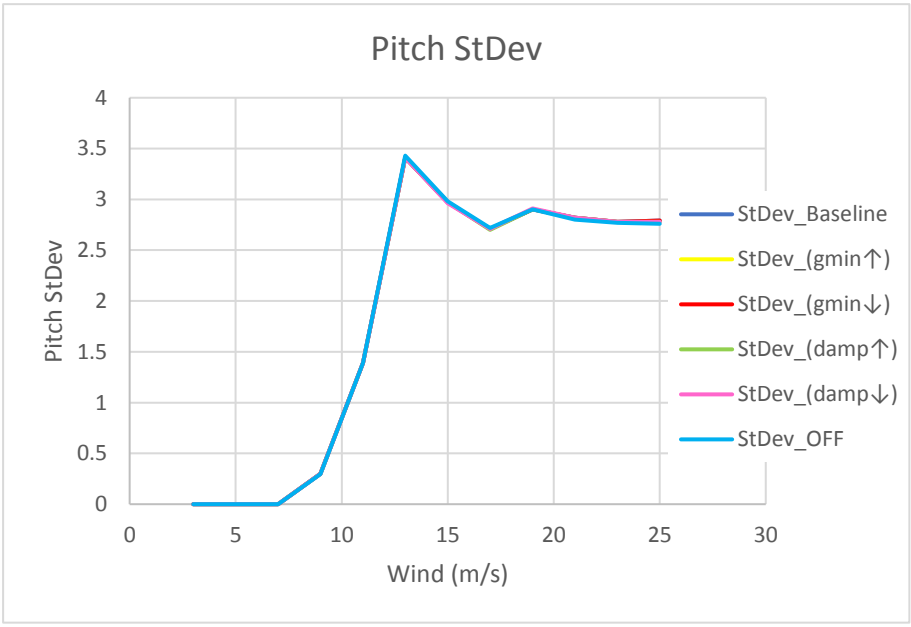

Figure 187: Pitch standard deviation for Scenario 6

As it can be seen in the previous graph, the modification of the 3P notch filter does not affect pitch duty too much.

The next graph represents the tower base momentum in the “y” axis (fore-aft tower base momentum).

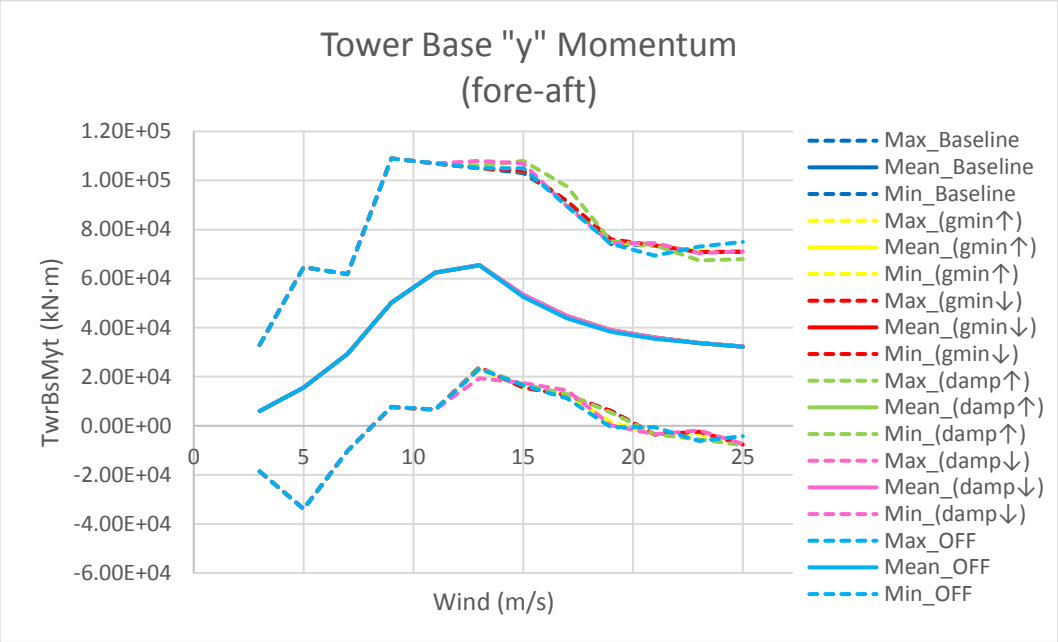

Figure 188: Tower base "y" momentum statistics for Scenario 6

The previous figure shows that the worst configurations for the maximum loads are when varying the filters damp (notch filter width Δ), especially when reducing it. Also, the load increases at 25 m/s when turning off the notch filter at the 3P frequency.

The next figure is a graph that represents the low speed shaft momentum with in the “x” axis.

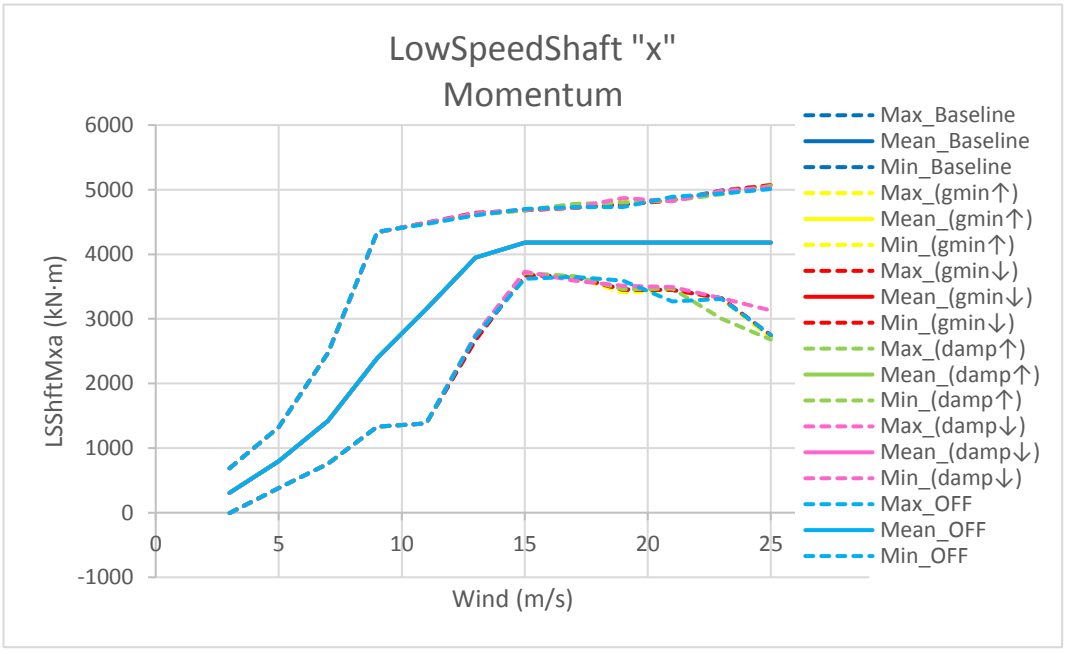

Figure 189: Low speed shaft "x" momentum statistics for Scenario 6

The maximum and mean loads do not vary significantly when changing the 3P notch filter's parameters.

7.7.3. Fatigue load analysis

Different element's damage equivalent load is represented in the spider chart below for the six different configurations of the 3P notch filter.

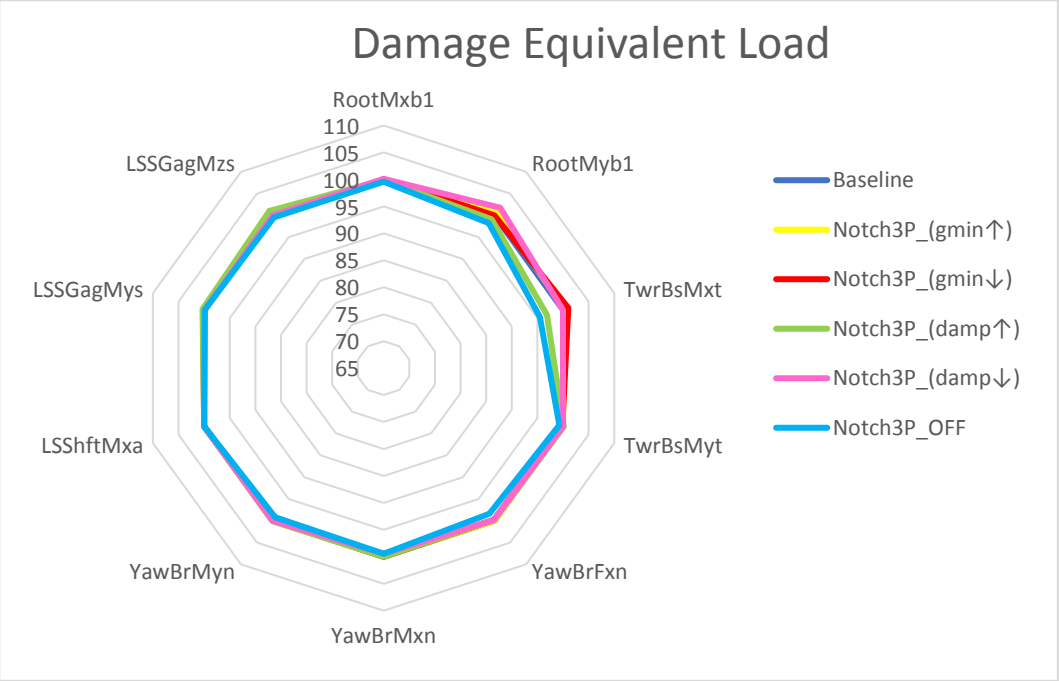

Figure 190: Fatigue load analysis spider chart for Scenario 6

According to the graph above, both increasing the filter's damp (notch filter width Δ) and turning it off reduce loads in the tower base in the "x" axis. Despite of this, given that the maximum load the tower must withstand is the one in the "y" axis and given the benefits of the 3P filter that have been observed throughout the Scenario's analysis, the decision is to keep the 3P filter turned on.

7.8. Conclusions

The results of the study of the previous 6 Scenarios are summarized in this section.

When varying a filter's parameters, some aspects of the system's behavior are improved and some others get worse. Depending on the system's application, different aspects such as open loop margins, closed loop behavior or structural loads will have priority in the control design.

This section classifies the best control configurations depending on the desired behavior. This way, the configuration with the most stars will be the one that suits best when looking for a certain performance, while the worst one will be the one with half a star. As it was observed in the previous section, varying some filters almost does not have effect on some behaviors and therefore, some cases will result in a tie: they will be represented in the table with the same amount of stars.

7.8.1.Scenario 1, Low Pass filter

In this section, the results of the analysis of Scenario 1 are shown. A table with the most suitable configurations depending on the desired behavior is displayed.

Scenario 1: Low Pass	Baseline	Case 0: 0.5 Hz	Case 1: 1Hz	Case 2: 2Hz
Open Loop	★★★	½	★½	★★
S (s)	★★★	½	★½	★★
T (s)	★★★	½	★½	★★
U (s)	★★	½	★½	★★★
Generator Power	★★★	½	★½	★★
Pitch Standard Deviation	★★★	½	★½	★★
Tower Base y Momentum	★★★	½	★½	★★
Low Speed Shaft x Momentum	★★★	½	★½	★★

Table 21: Filtering process configuration ranking for Scenario 1

The table above shows how introducing the 1st order low pass filter in the pitch loop would be beneficial (only at a cutoff frequency of 2Hz) to avoid having control action at high frequencies. This is very useful to reject noise that could enter the system as a disturbance.

7.8.2. Scenario 2, Notch DT

Next, the table with the most adequate filter configuration depending on the system's application is shown for Scenario 2, modifying the Notch filter at the drive train frequency.

Scenario 2: Notch DT	Baseline	Case 3: gmin↑	Case 4: gmin↓	Case 5: damp↑	Case 6: damp↓	Case 7: OFF
Open Loop	★★	★½	★★½	★	★★★	½
S (s)	★★	★★½	★½	★★★	½	½
T (s)	★★	★★½	★½	★★★	★	½
U (s)	★★	★★½	★½	★★★	★	½
Generator Power	★½	★½	★½	★½	★½	★½
Pitch Standard Deviation	★½	★½	★½	★½	★½	★½
Tower Base y Momentum	★★★	★★	★★½	★	★½	½
Low Speed Shaft x Momentum	★★	★★½	★½	★★★	★	½

Table 22: Filtering process configuration ranking for Scenario 2

Some of the system's aspects such as Generator Power or Pitch Standard Deviation do not vary significantly when making changes in the filter. Therefore, they have been represented in the table as a tie with 1 and a half stars each.

7.8.3. Scenario 3, Notch Sym

The next table shows the different filter configuration rating for each desired performance of the system.

Scenario 3: Notch Sym	Baseline	Case 8: gmin↑	Case 9: gmin↓	Case 10: damp↑	Case 11: damp↓	Case 12: OFF
Open Loop	★★	★★	★★	★★	★★	★★★
S (s)	★★★	★★★	★★★	★★★	★★★	★★
T (s)	★★★	★★★	★★★	★★★	★★★	★★
U (s)	★★★	★★★	★★★	★★★	★★★	★★
Generator Power	★★★	★★★	★★★	★★★	★★★	★★★
Pitch Standard Deviation	★★★	★★★	★★★	★★★	★★★	★★★
Tower Base y Momentum	★★★	★★★	★★★	★★★	★★★	★★★
Low Speed Shaft x Momentum	★★★	★★★	★★★	★★★	★★★	★★

Table 23: Filtering process configuration ranking for Scenario 3

Cases 8, 9, 10 and the Baseline scenario have the same gain and phase margin, which gives a tie between them. Varying the parameters of the notch filter placed at the 1st symmetric mode frequency has very little effect on the Generator Power, Pitch Standard Deviation and Tower Base momentum. Therefore, they are represented with a tie too.

7.8.4.Scenario 4, Notch 2Tss

In the next table, the classification of the best configurations depending on the desired performance is shown.

Scenario 4: Notch 2Tss	Baseline	Case 13: gmin↑	Case 14: gmin↓	Case 15: damp↑	Case 16: damp↓	Case 17: OFF
Open Loop	★½	★½	★½	½	★★½	★★★
S (s)	★★	★★½	★★½	★★★	★	½
T (s)	★★	★★½	★★½	★★★	★	½
U (s)	★★	★★½	★★½	★★★	★	½
Generator Power	★½	★½	★½	★½	★½	★½
Pitch Standard Deviation	★½	★½	★½	★½	★½	★½
Tower Base y Momentum	★½	★½	★½	★½	★½	★½
Low Speed Shaft x Momentum	★½	★½	★½	★½	★½	★½

Table 24: Filtering process configuration ranking for Scenario 4

Varying the parameters of the notch filter placed at the 2nd tower side-to-side mode frequency does not affect the Power, Pitch Standard Deviation or the Tower Base or Low Speed Shaft loads.

7.8.5. Scenario 5

The next table shows when the notch filter at the 1P is worth activating.

Scenario 5: Notch 1P	Baseline	Case 18: ON
Open Loop	★★★	½
S (s)	★★★	½
T (s)	½	★★★
U (s)	½	★★★
Generator Power	★★★	½
Pitch Standard Deviation	★★★	½
Tower Base y Momentum	★★★	½
Low Speed Shaft x Momentum	★★★	½

Table 25: Filtering process configuration ranking for Scenario 5

The notch filter placed at the 1P nonstructural frequency lowers the open loop margins and it slows down the system (lower band with in the closed loop disturbance rejection graph). On the other hand, both tracking and control sensibilities show that it attenuates the 1P frequency. The control strategy could only afford activating the 1P notch filter if it was a more stable system (bigger open loop gain and phase margins).

7.8.6. Scenario 6

The table below shows a ranking of the 3P notch filter configurations depending on the performance requirements.

Scenario 6: Notch 3P	Baseline	Case 19: gmin↑	Case 20: gmin↓	Case 21: damp↑	Case 22: damp↓	Case 23: OFF
Open Loop	★½	★½	★½	★½	★½	★★★
S (s)	★½	★½	★½	★½	★½	½
T (s)	★½	★½	★½	★½	★½	½
U (s)	★½	★½	★½	★½	★½	½
Generator Power	★½	★½	★½	★½	★½	½
Pitch Standard Deviation	★½	★½	★½	★½	★½	★½
Tower Base y Momentum	★★★	★★½	★★	½	★	★½
Low Speed Shaft x Momentum	★★★	★½	★★½	★	½	★★

Table 26: Filtering process configuration ranking for Scenario 6

By varying the filter's depth and width (Δ), many behaviors such as the Open Loop performance and the Disturbance S (s), Tracking T (s) and Control U (s) sensibilities are not affected.

Turning the filter off is good for open loop performance because it increases stability margins. As for the closed loop sensibilities, the best configurations are the ones where the filter is activated because it attenuates the 3P frequency, even though turning off the filter helps disturbance sensibility rejection, as it lowers the response's peak and increases the band width.

Chapter 8: Conclusions

8.1. Conclusions

In this project, a classical wind turbine control strategy based on Bossanyi [1] has been developed. The main objective when designing the controller block was to optimize both the power and the active controls for the proposed Upwind 5MW onshore baseline wind turbine model. While doing so, several other objectives have been fulfilled.

· During this project, some traditional wind turbine control strategies have been learned. The main strategies that have been implemented in the control scheme proposed in this project are a **Pitch Control** loop, a **Torque Control** loop, the **Drive Train Damping** (DTD) and the **Active Tower Damping** (ATD). Both the pitch and control loops are part of the regulation control strategy, they control the generator speed and they have been designed for Annual Energy Production (AEP) maximization. The DTD and the ATD are active control strategies, and they have been introduced to lower the wind turbine's loads. Also, the generator speed is thoroughly filtered in the regulation control loops with the objective of eliminating any unnecessary control action in the frequencies that must be avoided due to their effect in the wind turbine's structural loads.

· When developing this project, the learning of **FAST**, an aeroelastic engineering code for **simulating** the dynamic response of wind turbines was essential. Both [6] and [7] have been really helpful for the understanding of FAST, as it is a very complex tool and a lot of parameters and settings must be taken into account when simulating and linearizing.

· The fact that FAST allows the incorporation of its model to **Simulink** was crucial for the decision of the environment where the control was going to be designed. As a consequence of the development of this project's control strategy, a deep learning of the MATLAB Simulink environment has been carried out. Developing the control strategy in Simulink has a lot of advantages. For example, this way, the control is much more visual and intuitive than if the strategy was developed with code. Also, in case any further projects are based on this project's control strategy, either for the strategy's improvement or for new strategy testing, the fact that the model has been designed in Simulink makes it a lot easier to understand. On top of that, any variations can be introduced in a very dynamic and easy way.

· Due to the understanding of the digital implementation of the control strategy, it was necessary to **discretize** the different control blocks to allow the further execution of the project. Despite the fact that the control is designed with continuous-time transfer functions, the digital implementation of the control is valid due to the small enough discretization sample time that has been chosen, $T_s = 0.01s$.

· After building the discrete controller blocks in the Simulink environment, a control library has been created. This **Simulink library** contains the following blocks: 1^{st} order low pass filter, 2^{nd} order low pass filter, high pass filter, band pass filter, notch filter and a PID block. These blocks can be copied from the control library to the Simulink model where the FAST model is and, since they are linked blocks, any changes introduced into the blocks that are in the library will be automatically updated in the block in the Simulink model.

· One of the first steps in the actual control strategy design was the extraction of the **linearized** representations of the dynamic aeroelastic wind turbine model with FAST. This is key for the continuous-time Laplace design because this way, the plants of the model are obtained for different operating points. This allows checking the control performance in the time and frequency domain before implementing it in the Simulink model.

· When checking the system's behavior in the time and frequency domain, an optimized control performance was sought. The use of **sisotool**, a MATLAB GUI application that facilitates feedback loop SISO (single-input single-output) controller design has made the control optimization a lot easier. Sisotool allows an online view of the system's performance while carrying out the control tuning, which is a very visual way of seeing which control elements affect which behavior the most. The use of this tool has been very useful for the control tuning of the designed strategy.

· Once the control was tuned, the next step in the validation of the strategy was to carry out a load and statistical analysis of the system's response. In this project, only fatigue loads were analyzed. To do so, the fatigue-life estimator **MLife** has been used. MLife is a MATLAB based postprocessor for fatigue load analysis developed by NREL (National Renewable Energy Laboratory) that generates short-term damage, fatigue-life damage equivalent loads, lifetime damage, time until failure, etc. At the same time, it also performs statistical calculations including minimum and maximum values, mean, etc. All of this information is essential for the control validation and therefore several analysis have been carried out with different control configurations in order to test the active control strategies: the Drive Train Damping (DTD) and Active Tower Damping (ATD).

· Once the control was tuned, the first step in the control **validation** was the simulation of the system under different conditions such as a ramp wind or a wind input that increases by steps of 1m/s from cut in up to cut out wind speed. Some important aspects of the control's behavior such as how tightly the generator speed is controlled in the above rated zone can be easily seen with these simulations.

· To fully validate the control strategy, the final step was to carry out a **load and statistical analysis** of the system's response. In this project, only fatigue loads were analyzed. To do so, the fatigue-life estimator **MLife** has been used. MLife is a MATLAB based postprocessor for fatigue load analysis developed by NREL (National Renewable Energy Laboratory) that generates short-term damage, fatigue-life damage equivalent loads, lifetime damage, time until failure, etc. At the same time, it also performs statistical calculations including minimum and maximum values, mean, etc. All of this information is essential for the control validation and therefore several analysis have been carried out with different control configurations in order to test the active control strategies: the Drive Train Damping (DTD) and Active Tower Damping (ATD).

· An extra validation process that this project's classical control scheme went through is its comparison to another Simulink implemented control strategy, the control strategy published by the **Delft University** [2]. The two control systems' behaviors were compared and a study of both control's fatigue loads and statistics was carried out too.

· With the fully validated control strategy, the ultimate objective of studying the filtering process of the pitch control loop was finally carried out. The width and depth of the different filters introduced in the pitch control loop were modified a 10%. Then, the continuous-time and frequential behaviors were compared and a fatigue load and statistical analysis was carried out. As a result of this study, a **guide on generator speed filtering** depending on the specific application's restrictions has been developed in Section 7.8. This guide is in the form of tables, and it rates the different filter configurations from best to worst depending on the system's desired performance. This way, depending on the control's purpose, such as higher AEP, lower pitch duty or lower load in a certain component, the tables indicate the best filter configuration.

8.2. Industrial implementation

The control strategies designed for wind turbines are implemented into a PLC (Programmable Logic Controller). For this project to be implemented industrially, some changes would have to be made in the control scheme. For example, communications with the electric converter have not been considered and so an interface that connects the control to it would have to be created.

Another issue that must be taken into account is that the wind turbine control designed in this project does not have yaw control. All the simulations have been carried out with three dimensional winds of 0 m/s mean in the "v" direction, which is the effect that a well designed yaw control would have. This way, if the control was to be implemented into a PLC, a yaw control should be added to the control scheme.

Also, the control strategy of this project only has an emergency stop in case the wind turbine has an overspeed. It would be convenient to add more alarms and warnings before implementing it to a PLC.

On the other hand, the control has been implemented in a discrete-time form and therefore the power and active control are ready to be programmed into the PLC tasks destined to calculate pitch and torque signals of the torque control loop, pitch control loop, DTD and ATD.

The next figure shows a scheme of a wind turbine's PLC.

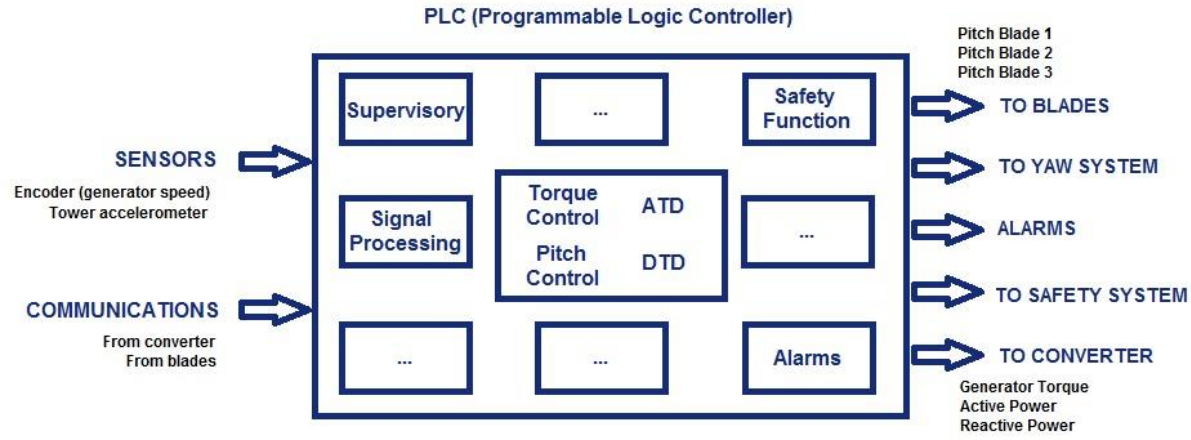

Figure 191: Wind turbine PLC scheme

The previous scheme shows how the designed control strategy is only part of what has to be implemented into a wind turbine's PLC.

8.3. Future work

Even though the results obtained in this project came up to the expectations, there are many aspects the control strategy that could be further developed and several improvements could be added to the existing scheme.

· The designed control scheme has numerous filters, which are all initiated at 0. This causes the system to take time since the simulation starts until the filters reach the actual values that correspond to that operating point. A good improvement for this control scheme would be studying and improving the filter's initializations.

· Another improvement the strategy could benefit from would be an upgrading of the transition zone coupling. The existing control activates the above rated zone and deactivates the below rated zone at the same instant. The pitch control is saturated to the minimum value when the operating point is below rated and the demanded torque is saturated to the rated value when working in the above rated zone. This way, a rapid change between the two zones (given for example by a wind gust at a wind speed just below the rated wind speed) would provoke the blades not to act until the generator torque reached rated. This could cause the wind turbine to overspeed, and it could be avoided by introducing a double PI to control the transition zone. The input signal to this double PI is the difference between rated power and measured power. This way, when the operating point is still far from rated, the pitch angle is saturated to its minimum value and, as the the power increases, the double PI slowly starts increasing the blade pitch angle, with very slow dynamics [1]

The double PI would let the blades start pitching before the demanded torque reached its rated value, therefore improving the pitch-torque coupling.

· Also, the actual pitch control strategy has been designed in absolute terms. This means that it demands a certain pitch angle instead of demanding a certain speed at which the blade should rotate. Switching the pitch control loop into a rate demanding pitch control could improve the control's behavior as the PI would always vary at values close to 0 and this would act like some kind of anti-windup strategy.

· The existing control only has one emergency stop due to either generator overspeed or due to a programmed emergency button. Other warnings and alarms could be introduced to stop the wind turbine in case of excessive vibrations in the structure, in case of an unbalanced rotor (possible broken or damaged blade, ice in the blades…), etc.

· As the actual control scheme does not have a yaw control, a good addition could be the development of a yaw control strategy, to have the wind turbine align with the wind.

· The load analysis that have been carried out in this project are all fatigue analysis. It could be interesting to complement this study with an extreme-event load analysis to test the control strategy in a different aspect.

· Finally, the wind turbine's starts and stops have not been properly developed. Only an emergency stop has been created by taking the blades to 90º (capturing the least amount of energy as possible and slowing down the rotor) and demanding no electric torque to the generator. A slower and safer stop would be beneficial for the wind turbine loads.

Chapter 9: References

[1] E. Bossanyi, "The Design of closed loop controllers for wind turbines," *Wind Energy*, 2000.

[2] S. P. Mulders and J. W. van Wingerden, "Delft Research Controller: an open-source and community-driven wind turbine baseline controller," *IOPscience, J. of Phys.: Conf. Ser. 1037 032009*, 2018.

[3] "REN21 data - REN21", *REN21*, 2019. [Online]. Available: http://www.ren21.net/status-of-renewables/ren21-interactive-map/.

[4] "Tecnología y mercado eólico," class notes from Eolic Systems by Pablo Sanchis Gúrpide, Electric and Electronic Engineering Dept., Public University of Navarra, 2017.

[5] "Extracción de la energía del viento," class notes from Renewable Energies by Alfredo Ursúa Rubio, Electric and Electronic Engineering Dept., Public University of Navarra, 2016.

[6] J.M. Jonkman and M.L. Buhl Jr., "Fast User's Guide," National Renewable Energy Laboratory, Aug. 2005.

[7] P. J. López Bracot, "Desarrollo de un entorno de validación profesional que facilite el diseño fiable de estructuras de control y estimadores de cargas en aerogeneradores," M.S. thesis, Pub. Univ. of Navarra, Jan. 2018.

[8] *Wind turbines. Part 1: Design requirements,* IEC 61400-1:2005. Third Edition, Jun. 2006

[9] J. Jonkman, S. Butterfield, W. Musial, and G. Scott, "Definition of a 5-MW Reference Wind Turbine for Offshore System Development," National Renewable Energy Laboratory, Feb. 2009.

[10] A. Díaz de Corcuera, "DESIGN OF ROBUST CONTROLLERS FOR LOAD REDUCTION IN WIND TURBINES," Ph.D. dissertation, Univ. Mondragon, Feb. 2013.

[11] J. Berro Bariain, "Modelado de incertidumbre en sistema de comunicaciones y actuadores de un aerogenerador y diseño de algoritmos de control inmunes a sus efectos," M.S. thesis, Pub. Univ. of Navarra, Sept. 2018.

[12] "Notch filter with varying coefficients – Simulink – MathWorks Spain," es.mathworks.com, 2019. [Online]. Available: https://es.mathworks.com/help/control/ref/varyingnotchfilter.html.

[13] J.L. Rodríguez Amenedo, J.C. Burgos Díaz and S. Arnalte Gómez, *Sistemas Eólicos de producción de energía eléctrica*. Editorial Rueda SL, 2003.

[14] "Apuntes de Ingeniería de Control", class notes from Daniel Rodfíguez Ramírez and Carlos Bordóns Alba, Systems and Automatics Dept., Public University of Navarra, May 2007.

[15] "Frequently Asked Questions (FAQ) | NWTC Information Portal", *Nwtc.nrel.gov*, 2019. [Online]. Available: https://nwtc.nrel.gov/FAQ

[16] Biblioteca de la Universidad Pública de Navarra. Oficina de Referencia. "Guía para citar y referenciar. IEEE Style," 2016. [Online]. Available: https://goo.gl/LaUj46.